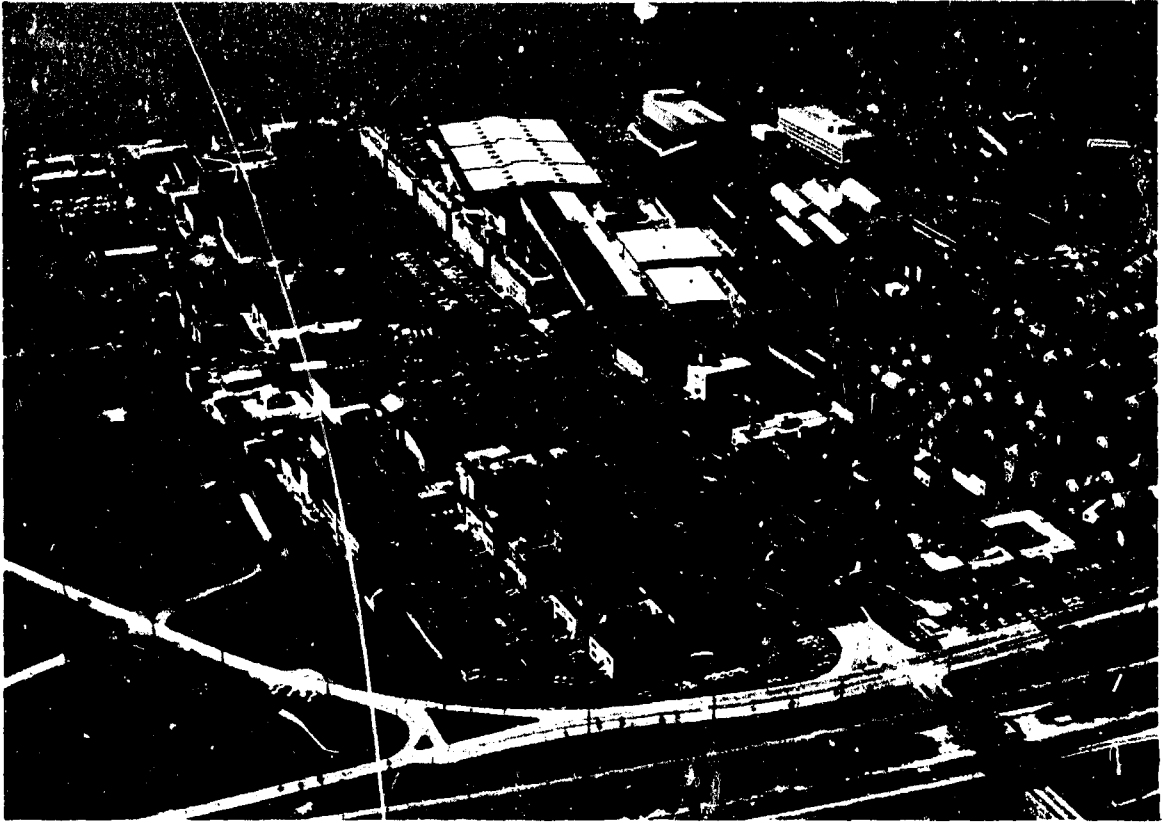


AD 700 249

1968 ANNUAL REPORT
NAVAL RESEARCH LABORATORY



Naval Research Laboratory – 1968

PREFACE

On July 2, 1968, the Naval Research Laboratory completed 45 years of service to the Navy. These years have seen the Laboratory grow from an initial group of 90 individuals working in radio and underwater sound to a current staff of 3,500 scientific and support personnel engaged in a broad spectrum of research and development in the physical and mathematical sciences.

The continuing policy which has supported a substantial program of research in the fundamental sciences, in parallel with a program of direct mission-related applications, has produced a distinguished record of contributions to national defense and scientific knowledge. The continued success of this policy quite obviously depends upon the excellence of the Laboratory's professional staff and their supporting services and facilities. Essential also, given finite resources and an environment of rapidly expanding science and related naval implications, is the balance and selectivity of the research program. The body of this report describes the unclassified portion of that program. The introductions to the program descriptions provide an overview of current program emphasis and direction.

This document has been prepared to report the activity and achievements of the past year. I believe it also reflects the quality and significance of the work accomplished. It is hoped that it will prove both informative and useful to all who sponsor, or share an interest in, work at the Naval Research Laboratory.

J. C. Matheson

James C. Matheson, CAPT., USN
Director
Naval Research Laboratory

CONTENTS

PREFACE	iii
THE NAVAL RESEARCH LABORATORY	1
THE RESEARCH PROGRAM	6
HIGHLIGHTS	8
RESEARCH AREAS	12

Electronics

An Overview	12	Frequency Translation of Laser Radar Signals	22
Hypervelocity Ballistics	12	A High-Performance Analogue Processor for Long-Range High-Frequency Radar	23
Kelvin Wake Analysis	13	Radar Detection of Nonfluctuating Targets in Log-Normal and Contaminated-Normal Clutter	23
Electromagnetic Propagation Through Gaseous Exhausts	15	Centralized Electronic Control	25
Solrad	16	Frequency and Time Instrumentation	26
Closed Cycle CO ₂ Laser	16	Antenna Multicoupling	26
Controllable Light Transmission Films	17	Flight Tests of the NRL Mark III Omega Aircraft Receiver	27
Microwave Shipboard Communications	17	Very-Low-Frequency Propagation (Navigation)	29
Spherical Airborne Antenna Coverage	17	Very-Low-Frequency Propagation (Communications)	29
Theory of Radar Sea Clutter	18		
Radar Target Scintillation	19		
Ionospheric Earth-Backscatter Investigations Carried Out by Precision Faytracing	20		
Dynamic Behavior of the Ionosphere as Determined by Radar Observations of Artificial Plasma Clouds	21		

Materials

An Overview	30	Compensation for Thermal Distortion in Glass Lasers	49
Separation of Water from Fuels	31	Third-Order Nonlinear Reflection Studies	49
The Behavior of "Free Molecules" in the Atmosphere	32	Atmospheric Depolarization of Laser Light	50
Fire-Retardant Paint System for Ship Interiors	33	Underwater Light Source	51
Inhibition of Corrosion in Navy Boilers	33	Elastic Constants Determined from X-Ray Scattering	51
Chemical Reactivity of Pristine Glass	34	Negative Etching in Sodium Fluoride Crystals	52
Mass Spectrometric Studies of Cobalt Carbonyl Compounds	35	High-Pressure Measurements of Shear Strength	52
Advances in Electrochemical Research	36	Transient Radiation Effects in Quartz and Fused Silica	52
Unambiguous Assignment of Spin-Coupling Parameters	37	Lattice Vibrations and Infrared Absorption in Mixed Linear Chains	53
Rate Spectrum in Cleavage Fracture	38	Annealing of Radiation Damage in Solar Cells	54
Stress-Corrosion Cracking of High-Strength Steels	38	High-Pressure Transition in Bismuth	54
Differential Aeration Corrosion of Stainless Steel	40	Ammonium Halide Luminescence	55
Spin Wave Resonance and Radiation Damage in Thin Films	40	Impurity-Perturbed Defect Centers in Alkali Halides	56
Environmental Effects at Elevated Temperatures	41	V _i Centers in Alkali Halide Crystals	56
Sintering of Porosity in Bicrystals of Niobium	42	Large Zero-Point Spin Deviations in an Antiferromagnet	57
Interfacial Energies in Metals	43	Vibrations of Atoms in Solids - Localized or Extended?	57
Gas-Metal Reactions	43	Exchange Coupling of Magnetic Ions	58
Influence of Oxygen on Formation of Surface Slip Bands	45	Potential Electrolyte for a Truly Dry Cell	58
Physical Properties of Incipient Ferromagnets	46	Dosimeter for High-Energy Pulsed Radiation	59
Fracture Toughness of High-Strength Metals	46	Electronic Transport Phenomena in Simple Metals	60
Neutron Spectra Related to Radiation Damage	48		

CONTENTS

Materials – Continued

Electronic Impurity States and Optical Phonons in Semiconductors	61	Effect of Adsorbed Films on Evaporation of Volatile Liquids	65
Radiation Damage to Hereditary Material	63	Mechanism of Action of Dry-Film Lubricants	65
Structure of Poison-Dart Frog Venom	63	Effect of Adsorbed Monolayers of Water on Solid Surfaces	66
Biological Adhesion	64	Bond Formation in Transition Metals	66
Surface Chemistry of Liquid-Liquid Interfaces	64	Growth of PZT Crystals	67
		Fire Protection for Aircraft Carriers	67

General Sciences

An Overview	68	Nuclear Structure Investigations by Inelastic Electron Scattering	86
Extreme Ultraviolet Spectroheliograms and Heliograms	69	Research Program with the Sector Focusing Cyclotron	86
Solar Monitoring	71	New Approach to Bound States of Two Spin Waves in Heisenberg-Type Ferromagnets	87
Solar X-Ray Spectral Studies	71	Iteration Procedures for Analysis of Scattering Processes	87
The Solar Corona	72	Thermal Blooming of Laser Beams	88
Advances in Extreme-Ultraviolet Photographic Techniques	74	Collisionless Shock Wave Research	89
Far-Ultraviolet Airglow Studies	74	Hard Core Theta-Pinch	89
Far-Infrared Astronomy	74	High-Brightness Glass Laser	90
X-Ray Astronomy Program	75	Information Systems	91
Navigation with the Radio Sun	75	Phased-Array Radar	91
Radio Variability of Quasars	76	Analytic Functions and Their Applications	92
Polarization Properties of Cosmic Radio Sources	78	Analysis of Noncentrosymmetric Crystal Structures	92
Magnetic Fields and Particles in Our Galaxy	77	Polynomial Approximations on the Whole Real Line	93
Effect of Mass on Frequency	79	Statistical Decomposition of Mixtures	93
Analysis for Trace Amounts of Carbon and Oxygen	81	Primitive Roots	94
X-Ray Spectrochemical Analysis	81	Research Computation Center Activities	94
A Neutron Coincidence Detector for Safeguards Inspections	82	Mean Path Length of Cosmic Rays	94
The Nature of Neutron Capture	83	Confinement of Cosmic Rays	95
Ion Implantation	84	New Telescope for Detecting Cosmic Gamma Rays	96
Charged-Particle Energy Losses and Fluctuations	85		
Triton-Induced Nuclear Reactions	85		

Oceanology

An Overview	97	Atmospheric Space Charge Over Water	102
Assured Range Studies	97	Cloud Nuclei	103
Statistics of Scattered Acoustic Pulses	98	Stratospheric Water-Vapor Distribution	103
Scale Model Acoustic Studies	99	Foam Separation of Trace Organic Substances in Sea Water	104
Sonar Calibration at Simulated Great Depths and Low Temperatures	100	Trace-Element Measurements in Marine Animals	105
Cavitation Threshold	100	Marine Geochemistry of Fluorine	106
High-Power Underwater Sound Source	101	The Density Gradient Column as a Tool for Measuring Sea-Water Density	106
Reliable Deep-Submergence Hydrophone	101	Study of Phytoplankton by Spectroreflectometry	107
Marking the Ocean Surface with Artificial Sea Slicks	101		
Carbon Monoxide and Methane at the Air-Sea Interface	102		

CONTENTS

Oceanology – Continued

<i>Scorpion Search</i>	108	Structural Analysis of Cable Systems	111
Optimum Packing of Hollow Spheres in Buoyancy Materials	109	Experimental Approaches in Shock Design Research	111
The Strength of Annealed Bulk Glass for Possible Deep-Submergence Structures	110	The Reliability of Nuclear-Power Instrumentation for Oceanographic Research.....	112

CONTRIBUTIONS TO SCIENCE AND TECHNOLOGY

Papers Published in Scientific Journals	114
Formal NRL Reports	126
Patents Received	131

RECOGNITION OF PERSONNEL

Honors and Incentive Awards	134
Research Publication Awards	136
Scholarship Awards	137
Research Associateship Awards	138

THE NAVAL RESEARCH LABORATORY

The Naval Research Laboratory is a field activity of the Office of Naval Research (ONR), reporting to the Chief of Naval Research, who is directly responsible to the Assistant Secretary of the Navy for Research and Development.

NRL was founded in 1923 to ensure that advancements in science and engineering could be readily applied to the Navy's needs. Towards that end, the NRL research program has developed into a comprehensive and coordinated effort in the physical, mathematical, and environmental sciences. An extensive basic research program is closely coupled to a broad effort in applied research and development devoted to both immediate and long-range technical problems of interest to the Navy. Where uniquely qualified, the Laboratory also provides consultative services and conducts research and development for other elements of the Defense Department and agencies of the Government.

Current sponsors of the research program include ONR; the Naval Systems Commands; the Advanced Research Projects Agency; the Defense Atomic Support Agency; the Atomic Energy Commission; the National Aeronautics and Space Administration; and various elements of the Army and Air Force. The funding level of sponsored research at NRL during fiscal year 1969 was approximately 97 million dollars.

There are three major organizational units of the Laboratory: the Office of the Director, the Research Department, and the Support Services Department.

Within the Office of the Director are the Military Staff Office, the Office of the Comptroller, and the Civilian Personnel Office.

NRL's Cyclotron building



THE LABORATORY

The Research Department, headed by a civilian scientist as Director of Research, is organized into four areas: electronics, materials, general sciences, and oceanology. Each area is headed by an Associate Director of Research who administers the work conducted by the scientific divisions and the special research groups within that area.

Each of the major scientific divisions consists of approximately 100 scientific, technical, and administrative personnel, headed by a Division Superintendent. The smaller organizational units (average of 10 persons), shown in the table, have special functions which are indicated by their titles or discussed in more detail elsewhere in this volume. There are three special organizations, each headed by a Chief Scientist who occupies a corresponding honorary "Chair of Science."

Organizational Units of the Research Department

Area	Major Scientific Divisions	Other Research Groups
Electronics	Applications Research Electronics Radar Communications Sciences Electronic Warfare	
Materials	Chemistry Metallurgy Solid State	*Laboratory for the Structure of Matter *Laboratory for Chemical Physics Central Materials Research Staff Shock & Vibration Information Center Combustion Suppression Research Center
General Sciences	Space Science Nuclear Physics Plasma Physics Mathematics and Information Sciences	*Laboratory for Cosmic Ray Physics Health Physics Staff SOLRAD Project
Oceanology	Acoustics Underwater Sound Reference Ocean Sciences Ocean Technology	Ship Facility Group Non Acoustic ASW (R&D) Task Group

*Special organization headed by a Chief Scientist who occupies a corresponding "Chair of Science."

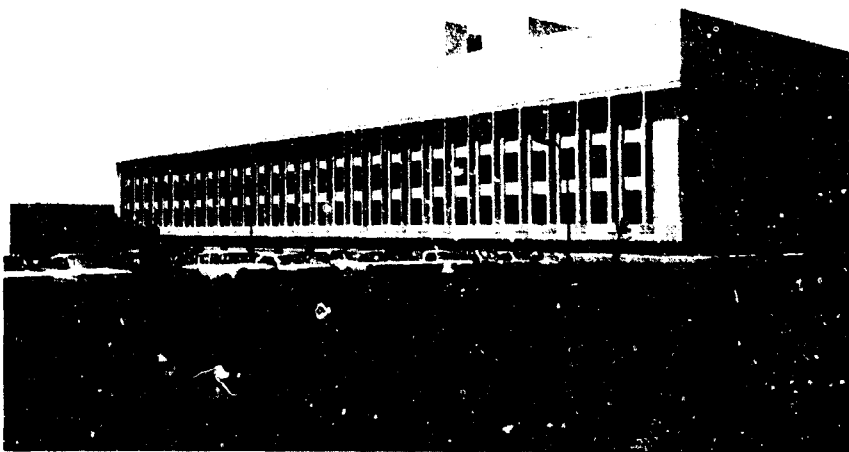
THE LABORATORY

Backing up the research programs in all of the areas mentioned above is the Support Services Department, whose many capabilities include mechanical, electronic, and project engineering staffs; technical drafting; numerous shops (machine, sheet metal and welding, plastics, foundry, pattern, plating, printed circuit, electronic assembly, microelectronic, and electronic model); the supply of all needed materials; editorial, printing, exhibit, and graphic-display services; patent counseling; and one of the Nation's finest technical libraries. The responsibilities for these supporting services fall within the purview of five major divisions (Supply, Technical Information, Engineering Services, Public Works, and Chesapeake Bay) and three staff offices (Management Engineer, Patent Counsel, and Medical Staff).

Operations and Technical
Services building



New laboratory building oc-
cupied by the Space Science
Division

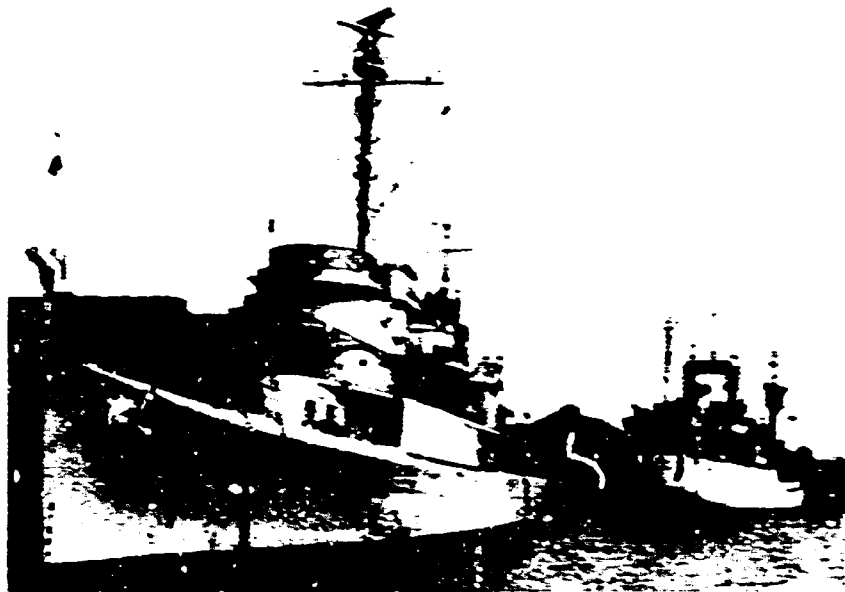


THE LABORATORY

The staff of the Laboratory consists of approximately 3,000 civilian employees and a military complement of 24 officers and 60 enlisted men. The research staff consists of over 1,200 scientists and engineers, almost half of whom have advanced degrees (about 270 doctors and 300 masters). Supporting these researchers are some 600 technical assistants and over 1,600 general, clerical, and shop personnel.

At the main site of the Laboratory, located on the east bank of the Potomac River in southwest Washington, D.C., a variety of major equipment and facilities is available to and used by the scientific staff. Among these are a 75-million-electron-volt (MeV) sector focusing cyclotron; a high-level radiation laboratory; a high-field (150 kilogauss) magnetic facility; Isotac (60 MeV) and Van de Graaff (5 million volts) particle accelerators; a multimegawatt-degree thermonuclear research (8 inch) facility; a research computer center (with a CDC 3600 computer); two large transfer-model and -materials test units; several vacuum chambers; and a space simulation facility.

For conducting specific experiments that cannot be performed at the main site, NEI has several field stations. The largest of these, the Chesapeake Bay Division (CBD), Maryland, has a variety of equipment including several large radar antennas and light-gas hypervelocity guns. Associated with CBD is Tipton Island, which is used as a terminal for over-the-water light path investigations. Some of the field sites are built solely around radar antennas, radio telescopes, and related systems devices. These include the Radio Astronomy Observatory at Maryland Point, Maryland; Space Surveillance Stations at Rendonville and Roma, Texas; and communications research facilities at Hybla Valley, Virginia; Stamp Neck and Waldorf, Maryland; and Sagar Grove, West Virginia.



NEI's research ships, the *Gambel* and the *Mearns*, at port in Washington, D.C.

THE LABORATORY

In addition, NRL has a Transducer Calibration Facility at Seneca Lake, New York; a Marine Corrosion Laboratory at Key West, Florida; an Underwater Tracking Facility at Argus Island (near Bermuda); and a large gondola suspended beneath the Chesapeake Bay Bridge, Maryland, for studies of the air-water interface.

For investigations requiring mobile research facilities, NRL has five airplanes equipped with scientific instruments especially useful in the conduct of studies in the communications sciences, oceanology, and in some of the space sciences. For similar requirements, NRL has two oceanographic research ships, the *USNS Mizar* and *Gibbs*, and access to several other types of naval surface ships and submarines.

The Laboratory initiated in 1961 a long-range building program to provide facilities adequate to requirements for research in the decades ahead. The acquisition of adjacent land has more than doubled the original acreage of Laboratory grounds; obsolescent buildings constructed hastily during World War II have been demolished to make room for new ones; two new general purpose laboratories have been built and occupied by the Electronics and Space Sciences Divisions; a major nuclear physics research facility (cyclotron) has been completed and placed in operation; an operations and technical services building has been constructed and occupied by the Public Works and Technical Information Divisions and the Office of the Comptroller; and the construction of a new chemistry building, scheduled for occupancy in the summer of 1970, was initiated this year. The modernization plans for future years call for the construction of additional general purpose laboratories, an acoustic and oceanographic research center, a new administration building, and a central library.



Model of new buildings which will eventually occupy the additional acreage acquired for NRL's expansion. Some of the structures have already been erected. The Cyclotron building, for instance, appears in the lower right-hand corner.

THE RESEARCH PROGRAM

In the view of the management and personnel of NRL, our mission is to operate an outstanding research center devoted to good science and its application to the special interests and needs of the community that supports the Laboratory. Good science is easily evaluated in the context of the larger professional world within which our staff functions. We judge ourselves by all of the attainments of our research—our publications, the invitations we receive to present papers, our memberships on committees of national professional societies, the consulting services we provide, the books published under our by-line, the colloquia we are invited to attend, and so forth. We believe the material contained herein constitutes strong evidence that the Laboratory has satisfied its obligation to practice good science.

We accommodate the needs of our sponsors by performing research and initiating its translation into advanced prototype equipment for use by the Fleet and other Service units. Our success in these endeavors must be judged by the degree to which we satisfy such needs. Since much of our applied work is of a classified nature, its scope and import are not reflected in this review. However, we feel that the Laboratory's continued growth and assumption of new responsibilities are reliable measures of our success in these areas.

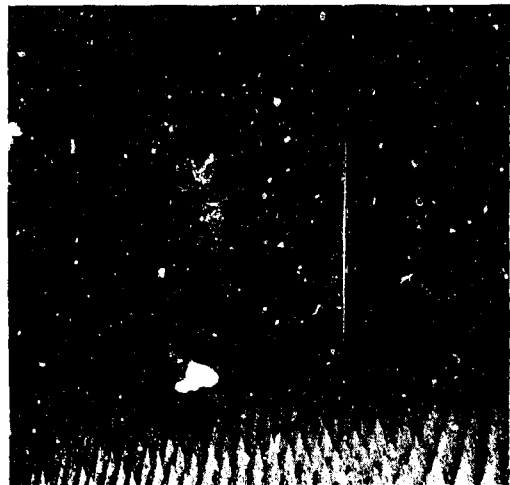
Above and beyond the formal responsibilities given in our mission statement, we feel that we have an overriding responsibility to be good citizens in the Navy and Department of Defense community. The degree to which NRL scientists and engineers partake in technical dialogs with their sponsors is not reflected in this document. Nonetheless, we believe that our technical interactions with various Navy organizations constitute one of our most important contributions.

Finally, we believe that in times of stress or crisis we must be available to help in any way that is necessary. While we are justly proud of the many NRL staff members who worked round the clock seven days a week during the successful search for the Scorpion, we are also very

GENERAL SCIENCES—Linear accelerator



ELECTRONICS—Anechoic chamber



THE RESEARCH PROGRAM

proud of our many staff members who worked equally hard on a large variety of projects that are not as well publicized.

Besides being a year of great accomplishment, 1968 was a year that witnessed many changes at the Naval Research Laboratory. During the year, the Laboratory undertook many important new and expanded programs. Among them was a major expansion of our program in under-sea acoustics which involved the assumption of the responsibilities formerly held by Hudson Laboratories of Columbia University. We were asked by the Director of Navy Laboratories to become a lead laboratory in the field of electronic warfare. Various large programs were either expanded or initiated under the sponsorship of the Advanced Research Projects Agency and the Defense Atomic Support Agency.

To facilitate the concentration of our efforts on areas of heightened interest, the Laboratory underwent a number of internal reorganizations and realignments of personnel. In addition, the technical caliber of our staff has been upgraded significantly. We were fortunate in having been able to recruit many competent senior scientists. As a result, we enter the year 1969 a stronger organization that is better able to satisfy the needs of our sponsors. These developments bode well for a productive and interesting future.

As explained above, the expositions presented here account for only a portion of the Research Department's 400 or more projects. Our reports are arranged according to the organizational units (areas and divisions) in which the work was performed.

Alan Berman

Alan Berman
Director of Research
Naval Research Laboratory

OCEANOLOGY — Acoustic research on the *Mizar*



MATERIALS — Metals research



HIGHLIGHTS

ELECTRONICS AREA

Laser Radar. Very large doppler (frequency) shifts will be encountered when lasers are used to identify fast-moving objects such as supersonic aircraft or orbiting satellites. Because intermediate-frequency amplifiers will be used to process these doppler-shifted target signals, a means must be devised for frequency shifting the laser so that the difference between its new shifted frequency and the doppler-shifted frequency of the return signal can be handled by the amplifier. NRL has demonstrated that birefringent optical materials placed in a rapidly rotating magnetic field may achieve the frequency shifting of the laser.

Radar Sea Clutter. A better basic understanding of wind-generated sea-surface waves is necessary if the radar-system designer is to improve radar performance in this area. NRL scientists have developed a mathematical model describing the scattering of radar signals by the sea's surface. This model gives results which are in good agreement with data obtained by aircraft and ships.

Solrad. In an effort carried out cooperatively with the general sciences area of the Laboratory, the electronics area has been conducting design, test, launch, and monitoring activities with regard to the Solrad series of satellites. The combined effort comes under the direction of the Solrad project team. For specific accomplishments in 1968, see the general sciences area highlight entitled "Solar Monitoring."

Ionospheric Raytracing. With the use of a computer-assisted program developed by NRL, the ionospheric propagation of high-frequency radar waves may be depicted by means of ray profiles. In particular, profiles for the Earth-backscatter echo can facilitate the investigation of traveling disturbances and gravity-wave effects in the ionosphere.

Artificial Plasma Clouds. The internal motions of violently turbulent regions of the lower ionosphere can now be studied in detail by means of NRL's sophisticated coherent pulse-doppler research radar. Statistical descriptions of the duration, relative velocities, and amplitudes of these turbulent regions are obtained by observing the evolution of cesium- and barium-seeded artificial plasma clouds injected into the ionosphere by rocket-launched projectiles.

Rocket Exhausts. Rocket exhausts interfere with electromagnetic signals relied upon to detect, track, or guide rockets. As a result of NRL's studies of this problem in its space, altitude, and velocity chamber, it is now possible to predict, and thus make allowances for, the amplitude and phase modulation of these signals in terms of rocket altitude, propellant type, and signal frequency.

Precision Time and Frequency. Since 1967, NRL has provided frequency monitoring equipment for many of the Navy's ships. Use of this equipment has resulted in a dramatic improvement in adherence to assigned frequencies and thus in an enhanced reliability in Fleet communications. During the past year, for example, a central time and frequency system was developed for installation aboard the USS *Nimitz* (CVAN-68).

Airborne Antennas. With the NRL-designed Hart-lobe antenna system, the long-standing problem of blindspots in airborne beacon reception, due to shielding of the antenna by the airframe itself, has been solved. Flight tests have demonstrated that a nearly omnidirectional signal-reception capability is obtained at various ranges and for various airplane bank angles. Overall system performance is noway compromised by the system.

Omega Aircraft Receiver. The recent 8,000-mile transatlantic flight test of the NRL-developed Mark III Omega receiver demonstrated the extreme reliability and accuracy of this all-weather system. With a computer incorporated in the system, longitude and latitude readings were instantaneously generated for the pilot. In very adverse weather, when all other navigation signals were obliterated, Omega signals continued to be received by the aircraft.

MATERIALS AREA

Mass Spectrometric Studies of Cobalt Carbonyl Compounds. A mass spectral study of a series of cobalt-carbon and cobalt-phosphorus compounds showed that the energies of the Co-C and Co-P covalent bonds are essentially identical but much stronger than that of the Co-H bond. Also, their mass spectral fragmentation patterns suggest that all of the trifluorophosphine carbonyl cobalt hydrides have a distorted trigonal bipyramid structure. The foregoing are findings which have both fundamental

and practical applications in biological systems and in the catalytic cracking of hydrocarbons.

Fire-Retardant Paint System for Ship Interiors. A technique has been developed for rendering a combustible paint fire-retardant. This result is achieved by use of a thin water-based undercoat containing materials that interact under the influence of heat to produce a powerful flame-extinguishant. The undercoat can be used effectively in combination with any type of decorator topcoat, but it was developed especially for use with the nontoxic acrylic latex paint, also an NRL product, now required for submarine interiors and other enclosed environments.

Stress-Corrosion Cracking of High-Strength Steels. Metallurgists at NRL have developed a technique by which the chemical reaction in a propagating stress-corrosion crack can be frozen at any point in its occurrence. This effect is achieved by immersing the fracture specimen in liquid nitrogen. When the specimen is later broken open for examination of the stress-corrosion-crack surface, most of the corroded to be analyzed is still in the place where it occurred. Data obtained thus far for 11 steels representing a wide range of metal compositions have corroborated an earlier NRL finding that stress-corrosion cracking in these materials is a dual process, partly chemical and partly mechanical.

Interfacial Energies in Metals. Metal physicists at NRL, using their own technique of hot gradient electron microscopy, have been able to observe directly the microstructural details of metal-metal interfaces at very high magnification (over 100,000X). Investigations of the surface tension balance, established at a point where a grain boundary surface meets the solid-liquid interface, have produced the first absolute values of the solid-liquid interfacial energy in a metal.

Physical Properties of Incipient Ferromagnets. An intermediate electronic state is that of "incipient ferromagnetism"—a strongly paramagnetic state that exhibits properties somewhere between those of superconductors and ferromagnets. NRL researchers have observed anomalous physical properties that arise from true many-body effects in several binary alloy systems which, over certain ranges of composition, are incipient ferromagnets. Certain temperature dependences have been theoretically explained and related to the strength of electron-

electron interaction. An unusual low-temperature heat capacity, a condition related in theory to enhancement of the effective mass of electronic quasiparticles, also has been observed for these incipient ferromagnets. When these and other fundamental properties are fully elucidated, the potential use of incipient ferromagnets in shipboard devices can be enhanced or their limitations more clearly defined.

Compensation for Thermal Distortion in Glass Lasers. A simple, inexpensive method has been developed to cancel out the thermal distortion produced in glass lasers as a result of optical pumping. It is based on the circulation of water from two reservoirs into the laser cavity. With optimum temperature control of the water and precise timing in firing the laser, the thermal gradient caused by optical pumping can be canceled by the thermal gradient caused by the cooling water. The method is applicable to any glass or crystalline laser system in which improved angular divergence of the beam is desired.

Atmospheric Depolarization of Laser Light. Recent experiments at NRL have indicated that a polarized laser light beam will not be appreciably modulated by the atmosphere. The measurements were made at night through relatively clear air. Those made over a 600-meter path gave negative results, and it was concluded that any atmospheric depolarization present affected less than 10% of the light signal.

Lattice Vibrations and Infrared Absorption in Mixed Linear Chains. Material scientists devised a method for calculating the frequencies and amplitudes of lattice vibrations of disordered crystal systems of the type $A_n B_{m-n} C$ and the infrared absorption associated with them. The method is an extension of one developed here earlier for binary chains. It applies to the analysis of recently measured spectra of mixed crystals, such as cadmium-zinc sulfide and cadmium sulfide-selenide.

Third-Order Nonlinear Reflection Studies. Third-harmonic signals of a neodymium laser reflected from a liquid medium (hexafluoroacetone sesquihydrate with additions of fuchsin red dye) were measured under conditions of phase matching and varying degrees of phase mismatching. The experimental results were found to be in good qualitative agreement with predictions from theory. A theoretical estimate of the phase of the reflected third-harmonic wave for various angles of incidence was developed.

HIGHLIGHTS

and the predicted nonlinear phase shifts may now be confirmed experimentally.

V⁺ Centers in Alkali Halide Crystals. Electron paramagnetic resonance measurements at NRL have corroborated recent optical evidence that the interstitial halogen atom in the simplest ionic solids (e.g., alkali halides) tends to be located adjacent to a substitutional impurity ion. This finding has led to the first detailed description of the structure of the impurity-associated defect center (the so-called V⁺ center) in potassium chloride and constitutes one further step toward the understanding of radiation damage in more complex, and impure, materials.

A Molecular Trap. The crystal and molecular structures of an unusually large organic clathrate, first synthesized by Diani in 1914, have been determined by NRL chemists. This result should facilitate studies of the structure and properties of "guest" molecules that are trapped within the cage-like cavities of organic clathrates.

Mechanism of Action of Dry-Film Lubricants. Surface chemists have developed a new theory which makes it possible to predict the coefficient of friction for any dry-film lubricant on any harder supporting surface. The values thus far are in close agreement with those obtained previously by tedious measurements for a wide variety of lubricants. Thus, in future studies of candidate materials for solid lubricants, one time-consuming series of measurements may be eliminated.

GENERAL SCIENCES AREA

Confinement of Cosmic Rays. Our ignorance of the regions in space where cosmic rays are magnetically trapped and of the duration of this confinement has been partially dispelled by an NRL analysis of information on the "light" cosmic ray elements and by Laboratory calculations of effects of their nuclear fragmentation. The results indicate, but do not yet firmly establish, confinement mainly within the Milky Way disk.

Solar Monitoring. Solar x-rays were monitored continuously during 1968 by a variety of NRL instruments carried by OGO IV, OGO V, OSO IV, and Solrad IX. Within 24 hours after the emissions were recorded aboard Solrad IX, x-ray time histories were compiled for scientific investigation and for

the prediction of radio communication disturbances, solar-induced terrestrial disturbances, and space operation hazards. The recent Apollo VIII spaceflight benefited directly from Solrad-based predictions of the likelihood of solar flare x-ray hazards.

Far Infrared Astronomy. Several point sources of unexpectedly high intensity were observed by long-wavelength (10-30 micron) infrared sensors carried by an NRL rocket. If these sources are normal galaxies, many of them radiate far more energy in the far infrared (thermal region) than they do in the rest of the spectrum. These results have major cosmological implications.

Extreme Ultraviolet Spectroheliograms. Spectroheliograms obtained by NRL rocket-borne instruments have revealed solar features as small as 10 seconds of arc. The spectral resolution was so good that the features formed by Si XI (503.4A) and He II (303.78A) radiation could be distinguished one from another, making it possible, for example, to determine that the coronal emission above the limb of a specific He II image originated entirely from Si XI.

Measurement of Trace Amounts of Carbon and Oxygen on Surfaces. A new technique has been developed at NRL for the determination of trace surface contaminants of carbon and oxygen, and it has been applied to gold samples whose cleanliness was critical to a series of chemical experiments. The sensitivity of the technique is such that as few as 10^{11} atoms per square centimeter (about 10^{-4} atomic layers) of C and 10^{12} atoms per square centimeter (about 10^{-2} atomic layers) of O can be detected.

Neutron Capture. According to the usually accepted theory of neutron capture, the highly excited capture states are so complex that there is little likelihood of regularity in the de-excitation gamma transitions. Recent studies by NRL have tended to contradict this theory by indicating that there is regularity. This regularity, along with an observed preference for particle states over hole states, is suggestive of a direct capture mechanism.

Thermal Blooming of Laser Beams. Thermal blooming, or the continuous lowering of the power density of laser beams owing to the diverging lens effect of the medium traversed, has been an obstacle to the development of high-power lasers for communications, ranging, and similar applications. Interferometric

observations made by NRL scientists of the index-of-refraction changes that arise in thermal blooming have enabled the investigators to correlate spatially and temporally resolved data on the index-of-refraction variation with the observation of thermal blooming. This constitutes an important step toward achievement of the laser applications mentioned above.

Phased Array Radar. NRL has made promising progress in efforts to develop a methodology for taking advantage of the inherent flexibility of a phased array radar (one which continually monitors its own activity and modifies its parameters to achieve nearly optimum performance at all times). In 1968, this progress consisted primarily of the production of a simulation model of the search mode for such a radar.

Information Systems. In its efforts to develop an information system capable of identifying all mobile platforms above, under, and on the world's oceans, NRL has conducted methodological investigations aimed at providing a means for deriving the maximum amount of valid information from the very large number of reports, including incomplete and erroneous ones, expected to be delivered to the system. Several candidate algorithms have been developed which associate multiple reports arising from a common object, and work is continuing in this area. Also, NRL is developing a computer test bed for evaluating candidate methodologies and for determining information needs not presently being satisfied.

Analytic Functions and Their Applications. An especially useful class of entire functions, that of bounded index, has been defined and studied with reference to average size and rate of growth of the functions and their derivatives, their representation by power series, and their distribution of values and zeros. It has been found that functions of this class are necessarily of exponential type, and their partial characterization in terms of the comparative rates of growth of the functions and their derivatives has been accomplished. These and other results obtained have important applications to problems in science and engineering.

OCEANOLOGY AREA

Scale Model Acoustic Studies. A major acoustic testing facility—a well-instrumented tank 22 feet in depth,

30 feet in diameter, and 116,000 gallons in capacity has been constructed at NRL. Associated equipment provides for the rotation of test transducer arrays to obtain complex underwater acoustic patterns. The tank is the first to have the capability of positioning a test device in three coordinates.

Marine Geochemistry of Fluorine. Using an ion-specific electrode, NRL scientists have developed a simple, accurate, and rapid method for analyzing fluorides in seawater. The accuracy of the method has been verified by the comparability of results obtained from measurements of fluoride in seawater samples by both the new method and the well-established photonuclear activation technique. The rapidity of measurement is indicated by a two-minute-per-sample processing time.

Scorpion Search. After six months of searching for the USS *Scorpion* in the Atlantic Ocean, NRL's research ship USNS *Mizar* located the submarine's hull in more than 10,000 feet of water. The principal sensors used were a wide-angle-lens survey camera, a side-looking sonar, and a proton precession magnetometer, which were towed about 30 feet off the bottom. A total of 143,000 ocean-bottom photographs was taken in a 12-square-mile area, 10,000 photographs of portions of *Scorpion's* hull.

Sonar Calibration. A new facility placed in operation at NRL in 1968 permits underwater sound transducers up to 3 feet long and 5 inches in diameter to be calibrated at frequencies ranging from 10 cycles per second to 4 thousand cycles per second, at temperatures ranging from the freezing point of seawater to -40°C , and at simulated ocean depths as great as 22,500 feet. Both absolute and comparison calibrations can be made.

Glass for Deep-Submergence Structures. Despite the well-known fact that the strength of annealed bulk glass is limited by surface flaws, the material is being considered for use in fabricating deep-submergence structures. Measurements made by NRL have established the rates of crack growth as a function of pressure and humidity, thereby providing a means for predicting the times required for small surface cracks to grow to critical size. Selection of the optimum glass composition, however, will require the accumulation of much more data.

ELECTRONICS

An Overview: by Claud E. Cleeton, Associate Director of Research for Electronics

The five divisions that comprise the electronics area of investigation at the Naval Research Laboratory made substantial progress during 1968 in fields highly relevant to Navy needs. In addition, some reorganization in the divisions took place in order to enhance their ability to respond to research and development problems. Since many of this area's achievements for 1968 stem from classified investigations, the reports given here do not provide complete coverage. (For example, accounts of work by the Electronic Warfare Division are almost exclusively classified, so its activities are not covered here.) Nevertheless, the reports included are, in general, representative of progress during 1968.

Research-supporting facilities and capabilities have expanded during the year to keep pace with ever-growing Navy needs. For example, research in electronics was enhanced by the continuously expanding capabilities of the supporting Research Devices Facility. Activity was centered in the important gas-laser field and involved difficult glass-envelope fabrication, optical-window preparation, electrical design, etc. Also during this period, workers at the silicon integrated circuit (microelectronics) facility installed part of the equipment needed to provide a flexible research-oriented service. The mask-preparation center, which is being assembled for use during 1969, includes equipment for precision artwork and high-resolution photoreduction. A photolithographic laboratory, which is now being installed for the precise layout of artwork and for high-resolution photoreduction of solid-state and microelectronics devices, will be in operation during 1969.

The following reorientations were made during the year: the Energy Conversion Branch of the Electronics Division was disestablished, its program in superconducting devices dropped, and its resources applied to strengthening the program in electron physics. An extensive reorganization of the Radar Division was conducted and a new Radar Geophysics Branch created to study basic geophysical phenomena related to the propagation of radar signals, the effects of the Earth environment, and geophysically generated clutter echoes and electrical noise that compete with desired radar signals. The Radio Division was renamed the Communications Sciences Division. In order to bring under each branch of this division the technical activities which logically belong together, the former Radio Navigation Branch was disestablished and its sections reassigned as follows: the former Avigation Section became the Integrated Avionics Systems

Section of the Systems Integration and Instrumentation Branch; the former Ship Systems Section became the Navigational Applications Section of the Electromagnetic Propagation Branch; and the former Submarine Reception Section became the Sub-Surface Antenna Section of the Radio Antenna Branch. The position of Assistant for Command Support was established to improve the division's ability to anticipate future needs of the Navy in the communication sciences and to ensure that the division is kept aware of the constraints implied in some of the long-range planning presently under way.

APPLICATIONS RESEARCH

Hypervelocity Ballistics. NRL's studies of hypervelocity ballistics encompass both the launching technique and the impact phenomena associated with projectile velocities in excess of 10,000 feet per second. Velocities of this magnitude are usually encountered only by vehicles in a space environment. Knowledge of hypervelocity impacts is, therefore, of considerable importance to the potential protection or destruction of satellites and re-entry vehicles.

Projectiles are launched by a two-stage light-gas gun consisting of a compression piston and tube, high-pressure section, and launch tube. Prior to firing, the compression tube is filled with a low-molecular-weight gas, usually hydrogen, until a predetermined pressure is reached. Upon firing, the piston is accelerated down the tube, compressing the hydrogen. This lightweight gas, in turn, accelerates the projectile through the launch tube. A velocity of 35,200 ft/sec has been achieved for a 0.12-gram projectile.

The tests show that the impact phenomena observed in the 15,000- to 30,000-ft/sec velocity range is completely different from that observed at the more common gun velocities of under 5,000 ft/sec. Target craters formed by projectiles traveling at high velocity are shallow and hemispherical, whereas those formed at low velocity are deep and narrow. Also, at hypervelocities, projectiles can be completely destroyed as they perforate thin plates, whereas at low velocities they pass through such plates virtually undamaged.

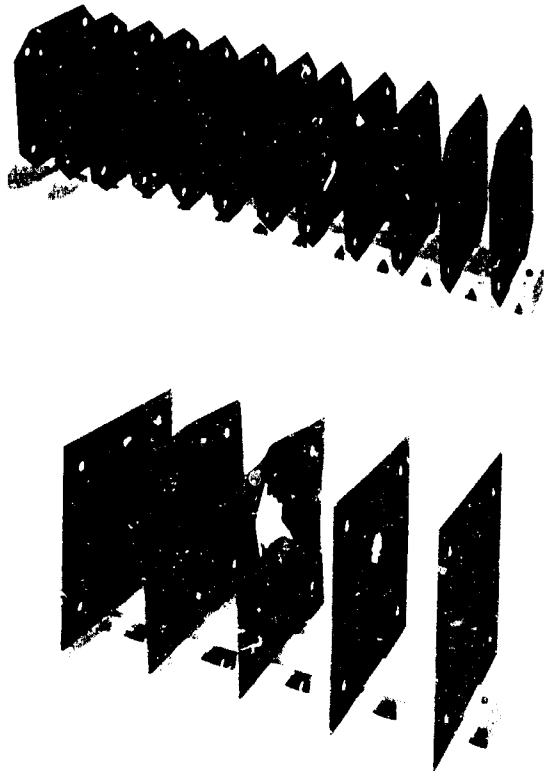
A five-year project undertaken to study the penetrating capability of metal rods impacting metal plates was completed in 1968. It was designed to increase the knowledge of the parameters affecting the pene-



A two-stage light-gas-gun range with a 3.25-inch-diameter compression tube. On the floor in the foreground is the powder casing, and sitting on the breech is a cylindrical aluminum piston. Beyond the compression tube, between the circular flanges, is the high-pressure section, and beyond that is the launch tube. The rest of the range consists of the cylindrical blast tank and the large rectangular target chamber at the rear.

tration of targets. This study has successfully determined the relationship between the length of rod lost as a function of the impact velocity, target-plate thickness, and rod and target materials. It has also established the relationship between these parameters and the diameter of the hole in the target plate.

Three significant firings were observed during the year: (1) a 6-gram steel rod with a length-to-diameter ratio of 15 was launched at a velocity of 15,000 ft/sec; (2) a 2-gram steel cone was launched at 15,200 ft/sec; and (3) a 0.25-gram 1/8-inch-diameter tungsten carbide sphere was launched at 23,400 ft/sec, a velocity which was made possible by a new sabot design involving a fiberglass material. A study of



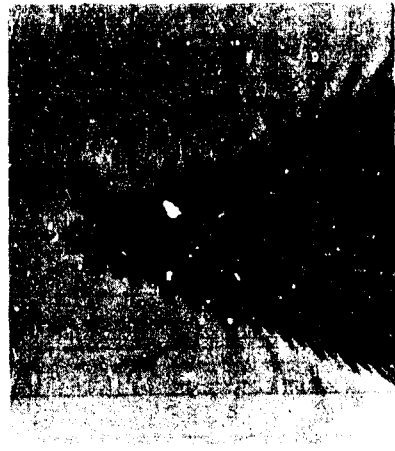
A 1-gram steel sphere impacting at 5,500 feet per second is able to perforate eleven 1/16-inch-thick aluminum plates spaced 4 inches apart (above). The same projectile impacting at 15,000 feet per second, however, is able to perforate only three of the same target plates (below).

spherical projectiles as small as 100 microns in diameter has demonstrated that the impact damage cannot be scaled simply by the projectile diameter, but instead as a function of the projectile size, velocity, mass, and other parameters.

Study results have improved the understanding of hypervelocity impacts, thus aiding the design of protective shields for space vehicles as well as the development of means for intentionally damaging such vehicles.

Kelvin Wake Analysis. A new technique has been developed and used by NRL in its continuing study of the detection and identification of disturbances which are produced in the water by moving objects and which may travel considerable distances before

being dissipated. The Navy is interested in these wave patterns and their characteristics because knowledge of them might lead to the development of a means of detecting wakes for marine traffic surveillance of both surface ships and submarines. An especially interesting set of disturbances is the Kelvin wake, which is a regular train of waves produced on the surface of a body of water by an object moving in the water. The surface disturbances have a definite pattern which can be identified among the general spectrum of surface waves. Although many studies have been made of this phenomenon, some charac-



An example of the Kelvin wake patterns produced by the 230:1-scale model configuration. The model submersible used was operated at a scaled depth and speed corresponding to those used in computing the wake.

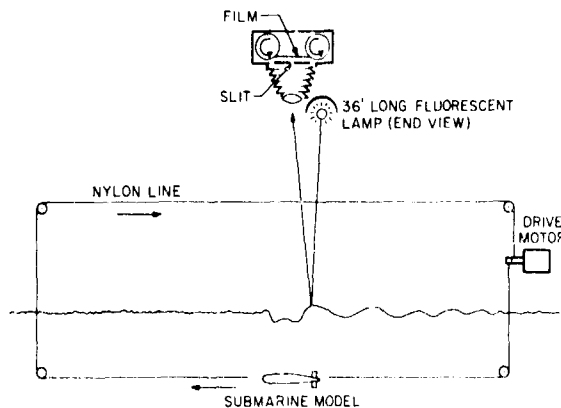


Computer-plotted vertical amplitudes of a Kelvin-type wake. Such wakes are produced on the surface of a body of water by an object moving in the water.

teristics of the wake patterns have not been well defined for a variety of conditions.

Based upon refinements of the Kelvin wake equation, a set of computer-plotted vertical wave amplitudes were converted to intensity patterns in which the light intensity is proportional to the vertical amplitude. The amplitude calculations were made for a submerged Rankine ovoid-type body operating at 20 knots and 75-foot keel depth. Correlation of this representation with a naturally generated wave pattern was made under carefully controlled conditions. A 230:1 scaled model was chosen and tested in the NRL pool. Uniform lighting of the entire wake pattern was achieved by means of a long fluorescent lamp which causes the wake's reflection from the water to fall on the narrow slit of a Sonne strip film camera. When the film is driven at a speed corresponding to the image motion of the scaled model, a recording of the accompanying wake delineating the crest and trough of each wave is produced.

The results of the study have demonstrated the ability to model the effects on wake patterns of variations in speed, depth, size, shape, and such environmental factors as wind and ambient gravity waves. The resulting photographs are being used in the continuing program to guide optical data processing and systems design efforts which will determine the feasibility of tracing vessels by means of Kelvin wakes.

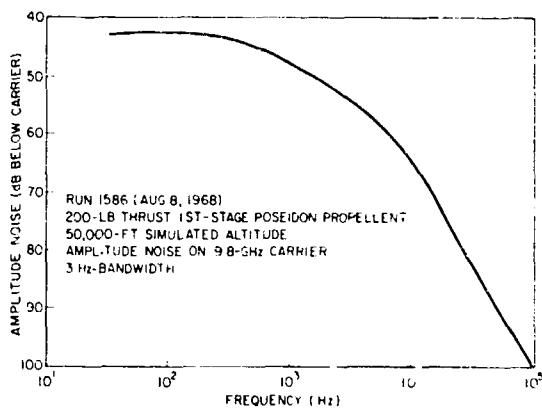


Schematic of the 230:1-scale model configuration chosen to correlate the computer-generated data with naturally generated wave patterns.

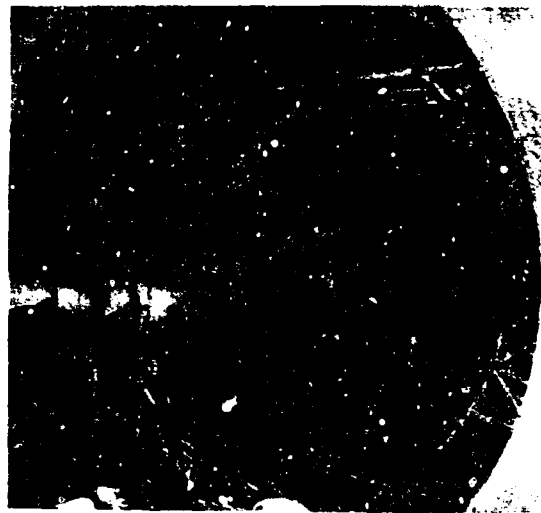
Electromagnetic Propagation Through Gaseous Exhausts. During the year, NRL has performed experiments to measure the effects on electromagnetic propagation of rocket exhausts in a high-altitude environment. These effects are important to the Navy in determining the accuracy and reliability of electromagnetic detection, tracking, and guidance systems when operating with targets that emit gaseous exhausts. The propagation path is distorted by turbulence, particle scatter, and ionization created by the gaseous exhausts. Improved knowledge of the effects of this distortion is needed in system design.

The attenuation and phase-shift measurements made at NRL indicate a definite dependence of these quantities on rocket altitude, propellant type, and electromagnetic frequency. There is also a strong indication that in many cases the received signal consists of the summation of two kinds of signals, namely the one that reaches the receiving antenna after traversing the rocket plume and the one that is guided along the curvature of the plume to the receiving station.

Measurements indicate that the rocket exhaust modulates the transmitted signals in both phase and amplitude. Although the exact shape of the curve varies as the area of the exhaust illuminated by the transmitting antenna is varied, phase modulation curves were found to be generally similar to amplitude modulation curves.



A rocket's exhaust modulates transmitted signals in both phase and amplitude. Shown above is the amplitude noise measured during one simulated 50,000-foot-altitude run. The shape of the curve varies as the region of the exhaust illuminated by the transmitting antenna is varied. Phase modulation curves are similar to amplitude modulation curves.



Measurements are made through the exhaust of a 200-pound-thrust motor burning a Poseidon-type propellant. Two focused-beam systems and one open-horn system (mounted in the ring frame) provide simultaneous data at three microwave frequencies. The motor on the rotating boom (left center) is mounted on a traversing cart to provide both longitudinal and transverse motion during a firing.

Although analysis of the data is not complete, it is already apparent that this research can be used for the evaluation of plume signal interference by various propellant types. For a given type of propellant, electromagnetic frequency, and rocket altitude, predictions can be made of the extent of communications blackouts due to signal attenuation or excessive noise levels. Also, in certain cases, the enhancement of communications due to wave bending around the exhaust plume can be predicted.

The experiments were conducted in the NRL space, altitude, and velocity chamber described in the 1967 *Annual Report*. During the year, instrumentation has been improved to measure phase shift, phase noise, amplitude shift, and amplitude noise. The instrumentation includes an ultraprecision quartz oscillator for phase stabilization of the klystron oscillators and hardening of the antenna horns and transmission lines to avoid acoustical interaction in the exhaust environment. Measurements have been made at 2.2, 9.8, and 24.0 billion cycles per second, both with transmissions across the plume and also at various angles between the plume axis and the line-of-sight path between transmitting and receiving antennas.

Solrad. On March 5, 1968, NRL's Solrad IX satellite, known also as Explorer 37 and 1968-17A, was launched by the National Aeronautics and Space Administration (NASA) from Wallops Island, Virginia, into an orbit inclined 59.4 degrees to the Earth's equator, with an apogee of 476 nautical miles and perigee of 275 nautical miles. At this time, the satellite began its continuous monitoring of bands of solar x-ray and ultraviolet emission, which are obscured from observation at the Earth's surface by absorption in the atmosphere. The information obtained increases the understanding of the physical processes involved in solar activity. This permits the establishment of the x-ray flare characteristics and their relation to radio communications disturbances, the development of techniques for predicting solar-induced terrestrial disturbances, and the estimation of hazards in space environment operations.

When Solrad IX is tracked by the NRL Satellite Tracking and Telemetry Station at Blossom Point, Maryland, the telemetry data are transmitted via telephone lines to NRL in real time. The data acquired as the satellite passes overhead, as well as the stored memory data acquired periodically, are processed at the Data Operations Center and transmitted, in special teletype message format, to all stations of the U.S. Air Force Solar Observation and Forecasting Network. These include activities of the Department of Defense, Environmental Science Services Administration (ESSA), NASA, and other organizations. The Space Disturbance Forecast Center of ESSA in Boulder, Colorado, is a prime user of this information; in addition to messages provided routinely, computer-generated plots displaying 10-14 hours of stored x-ray data are forwarded in facsimile to this activity. Furthermore, predictions of significant solar activity are provided directly to the Naval Communications Command to assist in the promulgation of Fleet radio propagation warnings. During 1968, 14 alerts were sent.

In the closing weeks of the year, NRL was called upon to support the Apollo VIII mission by using Solrad IX information to predict solar activity which might affect the environment through which the Apollo spacecraft traveled. For several days prior to the launch and during the flight, data were furnished as rapidly as possible to the Space Disturbance Forecast Center, which has overall responsibility to NASA for this support of the Apollo program. NRL participated in providing the best possible and most up-to-date space-environment in-

formation for Apollo VIII astronauts, for which it received a commendation from ESSA.

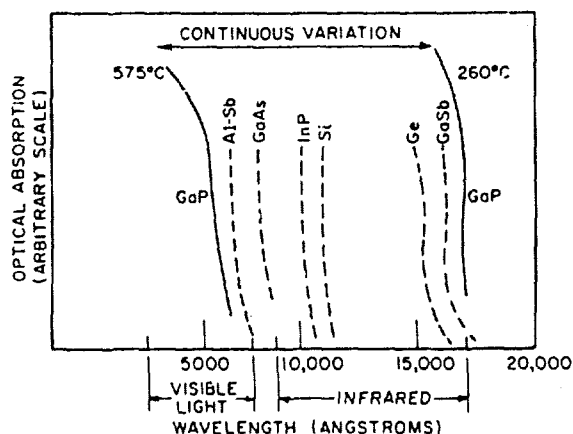
Special data-processing equipment is now under development to replace the majority of manual procedures presently required to provide quick-response processing of both the near real-time and the stored data. To support the Naval Air Systems Command exploratory development tasks in solar monitoring and to formalize objectives within the Laboratory by bringing participating groups together in a cohesive effort, the NRL Solrad project team was established in July 1968. (Prior to 1968, the Solrad monitoring experiment was being carried out cooperatively by personnel of the Space Sciences and the Applications Research Divisions. The formation of the Solrad project team further strengthened this cooperative effort.) Specifically, the project's objectives are to (1) develop, construct, test, evaluate, and provide launch support for Solrad satellites, (2) track, command, and acquire satellite telemetry, and (3) reduce, analyze, and transmit solar-emission data for scientific and application purposes.

ELECTRONICS

Closed Cycle CO₂ Laser. Until recently, CO₂ lasers required a flowing gas and cumbersome mechanical pumps. In 1968, NRL developed a noncirculating sealed-off CO₂ laser and operated it continuously for 1,050 hours without a catalyst at a continuous power level of 20 watts and an efficiency of 7.5 percent. The actual lifetime of the apparatus, which might be considerably more than 1,050 hours, was not determined because the experiment had to be terminated due to lack of facilities and space. The laser tube is 86 centimeters long, has a 1-cm bore, and is equipped with Brewster windows and external mirrors. Increased efficiency would have been obtained if the mirrors had been mounted internally. The tube gas fill was CO₂ and helium. The same efficiency and life could have been obtained with a tube fill of CO₂, He, and N₂, but that would have required that the tube be water cooled for long life because chemical reactions with the N₂ are sensitive to temperature.

The experiment has demonstrated that field-operated CO₂ gas lasers can be developed. Promising areas of application include communications and radar systems which transmit in the 10-micron low-attenuation "window" in the atmosphere.

Controllable Light Transmission Films. A discovery of controllable optical absorption in thin films of gallium phosphide (GaP) has been made at NRL. These films are evaporated onto quartz substrates in a high-vacuum chamber and then subjected to an annealing process at a temperature between 260°C and 575°C. The interesting characteristic of GaP is that different light transmission cutoffs are obtained for different annealing temperatures and that the annealing techniques provide a controllable light



As shown here, the optical absorption characteristics of thin films evaporated on a quartz substrate are dependent on the film annealing temperature. By varying this temperature, the optical characteristics of GaP may be made to span the range of many other semiconducting materials.

transmission cutoff that spans the range of almost all other common solid-state device materials.

An obvious practical application of the technique is in the fabrication of optical filters with different wavelength cutoffs or even variable wavelength cutoffs, all in one material. However, it may turn out that the most useful applications lie elsewhere. The light transmission cutoff characteristic is directly related to the width and nature of the forbidden energy gap in a semiconductor material. The possibility of varying the width of the gap of a single material through wide limits by a simple annealing process provides a powerful tool for the study of this semiconductor material and devices made from it. The next objective will be to study the detailed nature of the absorption band spectrum as a function of the energy gap.

The discovery is a result of NRL's continuing program of studying thin-film and surface phenomena

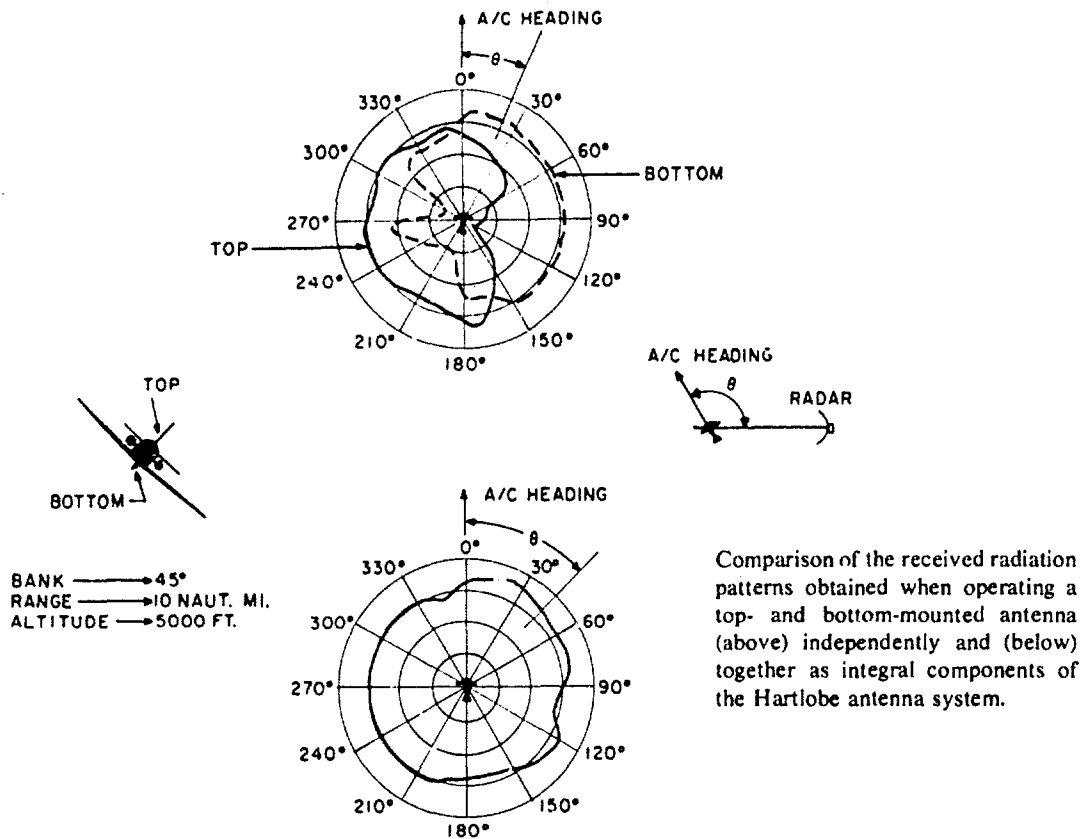
to obtain a better understanding and to improve the performance, efficiency, and reliability of solid-state thin-film devices.

Microwave Shipboard Communications. A means for achieving high reliability of shipboard microwave communications without providing excessive power to overcome fading has been developed. Experiments conducted at 37 billion cycles per second during the past year substantiate the conclusions of an analytical study that antenna diversity techniques are feasible for shipboard line-of-sight communications, especially at the higher frequencies for which the required antenna separation is conveniently small. With this approach, the transmitted signal is received by two or more receiving antennas. When the antennas are displaced in space, the received signals display different fade characteristics. Experimental results obtained in 1968 show that for certain antenna spacings a strong negative correlation exists between the received signals, and by summing the two signals the need for a large amount of excess power is eliminated. Calculations based on this experimental result indicate that the power required to provide a ship-to-ship communication link of a given range and reliability with this diversity system would be about 15 decibels lower (or 30 times less) than with a system having only one antenna.

The implementation of microwave systems for ship-to-ship and ship-to-shore communications will greatly improve the Navy's communications capability because microwaves are less affected by the weather than the shorter wavelengths of optical or infrared systems, and they also provide higher directivity and higher security through limited range than high-frequency systems, which use longer wavelengths.

Spherical Airborne Antenna Coverage. Early in 1968, flight tests were conducted on an engineering model of the NRL-developed Hartlobe antenna system. These tests showed a remarkable improvement in the performance of airborne transponder beacons used for identification of friend or foe (IFF) and air traffic control (ATC) purposes. The Hartlobe antenna system was developed by NRL to solve the long-standing problem of blindspots in airborne antennas due to shielding by the airframe.

Airborne antennas should be omnidirectional in order to satisfy the systems functions of communication, radio navigation, IFF, etc. Flight experiments



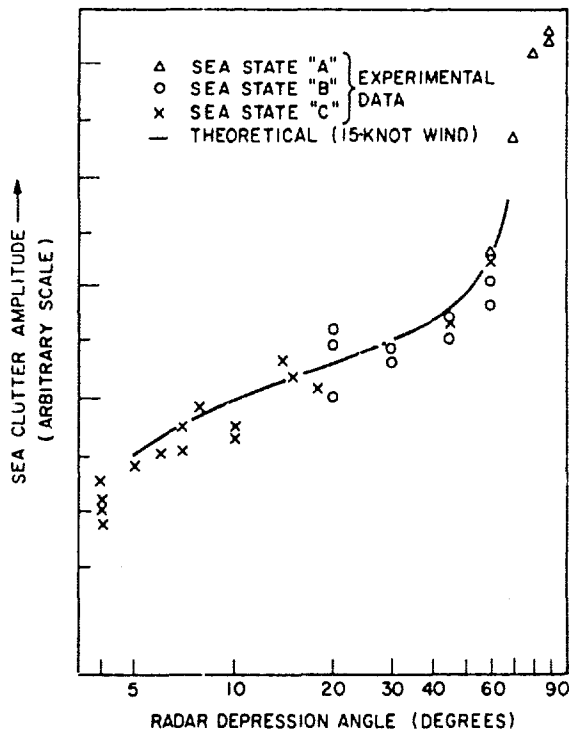
demonstrated that nearly omnidirectional antenna patterns were obtained at various ranges and airplane bank angles. These tests also gave assurance that the overall system performance was in no way compromised. The deep nulls encountered in signal reception when the aircraft employs only one antenna are very nearly eliminated in the Hartlobe pattern. The basic technique, as applied to beacon systems, consists of continuously monitoring the two antenna signals by means of beacon receivers connected to each antenna and of switching each transponder reply to the antenna receiving the stronger signal. Each interrogation is handled on an individual basis by means of pulse-by-pulse comparison.

The significant improvement in airborne spherical antenna coverage of IFF and ATC transponders and its obvious potential contributions to the success of military missions and increased safety have created great interest in the speedy adoption and implementation of the Hartlobe system by all three military services and by the Federal Aviation Agency. Currently, NRL is assisting the Naval Air Systems Command and Program Manager PM-8 (AIMS) in

setting up standards to assure satisfactory operation of this system when it is implemented.

Theory of Radar Sea Clutter. The lack of a good model of electromagnetic backscatter from the sea surface is a major impediment to the improvement of radar performance. By providing a better basic understanding of radar sea clutter caused by wind-generated waves, such a model would aid the radar-system designer.

During the past year, NRL has developed an improved mathematical model of this complex problem and has substantiated it experimentally. In this model, the strongest sources of the backscatter signal are the short surface-water wavelengths which satisfy the first-order Bragg reflection condition given by $2\lambda_w \cos \theta = \lambda_r$, where λ_w is the water wavelength, λ_r is the radar wavelength, and θ is the radar depression angle (angle of incidence). These small water waves are, of course, superimposed on the longer gravity waves and are therefore tilted out of the horizontal. The tilt has a large effect on the



A comparison of experimental data with predicted values of sea clutter amplitudes as a function of radar depression angle, showing how well the NRL mathematical model describes the complex problem of radar sea clutter. The experimental data shown above were obtained at 1,225 million cycles per second (L band).

horizontally polarized and cross polarized cross sections, and this effect is also included in the model.

Development of the model was aided by measurements taken under controlled conditions in laboratory water tanks. Good agreement was obtained between results of the model studies and data collected over open water by a specially instrumented NRL Super Constellation aircraft on vertical polarization at 428, 1,225, 4,450, and 8,910 million cycles per second. Good agreement also was obtained for horizontal polarization at the two lowest frequencies given above. The wavelength dependence and absolute value of the mean squared water-wave height spectra calculated from sea clutter cross sections are in reasonable agreement with oceanographically measured spectra and are consistent with an equilibrium or saturation spectrum for short gravity waves.

Measurements of the doppler spectrum of the backscattered signals from wind-generated waves in a wave tank are being continued to determine the

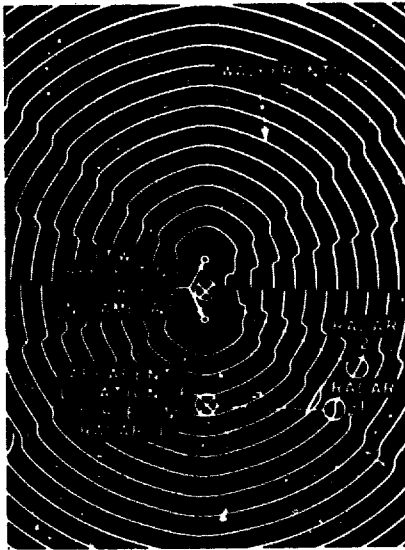
role of higher order scattering and to attempt to relate the properties of the doppler spectrum to the mechanisms of wave generation by the wind. Also, the Super Constellation will continue to be used to obtain more data at smaller angles of incidence and during higher sea states.

RADAR

Radar Target Scintillation. The advancing state-of-the-art in radar techniques has reduced systematic errors in airborne target location and doppler velocity determination to a low level. The major remaining limitation to superior radar performance is target scintillations which cause fluctuating errors in the radar information on the angle, range, and velocity of a target. The target scintillations result from the complex shape of the target as it presents several reflecting surfaces changing in relative position with respect to the radar. This is caused by the target's random yaw, roll, and pitch motions, which occur even when it is flying a "straight line" course. These motions cause the echo signals from the reflecting surfaces to change randomly in relative phase and amplitude. Since a typical radar cannot resolve the surfaces and look at them individually, it will observe a single echo signal composed of the summation of the echoes from the individual reflecting surfaces. This signal will scintillate because of the randomly changing relative phase and amplitude.

Previous analyses of radar target scintillations have shown the results of the scintillations on only specific radar systems. A 1968 NRL theoretical and experimental study of the target echo signal propagating in space has resulted in a new general concept of target scintillations. It is based on the fact that, as the echo signal propagates in space, distortions occur that are independent of specific radar systems. This concept provides a true description of target scintillations and of the relation between different types of target scintillation which are used, for example, to calculate the target doppler scintillation spectrum from data on target angle scintillation and rates of target motion. The concept can be readily applied to determine its effects on any type of radar target locating system, and it can also be applied to show the effectiveness of various diversity techniques and their relative merit for reducing target scintillation effects on radar performance. The theoretical relation between angle scintillation and doppler scintillation revealed by the concept has also been

verified by radar measurements. The theory shows, for example, that the Gaussian-distributed angle scintillation and rates of target motion of a Boeing 707 aircraft are accompanied by a doppler scintillation spectrum having the spike shape of a modified Hankel function. The theoretical spectrum was confirmed in shape and magnitude by high-resolution doppler measurements. This provides a simple means for using known data on aircraft to predict the doppler scintillation and resultant errors caused in doppler velocity measuring systems.

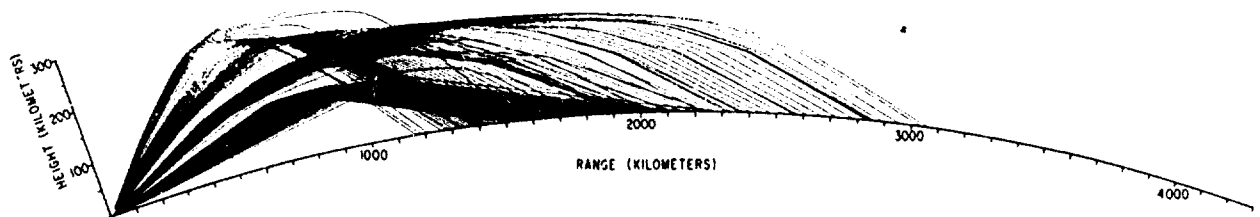


Phase fronts radiating from dual sources having arbitrarily selected equal-amplitude excitation, 180-degree phase difference, and three-wavelength separation. The relative amplitude at each point is inversely proportional to the relative range.

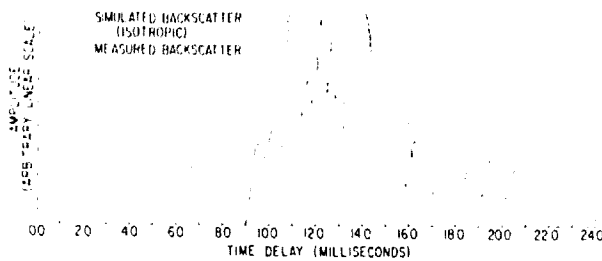
The new concept describes radar target angle scintillation as a distortion of the phase front of the echo signal, which in turn causes fluctuations in the apparent angle of arrival of the echo signal. In the figure, the phase fronts of the combined signal radiating from two point sources having a 180° relative phase are shown as the distortions which cause angle scintillation errors. A diagram of the situation would show that in the high-distortion regions, such as at radar 1, the apparent location of the source (along a direction normal to the phase front) falls far outside the physical area of the target. In a low-distortion region, such as at radar 2, the apparent location seen by the radar falls back within the area of the dual source. An actual aircraft target would cause distortions with random locations and slopes.

Ionospheric Earth-Backscatter Investigations Carried Out by Precision Raytracing. Investigations of the effects of ionospheric phenomena upon high-frequency radar have been made in which diagnostic ionospheric propagation techniques, including precise ionospheric raytracing, are used to predict the detailed distribution of Earth backscatter. In the present stage of these investigations, a computer-assisted program has been developed which enables the user to analyze radar-signal data at single-hop range from the radar site.

By means of a ray profile traced from a measured ionospheric electron density profile and the application of (1) the radar range equation, (2) an expression for ionospheric absorption, and (3) a statistical model for backscattering from rough surfaces, calculations are made to determine the distribution of the Earth-backscatter echo received by a high-frequency radar. This backscatter echo, in terms of power received and power *versus* time delay, is then compared with measured data to verify the accuracy of the backscattering



An example of a ray profile obtained from an actual measured ionospheric electron density profile. Since the density of the rays in the vertical plane is proportional to the radiated power in the direction of the rays, a graphic representation of the vertical-plane antenna pattern is obtained. Both E- and F-layer contributions are evident at all ranges shown.



An example of a verification of the close agreement of the calculated (simulated) Earth-backscatter echo distribution and the measured distribution in regard to (a) time-delay to the leading edge, (b) positions in time-delay of the two major peaks, (c) position of the pronounced null at 13 milliseconds, and (d) general shape and position of the tails of the distribution. Some of the discrepancies between the curves are attributed to the omission in the calculations of consideration of the variations in angles of incidence between the Earth and intersecting rays. The effects of this variation are now being incorporated in the calculation procedures and are expected to produce even closer correlations.

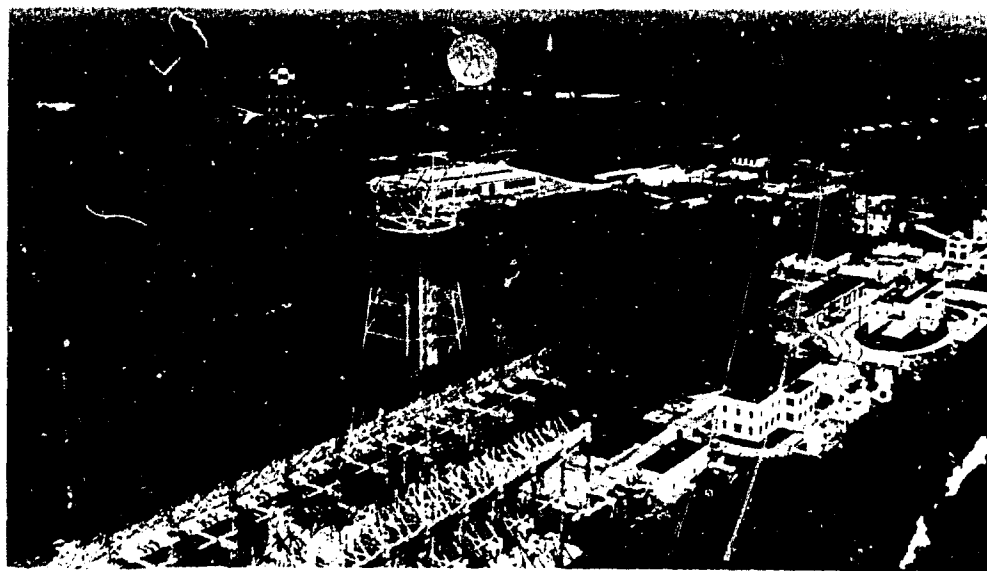
model and the measured electron density profile. When this is verified, the ray profile represents a description of transmitted power density within the volume illuminated.

These ionospheric raytracing and Earth-backscatter profile matching techniques have been used

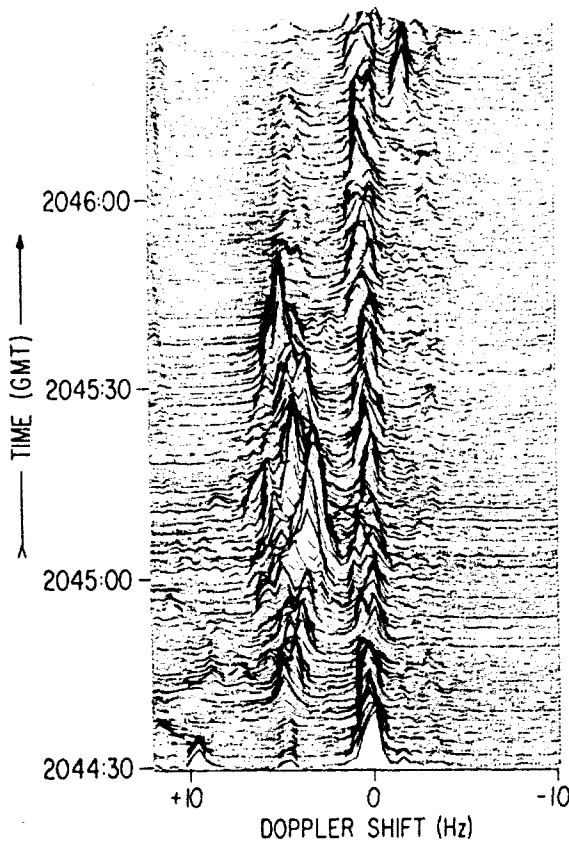
to investigate (1) the Earth's behavior as a scatter of decameter radiation at shallow incidence and (2) short-term evolutions of the ionospheric propagation path as represented by traveling disturbances and hydrodynamic-like gravity wave effects.

Dynamic Behavior of the Ionosphere as Determined by Radar Observations of Artificial Plasma Clouds.

The occasionally violent turbulence which characterizes the lower ionosphere, and which has gradually become accepted as an important influence in the creation and dissipation of sporadic-E layers, has been studied for many years by optical tracking of chemical clouds injected by rockets or gun-launched projectiles. Now NRL is making use of a sophisticated coherent pulse-doppler research radar having the appropriate frequency range and adequate signal-processing capability to probe the internal motions of these clouds and thus describe the turbulence in detail. The evolution of cesium- and barium-seeded artificial plasma clouds in the lower ionosphere is studied to determine statistical descriptions of the amplitudes, duration, and relative velocities of turbulent regions within the clouds. It should be understood that the techniques used are equally applicable to the study of turbulence, wind motion, and plasma resonance phenomena in the normal ionosphere as well, and such studies are proceeding. In this continuing program, a detailed description will be made



NRL's research radar installation on Chesapeake Bay, Maryland. The high-frequency radar is in the left foreground.



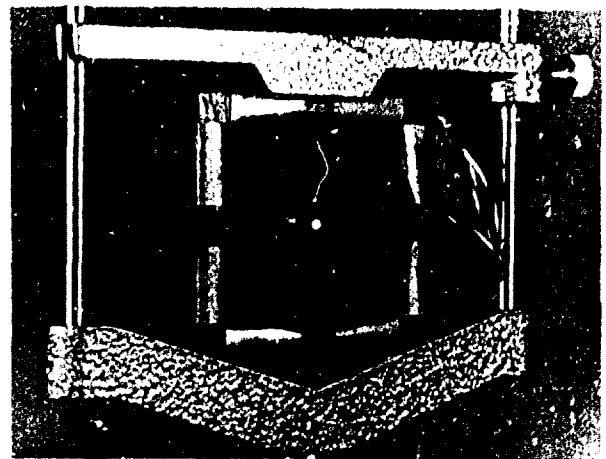
An example of the high-frequency radar data observed from a typical cesium-cloud release. The format in this figure is quasi-three-dimensional, displaying time, doppler shift, and signal amplitude. The irregular vertical band at zero doppler shift, which appears along the entire 2-minute display, represents an Earth-backscatter echo. The briefer, more diffuse signature, which appears centered on 4 cycles per second in the lower two-thirds of the figure, represents the cesium-cloud echo. Its irregular amplitude, which characterizes the turbulent motion, is illustrated by a few high, spectral-appearing peaks and by several lesser amplitude echoes distributed over about 1 minute in time and 4 cycles per second in doppler shift.

of the turbulence spectrum displayed by ionospheric fluid motions over a range of eddy sizes from 10 to 100 meters, a range which cannot be studied optically. This program promises to provide a missing link in describing the lower inertial and dissipation ranges of the turbulence spectrum of the lower ionosphere.

22 **Frequency Translation of Laser Radar Signals.** The development of laser radars faces the significant

problem of handling very large doppler (i.e., frequency) shifts which arise because of the very short wavelengths involved. Laser frequency shifts from hundreds (e.g., supersonic aircraft) to thousands (e.g., orbiting satellites) of megacycles may be encountered. In the presence of large doppler shifts in echo signals, some provision must be made for tuning either the laser transmitter or the reference signal at the receiver so as to maintain the difference frequency constant within the intermediate-frequency amplifier passband. Generally, the lasers used for this purpose cannot, in themselves, be tuned rapidly the required amount, so some other method of frequency shifting must be provided.

One possible solution to this problem has been demonstrated preliminarily at NRL in recent experiments in which optical frequency translation was achieved in the near-infrared by means of rotating magneto-optic birefringence in single-crystal yttrium iron garnet (YIG). Although visibly opaque, the ferrimagnetic material is transparent in the infrared. In the experiment, a circularly polarized infrared laser operated at 1.15 micrometers (11,500 angstroms) was beamed axially through a small rod of YIG which had been made optically birefringent by a transverse magnetic field. When the magnetic field is electrically rotated about the axis of the beam, a frequency splitting occurs in the transmitted signal, and the output then theoretically consists of a carrier component and a single sideband. The latter is the desired frequency-shifted component. If required, the carrier



Apparatus used to achieve optical frequency translation of laser light beams. The birefringent single-crystal YIG rod is the light dot in the center of the field coil assembly (the four dark areas around the YIG).

component can be virtually eliminated by optimizing the birefringence to 180 degrees. For experimental convenience, the magnetic field was rotated at 200 cycles per second to obtain a 400-cycle-per-second optical shift, which could be observed with an audio spectrum analyzer. Improved performance is expected from new variants of YIG, and these should prove suitable for achieving the very much larger frequency shifts required by laser radars.

A High-Performance Analogue Processor for Long-Range High-Frequency Radar. NRL has developed and is implementing a new, real-time signal- and data-processing system for use with its over-the-horizon high-frequency research radar facility located at its Chesapeake Bay Division. This system provides a theoretical maximum signal-to-noise ratio improvement and full processing gain and resolution for accelerating targets as well as constant-velocity targets. With precise signal matching and new signal spectral compression techniques, the detection and measurement of signals buried deeply in noise will be feasible, and the maximum possible radar sensitivity will be provided. A simple and direct analog implementation of the signal-processing system has been chosen as the most efficient and effective approach to the problem. Less electronic hardware is required and higher data rates are achievable without the paralleling of equipment in this system as compared with a system using digital techniques. Highly sophisticated signal-processing techniques are being used to control and minimize the undesired effects of clutter and interference.

When implemented, this processor will be the only one in existence providing all of the capabilities mentioned above. Its high resolution in both acceleration and velocity will greatly aid the identification of targets and permit an immediate separation of aircraft and missile targets. Present high-frequency radar signal processors, which have signal dynamic ranges from 30 to 60 decibels, are frequently disabled by interference that saturates signal channels and blocks target detections. The NRL system, which provides significantly higher dynamic ranges, will alleviate this problem.

An interim system developed by NRL was implemented in 1968. An improved model being developed from NRL specifications prepared in 1968 will be implemented during the coming year, providing a significant increase in the detection and identification capability of long-range high-frequency radars.

Radar Detection of Nonfluctuating Targets in Log-Normal and Contaminated-Normal Clutter. The accuracy with which the capabilities of radars can be predicted in terms of probability of target detection for given acceptable false-alarm rates under various sea conditions is important to the radar designer. In making these predictions in the past, the Rayleigh distribution has been assumed for describing the sea-clutter cross section. Previous sea-clutter measurements made by NRL by means of a high-resolution X-band radar with a 20-nanosecond pulse showed that the clutter cross section described by the Rayleigh model did not fit the measured data. Two studies completed at NRL during 1968 showed that the log-normal and noncoherent contaminated-normal distributions provide a much better fit to measured data and thus more accurate predictions of radar performance with respect to sea clutter.

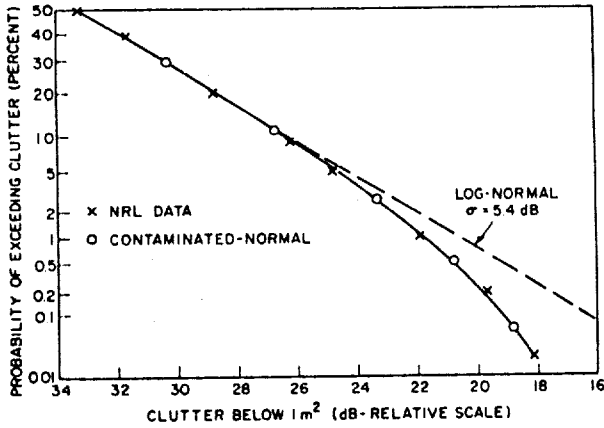
Measured and predicted results were compared for both a smooth and a moderate sea. It was found that the log-normal model provides a fair fit to the data for both sea states, but the tail of the distribution is still too long. The noncoherent contaminated-normal model provides a very good fit to the data for a smooth sea and a fair fit for a moderate sea, in both cases having a shorter tail than that of the log-normal model.

The probability of detection for a steady signal in log-normal clutter was computed, and families of detection probability curves *versus* signal-to-noise ratio (S/N) were plotted for false-alarm probabilities ranging from 10^{-2} to 10^{-6} and for the sum of N noncoherent pulses, N ranging from 1 to 30. For a sea state 2 and $N=30$, these curves showed that a S/N of some 8.8 decibels per pulse would be required for 90-percent probability of detection and a 10^{-6} false-alarm probability. The usually assumed Rayleigh model for sea clutter would require only 1.9 dB under the same assumptions of detectability. This is a significant difference because the wrong choice of model could lead to serious errors in prediction of radar performance.

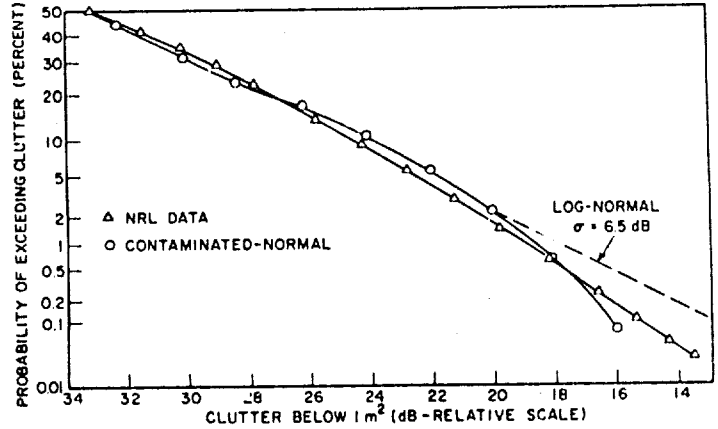
The coherent contaminated-normal distribution is given by

$$p(x) = \frac{(1-\gamma)}{\sqrt{2\pi\sigma^2}} e^{-x^2/2\sigma^2} + \frac{\gamma}{\sqrt{2\pi K^2\sigma^2}} e^{-x^2/2K^2\sigma^2}$$

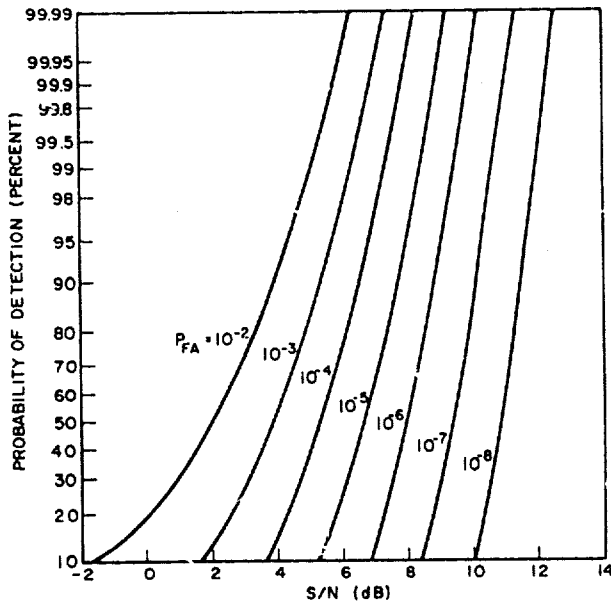
where γ is the contamination fraction, K is the ratio of standard deviations, and the noncoherent distribution is found by passing $p(x)$ through a voltage envelope detector. In the contaminated-normal



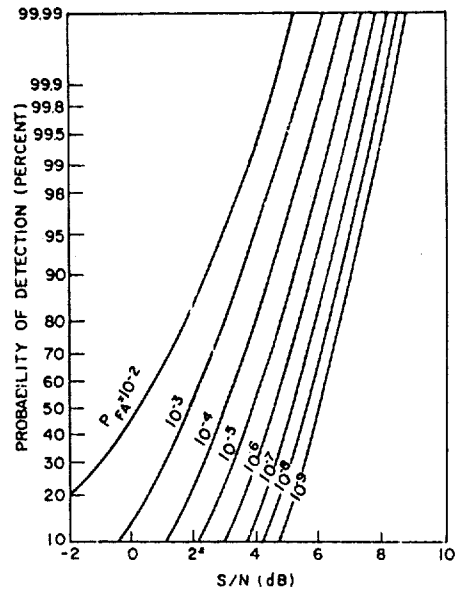
Comparison of NRL experimental data obtained from a smooth sea with a log-normal distribution ($\sigma = 5.4$ decibels) and with a contaminated-normal distribution ($\gamma = 0.25$ and $K = 2.25$).



Comparison of NRL experimental data obtained from a moderate sea with a log-normal distribution ($\sigma = 6.5$ decibels) and with a contaminated-normal distribution ($\gamma = 0.25$ and $K = 3.5$).



Probability of detection versus S/N according to the log-normal clutter model for probability of false alarm ranging from 10^{-2} to 10^{-8} and with $\sigma = 6$ decibels and number (N) of pulses integrated = 30.



Probability of detection versus S/N using the contaminated-normal clutter model with $\gamma = 0.25$ and $K = 2.25$. (smooth sea) for probability of false alarm from 10^{-2} to 10^{-8} and number (N) of pulses integrated = 30.

distribution investigation, the smooth sea was fitted by choosing $\gamma=0.25$ and $K=2.25$; the moderate sea was fitted by choosing $\gamma=0.25$ and $K=3.5$. Again, as in the log-normal case, expressions for the probabilities of false alarm and detection were developed for the noncoherent sum of N pulses by use of the characteristic function method.

Finally, probability-of-detection curves were plotted for the same parameters as used in the log-normal study. These curves showed that a S/N of 5.8 dB per pulse is required to obtain a 90-percent

probability of detection and a 10^{-6} false-alarm probability as opposed to the 8.8 dB and 1.9 dB required by the log-normal and Rayleigh distributions, respectively.

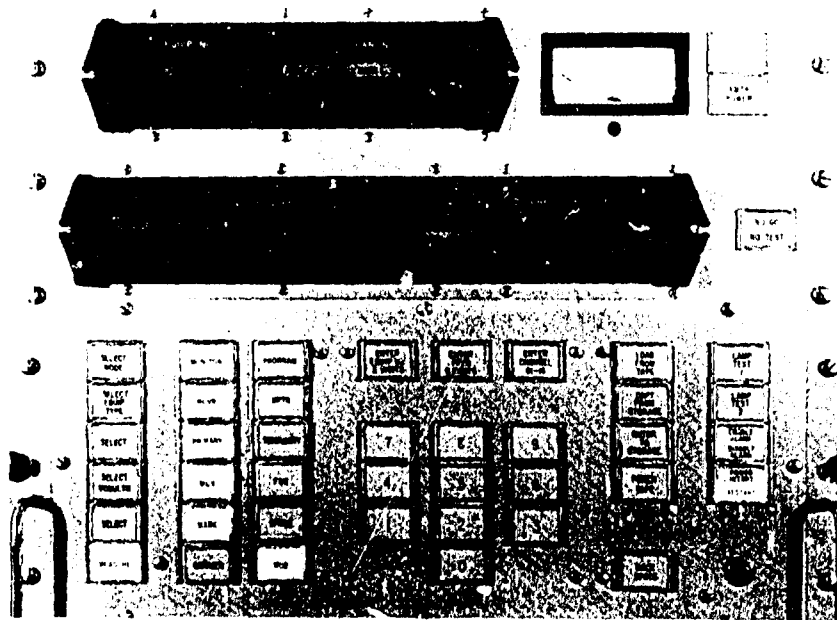
The use of log-normal and noncoherent contaminated-normal probability distribution models should be of interest to radar designers concerned with the sea states considered in the studies. Investigations in this continuing NRL program of other sea states await the completion of additional sea-clutter measurements now being made.

COMMUNICATIONS SCIENCES

Centralized Electronic Control. NRL has developed an on-line, nondisruptive, fast-acting frequency monitoring system (FMS) planned for installation aboard the USS *Nimitz* (CVAN-68). The FMS measures the frequency tuning accuracy of 35 high-frequency receivers and the output frequency of 16 high-frequency transmitters, including the frequency shift keyed (FSK) mark and space frequency components, and displays the resulting information on an

operator's control panel. The FMS will also be used to monitor relative transmitter output power, receiver operating sensitivity, and relative FSK channel levels.

The measurement technique utilized in the FMS was conceived and developed at NRL, and during the past year the system was fabricated under contract in accordance with NRL specifications and then evaluated by the Laboratory. The FMS will be installed as part of the facilities control console of the CVAN-68, where it will use frequency information provided by the central time and frequency facility



Frequency-monitoring system developed by NRL for future use on the CVAN-68. This system, which provides semiautomated monitoring capability for approximately 50 communications equipments, requires only minimum skill, judgment, and training on the part of the operator.

to be installed aboard that ship according to the plans described in the 1967 *Annual Report*. The system should increase enormously the reliability of naval communications.

The CEC research model has been expanded to include application of the basic element of time and frequency control to a simulated radar system. Preliminary studies show that some advantages include reduction of radial interference between two or more radars, as observed on the operator's planned position indicator, improved performance in a spot jamming environment through rapid frequency shifts, and positive control of radar transmissions in order to provide the capability for time sharing the frequency spectrum. The results of this study show that strong considerations should be given to taking advantage of the central frequency and time control element of CEC to increase the compatibility of existing and future radar systems.

Frequency and Time Instrumentation. A continuing NRL program is devoted to meeting an important and rapidly increasing Navy need of precision time and frequency. Instrumentation and techniques are developed for establishing, disseminating, controlling, and utilizing precision time and frequency. During the past year, NRL developed a central time and frequency system for installation aboard the USS *Nimitz* (CVAN-68), following its plans as described in the 1967 *Annual Report*. This system will function as a precise time and frequency reference facility serving a number of areas and systems aboard the ship. It will supply time codes continuously to remote units for display and reference and will provide standard frequency for disciplined devices requiring a high degree of precision and accuracy. Although the system as presently designed applies state-of-the-art techniques and equipments, it is amenable to future upgrading as improved components are developed. At present, it employs crystal oscillators which have frequency drift rates of several parts in 10^{10} per day. When the need arises, these may be replaced easily with cesium-beam frequency standards capable of maintaining the frequency to within 1 part in 10^{11} . Methods are provided for rating the oscillators against the Navy very-low-frequency (vlf) system and for setting the time from the Navy time signal transmissions or from radio station WWV. Great emphasis has been placed on providing high reliability, and strict guarantees have been built into the equipment to

prevent lapses in operation due to either power failures or system component failures.

In 1968, NRL assisted the Navy Electronic Systems and Ship Systems Commands by providing techniques for updating the performance of existing shipboard measurement equipment. An interface servosystem was developed by which the frequency of the shipboard signal generators could be controlled by a frequency counter. This increased the frequency stability and setting capability of the instrument from 10^5 to 10^7 , making it compatible with new synthesizer-controlled communication systems.

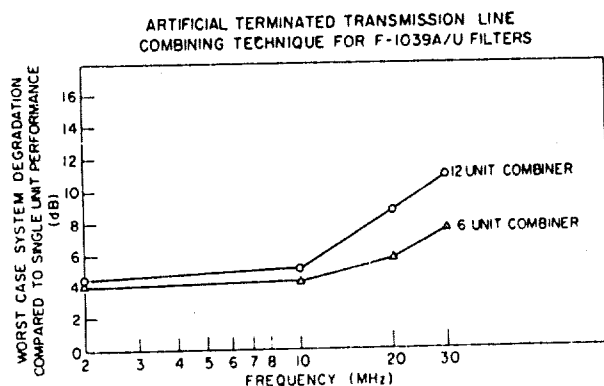
As a result of efforts begun in 1967, NRL has provided frequency monitoring equipment for many of the Navy's major ships. The installation of this equipment has resulted in a dramatic improvement in the adherence to assigned frequencies by Fleet units.

In 1968, NRL completed the installation of atomic frequency standards at all Navy vlf transmission stations. These provide frequency control to several parts in 10^{12} . NRL has made preliminary design plans of a system for the control of the frequency/time aspects of Navy communication stations from a single time and frequency reference within each station.

Antenna Multicoupling. The typical Navy shipboard environment imposes severe restrictions on the number of usable sites available for communication antennas which must serve numerous receivers aboard a ship. In order to take maximum advantage of available antennas, multicoupling techniques have been developed that permit individual antennas to be shared by many receivers and transmitters.

Commercially available F-1039A/U bandpass filters have been used to provide the preselector function between the antenna and radio receiver. During 1968, NRL investigated the possibility of combining large numbers of these filters to operate from single antennas over the 2-30-million-cycles-per-second (MHz) frequency range. Success of this endeavor would permit the Navy to implement available filters to ease antenna problems on existing ships. However, it was found that no more than three F-1039A/U filters in their original form could be operated from one antenna over the high-frequency range without encountering resonances that create unacceptable attenuation of incoming signals.

In order to permit more than three filters to be operated from one antenna, a new combining technique was designed by NRL in which the input



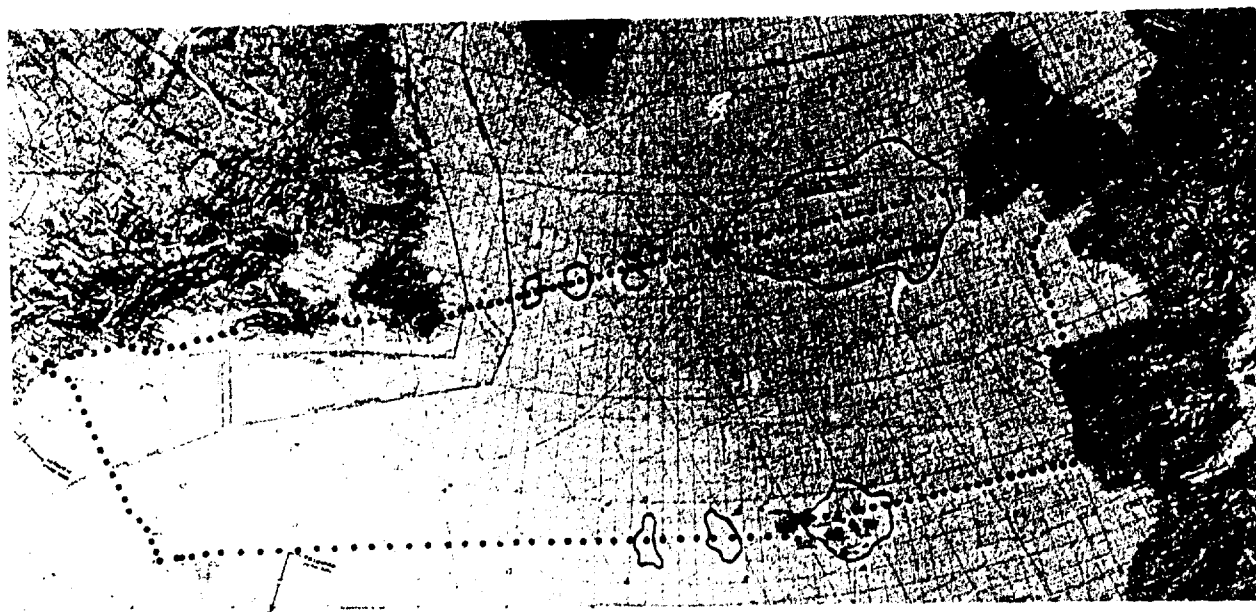
By properly modifying the input circuitry for commercially available bandpass filters, a group of such filters may be series-connected to a communication antenna to permit it to be shared by many receivers and transmitters. The theoretical system degradation for this type of combining (multicoupling) technique is shown for 6- and 12-unit systems.

circuitry of each filter simulates a section of 50-ohm transmission line. A group of filters, as modified, can then be connected in series between the antenna and a 50-ohm termination. The theoretical system degradation for this type of combining technique, as compared to single unit performance, is 3.5 decibels. This could be achieved only if the input impedance

characteristics of each filter are perfectly compensated and result in an insertion voltage-standing-wave ratio (VSWR) of unity. In laboratory tests, this goal is closely approached up to 10 MHz. Between 10 MHz and 30 MHz somewhat poorer performance is achieved because of a rising insertion VSWR characteristic. This technique provides the Navy with a means for implementing available receiving multicouplers on existing ships to enable the use of fewer antennas for a given number of receivers.

Flight Tests of the NRL Mark III Omega Aircraft Receiver. On September 6, 1968, the Deputy Secretary of Defense signed a Program Change Directive approving implementation of the Omega navigation system on a worldwide basis. Omega is a very-low-frequency radio navigation system that can be used by aircraft, surface ships, or submarines.

The significant contribution of the NRL-developed Mark III Omega receiver to this worldwide navigation system was demonstrated conclusively during an 8,000-mile transatlantic flight test in October 1968. With observers from the Federal Aviation Agency, the Omega Project Office, the Naval Air Systems Command (NASC), and the U.S. Coast Guard aboard, an NRL aircraft flew the following



Flight route for testing the NRL-developed Mark III Omega aircraft receiver.

ELECTRONICS

flight legs with the Mark III as the primary navigation system: (1) Naval Air Station, Patuxent River, Maryland, to Argentia, Newfoundland; (2) Argentia to Mildenhall, England; (3) Mildenhall to Madrid, Spain; (4) Madrid to the Azores; (5) the Azores to Bermuda; and (6) Bermuda back to Patuxent River. The system provided instantaneous readings of latitude and longitude during the entire flight.

The four Omega transmitting stations used during these flights are located at Bratland, Norway; Port of Spain, Trinidad; Haiku, Hawaii; and Forestport, New York. The flying time was reasonably well distributed between day and night and included sunrise and sunset periods at all transmitting stations and at the aircraft. Comparisons between Mark III position fixes and shore-based point-source systems' position fixes made at first contact and extreme range are shown in the table.

Except in some areas where the Bratland signal was used, the accuracy was about as expected. On a demonstration flight in England for Royal Air Force personnel, all fixes made on the basis of the Bratland signal indicated an offset of about 4 miles at about 120 degrees. This, of course, can be remedied by a propagation correction.

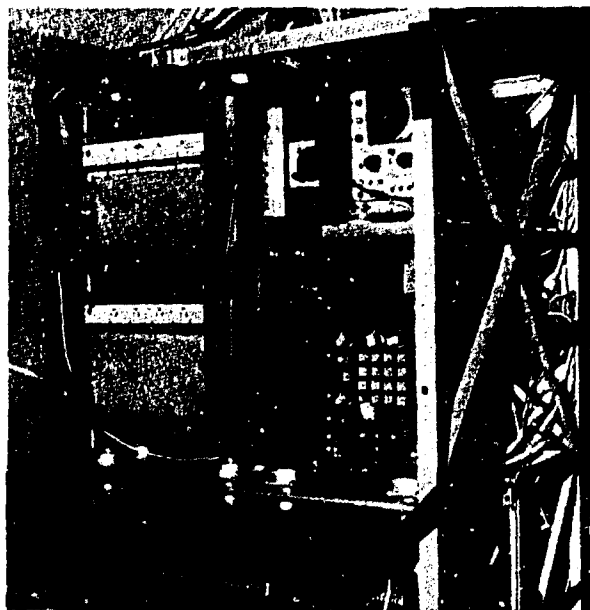
During the six overwater legs of the flight, Omega demonstrated an outstanding capability to tie into shore-based radio facilities. The average deviation from VOR-DME-TACAN (see table) was 1.4 nautical miles in distance and 1 degree in bearing. The reliability of the Mark III under adverse weather conditions was demonstrated vividly when at least three Omega signals were tracked over the entire trip without signal loss. On the flight leg from Argentia to Mildenhall, all Loran A, Loran C, and communications signals were obliterated for about three consecutive hours by severe rains and icing conditions, but the Omega signals were unaffected. The Mark III consistently tracked through the precipitation static, and on arriving within range of the short-range VOR-DME system at Shannon, Ireland, indicated a position difference of 3 nautical miles in range and 3 degrees in bearing.

Throughout the overwater flights, an Omega-actuated course deviation indicator (CDI) was used to provide steering directions to the pilots. The CDI displayed at all times the deviation from great-circle routes. Similar signals could have been coupled to the autopilot.

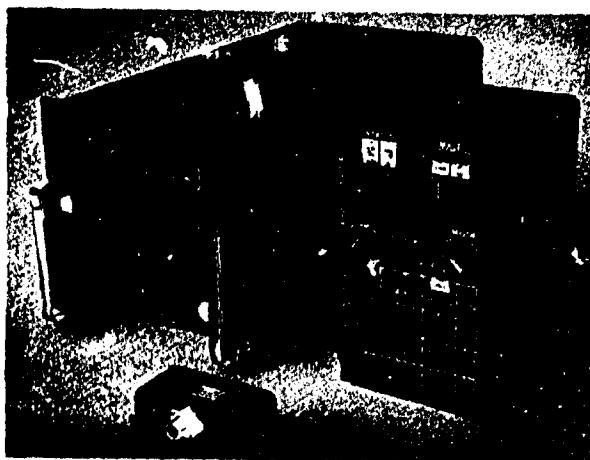
Additional flights across the United States and the Pacific Ocean to Hawaii and in the Caribbean area

with Army and Air Force observers aboard provided similarly satisfactory results.

The Mark III is the third in a series of Omega aircraft-receiver equipment designed and developed by NRL. It consists of an NRL-developed receiver section and a navigation computer designed and developed under an NRL contract.



Mark III installation in NRL's EC 121-K aircraft.



AN/ARN-99 (XN-L) Omega Navigation Set. This set includes a receiver-computer unit, control-indicator, and antenna-coupler unit. It is designed for use in any low- or high-performance aircraft and will operate with either an orthogonal loop or omnidirectional antenna.

Aircraft Approaching	After a Flight Length of		Omega Distance and Heading Difference vs TACAN or VOR and DME*		Distance from Destination
	Nautical Miles	Hours	Nautical Miles	Degrees	Nautical Miles
Argentina	1,200	6	1.4	0	72
Shannon	1,700	10	3.0	3	45
Madrid	500	2.5	†	0	†
Azores	1,000	5	0.75	0	128
Bermuda	1,800	9	2.5	3	132
Patuxent	600	3	0.25	1	76

*The acronyms TACAN, VOR, and DME stand for Tactical Air Navigation, Very High Frequency Omnitrange, and Distance Measuring Equipment, respectively.

†No distance measurement.

The receiver includes antenna couplers for loop and blade antennas, filters to eliminate adjacent channel interference, limiters to suppress impulse noise and provide constant output amplitude from the receiver, conversion of the signal frequencies to an intermediate frequency that is convenient for the computer, and timing circuits to produce gating waveforms which identify the incoming Omega signals to the computer. The receiver controller contains facilities for synchronization of the receiver timer with the incoming signals and for testing the receiver performance.

The computer processes the phase information contained in the signals to provide data useful for navigation, and it puts out such information as the present position in latitude and longitude, the distance and bearing to a destination, and the cross-track error (which can be coupled to an autopilot). Magnetic variations and phase corrections for a given time and location are manually inserted into the computer via a keyboard.

A prototype computerized Omega aircraft receiver (having a volume of less than 1 cubic foot and a weight of 45 pounds) will be delivered to NASC in the first quarter of 1969, and flight tests of the receiver are scheduled to begin in the second quarter of that year.

Very-Low-Frequency Propagation (Navigation). Studies were conducted by NRL during 1968 to determine the effects of multimode vlf propagation on the accuracy of the Omega navigation system.

With the use of instrumented naval aircraft, the phase variations were determined as a function of distance from an Omega transmitter. The investigations showed that the effects of multimode propagation were negligible during the daytime, but that they resulted in a nonlinear variation of phase with distance from the transmitter at nighttime. These data are now being studied so that a model can be developed to compute propagation correction factors necessary for the operational use of the system.

Very-Low-Frequency Propagation (Communications). NRL's propagation research program at very low frequencies (vlf) for 1968 has been devoted to a continuation of the data-collection effort started in 1967 employing special transmissions from the new vlf transmitting station NWC at Northwest Cape, Australia. Phase and amplitude information was recorded continuously at sites in Japan, Madagascar, Bahrain Island, the Philippine Islands, and Alaska. The information collected will be used by NRL in a statistical analysis to be performed during 1969. This analysis will permit further refinements in the vlf communications coverage prediction model.

The prediction model is largely empirical and is being updated continuously, as additional data on signal field strengths received in various geographic areas is made available, to provide the high confidence level required of effective coverage predictions for use in communication-systems design. A computer program has been developed by which worldwide contour maps of vlf communications reliability can be generated automatically from the recorded data.

MATERIALS

An Overview: by James H. Schulman, Associate Director of Research for Materials

The structures and properties of a wide range of materials, from individual pure compounds to complex aggregates of matter, are obviously the principal research interests of the divisions and special laboratories which comprise the materials area. Through an understanding of the effects of structure and composition on properties, the NRL researchers hope to learn how to tailor-make desirable new materials and to improve the mechanical, electrical, magnetic, optical, and thermal behavior of existing technologically important materials.

The term "materials," however, does not encompass the complete range of interest or motivation of the area. The research personnel are not exclusively "materials"-oriented; they are strongly phenomenon-oriented as well. For example, growth of special types of crystals is motivated by an intensive program of research on nonlinear optical phenomena wherein these crystals are used for frequency multiplication of laser light. Activity in nonlinear optics, in turn, is one of the more recent aspects of NRL's long history of investigations of luminescence phenomena in solids, which paved the way for the Laboratory's earliest researches on crystal and glass lasers. The concern with phenomena has carried NRL's materials scientists and engineers into many other areas not normally connected with materials research per se: for example, life support systems in closed spaces, such as submarines and the Sealab; fire suppression research; research on the mechanism of drag reduction by chemical additions to liquids in turbulent flow; night viewing devices; transient radiation effects in electronically active solids; and devices and systems for detecting electro-magnetic and corpuscular radiation, from the far infrared to gamma rays and high energy particles. The concern with phenomena as well as materials has fostered an interdisciplinary approach, albeit one which is based firmly on the fundamental disciplines of physics, chemistry, and metallurgy.

At the heart of a great deal of science and technology lie the problems of materials preparation, analysis, and characterization. The allusion is an appropriate one; like the operation of the heart, these important functions are often taken for granted and sadly neglected, with serious consequences. The NRL materials community is well aware of the vital importance of dealing with substances having either a quantitatively known high purity or a pre-determined impurity "doping," as well as known structures at the molecular and microscopic level. To obtain materials of this type, a variety of pre-

parative, analytical, and characterization facilities have been assembled over the years in the Chemistry, Metallurgy, and Solid State Divisions. Expertise has grown in special methods of crystal growth, microchemical methods, and compositional and structural analysis by various forms of spectroscopy. In order to promote the growth of these facilities and techniques and to make them more available to the entire Laboratory, a Central Materials Research Staff was formed during the past year. Besides undertaking to perform cooperative research in crystal growth and other necessary research in materials, this small group will initially attempt to coordinate the various facilities and skills that exist in the materials area and insure their maximum utilization. Attention to these basic materials problems will very likely be a continuing and ever-increasing necessity as the need grows for purer, larger, and more nearly perfect crystals as well as for increased sensitivity and accuracy in trace-impurity analysis and in the determination of stoichiometry.

The past year saw the beginning of the "decompression" of materials area research personnel. The move by the Space Science Division into its new quarters released urgently needed laboratory and office space to the Metallurgy and Solid State Divisions. The Laboratory's growing optics effort, now concentrated principally in the Solid State Division, benefited particularly from this long-awaited development. Without question, however, the major event of the year with respect to laboratory facilities was the ground-breaking for the new chemistry building, which is scheduled for completion in mid-1970. This will be a four-story structure of more than 140,000 square feet gross space provided with numerous specially designed features.

During the past year, materials area scientists were involved in a number of new cooperative activities of special interest. One of these is the Magnetic Materials Application Forum, which brings together scientists and engineers from the entire Laboratory to deal with current problems in the light of recent advances in the field. The charter of this group is similar to those of the NRL Laser Council and the Infrared Council, established last year as advisory staffs to the Research Directorate.

The Laboratory entered into a new relationship with the Center for Materials Research of the University of Maryland in 1968. Under a Memorandum of Understanding signed in the late summer, encouragement will be given to cooperative research between the two institutions and to direct interaction between

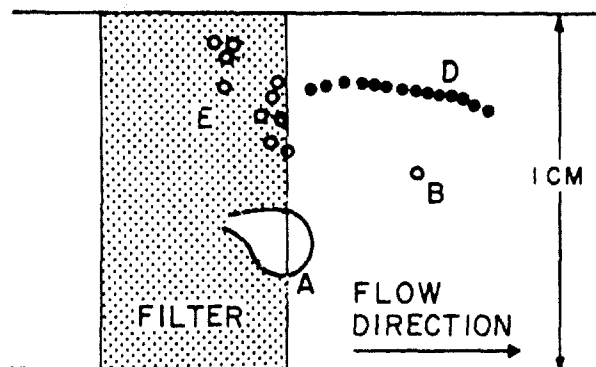
NRL researchers and the University faculty and students. This is the latest addition to the many existing close interactions—both formal and informal—between the materials area's scientists and prominent investigators in the academic world. Along these same lines, Metallurgy Division scientists continued their leading role as technical directors of the ARPA-sponsored stress-corrosion-cracking program in which the Laboratory's resources are coupled with those of industrial and university research establishments. The Solid State Division continued as the key element in a similar ARPA-sponsored investigation of the relation of glass structure and composition to its optical properties, and the attempt was made to broaden this effort to the mechanical properties of glass as well. In 1968, the Laboratory also renewed its participation in a consortium with the National Bureau of Standards and Naval Ordnance Laboratory with the aim of undertaking neutron-diffraction and neutron-scattering studies of solids by means of the new NBS 10-megawatt reactor.

The history of the past year includes the change in leadership of two divisions—Chemistry and Solid State. A select group, the Laboratory for Chemical Physics, was formed, with the former superintendent of the Chemistry Division serving as chief scientist. It is gratifying to note that these administrative changes were effected without perturbation of the high research output of the materials area, and it is believed that the program modifications now under consideration will increase the productivity demonstrated during the past year.

CHEMISTRY

Separation of Water from Fuels. Water is a critical contaminant of aircraft fuels because it is responsible for several major problems, such as corrosion, microbiological growth, and icing. Unfortunately, water in a fuel system is readily emulsified by the action of pumps or the high-speed flow of the fuel through pipelines, and these small droplets of emulsified water settle slowly from aircraft fuels, particularly JP-5, the jet fuel used in most naval aircraft.

The usual process of water separation is by passage of the fuel through a fiberglass filter. During the process, the small water droplets coalesce into larger drops, which can then settle from the fuel under the influence of gravity or be stripped from the fuel by a hydrophobic screen. The performance of the fiberglass



Stream of fuel passing through an operating fiberglass filter. Sketch shows modes of water release from the downstream face of the filter bed. (A) attached balloon-shaped drop, 1,500 microns; (B) released drop, 400 microns; (C) released droplet chain, 100 microns; (D) attached growing drops, 250 to 400 microns.

filter will be degraded somewhat by the presence of surfactants, occurring naturally or as additives, in the fuel.

In order to make the poorly understood problem of water separation more amenable to research, NRL chemists considered separately the three major processes involved: collection of emulsified water drops, passage of collected water through the fiber bed, and release of water from the downstream face of the fiber bed.

Computer calculations indicated that water drops as small as 1 micron in diameter could be readily collected by direct interception. This was verified experimentally for clean fuels, and, in keeping with the calculations, small fibers were found to be superior for this process. The surfactants did not markedly interfere with the efficiency of the collection process. Further, they did not alter the wettability of the

MATERIALS

fibers nor interfere with film drainage during the attachment stage of collection.

Variation of the fiber bed depth, composition, and packing density has shown that surfactants will alter the passage of collected water to the downstream face of the bed. For instance, with a standard corrosion inhibitor in the fuel, water passage is discontinuous if the bed is too deep. In such a case, a thread of water passing through the bed is severed and expelled as a jet.

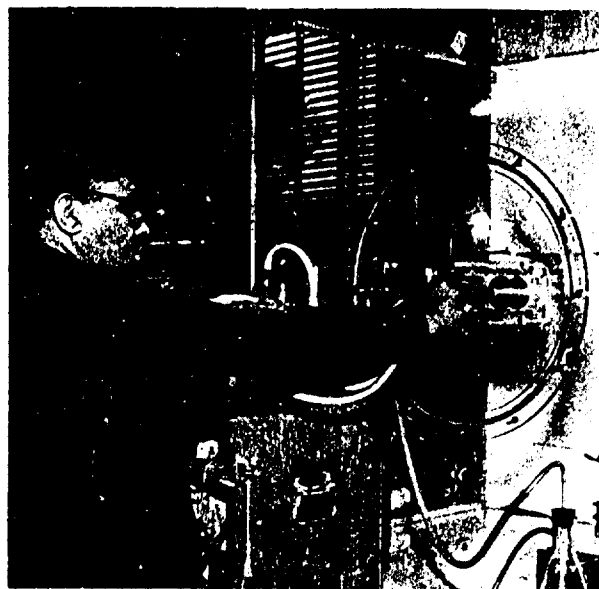
A continuous thread of water passing through a fiber bed will attach to the downstream fiber face and grow in size until the hydrodynamic forces overcome the fuel-water interfacial forces. The drop size may reach 1 or 2 millimeters in diameter. In the presence of a surfactant, the released drop is usually smaller. Surfactants also encourage a direct release of water that does not attach to the downstream fiber face. Frequently it takes the form of a droplet chain, resulting from Rayleigh instability of the water jet. Such chains typically consist of 20 to 30 minute droplets of uniform size. These droplets are too small to be settled by gravitational forces or stripped by screening.

Research to date has thus isolated an important mechanism that serves as a deterrent to the efficient separation of water from fuels: surfactants affect the fuel-water interfacial properties to encourage the release of water by jet action and subsequent Rayleigh instability. This novel concept, that fuel-water rather than fiber-water interfacial properties are significant, now suggests new research approaches to the problem of water separation.

The Behavior of "Free Molecules" in the Atmosphere. Radon, a naturally occurring radionuclide of the ^{238}U series, is responsible for the bulk of the radioactivity of the atmosphere. Radon is a noble or rare gas produced by radioactive decay of radium in the soil. It diffuses into the atmosphere, where it develops an equilibrium mixture of its own decay products, such as RaA (^{218}Po), RaB (^{214}Pb), and RaC (^{214}Bi), which are radioactive metals with half lives of 3.0, 26.8 and 19.7 minutes, respectively. Because of their high energies, these decay products are converted immediately to simple molecules containing oxygen or nitrogen. These are called "free molecules" as long as they are unattached. Their ultimate fate is determined by their diffusion and attachment to available surfaces, such as aerosol particles or container walls.

As might be surmised from their small size and consequently rapid diffusion rate, these free molecules are collected with extremely high efficiency, even by poor fibrous filters. They can even be filtered from a moving air stream by a simple uncharged-metal or plastic screen. This high preferential collection efficiency provides the means of distinguishing experimentally between the radioactive free molecules and those attached to aerosol particles.

NRL scientists are studying free molecule behavior by means of the radon descendants mentioned above. A 1.2-cubic-meter aerosol chamber was specially instrumented for this purpose. Results have shown that, when any quantity of aerosol is present, very few free molecules remain unattached; but when the atmosphere is clean and undisturbed, a considerable concentration of free molecules can exist. When the chamber atmosphere is rigorously cleaned by filtration and radon is allowed to grow into equilibrium with its descendants, appreciable quantities (25 to 50 percent) of the 3-minute RaA free molecules can be found, whereas the longer-lived descendants have either migrated to the walls or become attached to aerosol particles. From studies of this type it should be possible to obtain a direct measure of the rate of



An NRL chemist removes a filter from a specially designed aerosol chamber. By studying the "free molecules" that have been collected (in this case, the decay products of radon), the scientist can learn a lot about the amount and behavior of radioactive particles in the atmosphere.

diffusion of these small particles (molecular weight of about 250) in the atmosphere. Further, these radioactive products can be used to tag aerosols of small size (below the limit of measurement by optical means) for use in studying filtration mechanisms and evaluating filter media.

Fire-Retardant Paint System for Ship Interiors. In 1958, NRL scientists determined that contamination of nuclear submarine atmospheres by hydrocarbons was largely attributable to the organic solvents contained in oil-based paints that had been applied during construction, maintenance, or routine operation of the ships. To reduce this potential hazard, an acrylic latex paint was developed at NRL that could be applied during maintenance periods or, when necessary, during submergence if suitable precautions were followed. This paint was never formally adopted for Navy use because it lacked the equally desirable property of being fire retardant. Three proprietary, fire-retardant, latex paints were subsequently approved for submarines, but none of them contained all the properties considered necessary for their widespread use.

As a result of subsequent NRL research, a technique has been developed for rendering a combustible paint fire-retardant. This is achieved by use of a thin flame-quenching undercoat in combination with the regular decorative topcoat. The fire-retardant undercoat is a water-based material containing high proportions of chlorinated paraffin and antimony oxide which interact under the influence of heat to produce a powerful flame-quenching intermediate.

The primary purpose in using fire retardants only in the undercoat was to avoid detracting from the appearance of the topcoat. A further benefit is that fire-retardant additives are more effective when concentrated in the undercoat than when dispersed throughout the whole coating system.

This particular paint system, a fire-retardant undercoat and a decorative topcoat, is intended for application to noncombustible surfaces, such as bulkheads and nonflammable plastic-foam insulation. The coating system will burn under the influence of an extraneous flame, but it will immediately self-extinguish when the ignition source is removed or when the portion of paint directly exposed to the fire is consumed.

The water-based paints were not developed as replacements for the fire-retardant oil-based paints normally used in locations where adequate ventilation is available for months after their application,

although the two-coat approach to fire retardancy is applicable to any paint system. They are intended for use in situations where the prevention of toxicity and fire hazards during their application in an enclosed space is paramount.

Inhibition of Corrosion in Navy Boilers. Problems in boiler corrosion have been under investigation at NRL through a variety of approaches. A long-term study of corrosion in Navy steam boilers has experimentally and theoretically explained the formation, in alkaline media, of protective oxide films on the inner surface of these high-pressure vessels. The basic reaction involved in the formation of the protective film has been determined to be:



Unfortunately, localized concentrations of the alkaline solution can cause a breakdown in the protective film, permitting attack by the solution on the steel substrate in the form of pitting. Because the pits are potential sites for crack initiation, the chief concern in this study has been the prevention of catastrophic cracking of the vessel wall. Thus, the NRL efforts are directed toward a better understanding of corrosion reactions, including their effect on the formation, stabilization, and breakdown of protective films.

Earlier NRL research had demonstrated that lithium hydroxide (LiOH) is superior to NaOH as the alkaline medium. A cooperative pilot study on LiOH is now under way in a full-scale boiler at the Navy Ship Research Development Center (Annapolis Division).

More recently, radiochemical measurements were made involving osmotic pressure and the transport of helium and other gases through oxide films. The results demonstrated that magnetite films grown in 15-percent NaOH were porous to water. This finding verified a proposed mechanism for the film growth: the consumption of water by seepage through the film to the metal surface and by reaction with the iron increases localized concentration of the alkali and leads to subsequent pitting.

One important question in the study of film formation has been whether the hydrogen is generated at the metal-oxide interface or toward the water-oxide interface. Previously it was believed that if the hydrogen were formed at the iron-oxide interface it would pass through the iron more readily than if it were formed toward the water phase. To resolve this question, a "window" (to hydrogen) of silver-palladium alloy was placed in one end of an iron-tube

MATERIALS

capsule, and measurements of hydrogen permeation were made at two locations—the silver-palladium window and the tube wall. From the application of hydrogen pressure alternately to the outside of the tube wall and to the outside of the window, it was possible to determine the ease with which hydrogen permeated the oxide film and the metal wall. The path of hydrogen escape during corrosion could then be interpreted in terms of the location of the reaction and the rate at which hydrogen could pass through the corrosion film.

Several important findings resulted from these studies of hydrogen evolution:

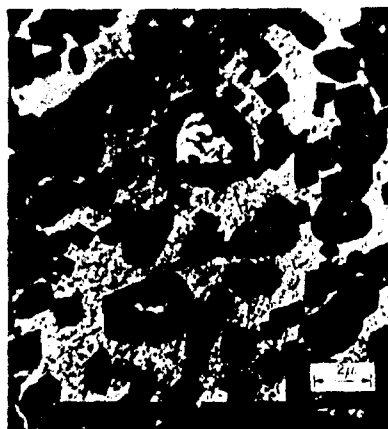
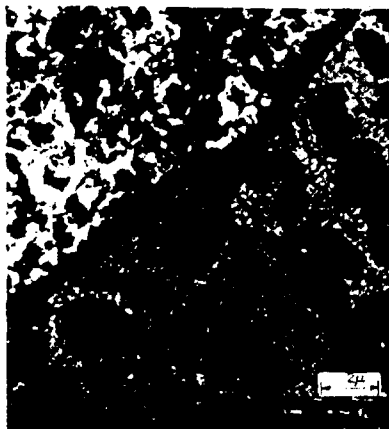
- A magnetite film is porous to hydrogen gas.
- In dilute solutions, hydrogen is evolved at the metal surface, either at the bottoms of pores or close to the surface at pore walls, and passes directly through the oxide and the metal in atomic form.
- Increased concentration of hydroxyl ions is produced in pores by the cathodic reactions on pore walls.
- The porosity of a film grown in an alkaline solution increases with alkalinity.

Recent electron microscopy studies at NRL have shown that the growth behavior of protective oxide films on mild steel in hot (300°C) alkaline solutions follows the pattern of formation of "active" and "passive" oxide films in water solutions at room temperature. The establishment of this relationship is important because, in addition to providing experimental confirmation of a crucial passivity postulate, it puts boiler corrosion studies, for the first time, squarely into the framework of electrochemical corrosion theory. This knowledge should in turn lead to the evaluation of boiler water additives in terms of specific rather than general effects.

Results of another NRL investigation suggested the use of ethylenedinitrilotetraacetic acid (EDTA) as a chelating (metal-ion binding) agent to prevent scale formation in a LiOH solution. Subsequently, nuclear magnetic resonance spectroscopy was used to study thermal decomposition of organic chelating agents in aqueous solutions heated to 200°C. EDTA was found to decompose rapidly by second-order kinetics at a rate dependent on the pH of the solution. The mechanism of decomposition suggested that some of the decomposition products themselves were good chelating agents. There were also indications that other chelating agents might be more thermally stable than EDTA. One such substance, commercially available nitrilotriacetic acid, has been laboratory tested and proposed for boiler evaluation at the Navy Ship Research and Development Center (Annapolis). Other chelating agents are being investigated.

Chemical Reactivity of Pristine Glass. A pristine (bare) glass surface is a great deal more chemically reactive under ambient conditions than is generally recognized. The chemical properties of glass, as well as its mechanical and physical properties, can limit the practical applications of this versatile material. Fundamental research in progress at NRL is directed toward the prime reactions of gas molecules, including water vapor, with the glass surface.

The experiments are conducted with very long, thin, glass fibers which provide maximum surface area for study. The fiber is drawn under precisely controlled conditions from a uniform glass melt onto a rotating metal drum. A suitable length of glass fiber (100-150 miles) of constant diameter (~8 microns) is obtained in about 30 minutes. The fiber sample



Electron micrographs of an iron oxide film grown on low-carbon steel in lithium hydroxide (pH 11) at 300°C. Here an "active" film is being displaced by a "passive" one. In the right-hand picture, transformation is almost complete; two small remaining areas of "active" oxide are indicated by arrows. The dark crystals rest on the upper surface of the "passive" film and presumably grow by precipitation from solution.

is immediately transferred from the drum to an evacuable cylindrical container for gas adsorption studies.

The sample's initial area can be calculated from its known length, weight, and density. Its surface area can also be determined from the amount of physical adsorption of nitrogen or krypton gas at low temperature (77°K). By this technique it is possible to measure surface area changes resulting from various treatments and to infer the chemical causes of such changes.

Typical results for a borosilicate glass (E-glass) commonly used in glass-reinforced plastics are as follows:

Treatment	Area (cm ² /gram)
Pristine E-glass fiber	2,450
Vacuum, 72 hours, 200°C	2,440
Water vapor, 90-150°C	1,970
Liquid water, 1 hour	3,400
3N HCl, 1 hour, 0°C	6,200

After a three-day treatment in vacuum at 200°C produced no change, it was found that a treatment of less than one day in water vapor at a lower temperature resulted in a 20-percent decrease in area. A possible explanation that water vapor catalyzes an unusually low-temperature sintering (sticking together) of touching fibers is being investigated. The substantial increases in surface area observed after an hour's treatment in water and in hydrochloric acid provide a quantitative determination of the surface reactions which are permanently changing the surface composition of the glass. After treatment with liquid water, the evacuated and outgassed glass surface adsorbed significantly more water vapor per unit than did the pristine glass. This behavior is compatible with the presence of neighboring Si-OH groups in the eroded surface.

Water vapor adsorption on pristine E-glass fiber occurs very rapidly and continues in measurable amounts over long time periods (days). Despite its smaller cross-sectional area, the water molecule appears to occupy about the same number of surface sites as do the inert atoms of krypton. The adsorption measurements with krypton or nitrogen actually give the monolayer coverage. In order to calculate surface area it is necessary to postulate a cross-sectional area for the adsorbed molecule. However, when combined with the initially known geometrical area of pristine glass fiber and the assumption of a surface

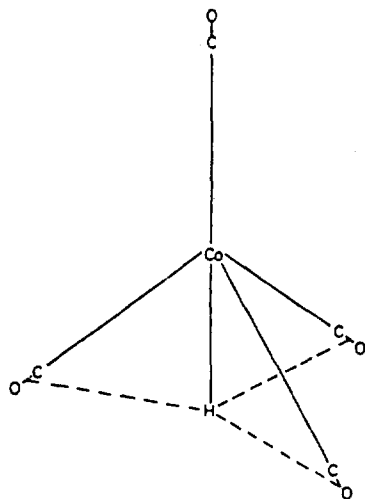
roughness factor of one, the adsorbed monolayer coverage yields an independent value for the area of the adsorbed molecule on glass. This is a fundamental quantity which has been long sought in surface experiments with particular glasses.

These measurements with pristine E-glass are a necessary preliminary to the main objective of the current research, i.e., to determine the effectiveness of various organic polymer barriers to water. Such barriers are crucially important in the performance of glass-fiber-reinforced plastics that are candidate materials for deep-sea submergent structures.

Mass Spectrometric Studies of Cobalt Carbonyl Compounds. A joint research project between the Naval Research Laboratory and the University of Pennsylvania has produced the first measurement of the cobalt-hydrogen bond energy. The nature of the cobalt-hydrogen and other cobalt bonds, such as the Co-C and Co-P, has great importance both in biological systems (vitamin B₁₂) and in the catalytic cracking of hydrocarbons. A mass spectral study has been carried out on the series of cobalt compounds $(HCo(CO)_x(PF_3)_{4-x})$, where $x = 0$ to 4. These studies included, for each compound, measurement of the fragmentation patterns (a plot of mass-to-charge of the various ions versus ion current intensity—a "fingerprint" of the individual molecule) and appearance potentials (variation of any ion current versus the energy of the ionizing electrons). The results showed that the Co-C and the Co-P covalent bond energies in these compounds are essentially identical (56 ± 15 kilocalories per mole) and are much stronger than the Co-H bond energy (4 ± 15 kcal/mole). The heats of formation of these compounds, calculated from appearance potential data, become more negative by approximately 200 kcal/mole for each CO that is replaced by PF₃. Since this change is the difference between the heats of formation (ΔH°_f) of PF₃ and CO, the nature of the covalent Co-C and C-P bonds in these compounds must be quite similar. The values for $\Delta H^\circ_f[HCo(CO)_x(PF_3)_{4-x}]$ are -173 ± 11 ; -381 ± 9 ; -579 ± 10 ; -783 ± 9 ; and -978 ± 14 kcal/mole for $x = 4$ to 0, respectively.

In the fragmentation pattern of these cobalt hydrides, it is possible to compare the abundances of the hydrogen-containing ions with those which have lost a hydrogen atom; that is, the relative amounts of $HCoL_y^+$ to CoL_y^+ , where L_y represents a total of from 0 to 4 molecules of CO and PF₃ in any combination. The results show that ions containing Co-H bonds are more abundant until two or more of the

covalently bonded molecules (CO or PF_3) are lost from the ionized molecules. This type of fragmentation can be explained by an intramolecular interaction between the equatorial molecules (CO or PF_3) and the axial hydrogen atom in the trigonal bipyramid structure. Such an interaction has been suggested previously to explain the infrared spectra of these hydrides. Thus the mass spectral fragmentation pattern data of these compounds provide strong support for a distorted trigonal bipyramid for the structure of all of the trifluorophosphine carbonyl cobalt hydrides where the equatorial molecules are bent toward the axial hydrogen atom.



Molecular model of $\text{HCo}(\text{CO})_4$. Intramolecular interactions between the axial hydrogen atom and the equatorial carbon monoxide molecules in $\text{HCo}(\text{CO})_4$ are shown by the dashed lines. These interactions, accounting for observed infrared properties, can be deduced from mass spectral fragmentation studies.

Advances in Electrochemical Research. Many Navy needs for isolated electric power sources could best be met with electrochemical systems. Such systems would continuously convert chemical energy directly into electricity—cleanly, quietly, and economically—to power submarines and deep submersibles. They would also find wide use in many other applications where isolated power sources are required.

The inherent disadvantage of electrochemical sources of power, such as storage batteries and

fuel cells, is their low energy output per unit weight and volume. Consequently, one of the oldest research programs at NRL is a continuous search for methods and materials that will lead to systems of minimum weight and maximum efficiency.

One of the primary problems to be solved is an understanding of the catalytic processes involved in electrode reactions. The specific aim is the development of electrodes on which fuels and oxygen can readily and continuously react in order that the cell can have a reliable high-power output over long periods of time.

Anodic Organic Reactions. Since formic acid is the simplest organic molecule (requiring the fewest electron transfer steps for complete oxidation) usable for fuel cell technology, knowledge concerning the reaction of formic acid at platinum electrodes is of particular importance in understanding the processes involved in anodic organic reactions. Three basic processes that occur at a platinum electrode in formic acid or formate solutions have been investigated at NRL: the reaction of chemisorbed oxygen atoms with hydrogen, formate species, or both; the formation of hydrogen atoms on the platinum surface derived from formic acid, formates, and hydrogen molecules; and the removal of these hydrogen atoms and their replacement on the surface by formate derivatives. This work has led to several important generalizations concerning low-temperature anodic reactions on suitable catalytic electrode materials in aqueous fuel cells.

- Atomic hydrogen is an excellent, and quite possibly the ideal, fuel for operation of a fuel cell anode at low polarization.

- Formic acid and formates, and possibly other organic fuels, can supply atomic hydrogen on clean platinum surfaces as fast as, or even faster than, molecular hydrogen.

- Dissociation of formates and other organic fuels to atomic hydrogen and free radicals is retarded by the adsorption of residues, which most likely are reaction products caused by the interaction of the free radicals with the electrode surface and with each other.

- Sulfuric acid and molecular hydrogen retard the formation of residues on the electrode surface that hinder dehydrogenation reaction. Thus one critical fuel-electrode problem appears to be finding a method of preventing the formation of organic residues on the electrode.

Behavior of Iron Electrodes. Another electrochemical approach at NRL is the study of electrode

reactions in high-purity, closed alkaline systems. High-purity iron has been employed as an electrode in sodium and lithium hydroxide solutions saturated with helium. The current passing over the electrode as a function of different increments of voltage was measured with a potentiostat, and the resulting data points were plotted to yield potentiostatic-polarization curves. In this system, the level of reactable impurities was reduced to about 10^{-6} parts per million, and the iron showed neither significant corrosion nor passive-type behavior. Depending on the potential, the primary reactions were the oxidation or reduction of hydroxyl ion and water. Iron was shown to act much like an inert noble metal, such as platinum, yet it is an excellent catalyst for the electrochemical oxidation of hydrogen and, in this respect, is superior to platinum.

To determine specific effects of impurities on the electrochemical behavior of iron, minute quantities of chloride ion were added to the solution. This completely changed the potentiostatic polarization relation, causing extensive iron corrosion and resulting in passive-type behavior. The catalytic properties of the iron electrode for the hydrogen oxidation reaction were virtually destroyed and were not restored until the system was returned to its original high-purity condition. These overall results have encouraged a continued study of high-purity iron as a possible fuel cell electrode.

Electrode Morphology. Important electrochemical surface phenomena are involved in high-energy-density cells, such as the silver-zinc cell, which are used in a number of military applications because they can deliver their energy at relatively high rates. Such cells actually operate at power levels considerably below their theoretical capabilities; thus the conditions which influence their performance has become the basis of a continuing investigation at NRL. It has been shown previously that one of the perplexing problems of the silver-zinc cell was the wide variation in the amount of electrical energy which could either be delivered to the cell or withdrawn from it, apparently dependent on the previous operational history of the cell. It was suspected further that the variation in energy was directly related to changes taking place in the electrode morphology during various operational modes. Consequently, a microscope technique was developed to study the morphological changes taking place in the silver electrode at various intervals during its charge-discharge cycling.

Microscopic examinations revealed that crystal size and shape (hence available reactive surface area) varied over a wide range that was dependent upon the method of charging or discharging. With most operating methods, the individual crystals tended to increase in size and decrease in number in proportion to the number of operational cycles. It was also discovered that crystal formation sometimes blocked the entrances of interior pores, which resulted in undesirable reduced interior porosity in the electrode.

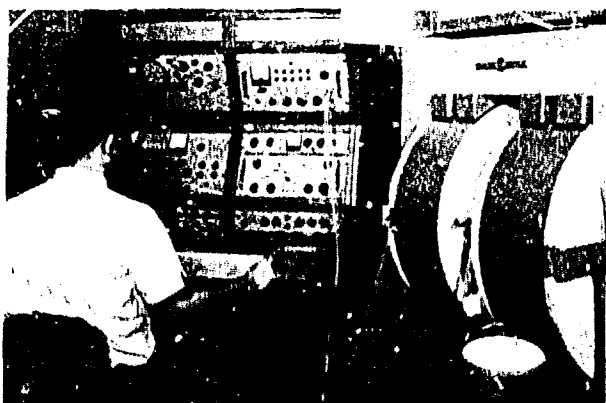
With the importance of electrolytically developed crystal morphology during both oxidation and reduction of an electrode clearly demonstrated, it becomes possible to estimate the total surface actually available for reaction, identify that portion of the reactive substance which is taking part in the reaction, and determine why certain portions do not react. Furthermore, it is expected that continued study of such phenomena will suggest means of increasing the total reactive surface of the electrode, thus increasing both the total quantity of available energy and the rate at which it can be delivered. These objectives will be achieved through improvements in operational methods and control of crystal morphology.

Unambiguous Assignment of Spin-Coupling Parameters.

The nuclear magnetic resonance (NMR) spectrum of a typical organic molecule consists of an array of lines whose positions and intensities are exactly definable in terms of two parameters: chemical shifts (δ 's), which number the chemically different nuclear environments within the molecule, and nuclear spin-spin coupling constants (J 's) which arise from the coupling of nuclear spin energy levels through the bonding electrons. The δ 's are proportional to the strength of the applied magnetic field, whereas the J 's are completely independent; thus the larger the δ -to- J ratio, the less do δ and J interact, and hence the simpler is the resulting spectrum.

Knowledge of J 's is of theoretical importance in the testing and formulation of theories of electronic and molecular structure and of practical importance in the construction of correlations from which the structures of new compounds may be elucidated. In many cases, however, especially for fluorine compounds, the degree of mixing between δ 's and J 's is so small that it is not possible to determine the signs and value assignments of J 's from high-field NMR spectra. This is true, even though NMR instrumentation has been moving toward the use of higher-strength magnetic fields (above 10 kilogauss),

MATERIALS



An NRL scientist records a nuclear magnetic resonance spectrum of an organic molecule. Such spectra reveal the chemical shifts and nuclear-spin coupling constants of the molecule, from which the structure of many new compounds may be determined.

which simplify the spectra and improve the signal-to-noise ratio.

A technique has been devised at NRL for routinely obtaining high-quality proton and fluorine NMR spectra at low fields (1.5 kilogauss), where the δ 's and J 's are of comparable magnitude and a maximum of interaction occurs. Computer analysis of the low-field spectra (a joint effort of NRL and the Food and Drug Administration) yields unambiguously the signs and value assignments of J 's. The technique is being applied to a variety of molecules for which the high-field NMR spectra do not allow extraction of this information.

METALLURGY

Rate Spectrum in Cleavage Fracture. Proper plasticity models of fracturing processes have long been sought by many research investigators. Among many possibilities is the concept that fracture may be controlled by local tensile plastic instability within the plastic zone around a crack tip. This general idea was fashioned at NRL into a quantitative theory which provided a consistent interpretation of experimental correlations between the plane strain fracture toughness (K_{Ic}) and plastic flow properties of the bulk material. The best initial correlations were obtained on a mild steel ship plate, a material of complex strain rate and temperature sensitivity. The strain hardening exponent (n), which is directly related to the strain

necessary to produce tensile instability, was found to correlate directly with K_{Ic} . The theory coupled the two with a simple size parameter (d_T), taken to be the diameter of ligamental bars envisioned as tying together the throat of the crack. In this model, crack instability occurs when these ligaments are stretched to the verge of tensile instability (necking), after which their rupture is inevitable. The larger these ligamental bars, the greater the stress and closely coupled strain field of the crack (i.e., the K_{Ic} level) required to bring the entire cell to instability and propagate the crack.

The existence of d_T cells was corroborated elsewhere by direct observation of sulfide-inclusion-nucleated tear dimples on fracture surfaces of a high-strength steel; these were interpreted as broken ligament residue. Stronger, indirect evidence supporting the model was found in another investigation of mild steel where a most distinctive pattern in both K_{Ic} and critical strain (E_c) values as a function of strain rate was found and matched. This pattern appeared at harmonic intervals of strain rate, suggestive of a lattice resonance effect. By analogy with optical spectra, it was called a "rate spectrum."

With the small fracture specimens used in this study, the rate spectrum could be observed only at low temperatures. The Atomic Energy Commission, concerned for the safety of heavy-walled nuclear reactor pressure vessels, has sponsored fracture toughness tests on much larger specimens. When the data for these large specimens were analyzed at NRL, two important results were obtained. First, the room-temperature fracture toughness, as measured directly, was indeed correctly anticipated by predictions of the d_T instability model. Second, and even more remarkable, the rate spectrum now appeared in room-temperature fracture and was identical in every respect with that previously discovered at low temperatures. The variations of K_{Ic} with strain rate are so precipitous and so large that they dominate the fracture toughness behavior. Indeed, they may be the key to safe use of mild steels in heavy sections. The basis for this phenomenon is a subject of great interest for both engineering and basic scientific aspects.

Stress-Corrosion Cracking of High-Strength Steels. The cracking of high-strength steels because of the simultaneous action of stress and a corrosive environment (such as seawater or atmospheric moisture) remains a major barrier to the more widespread use of these materials. This stress-corrosion cracking

process has long been considered to occur by either of two mechanisms: the dissolution of metal at the tip of the advancing crack, or the reduction of hydrogen by the general corrosion reaction and the redistribution of this hydrogen in advance of the growing crack. All attempts to analyze the chemical processes involved have been thwarted by three factors: the amount of corrodent within the growing stress-corrosion crack is exceedingly small; the chemical processes of greatest interest are those occurring deep within the crack; and the crack, having reactive walls, would be expected to act as a "chromatography column," sorting ions in some fashion so that the composition of the corrodent at the zone of most interest would differ from that near the mouth of the crack.

A technique has been developed in which a propagating stress-corrosion crack is frozen by immersing the specimen in liquid nitrogen. This freezing prevents further chemical reaction and ensures that most of the corrodent stays in place when the crack is later broken open to expose its still-frozen stress-corrosion crack surfaces. The specimen is then thawed, and the corrodent is analyzed immediately for pH and specific metallic ions in solution by pressing upon the fracture surfaces filter papers containing various pH and metal ion indicators. Knowing the values of both the pH at the growing-crack tip and the electrochemical potential enables one to use the Pourbaix method of analyzing corrosion behavior.

Data have been obtained for 11 alloy steels representing a wide range of metal compositions and stress-corrosion cracking resistances. For all the metals analyzed, the bulk corrodent was neutral (pH = 7) sodium chloride solution, but the pH of the corrodent at the advancing crack tip was found to be about 3.6. This acid condition is postulated to be due to the hydrolysis reaction $\text{Fe}^{2+} + 2\text{H}_2\text{O} \rightleftharpoons \text{Fe}(\text{OH})_2 + 2\text{H}^+$. The important result was that the data points for all 11 steels fell into that part of the Pourbaix diagram which indicates that hydrogen can be reduced from water, i.e., below the hydrogen reduction line. This suggests that the hydrogen mechanism is active. If so, the addition of a buffering salt to the corrodent, to hold the pH above the

hydrogen reduction line, should prevent stress-corrosion crack propagation. This concept was tested by adding sodium acetate to the corrodent. The presence of the acetate maintained the pH at 8 (above the hydrogen reduction line), and cracking did not occur. When the potential was depressed to below the hydrogen reduction line, cracking ensued at once!

Since cracking is observed only at points below the hydrogen reduction line, the necessary conditions for hydrogen embrittlement are met, and there are now no observations requiring the crack tip dissolution model.

The hydrogen model suggests that steels which exhibit high potentials and which corrode slowly, thereby permitting diffusion processes to oppose the accumulation of acid, should be the more resistant to stress corrosion. On the other hand, steels with low potential and also low intrinsic corrosion resistance would be expected to have poor resistance to stress corrosion. Both suppositions are in general accord with experimental results.

Electron microscopy of replicas of stress-corrosion fracture surfaces in high-strength steels has revealed the presence of ridges and peaks. These features are interpreted as terminal tensile failures of ligaments which were resistant to the corrosive factor. Thus, as has been found earlier for titanium, stress-corrosion cracking in high-strength steels is a dual process; part is the result of stress and a chemical reaction and part is essentially mechanical.

This work is part of a program funded by the Advanced Research Projects Agency in which academic and industrial laboratories also are involved.



Electron micrograph of replica of stress-corrosion fracture surface of a steel alloy. Broad featureless areas are considered to be due to simultaneous chemical action and stress. Ridges are interpreted as being formed by ligaments resistant to chemical effects that undergo plastic straining until they are torn apart. Magnification: 60,000X.

Differential Aeration Corrosion of Stainless Steel. Severe corrosion damage to stainless steels can result from differential aeration cells created at any point on the surface where the access of oxygen is limited (e.g. in a crevice or under some types of biological fouling). Such corrosion has been a continuing problem in ocean materials technology for many years. In principle, the problem could be eliminated by the substitution of more resistant alloys, but the stainless steels have many desirable qualities that call for their continued use.

It has been known for some years that Type 316 stainless steel is satisfactory for use in the sea if it is provided with reliable cathodic protection, i.e., electric bonding to a large cathode, such as a ship's hull. Type 316, however, is one of the more expensive alloys. Furthermore, many items fabricated from Type 316 are obtainable only by special order, which inevitably involves a delay in their procurement.



Stainless steel heat exchanger used in an acoustic project. This component failed as a result of differential aeration corrosion.

Studies to determine the reliability of the less-expensive Type 304 stainless steel were conducted on O-ring seals (which present an extremely severe differential aeration condition). The results demonstrated that, although differential aeration corrosion of Type 304 cannot be completely prevented by cathodic protection, the usual excessive corrosion associated with this alloy can be substantially reduced. Whenever the use of more resistant alloys is precluded, Type 304 fittings, if coupled to either zinc

anodes or structural steel, are adequate for long-term use in sea water.

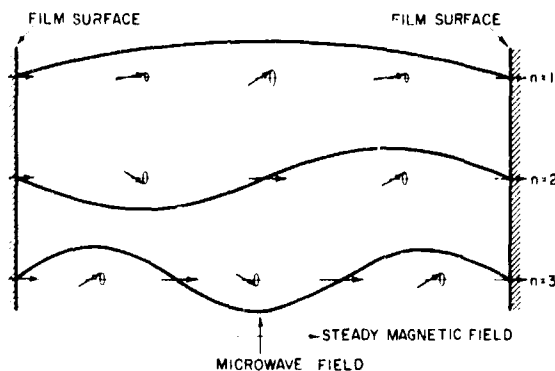
Along with the engineering experiment, an investigation into the solution chemistry of differential aeration corrosion was carried out by use of pH indicator papers and spot tests for metallic ions. This continuing investigation has already shown that differential aeration corrosion of Type 304 steel is always characterized by a very acid corrodent trapped in the area of low oxygen. The data indicate that the hydrogen ion concentration is too high to be completely accounted for by a reaction involving the iron in the stainless steel. The measured pH and available thermodynamic data suggest that the acidity is due to the hydrolysis of soluble chromium ions produced during the corrosion process.

The solution chemistry studies have indicated the desirability of investigating the application of an alkaline buffer to the mating surfaces of O-ring-type seals to mitigate the buildup of hydrogen ions. These studies should be useful also to the development of alloys resistant to differential aeration corrosion.

Spin-Wave Resonance and Radiation Damage in Thin Films. The increasing use of thin films in electronic devices and the continued interest in their use as computer elements make an understanding of their physical characteristics quite important. NRL scientists were the first to use a combination of two different techniques—spin-wave resonance and radiation damage—to determine the role that imperfections play in the characteristics of magnetic thin films. In addition to its use in the study of radiation damage in films *per se*, this approach provides a convenient and unique way to change the defect distribution in the film.

In spin-wave resonance, a ferromagnetic film in both a steady and a microwave field absorbs energy from the microwave field when the condition relating the microwave frequency and the magnitude of the steady field is satisfied. Although various spin-wave resonance modes can be excited, both the volume homogeneity of the magnetization and the surface anisotropy (and, hence, spin-pinning) affect the positions and intensities of the resonance absorption lines.

NRL studies of irradiated Permalloy films show that the spin-wave resonance fields are all decreased if the film is below a critical thickness (2,000 Å) and that, in general, the intensities of the even resonance modes are increased whereas those of the odd



Spin-wave modes ($n = 1, 2,$ and 3) of a ferromagnetic film, with the surface spins taken as pinned. Energy would be absorbed only by the $n = 1$ and $n = 3$ modes.

modes are decreased. These changes can be attributed to a change in the radial isotropic stress of the film and to a "freeing-up" of the spins at one surface of the film. In addition, it is found that for films thicker than 2,000 Å there is an increase in the resonance fields of the first two modes. This suggests that volume inhomogeneities, as well as surface (spin-pinning) changes, are playing a role in the spin-wave resonance patterns of these thicker films.

Since half-widths of the resonance lines do not change much with irradiation, even though in some cases the intensity changes by a factor of six, it is concluded that the spin waves are not interacting with the irradiation-produced defects and that the defects produced are smaller than the smallest spin-wave excited in the film (400 Å). After their irradiation, annealing the films at rather low temperature (200°C) changes the spin-wave resonance intensities back toward their original values, whereas the low-order resonance fields continue to increase for these thicker films. Thus, although the defects causing the changes in the surface anisotropy are annealing out, the volume inhomogeneities in the film are continuing to increase with anneal.

Environmental Effects at Elevated Temperatures.

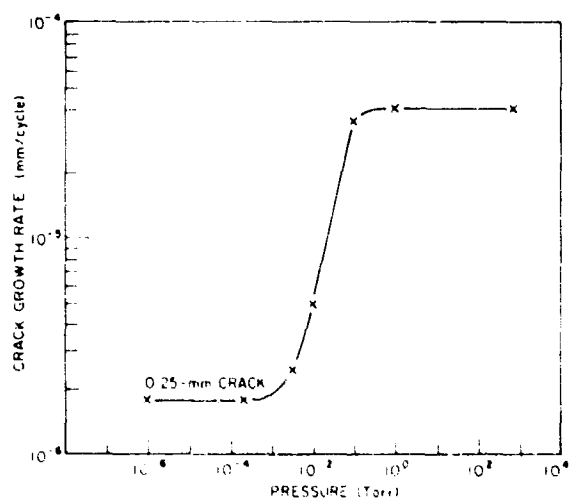
The deleterious effect of reactive gases on the fatigue properties of metals, a matter of concern in regard to many structures, has been related to an increase in rate of crack propagation. An understanding of the process by which this takes place could lead to better control of metal properties and thus to improvement in the reliability of structures. Several

explanations of the effects have been put forth, but experimental confirmation has been lacking.

In a detailed study conducted at NRL, the growth rate of a fatigue crack in Type 316 stainless steel was measured in an oxygen atmosphere at 500°C at a series of pressures from 10^{-7} to 10 torr. A regenerative drive machine was developed specifically for this purpose. The specimen was vibrated in reverse bending at its resonant frequency, and the observed decreases in frequency were used as a measure of crack length. It was found that rate of crack growth increased sharply at intermediate pressures but was insensitive to oxygen at very low and very high pressures. The critical transition pressure above which there was no further increase in growth rate may be interpreted in terms of a previously proposed model.

According to the model, the adsorption of gas on crack surfaces weakens the material there. In the transition region, with increase in pressure and thus in rate of surface coverage the crack velocity increases. The critical transition pressure is reached when the rate of surface coverage by the gas equals the rate of exposure of fresh surface at the crack tip. At pressures higher than that which produces saturation of the surfaces, no further increase in crack growth rate should be expected.

This concept was evaluated by a method developed at NRL for calculating the gas pressure at the critical point (where crack surfaces are being produced and



Effect of oxygen pressure at 500°C on rate of fatigue crack growth for Type 316 stainless steel at a bonding strain of 0.141 percent

saturated at the same rate). In this method, the time available for coverage of freshly exposed atoms at the crack tip is equated to the time it takes to saturate these surface atoms, as calculated from the kinetic theory of gases. It is assumed that the crack tip advances in small, discrete steps within the fatigue cycle and that the surface in each step is covered before the succeeding one is produced. The exposure time for each step is given by the interatomic spacing divided by the crack tip velocity. Then, from the kinetic theory of gases, the pressure necessary to saturate the surface within the exposure time can be calculated.

The critical pressure predicted by the method for crack growth rate in stainless steel at 500°C agrees well, within an order of magnitude, with the experimental value. Application of the method to data obtained in other investigations also produces good agreement between predicted and experimental values. These results indicate that environmental effects can be satisfactorily explained on the basis of gas adsorption.

Sintering of Porosity in Bicrystals of Niobium. A crystalline material is ordinarily composed of many, small, single-crystal grains of various orientations. The boundaries separating these grains can have a large effect on the properties and behavior of the material. An understanding of the nature of grain boundaries and of their interaction with other crystal defects, such as dislocations and atomic vacancies, is of great importance.

One of the most effective techniques for the study of grain boundaries is to create a boundary between two relatively large crystals; that is, to make a bicrystal of controlled orientation. Scientists at NRL have made bicrystals of niobium by vacuum-welding two single crystals at high temperature under light pressure. The boundary thus formed is identical to naturally occurring boundaries. Some porosity remains in the boundary after the crystals have been welded, but this can be removed by a sintering process of high-temperature annealing.

The kinetics of this sintering process can be related to the sintering of voids in a metallic powder compact and should provide information on the nature of the boundary and the dislocation structure. Void closure occurs by the migration of vacancies from the void pores to defects or external surfaces, where they can be absorbed. Experiments have been conducted to determine the sintering rate as a function



Photomicrographs of a niobium bicrystal boundary, showing decrease in porosity and accompanying dislocation density. Top: As welded. Bottom: Electroetched to develop pits at dislocation sites. Magnification: 100X.

of three variables: boundary misorientation, dislocation density and distribution as affected by welding pressure, and temperature. The percentage porosity is measured in sections cut perpendicular to the boundary, and the dislocation structure is examined by electroetching and decoration techniques developed at NRL.

It has been found that the sintering rate is initially quite high but decreases to a relatively low and apparently constant rate at long times. The rates are apparently independent of the boundary misorientation, a surprising result since the boundary would be expected to act as a vacancy sink. The large variation in initial rate has been related to changes in dislocation structure. Excess dislocations introduced during the welding process form subboundaries or are eliminated during the anneal, in times corresponding to the decrease of the sintering rate to a constant value. It was also found that the initial rate is strongly dependent on welding pressure, being higher for increased pressure, which produces an increased dislocation density. These results show that the dislocations can act as the principal vacancy sinks in the sintering of porosity.

Interfacial Energies In Metals. A knowledge of solid-liquid interfacial energies is important to the quantitative understanding of thermodynamic and kinetic interactions involved in most metallurgical solid-liquid processes. Previously, only indirect estimates of these energies have been available.

Using their own NRL-developed technique of gradient hot stage electron microscopy, NRL scientists have been able to observe directly the microstructural details of metal-melt interfaces at very high magnification (over 100,000X). Investigations of the surface tension balance established where a grain boundary surface meets the solid-liquid interface have produced the first absolute values of the solid-liquid interfacial energy in a metal.

The solid-liquid interfacial energy has been measured in pure bismuth over a range of crystallographic directions in the basal plane. An average value of 61 ergs per square centimeter was determined, which differs significantly from previously reported estimates based on rather indirect methods. A small anisotropy in the interfacial energy was detected and was shown to be responsible for many prominent micromorphological features of the solid-liquid interface. Similar considerations hold for many other metals, such as zinc, magnesium, beryllium, and tin, all of which are anisotropic in most of their properties.

Finally, the relationships found between grain boundary energies and solid-liquid surface energies have additional important metallurgical implications, since the behavior of metals near their melting point is frequently governed by the ability of the grain boundaries to resist melting and maintain structural integrity. Specifically, it was found that certain boundary dislocation structures are thermodynamically stable until the normal melting point is reached, whereas others become unstable below the melting point. The marked difference in stability seems to depend on very slight variations in the density of the dislocations in the grain boundary. The ability to control these structures may play an important role in the search for better high-temperature materials.

Gas-Metal Reactions. Ideally, the oxide formed on a metal in high-temperature service should completely isolate the structural alloy from the environment, stifle the reactions which formed the oxide barrier, and prevent property changes (structural changes) in the alloy. Unfortunately this ideal is never achieved, so alloy oxidation is a dominant constraint in a wide variety of Navy applications. Because the basic processes determining these limitations have not been fully explored, predictions of alloy behavior are based on simplified "model systems" which are not adequate.

NRL has explored some aspects of oxidation in systems as diverse as protective coatings for refractory metals and pure iron oxidation. Recent studies have shown that model mechanisms have been over-extended in the past. For example, measurements of increasing chromium solution in wüstite (Fe_{1-x}O) confirmed the lowering of the oxygen activity predicted by a pure iron model but showed an increase in the lattice parameter rather than the "predicted" contraction. These data are not sufficient to clarify the defect structure of this oxide, but when they are joined with other data, the combination cautions against generalizations derived for materials of low defect concentrations.

The importance of the surface reaction in the oxidation and carburization of Fe-Cr alloys in CO_2 -CO atmospheres has required a re-examination of the "model system," i.e., the oxidation of pure iron in CO_2 -CO. The complicated kinetic results characteristic of the conversion of iron to wüstite have been faithfully reproduced in these current studies. A variety of experimental techniques are being used, including kinetic measurements, x-ray data (for

MATERIALS

texture and oxide defect concentration), and optical and scanning electron microscopy (for microstructure and surface topography).

The evaluation of surface changes during oxidation has been greatly enhanced by use of the scanning electron microscope. The oxide formed in the initial period (2 hours) at 1,000°C in $\text{CO}_2/\text{CO} = 1.0$ shows a uniform, highly textured, wüstite layer and prominent wüstite needles. The growth kinetics of this period are nearly linear and are probably controlled by the reaction at the atmosphere-oxide interface. As the oxidation time is extended, a very rough and nonuniform oxide layer develops. After five to seven

hours, the surface morphology of the oxide has changed dramatically—and so have the reaction kinetics, the wüstite composition, and the oxide texture. After prolonged oxidation, the thickness and surface topography of the oxide become more uniform. The surface develops a pattern of square-based pyramidal pits bounded by planes close to the $\{111\}$ form. The rate of oxidation decreases but does not attain parabolic kinetics because steady state boundary conditions are not achieved, even after long oxidation.

In previous attempts to analyze the kinetics of iron oxidation, inappropriately simple boundary con-



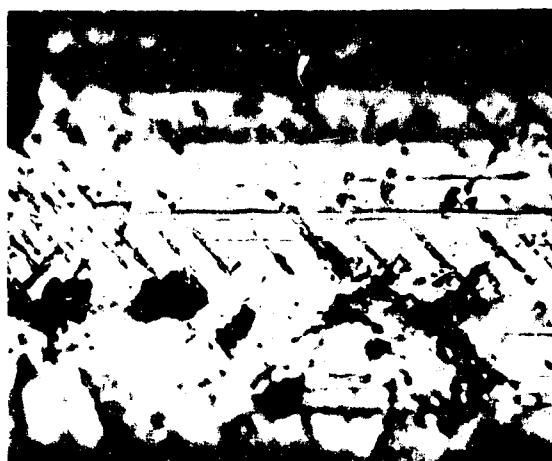
Photographs of secondary electron images showing surface of wüstite formed on iron oxidized at 1,000°C in $\text{CO}_2/\text{CO} = 1.0$ for two hours (at left) and for seven hours (at right). Magnification: 260X. The related perspective drawings were constructed from stereopairs of the photographs.

ditions have been assumed. One such assumption was that of a uniform, smooth, oxide layer during the entire growth period. Studies with the scanning electron microscope have shown that this is not a realistic assumption. It was also assumed that the wüstite composition remained at the iron:wüstite equilibrium value through the time of rapid oxidation (the five- to seven-hour period mentioned above). X-ray measurements of lattice parameters have shown that, in fact, a composition gradient develops in the oxide very early and that the surface composition of the oxide changes throughout the oxidation process.

The complexity of iron oxidation is not exclusively caused by a shift in the rate-controlling process from surface reaction to diffusional transport. Instead, there is an intervening period in which disruptive processes greatly alter the surface character and area of the oxide and produce very high oxidation rates. These same effects are evident in the oxidation of dilute Fe-Cr alloys (up to 5 weight-percent Cr) but are displaced by a much simpler sequence in higher Cr alloys (5 to 15 weight-percent Cr). This apparent paradox of the more complex alloy having simpler reaction kinetics (but with very different characteristics of the wüstite layers) suggests a strong influence of the metal-oxide interface reactions on the more dominant processes.

Influence of Oxygen on Formation of Surface Slip Bands. Metals under stress deform plastically by displacement or slip along crystallographic planes, and the cycling of the process leads to the initiation and growth of a crack. Where a plane on which slip has occurred intersects the metal surface, a step is produced, and these steps have the appearance of lines or bands. Inspection of the character of these slip bands can yield information about the deformation process. Because slip is often initiated at the surface, it would be of interest to know if it is influenced by the surrounding medium. This information could help explain the effects of environment on the failure of metals.

In metals undergoing fatigue, a reactive gas is known to accelerate crack propagation, but its effect on the preceding surface deformation and crack initiation is obscure. In a study of these early fatigue stages, Inconel X-750 sheet specimens, each containing a surface notch, were vibrated in reverse bending at 500°C in an atmosphere of 1-torr oxygen and in a vacuum of 6×10^{-7} torr. The experiments were interrupted periodically so that the notch surfaces could

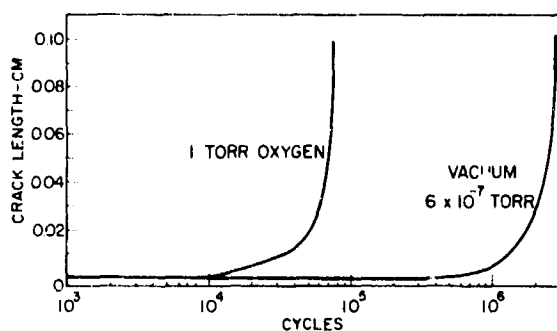


Photomicrograph of slip-band formation in notch of Inconel specimen vibrated at 500°C for 3.6×10^4 cycles in a vacuum of 6×10^{-7} torr (top) and in an atmosphere of 1-torr oxygen (bottom). Magnification: 500X.

be examined microscopically. Also, the rate of crack propagation was determined from decreases in resonant frequency of vibration which occur as the crack proceeds.

Curves of crack growth in 1-torr oxygen and in vacuum reveal that, for a comparable number of cycles, crack growth rates are higher in oxygen. As a result of the faster crack growth in oxygen and apparently earlier initiation of the crack, the fatigue life was about 37 times longer in vacuum than in oxygen.

The environment also affects the formation of slip bands which appear on the notch surface prior to cracking. Slip bands produced in vacuum are



Curves of fatigue crack growth in Inconel X-750 vibrated in reverse bending at 500°C and 0.17-percent strain in 1-torr oxygen and in vacuum.

widely spaced, whereas those produced in oxygen after the same number of cycles are finer and much more closely spaced. In a typical experiment, after 3.6×10^4 cycles, a fine crack had formed in oxygen but not in vacuum. The crack which later developed in vacuum followed the early, prominent slip bands.

Environmental influence on the development of surface deformation apparently can affect crack initiation. The finer and more closely spaced surface slip produced in oxygen appears to be related to chemisorption or oxidation of freshly exposed slip surfaces. Oxygen on the surfaces of the slip step may cause increased resistance to further slip on that plane, and other adjacent slip planes are activated, which accounts for the numerous slip bands. In contrast, the fresh slip surfaces produced in vacuum would not be quickly oxidized, and slip could be reversed and further cycled on the same plane. Oxidation of slip steps and transport of oxygen atoms into the interior of the crystal by the cycling can form strong obstacles to further dislocation motion. These obstacles also can serve to nucleate a crack.

These findings improve our understanding of environmental effects on metal properties and permit a more knowledgeable application of materials.

Physical Properties of Incipient Ferromagnets. Many metals have unique properties which can be interpreted only in terms of many-body electron-electron interactions. Two such properties, which also appear to be mutually exclusive, are superconductivity and ferromagnetism. Metals are either superconductors or ferromagnets but are never both. An intermediate electronic state is that of "incipient ferromagnetism"—a strongly paramagnetic state that exhibits

properties somewhere between those of the other two. Knowledge of this hybrid state should yield valuable clues for a better understanding of both the ferromagnetic and the superconducting states.

NRL scientists have been leaders in exploring the properties of several binary alloy systems which, over certain regions of composition, are incipient ferromagnets. These are the platinum-nickel and palladium-nickel alloys, which remain paramagnetic up to approximately 50 and 2 atomic-percent nickel, respectively. As the critical composition for the occurrence of ferromagnetism is approached, the alloys become increasingly strong paramagnets yet remain nonferromagnetic. In this region of composition, NRL scientists have observed anomalous physical properties which arise from true many-body effects. For example, at low temperatures, an electrical resistivity contribution varying as the square of the temperature and a thermal resistivity contribution varying as the first power of the temperature have been observed. These temperature dependences have been theoretically explained and related to the strength of the electron-electron interactions. As these interactions become stronger, the temperature coefficients of the two contributions increase extremely rapidly, although their ratio remains roughly constant.

Unusual low-temperature heat capacities also have been observed for these "incipient ferromagnets." The coefficient of the linear term in the low-temperature heat capacity has been found to vary extremely strongly as a function of electron interaction strength. Theoretically, this has been related to the enhancement of the effective mass of the electronic quasi-particles. In addition, the electron interactions have been found to result in an unusual composition dependence in the apparent Debye characteristic temperature. Finally, since the electron interactions are strongly functions of the magnetic field, the field dependence of many of the properties mentioned above has been examined in field strengths up to 100 kilogauss.

Fracture Toughness of High-Strength Metals. The tensile strength of a material is defined in terms of critical stresses which relate to the beginning of yielding and to the initiation of fracture. For brittle solids, yielding does not develop, the strength limit is attained with the onset of fracture, and catastrophic failure results. Metals generally yield and increase in strength by work hardening prior to the onset of

fracture. Measurements made on the usual specimens of smooth section may be misleading, however, as to the actual strength capabilities of a material. In structural applications, the presence of cracks or other notch-like defects results in very high stresses at the crack tips, and the first development of yielding is concentrated within a small plastic zone at the tip. The extent to which this microscopic volume of metal deforms instead of fracturing establishes the fracture strength of the total section.

In metals of high fracture toughness, large crack-tip plastic zones will develop which serve to blunt the crack and thereby permit the rise of nominal stresses to levels that will cause general yielding. In metals of low fracture toughness, fracture will occur in the plastic zone at levels of nominal stresses that may be far below the yield point. Thus, the most significant parameter of strength for metals or other materials is the "cracked body strength."

The development of high-strength alloys entails the control of complex, multiphase, microstructural conditions. In brief, while the metal must offer high plastic flow resistance at microscale (grain size and subgrain size levels of 10^{-4} to 10^{-6} centimeter), the flow must not be terminated by microfracture processes at too early a stage. In effect, the desired aim is microscale, crackless plasticity of high-activation stress intensity.

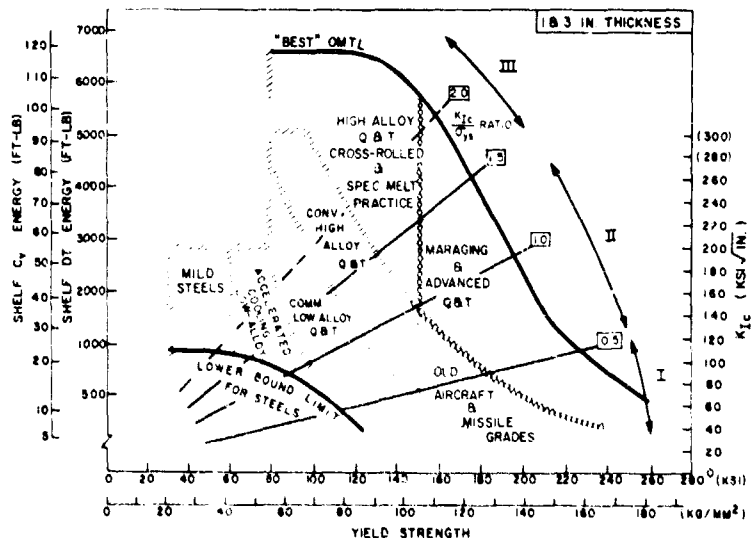
The apparent paradox in strength of materials is that microscopic "weakness," i.e., yielding with the creation of a plastic zone at crack tips, leads to macroscopic strength—the material will resist fracture even

in the presence of large cracks. Conversely, microscopic "strength," signifying too high a resistance to yielding at crack tips, leads to macroscopic weakness—the yield-resisting solid will fracture at very low nominal stresses in the presence of minute defects.

The critical fracture strength is defined by the parameter K_{Ic} ($\text{ksi} \sqrt{\text{in.}}$), which is the critical intensity of the elastic stress field at the crack tip. The size of the crack-tip plastic zone is proportional to the parameter $(K_{Ic}/\sigma_y)^2$, i.e., the ratio of the crack-tip stress field intensity to the nominal yield strength. This is basically an expression of the ratio between the force applied and the force required for yielding. The higher the ratio, the larger the plastic zone and the higher the energy absorbed by the metal prior to fracture. Formal fracture mechanics concepts provide for conversion of the ratio to critical flaw size and stress relationships. In practice, the ratio for a given metal thickness can increase only to some specific level beyond which general yielding occurs and flow rather than fracture dominates the failure process.

The complexities of these relationships have seriously impeded communication between research specialists working in the microstructural aspects of high-strength metals and design or materials engineers. Until NRL developed the dynamic tear (DT) test, there was no simple engineering test available which properly characterized the plastic zone size across the full spectrum of metal toughness—relatively brittle to fully ductile. The development of the DT test and its characterization in terms

Ratio analysis diagram for steels. Materials falling within the area of zone I will be characterized by critical flaws of minute dimensions, those within zone II by transition from small to very large critical flaws, and those within zone III by complete resistance to unstable fracture.



MATERIALS

of the K_{Ic}/σ_{ys} parameter have made it possible to resolve these complexities in a very simple manner. In fact, information which would otherwise require textbook-size descriptions may now be "compressed" into a simple diagram, called the "ratio analysis diagram" (RAD).

For example, the RAD for steels provides the following information in terms of the full yield-strength range for plate thicknesses of 1 to 3 inches:

The optimum material trend line (OMTL). This represents the current "leading edge of the technology" and indicates the best material for specific strength levels. Metallurgical research is aimed at developing materials with fracture properties beyond this current limit of the technology.

K_{Ic}/σ_{ys} ratio lines. These can be translated quickly into flaw size and stress conditions that will cause fracture.

Zonal regions of generic families of alloys, including processing variables. These define metallurgical factors for the developers of new alloys. In addition, they provide for the design engineer a means of deriving estimates of trade-offs for relative strength, relative quality, relative cost, etc.

Such diagrams have been worked out for the structural steels, titanium, and aluminum alloys and, except for aluminum, their respective weld metals. The diagrams may be "entered" by a variety of scales known to engineers, the most definitive for total range of toughness being that of the relatively inexpensive DT test. As additional information is obtained, the data points may be plotted on the diagram, and thus it serves as a data storage bank of utmost simplicity.

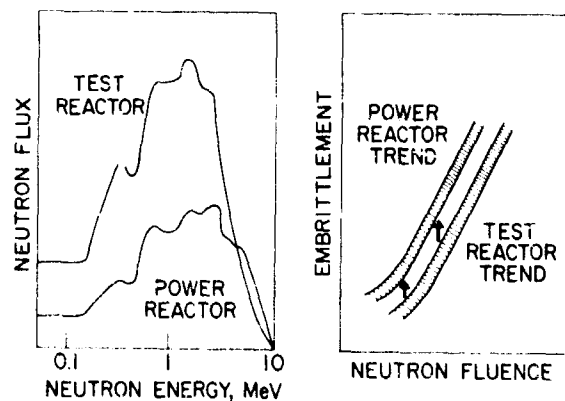
The DT test and RAD procedures have been utilized in critical Navy decision-making relating to the selection of metals, alloy development plans, and engineering design practice. At the request of the Naval Ship Systems Command, the test procedures are presently being reduced to Navy standard practice documents. The high interest of metal producers is evidenced by the installation of DT test equipment in a rapidly increasing number of industrial laboratories.

Neutron Spectra Related to Radiation Damage. Experimental studies over several years have provided extensive knowledge of radiation damage in structural steels. This knowledge has been developed to the point where it can be applied in situations involving operational reactors as well as in fundamental studies. One of the most important factors in either of these applications is a definition of the neutron environment in which a particular material was

exposed. The neutron spectrum (i.e., the number and distribution of neutrons by energy) can be changed drastically by different components of the reactor, such as the fuel element, the core structure, and the coolant or moderator. Thus it becomes extremely important to define the neutron spectrum not only for a specific test reactor but also for the reactor to which the data would be applied. Furthermore, it is imperative to know as much as possible about the contribution to damage by neutrons of various energy groups.

In order to resolve both questions, analyses based on advanced computer techniques have been made to describe the spectra for various reactors used in irradiation studies, and these are then related to changes in the mechanical properties of metals. By this procedure it has been possible to account for what appeared to be anomalous variations in radiation effects data. Furthermore, by comparing neutron spectra for test reactors (where most experiments are conducted) with those for power reactors, NRI scientists have developed techniques for analytical adjustment of the experimental neutron fluence values to those which would have been received in the actual power reactor. Such analyses permit a more confident application of radiation effects data to operating reactors.

The computer techniques for neutron spectrum analysis have been successfully tested by comparing embrittlement data for materials irradiated in test reactors with those for materials irradiated in power reactors. The results have proved that the usual spectrum at the pressure vessel of a light-water-cooled power reactor is more damaging than that at the normal irradiation position of a test reactor. This



Neutron spectral characteristics for light water power and test reactors and the resulting materials-embrittlement trends.

was shown to be the result of a higher average energy distribution of neutrons in power reactors and required adjustment of test reactor embrittlement data. In this way it has been possible to use a volume of test reactor data to project with confidence the embrittlement of a power reactor pressure vessel.

The computer spectral analyses have also permitted the evaluation of conventional approaches to the definition of neutron exposure and suggest that the procedure of reporting the number of neutrons having energies over 1 million electron volts should be modified to include neutrons of energies above 0.5 million electron volts in order to provide a better representation of the damage potential of the environment.

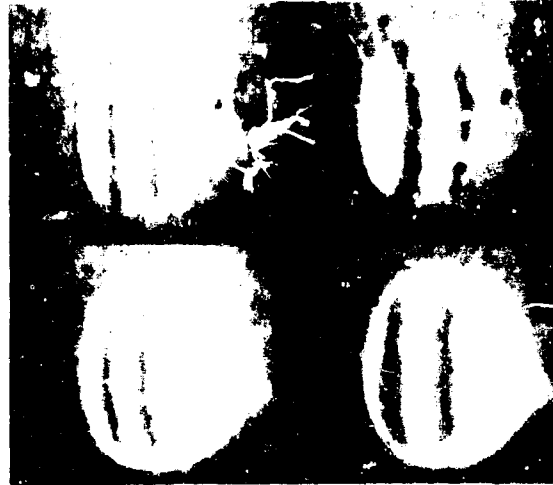
The computer evaluation program has recently been extended to test a number of different neutron damage models. Variations in resulting mechanical properties are the standard by which the different computer codes defining neutron spectra are being judged.

SOLID STATE

Compensation for Thermal Distortion in Glass Lasers.

A principal obstacle to diffraction-limited laser operation is thermal distortion of the glass rod associated with nonuniform absorption of optical pump radiation. Optical pumping can raise the energy of the laser ions to levels above the excited state required for laser action. The ions subsequently decay to the lasing level by a radiationless process which effectively produces heat. Since the laser rod absorbs more of the pump radiation near its surface than at its center, this results in nonuniform heating that causes the optical path length differences (distortion) in the rod; accordingly, the laser rod exhibits birefringence from the thermally induced stress.

Scientists at NRI have developed a simple, inexpensive method of compensating for thermal distortion produced by optical pumping. It is based on control of the temperature of the cooling water that circulates through the laser cavity. Control of water temperature is obtained by the circulation of water from two reservoirs into the laser cavity. The water in one reservoir is a few degrees above room temperature and that in the other a few degrees below room temperature. Approximately 30 seconds before the laser is fired, water from the cooler supply replaces the warmer water in the cavity. The surface of the rod, because it is in contact with the water,



Interferograms through a neodymium-glass laser rod before pumping (upper pictures) and during pumping (lower pictures). Left: Laser rod is in water of constant temperature. Thus, before pumping, the fringes are straight (upper picture), indicating no distortion. After pumping (lower picture), they become distorted. Right: Water temperature is decreased before start of pumping. Thus, the fringes are initially curved (upper picture) but become straight during pumping (lower picture) when compensation is achieved.

is cooled more rapidly than the center, and a thermal gradient is established which is opposite in sense to that subsequently produced by the optical pumping. With optimum temperature control and delay time, the thermal distortion caused by optical pumping is canceled.

This method of thermal compensation should be useful in any glass or crystalline laser system in which it is desired to improve the angular divergence of the beam. As one example, it has been helpful in obtaining reproducible mode-locked laser pulses in a neodymium-glass system.

Third-Order Nonlinear Reflection Studies. Recent studies at NRI have been directed toward the extension of the laws of optics to third order. A third-order optical process can be produced by inducing a nonlinear polarization in proportion to the third power of the electric field strength of a laser wave. It is this interaction which results in the production of the third-harmonic frequency of the laser. Harmonic radiation is usually studied by transmitting the laser wave through a nonlinear medium and observing

MATERIALS

the collinear harmonic radiation which is generated. In addition, there should be a reflected harmonic wave from the surface of the nonlinear medium. Although there have been a number of previous investigations of the generation of *reflected second-harmonic* radiation, the work carried out at NRL represents the first demonstration of the generation of a *reflected third-harmonic* wave.

The nonlinear reflection experiments were carried out by using a neodymium laser operating at 1.06 microns and observing the third-harmonic radiation reflected from a liquid medium at 0.353 microns. The liquid employed was hexafluoroacetone sesquihydrate to which additions of fuchsin red dye were introduced. This medium was selected because it is isotropic, it can withstand repeated exposures to high-intensity laser radiation, and its index of refraction can be tuned simply by adjusting the concentration of dye additive.

The liquid was placed in contact with a specially designed quartz prism so that the laser beam could be incident at the liquid surface in the vicinity of the critical angle for total internal reflection. It is precisely at the critical angle that one observes a much-enhanced, third-harmonic, reflected wave, particularly when the dye concentration is adjusted so that the indices of refraction at the frequencies of the laser and of the third harmonic are identical (so-called phase matching). The third-harmonic reflected signals also were measured with varying degrees of phase mismatching in the liquid.

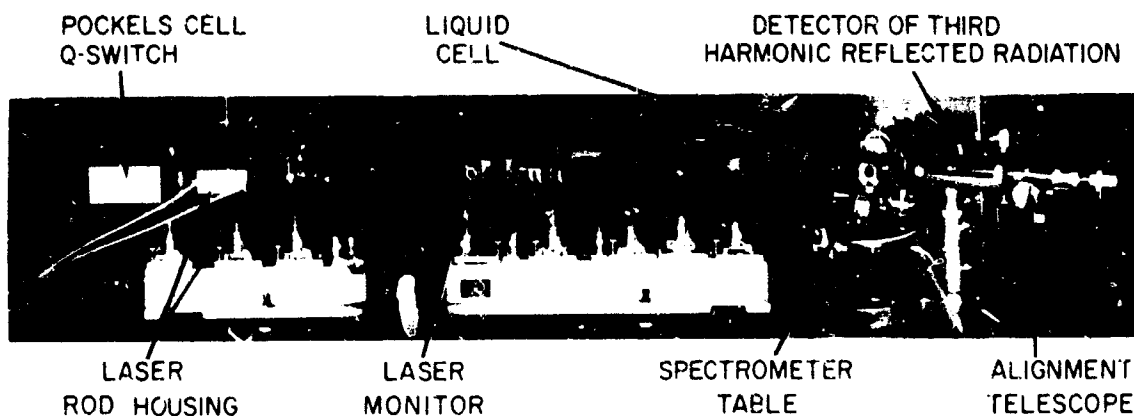
The experimental results of third-harmonic reflected radiation as a function of angle of incidence of the laser wave were found to be in good qualitative

agreement with predictions from theory. A theoretical estimate of the phase of the reflected third-harmonic wave for various angles of incidence was developed, and the predicted nonlinear phase shifts may now be confirmed experimentally.

Atmospheric Depolarization of Laser Light. In 1965 there were reports of observations which indicated that a polarized laser light beam would be heavily modulated by the atmosphere. Such an effect implied that several proposed optical systems then under study for naval applications would not work. NRL measurements, however, over a 2.3-kilometer path showed no modulation of the polarized beam. The equipment used for these measurements had a sensitivity of 10^{-6} (-60 decibels) in terms of the depolarization intensity ratio (S/N).

More recent measurements at NRL have been made with equipment of improved sensitivity and precision. The instrumentation developed for this purpose is capable of detecting depolarization (or polarization modulation) with an intensity ratio of 10^{-8} (-80 db). This increased sensitivity is achieved by the use of improved optical components and an optical bridge technique in which residual light in the depolarized, or signal, channel (that of orthogonal polarization) is balanced by a small controllable fraction of the polarized beam. This technique also minimizes the problems caused by scintillation-induced intensity modulation. This modulation, though severe, affects the signal and reference channels equally and so does not change the balance between them.

Measurements so far have been made at night through relatively clear air. Those made over a 600-



meter path gave negative results, and it was concluded that any atmospheric depolarization present affected less than 10^{-8} of the light signal. This very low figure shows that polarization modulation will not be appreciably affected by the atmosphere.

Underwater Light Source. NRL scientists have developed a unique underwater searchlight that offers several distinct advantages not available with conventional systems now in use. Its chief components are a 2.2-kilovolt, short-arc xenon lamp, a 10-inch-diameter reflector, and an igniter. The light can be adjusted to form an intense, narrow beam for long-distance communications or a diffuse, broad pattern for short-distance illumination.

One unusual feature of the NRL searchlight is that the lamp and reflector are not enclosed in a watertight housing. This reduces weight and bulk, eliminates the problems of window leakage or breakage, and permits easy access to the light source elements for adjustment or replacement. Further, undesirable heat build-up is avoided by dissipation of the heat directly into the water. Of equal importance is the fact that the light does not pass through a window that could attenuate the beam and limit its intensity and diameter. Successful operation of the searchlight under water is effected by insulating the electrical terminals of the lamp from the water by means of watertight connections and by applying a water-insulating rubber coating over the reflective coating



Newly developed underwater searchlight mounted aboard NRL's midget submarine, the SSX-1.

on the back of the reflector. The lamp igniter is enclosed in a watertight housing. Underwater cable is used throughout.

The xenon arc lamp has several distinct advantages over an ordinary filament bulb. It is more efficient and has a higher output of the blue-green light to which water is most transparent, it can be internally modulated for information transmission by direct variation of arc current, and it has a higher intrinsic brightness in a smaller radiating area so that a more intense, concentrated light beam can be projected.

The NRL searchlight has been operated successfully in fresh and salt water. It has seen considerable underwater service mounted atop NRL's midget submarine, the SSX-1. It has been tested in water pressures to 780 pounds per square inch (a simulated depth of 880 feet). After many hundreds of hours of underwater operation, it shows little sign of deterioration and continues to function satisfactorily.

Elastic Constants Determined from X-Ray Scattering.

It is of general scientific interest to know both the absolute values and the directional variances of the elastic constants of crystalline materials. This information is especially useful in the determination of interatomic force constants. Elastic constants are usually determined experimentally through measurements of ultrasonic wave attenuation. In this type of measurement, however, relatively large, preferentially oriented, single crystals are required.

Recently research was undertaken at NRL to determine the elastic constants of a small hexagonal crystal of holmium by measuring the diffuse scattering of x-rays with temperature. The pattern of scattered x-radiation contains information concerning the crystalline lattice vibrations and can be analyzed to yield not only the elastic constants but also other information pertaining to the frequency spectrum of the crystal. The measurements were made on a Picker automated diffractometer with a highly monochromatic x-ray source. The data were reduced and incorporated into a computer program which yielded all five of the significant elastic constants of the material.

This work represents an improvement over ultrasonic techniques because extremely small single crystals of arbitrary orientation can be employed. In addition, the automated technique should yield results of significantly improved accuracy over those obtained with older photographic methods of measuring thermal diffuse scattering intensities.

Negative Etching in Sodium Fluoride Crystals. The discovery at NRL of negative etching in sodium fluoride crystals has enabled NRL scientists to observe directly some of the reactions of point defects in crystals. Negative etching is the converse of positive or conventional etching in that pits, instead of pits, are formed at preferential sites. The apparent sensitivity of the etchant to small concentrations of calcium impurities (less than 10 parts per million) and its negative action may be caused by the cumulative nature of its reaction with impurities whereby an insoluble product is formed that adheres to the surface and prevents dissolution.

In studies of point defects in sodium fluoride crystals, positive etching was observed at individual dislocations and negative etching at grain walls. The positively etched individual dislocations appeared as conical pits; the negatively etched grain walls looked like black lines. In addition to revealing the positions of grain walls, the etchant has been found



Grain walls in sodium fluoride. Negative etching has revealed the initial position, the six intermediate positions, and the final position of the grain wall, which has moved intermittently to the right in response to tensile forces. These features are revealed because the negative etch reacts with impurities left behind when the velocity of the grain wall exceeds a critical value.

to respond to the presence of impurity clusters or small precipitates in these crystals. Thus negative etching provides a new tool for the study of the behavior of point defects in crystals.

High-Pressure Measurements of Shear Strength. NRL scientists are studying the shear strength of materials under high pressures by means of an inverted extrusion press. The results of this kind of measurement have already found applications in geophysics and are now being used in studies of dry lubricants.

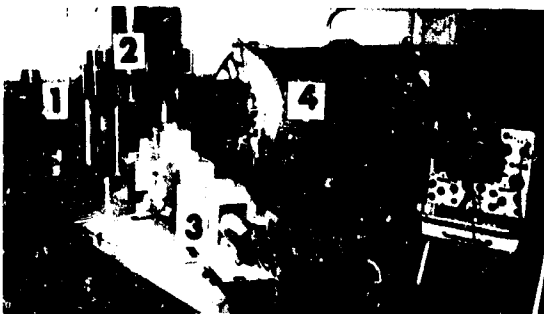
In cooperation with the Air Force Cambridge Research Laboratories, high-pressure shear strength measurements have been made on molecular crystals such as solid argon, metallic elements such as copper, and minerals such as olivine. The NRL group has found that data on these diverse materials all follow a simple and consistent pattern. When the shear strength is expressed as a function of temperature divided by the melting temperature of the element at shear, the data for the members of a given class very nearly coincide. The melting temperature varies considerably with pressure, as does the shear modulus of elasticity.

The pressure and temperature dependences of the shear strength of these several different classes of solids have been shown to follow a simple semi-empirical equation which is consistent with dislocation theory. In organic and other weak or low-melting-point materials the pressure effects tend to be large, and it is among these materials that many of the dry lubricants are to be found. These lubricants can be subjected to very high local pressures in many applications, and their behavior under such conditions should be known and, if possible, understood. The fact that the same mechanisms of shear seem to be acting in materials with such diverse types of bonding as the noble gases, metals, and minerals would indicate that some progress toward such understanding has been made.

Transient Radiation Effects in Quartz and Fused Silica. An important consideration in the design of any device of potential interest to the Navy is its performance in high-radiation environments such as might be encountered in space or in the vicinity of a nuclear blast. Crystalline quartz and glassy fused silica (both are forms of silicon dioxide, SiO_2) are commonly used as optical materials and in electronic devices. Consequently, the effects of nuclear radiation on these materials have been studied extensively.

Permanent radiation damage has been thoroughly cataloged, but it is only partially understood. Transient radiation effects have not been studied previously.

Investigations are being carried out at NRL to determine the nature of transient coloration induced in silicon dioxide by very short, extremely intense pulses of radiation. The pulsed radiation being used in the present experiments has an energy of 600 thousand electron volts and a duration of 3 nanoseconds. Samples of quartz and fused silica are maintained at a constant temperature (either 300°, 77°, or 4.2°K), and radiation-induced coloration is measured by observing the attenuation of a beam of monochromatic light passed through the region of the sample where the incident electrons were stopped. Initial pulse-induced attenuations as large as 30 percent for fused silica and 70 percent for quartz have been observed; these decayed to less than 1 percent of their initial values in about 1 millisecond. The maxima of the transient absorption curves occur at a wavelength of about 215 nanometers. Thus, a normally reliable quartz optical device could be effectively "blacked out" in the far ultraviolet region for as long as 1 millisecond if it should be suddenly exposed to a sharp burst of nuclear radiation.



Apparatus used to study transient optical effects induced by pulsed-electron irradiation. The major components are light source (1), dewar and sample chamber (2), monochromator and detector (3), and pulsed-electron source (4).

One of the findings of the current study is that the curves of transient absorption *versus* wavelength are nearly identical for crystalline quartz and various ultraviolet grades of fused silica. Moreover, these curves closely resemble the *permanent* absorption that can be induced in water-free fused silica by long-term exposure to intense radiation. This permanent absorption has been attributed by previous workers

to electrons trapped on dangling silica tetrahedral orbitals at vacant oxygen sites. Defects of this type have been designated E' centers. From the similarity of the absorption bands, it is tentatively concluded that short, intense bursts of radiation generate E' centers in a transient manner in all forms of silicon dioxide.

Transient luminescence of apparently intrinsic origin also has been observed after pulsed irradiation. Its decay is similar to that of the transient absorption; therefore, the absorption and luminescence are evidently caused by the same transient defect. The precise nature of this defect and its relationship to the stable E' center are now being investigated.

By understanding the process of formation and destruction of radiation-induced defect centers in these materials, NRL researchers hope to be able to counter undesirable changes in physical properties of the materials which occur after their exposure to high radiation doses. A case of obvious interest is the radiation hardening of metal-oxide semiconductor devices, in which silicon dioxide normally forms the oxide layer.

Lattice Vibrations and Infrared Absorption in Mixed Linear Chains. In recent years, much attention has been focused on the calculation of lattice vibration effects caused by point impurities. The extension to the more complicated case of the general disordered system, such as that which occurs in glassy materials, has received relatively little emphasis. The defect vibration problem has often been formulated in terms of the Green's function approach, in which the changes in the lattice vibration spectrum are expressed in terms of the vibrations of the ordered system. While such an approach can be used for dilute impurities, it has not proved feasible for describing the general disordered system. Alternatively, the vibrations of some simple disordered systems can be calculated by direct methods adaptable to high-speed electronic computers.

During the past year, the lattice vibrations and the infrared absorption of mixed linear chains of the type $A_xB_{1-x}C$ have been calculated as large amounts of experimental data on the infrared and Raman spectra of mixed crystals of types CdS_xSe_{1-x} and $Cd_xZn_{1-x}S$ have been accumulated. In earlier attempts, the situation was oversimplified by the use of average force constants and masses rather than a microscopic lattice dynamical approach.

The vibration frequencies and atomic amplitudes have now been calculated by use of a lattice dynamical approach for mixed linear chains. The method is an extension of one developed earlier at NRL for

binary chains. It can be used for any chain having nearest-neighbor interactions and any arbitrary set of masses and nearest-neighbor force constants. This shows that the lattice dynamical approach is quite practical, even for highly disordered systems. The calculated results are in qualitative agreement with the experimental data.

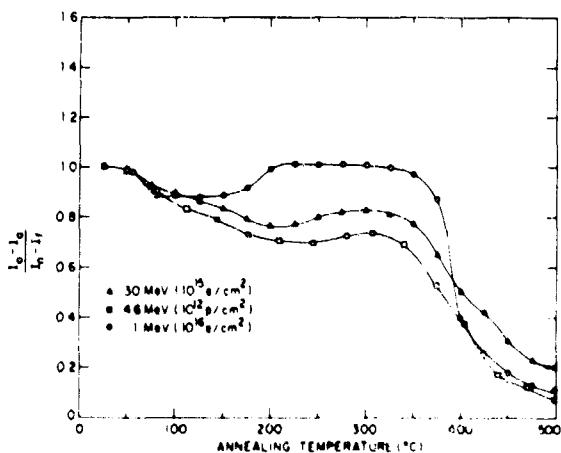
Annealing of Radiation Damage in Solar Cells. Numerous experiments carried out in space and in the laboratory have shown that if a solar cell is bombarded by electrons and protons there will be a degradation of its photoelectric properties. In a silicon solar cell, this radiation damage generally takes the form of isolated point defects caused by displacements of silicon atoms. If, however, the silicon cell is bombarded by high-energy protons and neutrons, a significant portion of the radiation damage will be in the form of clusters of point defects. Post-irradiation thermal annealing studies at NRL have revealed that, if the damaged cell is heated to a sufficiently high temperature, its photoelectric properties can be restored almost completely to the pre-irradiation level. An important part of this work has been the study of the radiation damage process in solar cells as a function of the bombarding particle and its energy.

Thermal annealing experiments with silicon single crystals doped with boron have established that a broad, gradual annealing stage between 50° and

200°C is characteristic of the defect clusters. The annealing of isolated point defects produced by 1-million-electron-volt (Mev) irradiation exhibits an annealing stage near 380°C.

Defect clusters are produced in silicon by a series of displacements of atoms from their normal lattice sites when the energy imparted by the bombarding particle is several times greater than the displacement energy of a silicon atom (~25 electron volts). When the partition of energy between ionization and displacement for recoil atoms in silicon is taken into account, it is found that only electrons of energies greater than 15 Mev can produce significant numbers of displacements (~100) for cluster formation. Previous studies indicate that the influence of clusters comprising less than this number of displacements is too small to affect the electrical properties of silicon measurably.

To determine whether or not high-energy electrons would produce defect clusters, silicon solar cells of the same type as described above were irradiated by electrons of 30-Mev energy at the NRL linear accelerator. It was found that an annealing stage appears over the same temperature range as that identified with the breaking up of defect clusters in proton- and neutron-irradiated solar cells. The similarity of the results for protons and high-energy electrons indicates that higher energy electrons do indeed produce defect clusters in silicon and that 30-Mev electrons can be used to simulate proton damage. Further studies established that this annealing stage is independent of the dopant used in solar cells or of the concentration of residual oxygen impurity present.



Annealing recovery of the short-circuit current output of 10-ohm-centimeter, n-on-p, silicon solar cells following irradiation by 1-Mev electrons, 4.6-Mev protons, and 30-Mev electrons at 30°C. The ordinate shows the unannealed fraction of the short-circuit current.

High-Pressure Transition in Bismuth. The structural transition in bismuth under pressure, with the accompanying changes in electrical resistance, have been widely used for the past 20 years as calibration points for high-pressure equipment. The Bi III-V transition, occurring at about 88 kilobars, has been especially valuable as a fixed point for equipment designed to operate in the 100- to 200-kilobar region, in which calibration points are fewer and much less well defined. The x-ray-equipped tetrahedral press recently installed at NRL has been used to make an independent determination of this point, because its value has been brought into question by the results of recent measurements at Brigham Young University. The university scientists announced that this transition actually occurs at 75.4 kilobars, a 15-

A scientist uses NRL's tetrahedral press and associated x-ray equipment to study the structural transition of bismuth under pressure. The newly installed research tool is capable of producing pressures of over 100,000 atmospheres (100 kilobars) in a volume of 1 cubic inch.



percent shift downward, based on measurements made with a similar press.

The NRL measurements established a value of 74.0 kilobars. The experimental procedure was substantially the same as that used at Brigham Young. A bismuth wire was imbedded in a matrix of sodium chloride, and both were held at the center of a boron-plastic specimen holder placed in the press. The resistance of the bismuth was monitored as a function of pressure, and the pressure was determined by observing the change in the lattice constant of the sodium chloride as derived from its x-ray diffraction pattern.

The resulting value, based on only two runs, was slightly below the value of 75.4 obtained at Brigham Young but could nevertheless be considered corroborative. A working value of 77 ± 3 kilobars was subsequently agreed upon at the National Bureau of Standards' Conference on the High-Pressure Environment held in October 1968, and the NRL value was included in these deliberations. In addition to being quite timely, these experiments were of value in testing the new press and indicating areas where its operation could be improved.

Ammonium Halide Luminescence. The intrinsic luminescent properties of alkali halide crystals at low temperatures have been investigated for some time. Through a series of experiments that included measuring the polarization characteristics of the luminescence, NRL scientists have identified the center as a "self-trapped exciton." This center may be

regarded simply as a localized halide-ion pair in a bonding excited state. The emission data are consistent with theoretical interpretations based on the electronic states that arise in such a center.

Recent efforts at NRL have extended these studies to include ammonium halide crystals. One reason for investigating the ammonium halides is that they have the body-centered-cubic structure in the low-temperature phase as compared with the face-centered-cubic structure of most alkali halides. A more practical reason for investigating radiation effects in ammonium halides is that their high hydrogen content makes them promising candidates for use in fast-neutron dosimetry.

Under continuous x-ray excitation at 4° and 77°K , a single broad emission band was observed at wavelengths of 2,550Å in ammonium chloride, 2,950Å in ammonium bromide, and 3,300Å in ammonium iodide. By correlating the polarization of the luminescence with the orientation of self-trapped holes (a bound pair of nearest-neighbor halide ions with a single electron deficiency), the source of the luminescence has been identified as a self-trapped exciton, similar to that previously found in the alkali halides. By measuring the decay time of the luminescence after pulsed x-ray excitation, it was found that the 2,950Å band in ammonium bromide consists of two overlapping emissions of almost identical energy and band shape.

A technique was developed in the course of these experiments whereby the individual polarizations of overlapping bands could be measured by resolving

them on a time scale when they could not be resolved spectrally. One component has a lifetime of the order of 10 nanoseconds and has its electric vector parallel to the halide-ion pair axis. The other component is polarized perpendicularly to the pair axis and has a stronger lifetime of 800 nanoseconds. A comparison of the properties of these transitions with those observed in the alkali halides led to the conclusion that the self-trapped exciton states are essentially the same in the two materials. In particular, a singlet state evidently initiates the 10-nanosecond allowed transition, while a triplet state initiates the long-lived or forbidden transition. Magneto-optic experiments now being conducted are expected to yield more detailed information about the nature of these states.

Impurity-Perturbed Defect Centers in Alkali Halides.

The effects of radiation damage have been extensively investigated in the alkali halide crystals, and the simplest and best-known atomic defect has been found to be the F center, an electron trapped at a negative ion vacancy. One of the more interesting aspects of the F center's behavior is its ability, as a result of optical excitation, to move through the lattice and to aggregate or become trapped at other defects. In intentionally doped samples, the most common of these compound defects is the F_A center, an F center with a foreign alkali ion at a nearest-neighbor site. The impurity ion next to the F center has proved to be a very sensitive atomic-sized probe for studying the effect of static perturbations on the F center. For example, the F center has one optical absorption corresponding to its 1s-2p transition, whereas the F_A center has two, one of which lies on the low-energy side of the F band. The difference arises from a partial removal of a degeneracy of the F-center 2p state by the alkali ion.

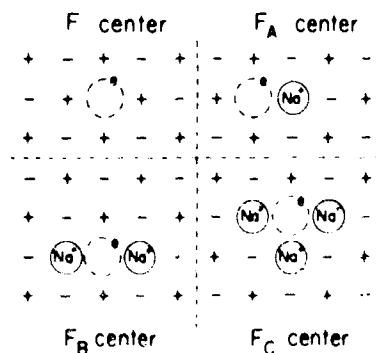
Scientists at NRL have now successfully produced and identified two new impurity-associated defects

which are of primary importance in heavily doped crystals. One is referred to as the F_B center, which in potassium chloride may be a linear array consisting of an F center located between two sodium ions, and the other is the F_C center, which is evidently three nearest-neighbor sodium ions forming an isosceles triangle around an F center. Among their interesting properties is the fact that each center has an absorption twice as far into the infrared region as that for the F_A center, evidently because the 2p function now interacts equally with two or more sodium ions.

V_1 Centers in Alkali Halide Crystals.

Progress has been made in the understanding of radiation damage mechanisms by studying their effects in simple materials. Since the alkali halides are among the simplest ionic solids, they have been subjected to close scrutiny for several decades. Among the multitude of defect centers produced by ionizing radiation in these crystalline materials, one of the basic atomic configurations consists simply of a halogen atom at an interstitial position in the crystal lattice. At low temperatures, covalent bonding occurs between the interstitial atom and its nearest anion neighbors, forming, in the case of potassium chloride (KCl) below 40°K, the linear molecule-ion Cl_4^{3-} , called the H center. This defect H center can absorb light, making it a "color center." Because it has an unpaired electron, it is paramagnetic.

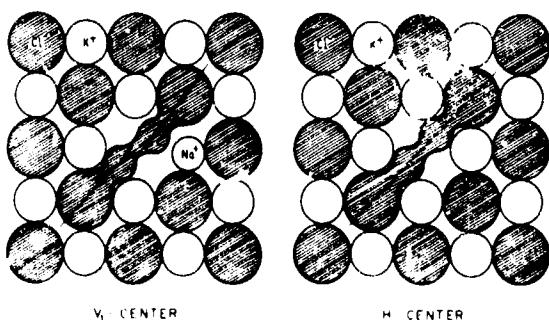
Recent optical evidence indicated that the interstitial halogen atom tends to be located adjacent to a substitutional impurity alkali ion. Electron paramagnetic resonance (EPR) measurements at NRL have corroborated this identification and have provided the first detailed description of the structure of this impurity-associated defect center, designated V_1 . In potassium chloride it is found that the presence of the substitutional impurity ion bends the bond axis of the two central chlorine atoms of the Cl_4^{3-} molecule-ion by about 5 degrees from the normal lattice angle. Further, the unpaired electron distribution is strongly perturbed from its condition in the normal, linear, Cl_4^{3-} H center. The interstitial Cl^0 of the V_1 center can be stimulated within its optical absorption



Schematic representation of F centers in potassium chloride lattice. The F center is an electron trapped at the site of a chloride ion vacancy. The F_A , F_B , and F_C centers are, respectively, an F center with one, two, and three sodium ions substituted at nearest-neighbor potassium sites. The potassium ions are represented by plus signs, the chlorine ions by minus signs.



An electron paramagnetic resonance spectrometer is used to determine the structure of radiation-induced defect centers in potassium chloride.



Models of H and V_K centers in potassium chloride. The bending of the bond axis in the V_K center is due to a substitutional sodium impurity ion.

band to move from the vicinity of its associated impurity ion, and these changes are seen directly by EPR. Another type of motion observed is one in which the interstitial atom moves only among sites neighboring the impurity atom.

This study of impurity-associated defect centers in alkali halides constitutes one further step toward the understanding of radiation damage in more complex, and impure, materials.

Large Zero-Point Spin Deviations in an Antiferromagnet. Antiferromagnetic materials have potential application as components of infrared and millimeter-wave devices. The magnetic properties of these materials are under continuing investigation at NRI. In one aspect of these studies, the elusive and difficult-to-measure phenomenon known as "zero-point spin

deviation" (i.e., the deviation, at the absolute zero of temperature, of the sublattice magnetization in an antiferromagnet from that in a "corresponding" ferromagnet) has been determined by resonance methods. The material used was K_2MnF_4 , which has the important virtue of an ideal, two-dimensional, antiferromagnetic structure. Previous determinations of such a spin deviation have been qualitative at most because the materials measured had three-dimensional antiferromagnetic structures in which the spin deviations are intrinsically small and partly obscured by various perturbations.

For this determination, the values of the transferred hyperfine interactions (which result from interactions between the Mn^{2+} electrons and the ^{19}F nuclei) were obtained from electron spin resonance (ESR) measurements on K_2ZnF_4 (which is isomorphous with K_2MnF_4) doped with Mn^{2+} and from nuclear magnetic resonance (NMR) measurements on the ^{19}F nuclei in K_2MnF_4 . The spin deviation deduced from the combined ESR and NMR results was found to be large and in good agreement with theory.

Vibrations of Atoms in Solids—Localized or Extended?

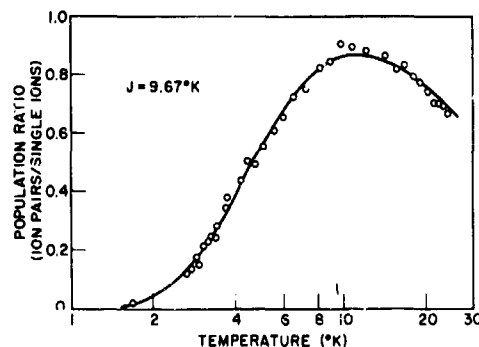
The first paper on the vibration of atoms in solids is still the most famous one: Einstein, in 1906, assumed that all atoms move about their equilibrium positions at the same frequency. By taking Planck's hypothesis of quantized energy states seriously, he was then able to explain the formerly mysterious deviation of the specific heat of solids from the classically expected value and thus provided one of the early confirmations of quantum theory. Although his far-reaching conclusions were found valid, the detailed model for atomic vibrations was oversimplified. In fact, each atom is not tied to some fictitious "hitching post" located at its equilibrium position; it is bonded to other neighboring atoms, and the forces that control one atom's motion depend not only on its own displacement but also on the displacements of its neighboring atoms and, indirectly, on those of all the atoms in the solid. As shown by Born and Von Karman in 1913, the resulting atomic motions in "ordered" solids (i.e., in crystals) are thus far from localized; rather, they are of the nature of waves penetrating the entire solid. The extensive field of "lattice dynamics," developed over the past few decades at NRI and elsewhere, is based on this view.

It is only recently that localized vibrations have been observed and studied again. They have been found to occur in solids containing impurities that

are the lighter atoms of the host lattice. The localized-vibration approach, which is inherently simpler than the ordinary theory of lattice dynamics, has now been justified also for disordered solids, such as alloys and mixed crystals, that contain more than one species of atoms in an irregular sequence but in an ordered matrix. These vibrations can be investigated easily in detail by studying the vibrations of very small solids. It has been observed that local vibrations appear whenever a group of atoms contains light atoms bounded by a sufficient number of heavy atoms. (The number that is "sufficient" depends on force model, mass ratio, and dimensionality, but it is generally small.) The density of these local modes of vibration that would appear in the spectrum of the large solid can then be computed from the probability of the occurrence in the large solid of the small configuration of masses that produces each. Detailed calculations for one-dimensional models have given results in agreement with previously observed peaks in the frequency distribution. Similar features have been predicted for two- and three-dimensional structures, but their intensity, compared with the continuous part of the spectrum, has been smaller.

It is intriguing that localized vibrations have been observed again, and as a major component of the vibrational spectra of disordered solids. The spectra of these solids were expected to be particularly complex. Their comparative simplicity improves the outlook for the success of further studies of the lattice vibrations of disordered solids.

Exchange Coupling of Magnetic Ions. The properties of magnetic crystals have been extensively exploited in various microwave devices. The existence of these useful properties depends on the spatial ordering of the spins, caused by the exchange interaction between pairs of nearby magnetic ions, that occurs in these materials. In the simplest cases, this exchange interaction is described mathematically by the Heisenberg hamiltonian $\mathcal{H} = J S_1 \cdot S_2$, where J is the exchange constant. This isotropic expression is especially accurate for S-state ions, such as Mn^{2+} , which have no orbital angular momentum. The value of J can be determined for a given compound from macroscopic magnetic measurements. The J value obtained, however, is rather dependent on the importance attributed to exchange interactions with magnetic ions more distant than nearest neighbors. As a result, any method which directly measures this exchange interaction for a known pair of ions allows



Typical electron paramagnetic resonance data used to determine the exchange constant J of exchange-coupled Mn^{2+} pairs in $KZnF_3:Mn^{2+}$. The population of the $S = 1$ state (ratio of pair to single ion intensity) of a nearest-neighbor Mn^{2+} pair is plotted as a function of temperature and compared with the theoretical expression for that state (solid line). The value $J = +9.67^\circ K$ is found from a least-square fit of the data to theory.

an evaluation of the theoretical calculations which are now becoming possible.

With this end in view, the electron paramagnetic resonance of exchange-coupled pairs of Mn^{2+} ions has been observed in Mn^{2+} -doped $KZnF_3$, which has a cubic perovskite structure. The $Mn:Zn$ ratio used was approximately 0.01. The angular dependence of the Mn^{2+} pair spectrum showed that the pair axes are along the three cube edges. Thus the Mn^{2+} pairs are nearest magnetic neighbors and are expected to be antiferromagnetically coupled. From the temperature dependence of the intensity of selected pair lines in the region of 1.5° to $25^\circ K$, the exchange constant J is found to be $+9.9^\circ K$, a value in good agreement with the magnetic properties of pure $KMnF_3$. This agreement confirms the assumption, which was based on the unusual crystallographic structure of $KMnF_3$, that only nearest-neighbor exchange interactions are important in that material.

Potential Electrolyte for a Truly Dry Cell. The usual dry cell is dry only on the outside. Inside of the cell is a paste-like electrolyte, which enables the cell to discharge when not in use. This undesirable characteristic, among others, has led to an increased tempo, on the part of military and civilian users alike, in the search for new battery materials. In recent years, several batteries have been developed that contain



An NRL scientist measures the ionic conductivity of ammonium chloride single crystals at elevated temperatures. These and similar materials have potential use as solid electrolytes in dry cell batteries.

solid electrolytes having high ionic conductivity and little or no electronic conductivity.

NRL scientists have been studying the ionic conductivity of several solids in the alkali and ammonium halide families. The results of their experiments have provided new insights into the atomistic mechanisms that permit ions to move through the lattices of ionic crystals. This work has given evidence for interactions between the charge carriers, for the influence of the thermal vibrations of the ions, and for the possible existence of single, double, and even triple lattice vacancies.

Most recently, the NRL scientists have measured the ionic conduction of ammonium chloride single crystals in their regular (NH_4Cl) and deuterated (ND_4Cl) forms, during which the relatively rapid motion of the hydrogen ion was verified. The practical application of this material in a solid state battery will require further study.

Dosimeter for High-Energy Pulsed Radiation. For the first time, a dosimeter has been developed which can be used to measure doses deposited in material by very short pulses (300 microseconds or less) of

high-energy ionizing radiation. Its principle of operation is the optical fluorescence produced when ionizing radiation is absorbed in dilute ruby (Al_2O_3 with a chromium content of about 0.001 percent). The fluorescence observed is at wavelengths of 6,943A and 6,929A (commonly known as the R lines) and has a lifetime of 3 milliseconds.

In the experimental arrangement, a ruby crystal is exposed to the same pulse of ionizing radiation that passes through a test material. The resulting ruby fluorescence is detected by a photomultiplier (out of the direct path of the radiation beam), displayed on a fast oscilloscope, and recorded photographically. In this application of the dosimeter, a light shield is used to prevent spurious fluorescence from interfering with the dose measurement. For situations in which the radiation does not penetrate the test material, the ruby dosimeter may be placed elsewhere in the radiation field.

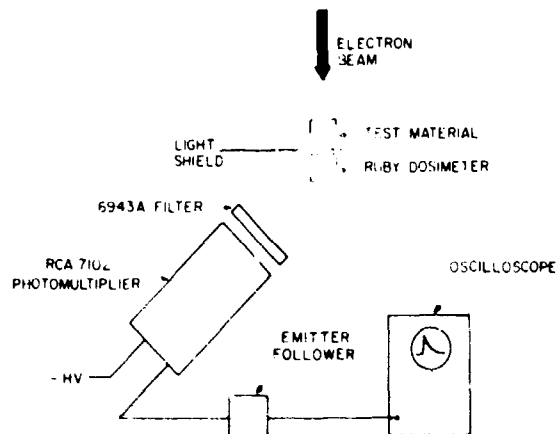


Diagram of NRL's ruby dosimeter system used to measure doses deposited in materials by very short pulses of high-energy ionizing radiation. The electron beam impinges on the ruby dosimeter. The R-line fluorescence is detected by the optically filtered multiplier and coupled by an emitter follower to the oscilloscope.

A plot of fluorescence intensity *versus* dose is linear when the intensity is measured 1 millisecond after a 0.5-microsecond linear-accelerator pulse of 30 million electron volts. The 1-millisecond delay avoids radiation-induced detector noise that generally occurs during the first few hundred microseconds. The linear relationship of the fluorescence intensity with dose makes it possible to use the photomultiplier response

as a direct measure of the relative dose delivered. This linearity was found to hold for absorbed doses up to 1×10^6 rads (ruby) per pulse, the maximum attained on the NRL linear accelerator.

The two distinct advantages of this dosimeter are that the dose can be determined immediately and that the dosimeter is reusable without any treatment, at least for cumulative doses up to 10^6 rads (ruby).

Electronic Transport Phenomena in Simple Metals. Understanding the electrical resistivity of metals at low temperatures and the increase of this resistivity due to magnetic fields (i.e., magnetoresistance) constitutes one of the most fundamental problems of solid state physics. The theory of these transport phenomena (charge motions) requires detailed knowledge concerning the anisotropy of the intrinsic parameters of both the electronic band structure with its associated Fermi surface and the electronic scattering mechanisms responsible for the mean free path. The scattering mechanisms responsible for the mean free path and its anisotropy are of great interest in solid state physics, but very little progress has been made in understanding these mechanisms because definitive experiments have been lacking. Values for the Fermi-surface and mean-free-path parameters cannot be obtained separately from resistivity measurements made in the absence of a magnetic field (H). Field-free measurements yield only a combination of their values and, furthermore, only the average of their combined magnitude. Magnetoresistance measurements at high H , however, can determine the anisotropy of these combined parameters.

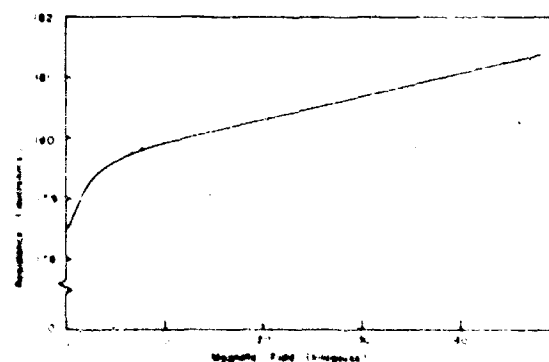
Over the past decade, intensive research on metals has produced a virtual explosion of experimental and theoretical information which does provide the desired Fermi-surface parameters separately. All non-Group I metals have multiple Fermi surfaces with very complex shapes and are extremely difficult to treat theoretically. Each of the Group I metals has only a single Fermi surface. While the Fermi surface shape for the noble metals is still somewhat complex, for sodium or potassium it is very simple and is spherical to 0.1 percent. Thus, sodium or potassium closely approximate a free-electron metal and should be most suitable for theoretical treatments.

Standard magnetoresistance theories have been extraordinarily successful in *qualitatively* explaining the principal characteristics of the magnetoresistance

for the simple noble metals as well as for the complex, non-Group I metals. For 40 years these theories have repeatedly predicted that the magnetoresistance should become independent of H (i.e., saturate) at high H for such free-electron metals as sodium and potassium. Until this year, however, all attempts to verify this saturation theory revealed only linear behavior.

NRL scientists had been studying the magnetoresistance of pure metals at extremely low temperatures in order to identify the best conductors for cryogenic magnets. As an outgrowth of this study, experimental techniques developed for observing the intrinsic saturating behavior greatly reduced the magnitude of the macroscopic linear effects. They also showed that the magnetoresistance of potassium would exhibit the long-sought intrinsic saturating behavior, which until now has been well masked by the superimposed, overwhelmingly linear behavior. The percentage of the resistance from $H = 0$ to saturation, $(\Delta R/R_0)_s$, was at least 100 times smaller for potassium than the $(\Delta R/R_0)_s$ values observed previously for more complex metals. The masking linear behavior was found to be caused by macroscopic rather than intrinsic phenomena. These macroscopic phenomena are the distortions of the electric field and the potential distributions in a magnetic field caused by nonuniform current distributions and the effects of the sample geometry. The distortions give rise to a magnetoresistive voltage proportional to the absolute value of the Hall voltage, which is linear.

The quantity $(\Delta R/R_0)_s$ is a direct measure of the combined anisotropies of the Fermi surface and the



Resistance versus magnetic field for potassium at 4.2°K. The solid curve indicates both a saturating and a linear behavior. The dashed line represents the linear component of the solid curve.

mean-free-path. The very small observed values of $(\Delta R/R_0)$, are still 100 to 1,000 times too large to be explained by the accurately known Fermi-surface anisotropy of about 0.1 percent. Therefore, the observed $(\Delta R/R_0)$, must be due to a large mean-free-path anisotropy. This can most probably be attributed to electron-phonon scattering anisotropy caused by the highly anisotropic phonon dispersion recently revealed in measurements of potassium. The current experiments represent a breakthrough in obtaining the quantitative mean-free-path information necessary for a more complete understanding of the fundamental theory of electrical resistivity and magneto-resistance.

Electronic Impurity States and Optical Phonons in Semiconductors. As an outgrowth of research on far-infrared detectors, an investigation has been made of the coupling of electronic impurity states in semiconductors to the thermal vibrations of the ions. Certain of the thermal vibrations are characterized by the ions of opposite charge moving in opposite directions, so that a macroscopic electric field is produced during the vibration. Because of their macroscopic electric field, these particular thermal vibrations, known as longitudinal optical phonons, strongly scatter charge carriers such as electrons or holes. This scattering is an important factor in determining the electrical resistivity of the material and its performance in devices.

When a semiconductor is placed in an external magnetic field, the conduction electrons execute circular orbits and may absorb or emit electromagnetic radiation, a phenomenon called cyclotron resonance. For n-type indium antimonide (InSb) in magnetic fields between 10 and 100 kilogauss, cyclotron resonance occurs in the infrared spectral region. When the InSb is cooled to liquid helium temperature, the conduction electrons become localized at impurities, and the cyclotron resonance line is shifted to a higher frequency.

If the magnetic field is adjusted so that the impurity-shifted cyclotron resonance frequency coincides with the frequency of the longitudinal optical phonons, one may expect interesting effects arising from the interaction of the impurity electrons with the macroscopic electric field of the phonons. NRL scientists have carried out such an experiment using n-type InSb and have found that the impurity-shifted cyclotron resonance line is split into as many as six subsidiary peaks. This splitting is striking confirmation of the importance of the coupling of the impurity

electron to the longitudinal optical phonons and corresponds to scattering of the electron by the phonons from an excited intermediate state to a number of discrete final states of the impurity.

In a related investigation, NRL scientists have further shown that electrons in InSb are not strongly coupled to transverse optical phonons which, in contrast to longitudinal optical phonons, are not accompanied by a macroscopic electric field. This result demonstrates the importance of the macroscopic electric field in the scattering of current carriers by phonons.

STRUCTURE OF MATTER

A Molecular Trap. Inclusion compounds are defined as molecular combinations in which one component, the "guest," fits into a cavity in the other, the "host." When the cavity is a three-dimensional enclosure that traps the guest molecule from all sides, the host is referred to as a clathrate or cage structure. No ordinary chemical bonds need exist between the atoms of the two compounds.

There are six basic types of inclusion compounds, characterized by the shape of the cavity found in the host. These compounds are finding uses in industry. Water clathrates, for example, are used in reclaiming fresh water from sea water. Inclusion compounds also play a role in the chemistry of living cells. Proteins form inclusion compounds which are shape-dependent. This shape-dependence accounts for biochemical specificity.

Water clathrates, often called gas hydrates, are perhaps the best-known inclusion compounds and have been the subject of extensive chemical and x-ray investigations. Until lately, however, very little x-ray work beyond the determination of the space group and the cell dimensions has been attempted on large organic inclusion compounds such as the cyclodextrins and Dianin's compound (first prepared in 1914). A. P. Dianin observed that his compound formed crystalline adducts with ethanol, acetone, acetic acid, chloroform, and ether. This guest list

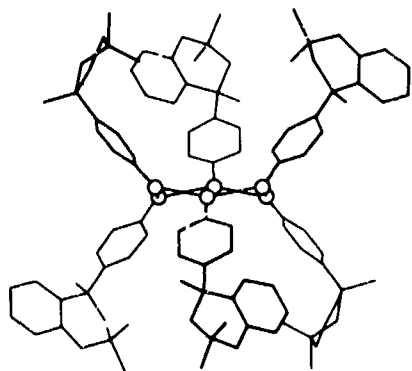


Chemical formula of Dianin's compound, $C_{12}H_{20}O$.

MATERIALS

was later expanded to approximately 40 compounds by Baker and McOinic, and it could grow even larger. In 1955, Powell and Wetters did some preliminary x-ray work to determine the space group and cell dimensions. The actual structure was not solved at that time, but it was predicted that Dianin's compound formed inclusion compounds of the cage or clathrate type.

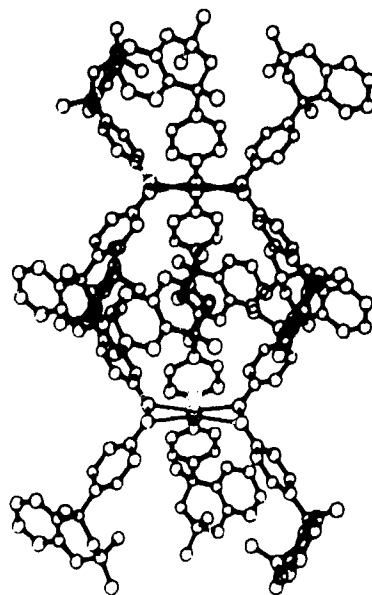
The crystal and molecular structure of Dianin's compound has been solved recently at NRL. Six molecules of Dianin's compound are linked, through hydrogen bonding of the OH groups, to form a large complex which then enters into the cage formation.



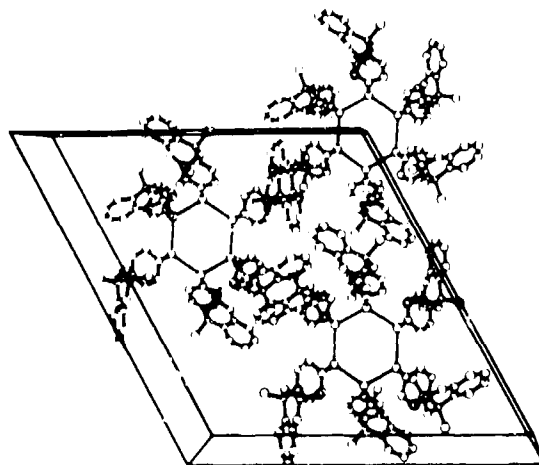
A single complex formed by six molecules of Dianin's compound held together by hydrogen bonding of the OH groups.

A single complex resembles two truncated cones having in common their smaller bases formed by the hexagon of hydrogen-bonded oxygens. The space group of the crystal is $R\bar{3}$. In this space group the cages are formed by piling the complexes directly above each other *ad infinitum*, with their symmetry axis parallel to the c-axis, to form long columns of successive enclosures. Most of the cage is formed when two of these complexes stack together with one hexagon of hydrogen-bonded oxygens forming the floor of the cage and the next hexagon of hydrogen-bonded oxygens one unit cell away along the c-axis forming the ceiling. Bounding of the cage is completed by one molecule from each of its six nearest neighboring complexes. In this way the long columns are interrelated, and the only spaces in the cell large enough to ensnare a guest molecule lie within the cagelike cavities of the host.

Determining the structure of the host molecule is only the beginning of this study. It should now be



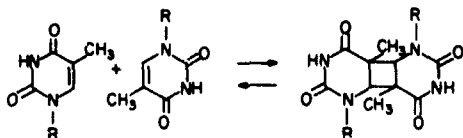
Two complexes of Dianin's compound stacked together to form a cage.



Contents of the unit cell of Dianin's compound, drawn looking down the c-axis.

possible to study the detailed structure of the guests which, by themselves, at room temperatures often form poor crystals or none at all. The large number of inclusions that can be formed with Dianin's compound provides an unusual opportunity to make an extensive study of the structures and properties in the relatively new field of organic clathrates.

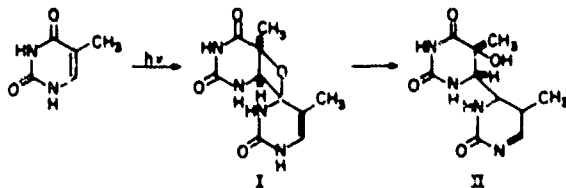
Radiation Damage to Hereditary Material. One of the serious consequences of irradiating human tissue is the damage that occurs to the hereditary material DNA. It was found in 1960 by Wang (at Tufts University) and Beukers, Ijlstra, and Berends (in the Netherlands) that the thymine bases in a DNA molecule can react to form dimers of the following type:



where R represents the remainder of the DNA chain to which the thymine base is attached. Since the DNA molecule acts in terms of a sequential code, the formation of the dimer constitutes a damaging perturbation. Interestingly, other radiation can reverse the reaction by breaking the dimer, as indicated by the backward arrow.

Recently, Varghese and Wang (now at Johns Hopkins University) found a new product, formed from two thymine bases upon the irradiation of DNA. The same product can be obtained upon irradiation of the free bases. This material was shown to be different chemically from the dimer described above, and it has not been possible to reverse the reaction by use of additional radiation. It would appear, then, that this type of radiation damage would be even more difficult to correct. In any case, a first step in prevention or correction is to identify the chemical composition and molecular geometry of the product.

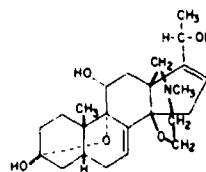
Professor Wang sent one small crystal of the new reaction product to the Naval Research Laboratory for structure analysis by x-ray diffraction. Advances by NRL scientists in solving the phase problem in x-ray structure analysis have made this method particularly well suited for determining the composition and geometry of unknown materials. The structure determination was carried out, and the molecular formula and configuration were established to be as shown in Formula II, below. The reaction can be described by:



One of the benefits from determining the end product of a rearrangement reaction is the opportunity afforded to postulate the intermediate steps in a reaction mechanism. Formula I represents such a postulate.

Further investigations are proceeding in this area. For example, Wang has recently isolated an adduct made from three thymine molecules. The determination of the composition and configuration of this molecule will make a very interesting and worthwhile study. Information from investigations of this type is quite useful in the fields of genetics and radiation damage to hereditary material.

Structure of Poison-Dart Frog Venom. The Colombian poison-dart frog, *Phyllobates auretaenia*, produces in its skin a venom which the native Indians use to tip their arrowheads when hunting game. The venom is the most potent yet discovered. It has a toxicity about 250 times that of strychnine, but, to be active, it must be introduced into the body through the pierced skin. Taken orally, it is harmless. Biochemists from the National Institutes of Health traveled to Colombia to collect about 4,000 frogs and extract their venom. (The frogs, which are only 2 to 3 centimeters long, are too delicate to survive a trip to Washington.)

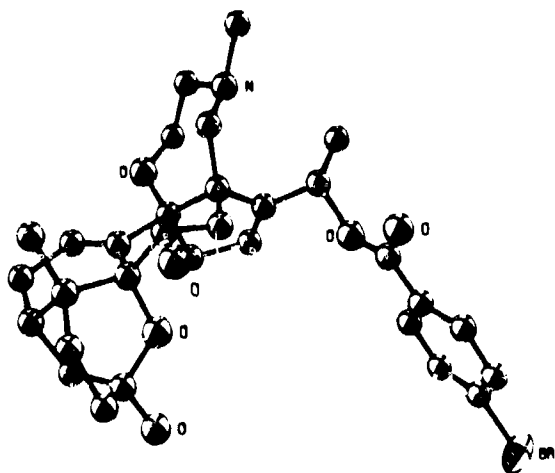


Chemical formula of batrachotoxin A, $C_{24}H_{35}NO_5$
(R = H, Br, C_6H_4CO-).

The major alkaloid fraction isolated from the frogs consists of batrachotoxin, isobatrachotoxin, and pseudobatrachotoxin, all $C_{24}H_{33}NO_4$. Pseudobatrachotoxin is very unstable and is readily converted to batrachotoxin A ($C_{24}H_{33}NO_5$) with the formal addition of H_2O . Such minute amounts of the purified alkaloids were available that it was not feasible to establish the structural formulae by chemical analyses. Hence, x-ray diffraction analysis, which can handle extremely small specimens, was indicated. Thus far, the only crystals suitable for an x-ray analysis were those of the O-p bromobenzoate derivative of batrachotoxin A.

MATERIALS

A very small crystal ($0.05 \times 0.03 \times 1.0$ millimeter) of this derivative was sent to the Naval Research Laboratory for x-ray analysis. Because the bromine atom occurs on a cell edge in the unit cell, phases based on the heavy atom would lead to a fourfold ambiguity. In addition, the relatively weak scattering from carbon atoms and the very limited number of data obtainable from the small crystal prevented the use of the classical heavy-atom technique for structure determination. Two peaks could be recognized as corresponding to oxygen atoms in the fourfold ambiguous Fourier map obtained from a knowledge of the phases from the bromine atom position. The bromobenzoate group could thus be located, and the complete structure was established by using a recycling procedure based on a partial structure and employing the tangent formula developed at NRL.



Structure of Colombian poison-bart frog venom.

The structure of batrachotoxin A is quite novel. It is both an alkaloid derived from an animal source and also a steroid. Its structure resembles that of digitoxigenin, a component of digitalis, the well-known heart drug. It is therefore not surprising that the lethal effect of the venom derives in part from its action as a cardiotoxin.

CHEMICAL PHYSICS

Biological Adhesion. In contrast to the substantial progress which has been made in understanding and controlling adhesion in man-made systems, knowledge of the mechanisms governing adhesion in bio-

logical systems remains far from complete, despite extensive investigation by the traditional techniques of biology and medical science. NRL scientists have attempted a new approach whereby knowledge gained from past, basic surface-chemical studies could be used to provide advantageous starting points in the search for a better understanding of biological adhesion.

This interdisciplinary approach has already resulted in improved insight into the role of the naturally occurring adhesives and adhesives encountered in biology. The NRL workers have pointed out that viscous liquids, particularly those thickened by natural biopolymers, could serve as useful adhesives in the relatively mobile and conformable systems found in living organisms. Adhesives which fail to solidify result in joints of limited technological significance because of their relatively low resistance to shear. Such adhesives may be far more important in nonrigid biological assemblages, however, where efficient mating of contours permits an intervening liquid film to function as an adequate adhesive. Moreover, the susceptibility of naturally occurring thickening agents to cross linking or to depolymerization by dilution or enzymatic action would account for the rapid and reversible changes characterizing living systems. These results thus provide guidance in designing synthetic adhesives for biological systems.

Specific mechanisms have been identified by NRL scientists as highly probable causes of both surface attraction and modification in the contact interaction of blood with foreign solids, such as plastic or metal biological or surgical implants. The implications for blood coagulation and thrombus formation should influence future research on plastic prosthetic implants, including their selection and design. Finally, a surface-chemical interpretation of reported cell-aggregation studies sheds some light on possible causes for the development of mobility in cancer cells.

Surface Chemistry of Liquid-Liquid Interfaces. Recent NRL studies of the spreading of several classes of polar-nonpolar organic liquids on water have shown that two of the most basic physical interactions between two liquids—interfacial surface tension and mutual solubility—can be measured with simple surface-chemical methods.

It has been proved theoretically and experimentally that the interfacial tension between two liquids can

be accurately calculated from the spreading pressure of one upon the other. Especially important is the fact that the calculated values of interfacial tension are as precise as the best reported values obtained by direct measurement, if not more so. Moreover, it is very difficult to make an accurate direct determination of interfacial tension because every method used is extremely sensitive to traces of surface-active impurities, present in either of the liquids or in both, that diffuse to and adsorb at the interface. Use of the spreading pressure method not only eliminates or minimizes this difficulty but also provides much greater speed of the measurement—a few seconds as compared with hours.

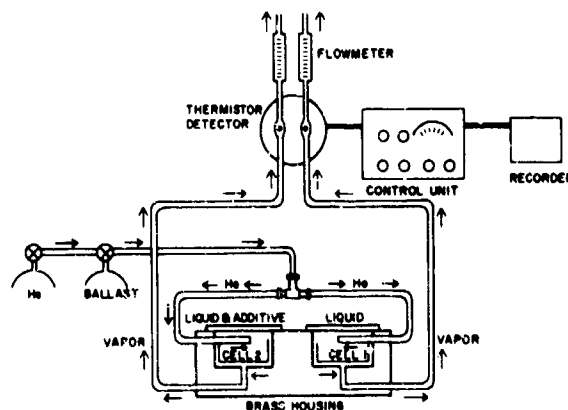
This investigation also showed that interfacial tension data can be used to estimate the solubility of water in an organic liquid. Since few reliable or consistent literature values for interfacial tension and water solubility are available and their direct measurement is very difficult and time consuming, the results of this work will be of increasing interest, not only to investigators in physics and chemistry but to those in biochemistry, physiology, and pharmacology.

Effect of Adsorbed Films on Evaporation of Volatile Liquids. A study has been made to determine the effect of adsorbed surface-active molecules on the rate of evaporation of volatile organic liquids. The soluble, partially fluorinated additives investigated were those which previous research had proved to be the most surface-active agents for organic liquids. When these were adsorbed from solution, no change in the rate of evaporation was observed under a variety of the most favorable experimental conditions for adsorption of closely packed films. Monolayers of insoluble surface-active compounds at the air-liquid interface also produced no detectable reduction in the rate of evaporation of organic liquids. Even insoluble, multimolecular films of the most surface-active silicones did not significantly reduce the rate of evaporation until the film thickness was increased to at least 0.04 millimeter, a very thick film compared with the thickness of a monolayer, which is approximately 2.0×10^{-6} mm. Hence, fluorocarbon surface-active compounds by themselves would not be expected to decrease gasoline evaporation.

It has also been found that thin, metastable films of water could be spread on the surface of most volatile organic liquids if certain partially fluorinated surface-active additives were used as wetting agents. Only when these aqueous films reached a thickness of

approximately 0.005 mm did they begin to have a significant effect on the evaporation rate.

These results prove that, in the so-called Light Water mixtures used for extinguishing fuel fires, the fluorocarbon additives cause the aqueous surfactant solution to spread on the fuel or other volatile organic liquid. These additives may improve the properties of the aqueous foams, but they will not by themselves impede the rates of evaporation of the organic liquids. It can be concluded that the only effective evaporation barrier present in Light Water foams is the thick layer of water trapped in the wall of each foam bubble or left on the fuel surface as a thick film.



Dual-cell thermal conductivity apparatus used at NRL for measuring relative rates of evaporation of volatile liquids.

Mechanism of Action of Dry-Film Lubricants. Thin solid films of low shear strength are now widely used to lubricate sliding systems in which oils or greases are inadequate. Results of an earlier pioneering investigation at NRL suggested that, as a first approximation, the coefficient of friction for many such dry films was equal to the ratio of the mean yield pressure of the film material to that of the substrate. It was pointed out, however, that one factor neglected in the derivation of this relationship was the effect of pressure on the shear strength of the film.

Recently, in a reanalysis of the problem, variation of shear strength with pressure was incorporated into the relationship as a significant factor. The new theory has made it possible to predict the coefficient of friction for any dry-film lubricant on any harder

supporting surface. The equations derived also express the pressure on the film in terms of the elastic or plastic properties of the supporting solid.

The measured coefficient of friction of such diverse solid-film lubricants as gold, paraffin, and molybdenum disulfide under a variety of conditions closely approximated that predicted by the new quantitative relation. Therefore, it is now possible to eliminate much of the old trial-and-error approach and to predict the potential of any solid material for use as a dry-film lubricant. Two prerequisites for any candidate material would be a low shear strength at atmospheric pressure and a low rate of increase in the shear strength with increasing pressure.

Effect of Adsorbed Monolayers of Water on Solid Surfaces. Recent NRL investigations have elucidated the influence of adsorbed water on the wetting and spreading behavior of pure nonhydrophilic (non-water-loving) liquids on solid surfaces. The interaction between a liquid and a solid surface can be quantitatively expressed by a parameter called the critical surface tension of wetting (γ_c). A liquid having a surface tension greater than γ_c will not wet or spread on the solid, whereas one with a value below γ_c will completely spread over the surface. When the interaction arises from dispersion forces only (that is dipole-dipole polarization forces), γ_c is expected to be the same for all such series of homologous liquids. If, however, nondispersion forces also are active, γ_c is increased by an amount proportional to the contribution of such nondispersion forces.

The wetting behavior of a number of nonhydrophilic organic liquids on solid surfaces which were fully or partially coated with water molecules was shown to follow the same fundamental laws. Here, the nondispersion forces acted between the water film and the contacting organic liquid molecules.

A variety of high-energy hydrophilic solid surfaces such as glasses, minerals, metals, or metal oxides were investigated. The formation of only a fraction of a monolayer of water adsorbed at a relative humidity (RH) of 0.6 percent converted each high-energy surface to one of very much lower energy, with a coincident reduction in γ_c ; additional water adsorption at 95-percent RH formed a more condensed film and further lowered the γ_c value. Furthermore, the γ_c values at each extreme of RH were nearly

identical for all of these diverse solid surfaces. Thus it was concluded that, after exposure to a humid atmosphere, the surface energy of any clean, smooth, high-energy hydrophilic surface depends on the concentration of water adsorbed on the surface and that the chemical nature of the underlying substrate has little other effect on wetting and spreading properties of any nonhydrogen-bonding liquid. A monolayer of adsorbed water thus exerts an important influence.

Unless the solid surface is completely free of adsorbed water molecules, spontaneous spreading of many organic liquids will be impeded, with concomitant decreased adhesion of the liquid to the solid. These results also support the frequently used assumption that adsorbed water lowers the surface energy and so assists in crack propagation.

CENTRAL MATERIALS RESEARCH

Bond Formation in Transition Metals. A new approach to the formation of bonds between atoms in transition metal compounds and alloys promises to increase our understanding of this important class of materials. This approach, developed by an NRL scientist, involves the chemical concept of concentrating electron density into the areas between atoms. However, each bonding orbital (composed of atomic wave functions) concentrates the electron density into two different directions simultaneously, instead of the usual single bonding lobe. This new feature results in fairly unique descriptions of the bonding and local orbitals and is necessary because each atom interacts strongly with more near neighbors than the number of available bonding orbitals of the usual type. It is well known that the predominant coordination numbers (i.e., near neighbors) observed in transition metal compounds are 12, 14, 15, and 16. The higher coordination numbers (14, 15, and 16) are often associated with the formation of the brittle, and structurally complex, phases. In these phases it has been shown that particular transition elements prefer certain coordinations. These preferences can now be partially understood in terms of the atom's position in the periodic table and in terms of the atomic d-orbital character used in the bidirectional bonding orbitals required for each different coordination number.

The method has been applied recently to the Laves phases, which belong to a large, well-known class

of intermetallic compounds of the composition AB_2 . One of the problems in the understanding of these materials is that the A-atom has unusually short interatomic distances with four of its near neighbors (also A-atoms) but normal distances with twelve B-atom neighbors. Treating the atoms as hard spheres, as is often done in discussing the packing of atoms in alloys, produces a contradiction. It suggests that the A-atom is in a state of severe compression with respect to the A-near-neighbors but is not compressed with respect to its interaction with its B-atom neighbors. This contradiction is resolved by the use of bidirectional orbitals, which points out that the orbitals forming the bonds between A-atoms have a much larger atomic d-orbital character than those of the A-B bond and accordingly should have a smaller effective radius in that direction.

Growth of PZT Crystals. The more general piezoelectric properties of lead zirconate titanate (PZT) as a ceramic material have been known and used effectively by the Navy for many years. A more detailed understanding of this material is needed, however, including such factors as domain characteristics, interaction between domains, and domain wall motion, because it is these factors that govern a majority of the properties important to the use of ceramics in sonar systems. No adequate investigation has been made of these factors because single crystals of PZT of good quality large enough for such studies have not been available.

NRL has developed a technique for growing crystals of sufficient size to be useful in the detailed study of domain and piezoelectric properties. The crystals are prepared by flux growth from a solution of PZT in lead borate at an elevated temperature. Pure powdered mixtures of lead oxide, zirconium oxide, titanium oxide, and boron oxide are placed in tightly covered platinum crucibles and heated to 1200°C to form a solution of PZT in the borate melt. The crucibles are cooled in a carefully controlled and programmed oven at a very slow rate over a temperature interval of several hundred degrees. The crystals nucleate and grow from the melt during the slow cooling process. The oven is then cooled to room temperature, the crucibles are opened, and the borate flux in which the PZT crystals are imbedded is leached out by solvents. Crystals $5 \times 5 \times 3$ millimeters in size have been produced from flux melts of PZT and are now being evaluated.

Research directed toward the understanding and control of the piezoelectric properties of PZT will contribute to our fund of basic knowledge concerning ceramic solids. It will also lead to more reliable sonar transducers and other devices useful to the Navy.

COMBUSTION SUPPRESSION

Fire Protection for Aircraft Carriers. The modernization of aircraft carrier fire-extinguishment systems is imperative if future catastrophes, such as those aboard the *Forrestal* and the *Enterprise*, are to be averted. At NRL, efforts in solving this problem have been directed toward an extended use of Light Water in all the fire-protection systems. Light Water is an effective mixture of perfluorinated surfactants produced commercially and developed by NRL chemists for use in extinguishing fuel fires and halting flammable vapor emission from fuel surfaces.

Early in 1968 a new fire-protection concept for carrier flight decks was explored in which the nuclear-fallout-washdown nozzles already built into the flight deck could be used as part of the fire-fighting system. Laboratory tests indicated that the Light Water solutions introduced directly into the sea water systems supplying these nozzles would immediately extinguish jet fuel fires burning on the deck. It was also found that Light Water solutions applied from existing overhead water sprinklers used on carrier hangar decks should be equally effective in extinguishing spilled jet-fuel fires. (Ordinary water sprayed from these sprinklers would merely spread the fire across the deck.)

Recently, at the Jacksonville Naval Air Station, NRL engineers conducted full-scale "proof" tests on large fires equivalent to that aboard the *Forrestal*. Under these mock-up conditions, Light Water, when used in the shipboard high-capacity fog-foam system, was up to seven times more efficient than the old protein-type extinguishing agents. When used in the washdown system at impingement densities of 0.03 gallons per minute per square foot, it extinguished a mocked up flight deck fire in two minutes, even in a 30-knot wind.

As the result of an earlier NRL study, a change-over to the use of Light Water at naval air stations was made in 1968. Engineering studies are now under way at NRL to provide the design data necessary for equipping all aircraft carriers with Light Water.

GENERAL SCIENCES

An Overview: by Wayne C. Hall, Associate Director of Research for General Sciences

During the year, a new laboratory building was occupied by the Space Science Division and the E. O. Hulburt Center for Space Research, providing offices and laboratories for 140 scientists, engineers, technicians and the administrative staff. The Hulburt Center, an inseparable part of the Space Science Division, is an organizational concept which is jointly sponsored by the National Science Foundation, the National Aeronautics and Space Administration (NASA), and the Office of Naval Research. Its purpose is to bring university scientists to NRL for one- or two-year appointments so that they may conduct rocket and astronomy projects by means of the Laboratory's unique facilities and the military rocket ranges. At the same time, the Hulburt Center provides some of the character and stimulus of a graduate research center to the NRL program.

Many programs within the Space Science Division relate directly to military problems in infrared, night-vision systems, radiac devices, radio communications, navigation systems, and microwave radiometry. The major effort of the division (and the Hulburt Center), however, is in satellite, rocket, and radio astronomy. Consequently, in the new building are specialized laboratories housing some of the most unique research instruments for advanced rocket and satellite experiments.

Since the establishment of NASA, the Space Science Division has been a major participant in the NASA astronomy and geophysics programs. NRL has conducted observations from OSO-2 and -4 and OGO-1, -2, -3, -4, and -5, as well as many NASA-sponsored rockets. Further efforts are being supported in connection with OSO-F, -G, and -H; OGO-F; and the Apollo Telescope Mount project.

NRL early became involved in the use of radio telescopes. More recently, in radio astronomical work, the Laboratory has led the way in polarization measurements which identify synchrotron sources and reveal the scale of magnetic fields within radio galaxies, intergalactic space, and the local galaxy. Now the evolving research pattern in astrophysics includes very long base line interferometry and molecular line spectroscopy carried out by means of radio telescopes. Activities of the latter kind are performed cooperatively, e.g., with the National Radio Astronomy Observatory and leading university groups. Considering this breadth of program, history, and degree of collaboration with other institutions, the Laboratory expects much to come from the recently dedicated Space Science Building.

Another increasing effort concerns the application of nuclear technology to problems in non-nuclear areas. Extensive, well-instrumented, modern facilities now include a 75-million-electron-volt (Mev) cyclotron, a 5-million-volt Van de Graaff accelerator, a 60-Mev linear electron accelerator, and a 1-megawatt nuclear reactor.

In the past 12 months, the major applications of activation analyses techniques were for forensic purposes and for the determination of trace amounts of sodium and potassium in a solid-propellant matrix and of the existence of fractional atomic layers of impurities on highly pure, carefully polished surfaces. Nuclear accelerators were used to study transient radiation effects in electronic components and to implant selected ions in materials for experimental purposes. Further applications are expected.

At the end of 1967, a new research division, the Mathematics and Information Sciences Division, was formed. It includes the Research Computation Center, which provides operation and maintenance of general-purpose computers for the benefit of all divisions of the Laboratory and maintains a group of expert consultants on data collection and processing. This group also performs a number of other functions which have as their end goal the utilization of the computer sciences in the performance of Laboratory programs.

A second part of the new division consists of the former Mathematical Analysis Branch. Research in this area, which has been in progress for many years, concerns function theory; functional, integral, and differential equations; variational calculus; integral transforms; Eigen-value theory; and other branches of mathematics. In addition, this part of the division provides research support in areas of applied mathematics, with emphasis on the fields of probability and statistics, communication and control, and optimization and data analysis. It also engages in numerical analysis as required.

A third part of the division was developed during 1968 to work in the areas of the information sciences, including primarily logic, formal linguistics, information-theory systems analysis, computer-aided design, signal processing, and information retrieval. In the course of the year the branch began work on specific problems dealing with multisensor correlation; the development of certain components of digital hardware; the development of software, involving, for example, actuarial models for research personnel and models for data banks within the Research

Department; and, finally, small programs in logistics and command and control systems.

The research effort in the area of logistics has been hampered by the unavailability of a sufficient number of qualified personnel, but it is now beginning to move in the direction of specific problems in reliability of systems. This effort is expected to increase as qualified manpower is obtained. Research in command and control systems is expected to increase also. Currently, a small effort is under way directed toward the development of new systems with present hardware and the development of a system of the future which can be incorporated into the Navy Management System as technology improves.

In other defense research, a number of highly significant programs have been established or further enhanced. They include the development of

high-power lasers through studies of beam trapping, thermal blooming, ultraviolet lasers, Raman oscillators, and high-power glass laser systems. Another program involves the generation of highly intense x-radiation.

A considerable and very productive effort is devoted to nuclear weapons effects, diagnostics, and the preparation of computer codes which can be used to predict the behavior of nuclear weapons. New technologies have been derived for the generation of plasma and electron streams and for diagnosing and predicting their complex properties. With the backing of the cognizant sponsors within the Department of Defense, long-range programs have been established in all of these areas. They involve the collaboration of several large university research groups, each of which has entered into agreements for mutually cooperative endeavors.

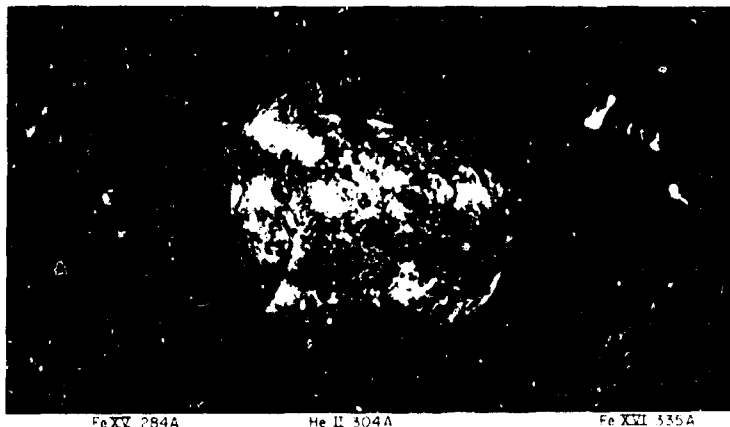
SPACE SCIENCES

Extreme Ultraviolet Spectroheliograms and Heliograms. Progress has continued in the refinement of the spatial resolution in extreme ultraviolet (XUV) spectral images of the solar disk. The first clear ultraviolet picture of the sun, made by NRL in 1959 from above the terrestrial atmosphere, showed details subtending as little as 30 seconds of arc. In contrast, the latest NRL spectroheliograms, taken from a rocket launched at the White Sands Missile Range, New Mexico, on September 22, 1968, revealed features as small as 10 seconds of arc. The images were recorded in two wavelength ranges, 170-370 angstroms (Å) and 550-630Å, with an objective spectrograph equipped with a single concave grating in a Wadsworth configuration. An aluminum film filter (about 1,000Å thick) was placed immediately in front of the film cartridge to block the intense, scattered, long-wavelength radiation. The performance of the instrument is demonstrated by the cleanliness of the spectroheliograms.

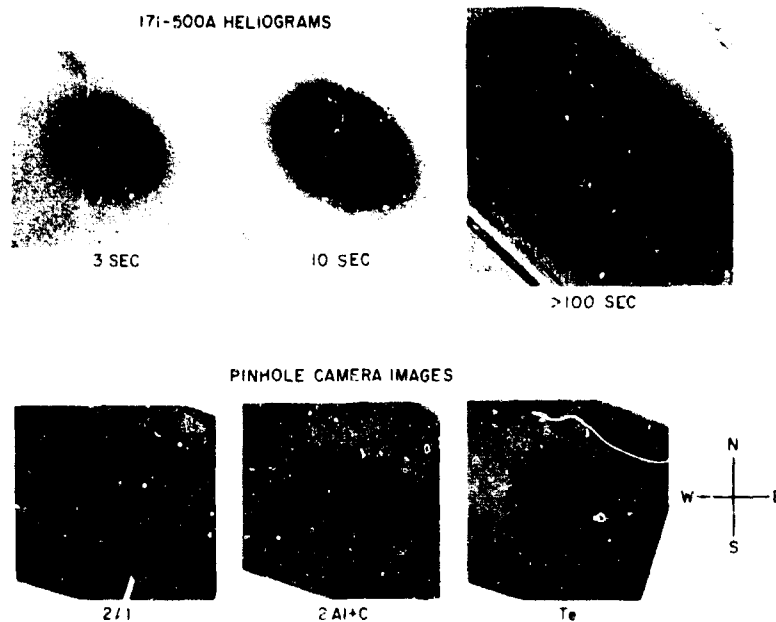
The solar-disk image in any one wavelength spanned an interval in the spectrum equivalent to a range of 27Å; the spectral resolution of 0.15Å was so good that the features formed by Si XI (303.4Å) and He II (303.78Å) radiation could be distinguished one from the other. This resolution made it possible to determine that the coronal emission above the limb of the He II image (near 10 o'clock in the September 22 spectroheliogram) originated from Si XI, with

none from the He II line emission. This confirms the suggestion of Scott Smith, a former consultant for the E. O. Hulburt Center for Space Research.

Emission from centers of activity was present in all lines, although the shapes and intensities of the regions were not alike. In the coronal lines Fe XV and XVI, for example, emission above the limb was conspicuous, whereas over the disk it was very faint but detectable. In the chromospheric lines He II (303.78Å), He I (584.3Å), O IV (554Å), and O V (629.7Å) emission over the disk was intense, and a coarse network was present. Many intense prominences were recorded in He II (304Å) and He I (584Å), but not in any other lines. In the other lines, the prominences appeared to be similar to absorption features in that they destroyed the continuity of the bright limb emission rings, which are characteristic of the high chromospheric lines, such as those of Mg IX. Dark filaments were present over the disk in all chromospheric lines. The intense coronal emission from McMath Plage No. 687, located on the limb at 12°N (about 10 o'clock on the He II image of the September 22 spectroheliogram), extended to an apparent height of 70,000 kilometers. In Fe XV and XVI, it was diffuse; in Mg IX, it appeared as a group of six or seven curved rays; and in Si XI, there was just a suggestion of structure. Projecting from the center of this Si XI (303.4Å) coronal feature was a long, thin, strongly curved plume that



Extreme ultraviolet spectroheliogram obtained on September 22, 1968, showing solar features in three relatively intense emission lines. The sun is photographed with the images obtained by longer wavelength ultraviolet displaced toward the right. The intense image formed by He II light is near the center, and the less intense Fe XV and Fe XVI are to the left and right, respectively. Images in other wavelengths are discernible, as discussed in the text.



Heliograms and pin-hole-camera photographs of the sun obtained on September 22, 1968, demonstrating the equatorial bulge formed by the extreme-ultraviolet corona.

extended to 300,000 km. This is believed to be a He II (303.78A) prominence of some kind, because it was not found in any other line. However, it has not yet been identified in available H-alpha images covering this period.

Positions of the intense coronal emissions shown in the September 22 spectroheliogram correlate well with the streamers depicted in the white-light coronagrams reproduced in "Solar Corona," an accompanying article.

Also carried on the September 22 rocket was a simple camera (heliograph) that photographed the solar disk, with the XUV radiation transmitted by an aluminum film filter (170A-600A), and three pinhole cameras employing several metal film filter combinations to isolate different spectral regions in the XUV. Exposures made by means of these instruments showed an apparent equatorial bulge. A similar feature had been observed on previous flights, but the interpretation of the data has been

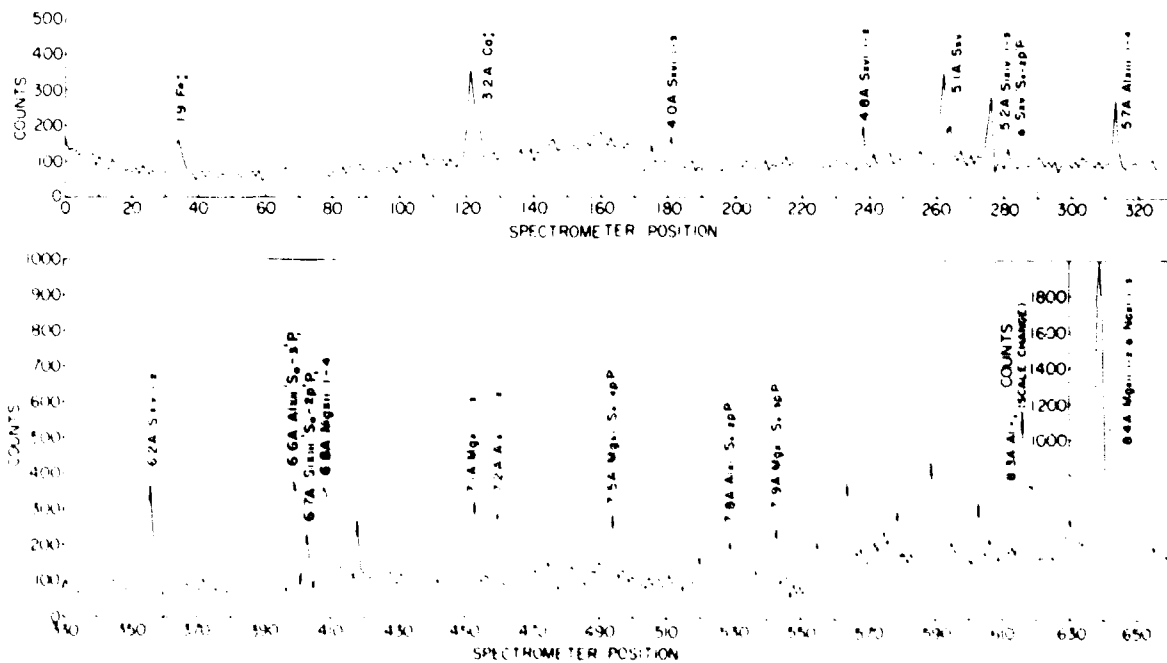
in question because "jitter" in the solar-pointing control, precession cone of the rocket, and optical aberrations in the cameras may have contributed to the "buge." On this flight, however, jitter and precession cone angle were very small. The three pinhole-camera exposures also confirm the results of the XUV heliograph experiment in that the cameras have no aberrations other than those caused by diffraction, which are symmetrical about the camera axes.

Solar Monitoring. The monitoring of solar-activity events by means of their x-ray emission was carried out successfully by a variety of instruments during 1968, most notably by ion-chamber assemblies aboard OGO-IV, OSO-IV, and Solrad-IX and by a proportional-counter spectrometer aboard OGO-V. Full-orbit (sunlit-portion) data from Solrad IX have been most valuable in that they have permitted the compilation of time histories of 0.5-3 angstrom (A), 1-8A, and 8-20A x-rays within 24 hours of the times the emissions were recorded aboard the satellite. The x-ray data obtained by Solrad were used to evaluate the likelihood of solar-flare hazard conditions during the flight of Apollo VIII.

The Solrad monitoring was performed cooperatively by the Space Sciences and Applications Research Divisions.

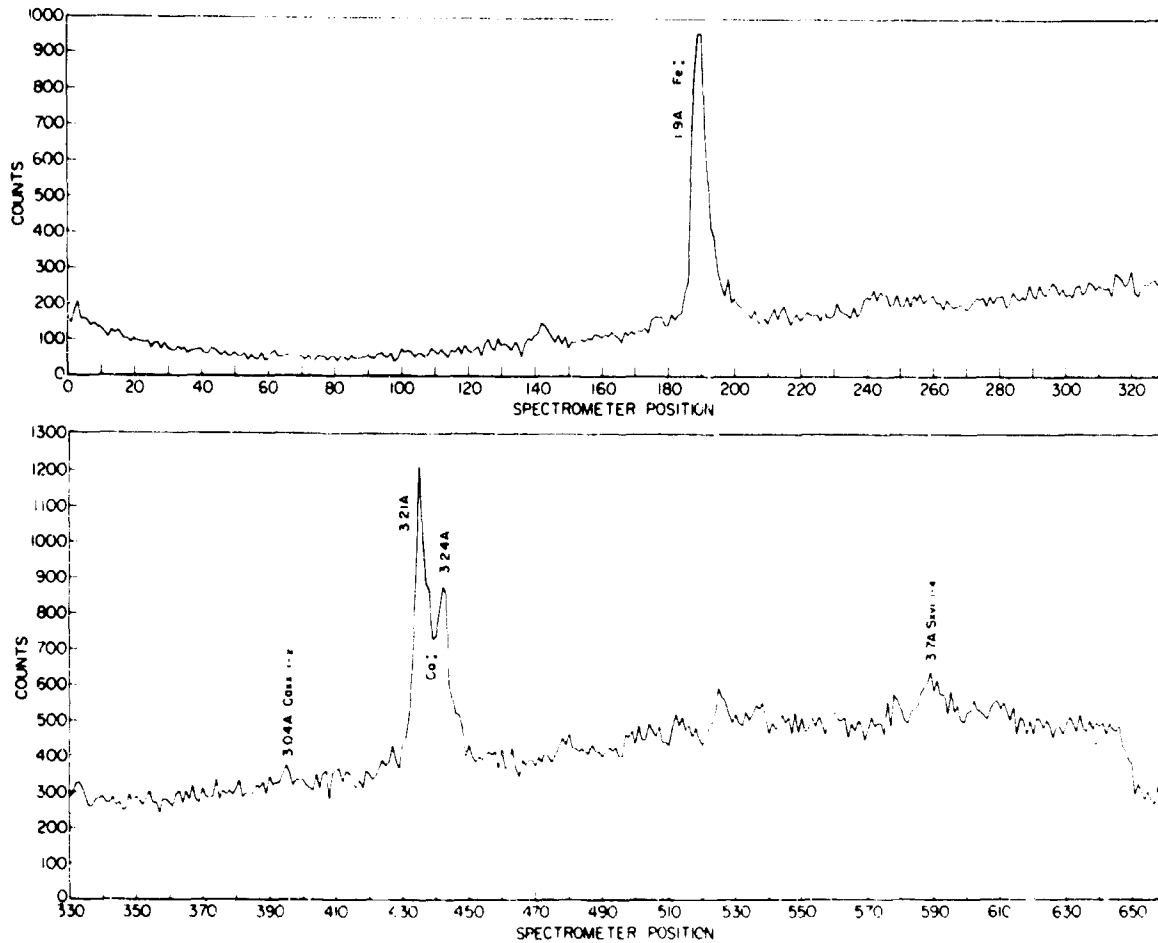
Solar X-Ray Spectral Studies. X-ray spectra of a considerable number of flares have been obtained from OSO-IV in the wavelength ranges of 0.5-4.0 angstroms (A) and 1.0-8.5A. An example of the emission spectrum of a class 3b flare is shown in the figures. The graphs consist of uncorrected data giving sensor counts per 0.88 second as a function of the step position of a Bragg crystal spectrometer. Several features in the spectrum are instrumental in origin. The rise in count rate at very short wavelengths is due to increased crystal reflectivity near grazing incidence, and the changes in continuum level that occur at 4.0A, 6.7A, and 8.0A are the result of K x-ray edges in the sensor gas and in system filters and windows. However, the appearance of these effects confirms that the continuum recorded by the instrument is truly a solar x-ray continuum.

The flare spectrum at short wavelengths is characterized by the dominance of continuum emission over line emission, by line emission arising from



Counts recorded from the ethylene diamine d-tartrate (EDDT) spectrometer for the class 3b flare on November 16, 1968 (2125 UT). The vertical axis represents counts per 0.88 second. The horizontal axis indicates spectrometer position in steps of six arc minutes. The wavelengths of the emission lines were calculated from this information.

GENERAL SCIENCES

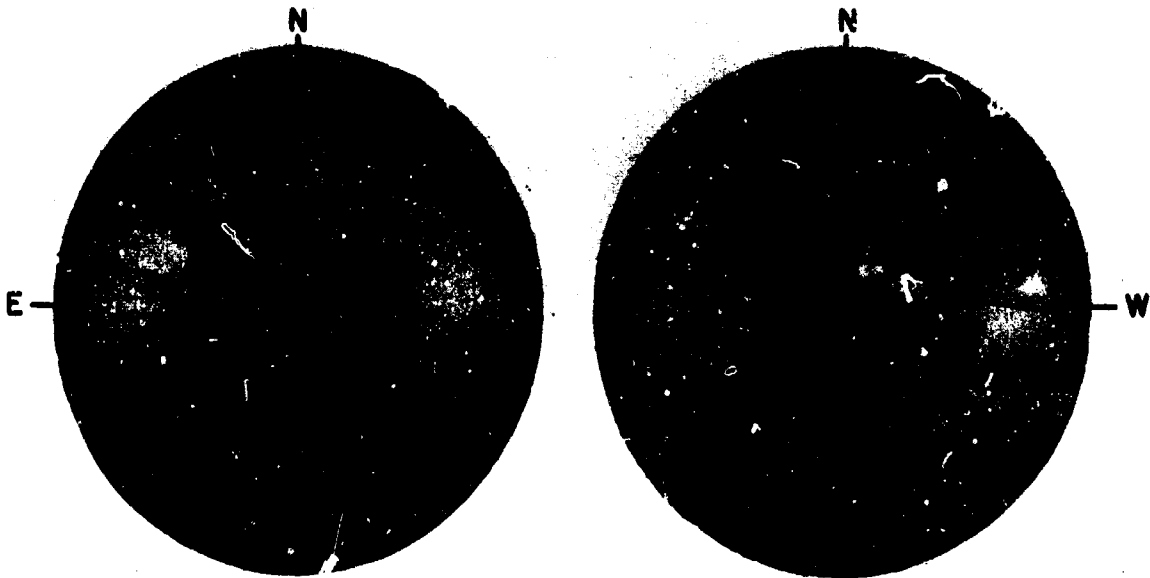


Uncorrected data derived from the LiF spectrometer for the class 3b flare on November 16, 1968 (2125 UT). The vertical scale represents counts per 1.28 seconds. The horizontal scale indicates spectrometer positions in steps of six arc minutes. The line identifications and wavelengths should be considered approximate, since θ is changing both because of the spectrometer drive and the motion in the view direction.

many ionization states of Mg, Al, Si, S, Ca, and Fe, and by inner-shell transition lines arising from the production of K-shell vacancies in ions still holding one or more L-shell electrons. Flare-plasma spectra are found to vary greatly from flare to flare.

The Solar Corona. Observation of the sun's white-light corona with rocket-borne coronagraphs is continuing under a program supported by NASA. In 1968, the coronagraph flights had a more specific purpose than surveying the corona at six-month intervals, as had been done previously. Two observations in quick succession, on April 27 and 29, were made to record short-term changes in the outer corona.

These flights were the first ones in the short history of rocket observations and in the long history of eclipse "chasing" during which the same solar streamers were photographed twice. All previous photographs have been single snapshots taken during aircraft or rocket flights that provided no opportunities for later observations. Although during the two-day interval between flights, the sun rotated a mere 25 degrees, unexpected and puzzling changes in the appearance of the streamers were revealed. Study of the photographs is still under way. In continuing studies, NRL scientists hope to unravel the behavior of coronal streamers more completely from the NASA-supported Orbiting Solar Observatory.

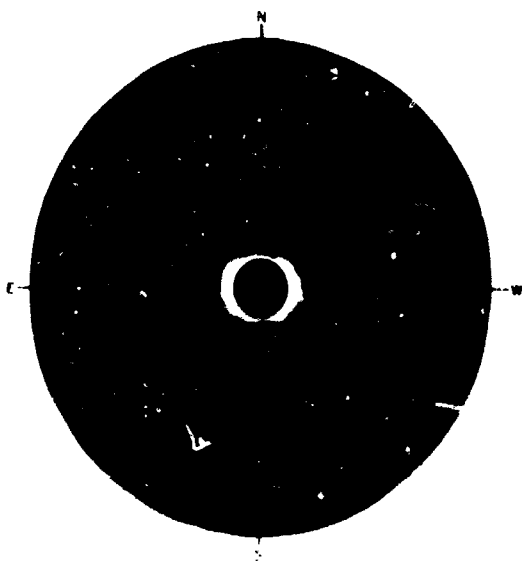


Photographs of the sun's outer corona (from 3 to 9 solar radii) taken from rockets launched on April 27 (left) and 29 (right), 1968. The sun is artificially eclipsed by a circular disk. The small black disk is the moon silhouetted against the corona. The eclipsed area in each photograph contains a sketch of the sun and its known active regions. The radial lines are where streamers would have been observed if each region had ejected a narrow beam of electrons straight outward.

H (OSO-H), which will carry aloft the NRL coronagraph to record the contortions of the streamers in a nearly continuous moving-picture fashion.

The flight of a coronagraph-equipped rocket on September 22 was timed to coincide as closely as

possible with a total eclipse in the USSR. The photograph obtained recorded the corona and streamers from three to nine solar radii from the sun, while the eclipse photographs from the USSR recorded the corona from the sun's edge to a distance of three solar radii. The rocket flight, therefore, served its intended function of recording the corona outward into a region not accessible to eclipse observers.



A rocket photograph of the sun's outer corona (from 3 to 9 solar radii) taken at 1530 UT, September 22, 1968. Into the occulted center has been introduced, to the proper scale and orientation, a USSR eclipse photograph taken at 1119 UT on the same day. Streamers which fade away into the Russian sky are seen to continue outward a large distance from the sun in the rocket photograph. (The photo was taken by M. N. Gnevyshev of the Pulkovo Observatory, USSR, using a camera obtained from D. H. Menzel, Harvard Observatory. Picture courtesy of the Douglas Advanced Research Laboratories of the McDonnell-Douglas Corp.)

Advances in Extreme-Ultraviolet Photographic Techniques. One of the vexing problems of photography from Earth-orbiting spacecraft is the fogging of the film, mainly by high-energy particles concentrated in the several particle belts. An evaluation of this effect has been accomplished by exposing photographic film strips to protons of an energy (20 million electron volts) comparable to that encountered in space. This was done in one of the first experiments performed with NRL's new 75-million-electron-volt sector-focusing cyclotron.

It was found that Kodak short-wavelength-radiation film is the least sensitive of the nine types of film strips tested and is the only extreme ultraviolet (XUV) sensitive film which can be used, for example, in NASA's Apollo Telescope Mount (ATM) 56-day mission, which has a circular orbital altitude of 220 nautical miles and an inclination of 30 degrees. A proton fog density of 0.2 can be tolerated before XUV spectral images (emission lines and continuum) are materially affected.

A technique was developed by NRL and Sigmatron, Inc., of California for the production of hitherto unobtainable very large (250- by 35-millimeter) aluminum film filters for isolating the 170 to 600 angstrom (A) region of the XUV spectrum. The single-layer films are supported on 70/inch wire mesh and are quite free of harmful pinholes. At a thickness of approximately 1,100A, the films are just opaque to the filament of a high-power tungsten lamp. The really remarkable achievement of the technique, however, is that it permits the production of filters that are sturdy enough to withstand an acoustical environment of 146 decibels—a sound level well above that tolerable by man.

Far-Ultraviolet Airglow Studies. One of the scientific mysteries of ionospheric physics has been the presence of a low level of ionization in the *E* and *F*₁ regions throughout the night. The normal *E* and *F*₁ regions are produced by absorption of ionizing radiations from the sun. After sunset, these regions should rapidly disappear by ion-electron recombination. During the night, low levels of ionizing radiations are present in starlight, but they are too low to maintain the observed lower-ionospheric electron densities.

In August 1967, a study was carried out with photometers capable of measuring radiations of wavelengths less than 1,100 angstroms (A). Analysis of the data has revealed the presence in the night sky of diffuse far-ultraviolet radiation identified as

hydrogen Lyman- β at 1.026A and as helium at either 304A or 584A. The levels of these radiations appear sufficient to maintain the observed electron densities of the nighttime *E* and lower *F*₁ regions.

The OGO-IV spacecraft carries an NRL experiment in which sets of far-ultraviolet sensors are directed toward the center of the Earth. Part of the results of this study were reported in the 1967 *Annual Report*. Among the new discoveries was the observation of far-ultraviolet airglow in the equatorial zone. The occurrence frequency of these glows, measured during the period August 1967 to February 1968, was most pronounced in October. The emissions are seen to be quite symmetrically located, completely encircling the Earth, at 12-15 degrees on either side of the magnetic dip equator. They are believed to be an ultraviolet counterpart of the intertropical red arcs. Recent comparisons of these data and data obtained by Barth from a scanning spectrometer that was also carried by OGO-IV show that the far-ultraviolet emissions are represented largely by oxygen lines at 1,304A and 1,356A.

The "dark aurora," observed in Lyman- α and reported on last year, is now believed to be of instrumental origin. The effect on sensor output was produced by transient charging of the sensor windows by electron streams which impact the auroral zone, presumably the same electron streams that produced the aurora underneath the spacecraft.

Far-Infrared Astronomy. Early in 1968, NRL flew its first long-wavelength (more than 10 microns (μ)) infrared-astronomy rocket to study diffuse and point-source radiation from the celestial sphere. The rocket instrument system (described in the 1967 *Annual Report*) included a Cassegrain-mirror telescope cooled to liquid-helium temperature and a set of four solid-state far-infrared sensors covering the spectral bands 10-30 μ , 10-120 μ , 10-1,050 μ , and 300-1,300 μ . Good data were obtained from a Ge:Cu sensor covering the 10-30 μ band. Several point sources of unexpectedly high intensity were seen. If these point sources are truly of celestial origin, they are believed most likely to be normal galaxies, and the fluxes observed mean that many such galaxies radiate much more energy in the far infrared (thermal region) than they do in the rest of the spectrum.

The first data on diffuse, background far-infrared radiation were obtained from an NRL 300-1,300 μ sensor flown in a Cornell University rocket. These

data indicate a flux level substantially higher than that expected on the basis of measured microwave-emission backgrounds, which are consistent with a 3°K black-body radiation temperature of space. Both the point-source and diffuse-background results have major cosmological implications, but these must be considered somewhat uncertain until they can be properly rechecked.

X-Ray Astronomy Program. During the past year, the advantages of the switch from large-area Geiger counters to proportional counters and the successful use of inertially referenced attitude-control systems in NRL's x-ray astronomy program have become apparent. The main achievement of the program in 1968 was an extension of x-ray astronomy to longer wavelengths. By means of counters having 1/8-mil Mylar windows, it was possible to carry out measurements in the 44-60 angstrom (Å) band. A source in Vulpecula that did not show up in the 1-10Å band of conventional rocket x-ray astronomy was observed in the higher band. In addition, a diffuse soft flux was observed at high galactic latitudes, and a flux was observed at lower galactic latitudes. The high-galactic-latitude flux is too intense to explain by extrapolation of the flux observed between 1-10Å (power law energy index = 0.4) and thus is believed to constitute a new component of intergalactic radiation. The high-latitude soft x-ray flux is believed to arise from hot intergalactic material in the 3×10^5 to 8×10^5 °K temperature range and at a rms density of $\sim 10^{-5}$ atoms cm^{-3} . The low-galactic-latitude soft background, on the other hand, is believed to represent unresolved radiation from many soft x-ray point sources similar to the Vulpecula source. From the point of view of cosmology, the hot-intergalactic-medium explanation of the high-galactic-latitude data is of considerable interest in that the medium's presumed density would account for about enough material to eventually stop the expansion of the universe by the action of gravity.

At shorter wavelengths, good-quality pulse-amplitude spectra were obtained for SCO XR-1, Cyg XR-1, and Cyg XR-2. Cyg XR-1 was again shown to have a spectrum strikingly different in shape from the hot-gas spectra of SCO XR-1 and Cyg XR-2. The SCO XR-1 spectrum was shown to have the behavior of a 65×10^6 -degree plasma containing less than 5 percent iron. The low percentage of iron was determined on the basis of the lack of strong emissions at the wavelengths of the Fe XXV and Fe XXVI

resonance lines. Some 250-thousand-electron-volt radiation was also observed, indicating no very great interstellar gas absorption between Earth and SCO XR-1.

A slow scan of the Cen A radio source was made in 1968. An elevated count rate was observed throughout the period of scan during which the Cen A radio emission lobes and optical center were in the field of view. The main portion of the radio lobes and the optical center occupy 4 degrees of angle in the scan direction—an interval that was covered during 40 seconds of a 200-second scan. The count accumulation during the 40 seconds of Cen A scan exceeded by 3σ that of the average 40-second count for the full 200 seconds of scan.

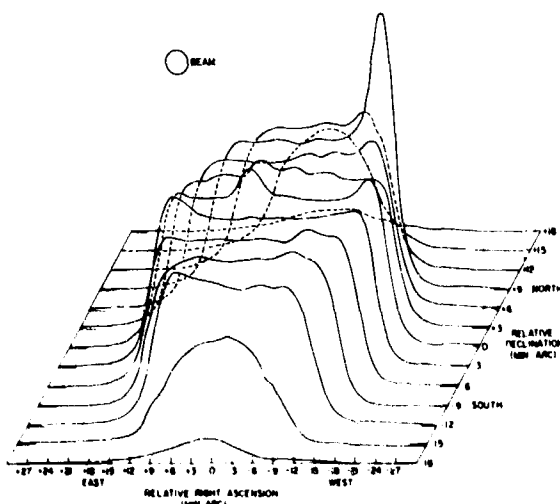
Navigation with the Radio Sun. The sun is an attractive source for navigation at both optical and radio wavelengths because of its great intensity. Navigation at radio wavelengths has the additional important advantage over that at optical wavelengths of all-weather capability. As an example of the useful intensity of the sun, a 3-foot-diameter parabolic antenna at 2-centimeters wavelength used with very simple receivers will give signal-to-noise ratios of several hundred. Even with the poor angular resolution of this small antenna of about 1-1/2 degrees compared with the size of the solar disk of about 1/2 degree, it is possible to determine the position of the apparent center of the sun to an accuracy of several seconds of arc. However, the apparent center as measured with low-angular-resolution equipment may not coincide with the geometrical center of the sun due to solar activity superimposed upon the uniformly bright disk of the quiet sun. This activity will distort the brightness distribution, causing the displacement of the brightness centroid from the geometrical center of the disk by sizable amounts, resulting in significant navigational errors. To assess the magnitude and frequency of these errors and their effect upon navigational systems, a high-angular-resolution study of the sun has been undertaken by means of the NRL 85-foot radio telescope.

The time of occurrence of individual activity is unpredictable, though the average solar activity varies cyclically with a period of 11 years. The major activity at centimeter wavelengths may be classed as either spots or bursts. Spots have typical lifetimes of 1 to 10 days and usually constitute less than 2 percent of the quiet sun flux. Bursts are of brief duration, with lifetimes ranging from a few minutes

GENERAL SCIENCES

to several hours, but they may be 10 or even 100 times more intense than spots.

The figure presents some results of the investigation of the brightness distribution over the sun at 2-centimeters wavelength being conducted by means of the NRL 85-foot telescope. The beam-width of the 85-foot antenna at this wavelength is only 3.3 minutes of arc, allowing the brightness distribution to be measured in detail. The average position measured by a smaller antenna with much poorer angular resolution can be computed from these data. The measurements were taken by scanning the sun at intervals of 3 minutes of arc, forming a raster covering the entire solar disk. Nine active sun spots were present on this day, with a flux greater than the sensitivity limit of the observations of a 1,000th of the quiet solar flux. The most intense spot, on the north-west limb of the sun, had a flux of 2.2 percent of the quiet sun and was the major contributor to shifting the brightness centroid from the geometrical center. The brightness centroid was displaced by 14 arc seconds at a position angle of 710 degrees. The minimum displacement observed to date is 4 arc seconds, with the average being about 9 arc seconds. By reference to these observations, the centroid position can be determined to an accuracy of less than 3 arc seconds, which is less than a 600th of the size of the solar disk.



A typical observation of the brightness distribution over the sun at 14.50 billion cycles per second made on October 10, 1967. The raster scans are shown, but they have been displaced and skewed for clarity. The beam of the 85-foot telescope is represented by the circle in the upper left corner.

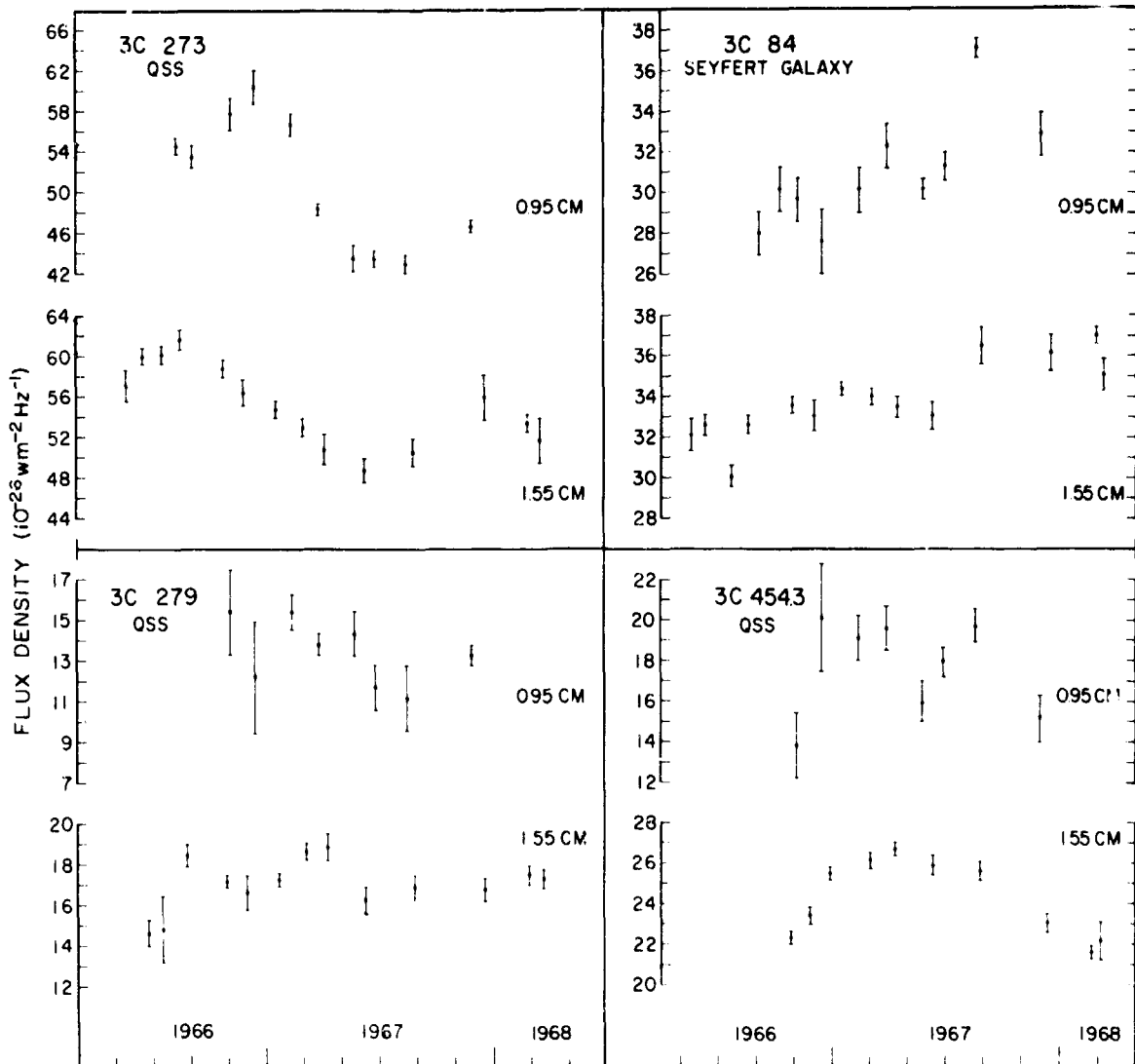
Measurements of this kind provide information on the frequency of occurrence and magnitude of navigational errors due to solar activity. In addition, they provide a means of correcting the errors and of evaluating different sources of error which otherwise could be masked in a navigational system under test.

Radio Variability of Quasars. About seven years ago, through the cooperative efforts of radio and optical astronomers, it was discovered that certain celestial objects previously regarded as faint bluish stars are, in fact, not stars but massive, very distant objects which radiate huge amounts of energy in the radio and optical regions. Their radio energy is believed to be generated by the synchrotron radiation process, in which highly energetic electrons emit radiation while spiraling around the lines of force in a magnetic field.

Understanding these quasi-stellar sources and their energy-generation and radiation processes is of first importance in astrophysics and of great potential practical importance.

Recently, astronomers made the surprising observation of large variations in the intensity and polarization of the radiation from these objects in time periods of less than a year. These variations have provided a new means of investigating the physical properties of the sources. Through such studies, for example, it has been found that certain peculiar galaxies, so-called Seyfert galaxies, share some of the properties of quasars, including temporal variability of radiation characteristics.

Accurate measurements of the quasars 3C 273, 3C 279, and 3C 454.3 and of the Seyfert galaxy 3C 84 made at NRL over a period of two years at wavelengths of 9.5 millimeters and 1.5 centimeters showed large intensity variations; in some cases several peaks were recorded, as shown in the figure. The variations observed are generally consistent with the interpretation of the variable radiation which results from expanding clouds of radiating relativistic particles. The relativistic particles might be injected into the source region by explosions similar to those that create supernova, but on a much larger scale. It would be expected that the radiation from the cloud would increase with time until the expanding cloud becomes optically thin and that the radiation then would begin to decrease. The observation of repeated peaks of intensity can be explained qualitatively by such a process.



Intensity variations of the quasars 3C 273, 3C 279, and 3C 454.3 and of the Seyfert galaxy 3C 84 over a two-year interval at two wavelengths, 9.5 mm and 1.55 cm.

Measurements of linear polarization made at 1.5-cm wavelength over the second year of the intensity investigations show little evidence for variation of the polarization of these sources, except for 3C 454.3. The degree of linear polarization of 3C 454.3 increased from less than one percent to more than two percent during that year. Over that period, the total intensity decreased, suggesting that the radiation of the variable component is unpolarized or that its polarization increased greatly as its intensity decreased. Separate measurements made in 1965 and

1967 at 2-cm wavelength of seven intensity-variable sources show that the degree of polarization of the quasar 3C 279 doubled during this interval, whereas the degree of polarization of 3C 120 decreased. Simultaneously, the total intensity of both sources increased, suggesting that in one case the radiation of the variable component was polarized, while in the other case it was not.

The varying source components must have very small angular diameters (of the order of 10^{-4} arc seconds) and be at very great distances from Earth

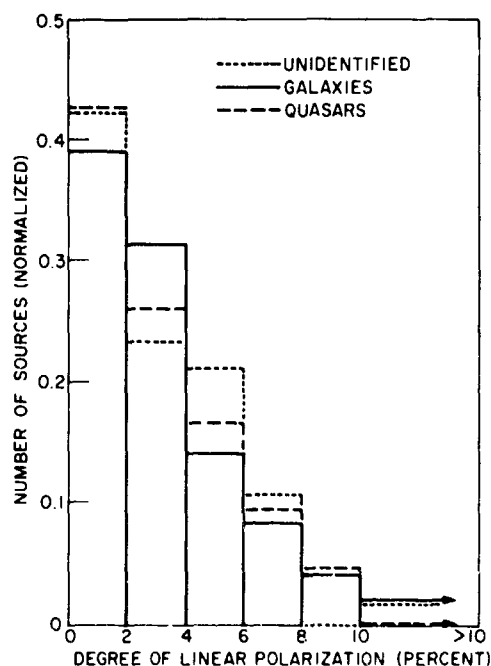
GENERAL SCIENCES

for variations with periods of less than a year to occur. Investigations of the components by long base line interferometry at the short wavelength of 2.8 cm were begun in December 1968 by the NRL Maryland Point Observatory and an observatory in Germany. If the data analysis is successful, this experiment will give a resolution of 3×10^{-4} arc seconds.

Polarization Properties of Cosmic Radio Sources. In 1956, radio astronomers at NRL discovered that some of the radiation from supernova remnants is partly linearly polarized at short radio wavelengths, and in 1961 they showed that the radiation from extragalactic radio sources is also linearly polarized. These findings were a basic part of the evidence that the radiation is generated by the synchrotron process—that is, the radiation is generated by relativistic electrons moving in helical orbits in magnetic fields. The polarization of the radiation from cosmic radio sources is an important source of information about the distribution of magnetic fields and relativistic particles in the source region and, consequently, about the structure and physical characteristics of these discrete regions in the universe. In addition, knowledge of the polarization and other radiation properties of cosmic radio sources has practical importance because of the potentialities of the sources as radio reference points for navigation systems and for the calibration of radio and radar systems.

Since 1961, large programs of polarization studies have been pursued at NRL and other radio astronomy observatories. As a consequence, the polarization properties of about 275 sources have been measured at various wavelengths. The results show that the radiation from the majority of cosmic radio sources is partly linearly polarized at wavelengths shorter than about 30 centimeters. The degree of polarization varies from source to source but generally decreases toward longer wavelengths. At NRL, the polarization characteristics have been determined for 135 sources at 25-cm wavelength, 156 sources at 21 cm, 99 sources at 6 cm, 50 sources at 2.9 cm, 29 sources at 2 cm, and 3 sources at 9.5 mm. In general, the polarization characteristics of radio galaxies, quasi-stellar sources, supernova remnants, and unidentified sources are about the same, showing, in this respect at least, a similarity of the radiating properties of these different types of cosmic radio sources. No outstanding correlations have been found between the polarization characteristics of the

integrated source radiation and source properties. An analysis of 239 extragalactic sources for correlations between degree of polarization at 21-cm wavelength and intrinsic source properties showed that the polarization characteristics are similar for sources having a wide range of other properties. The degree of polarization ranges from 0 to about 10 percent, with the degree ranging between 0 and 2 percent for

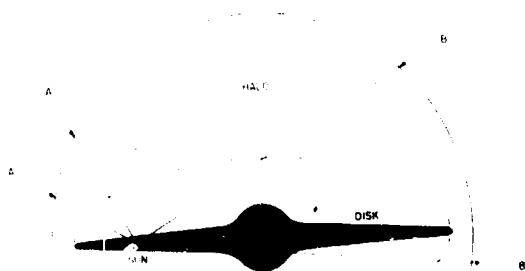


Linear polarization of extragalactic radio sources at 21-cm wavelength. The distributions of relative numbers of sources with degree of polarization are similar for quasars, radio galaxies, and unidentified sources.

about 40 percent of the sources considered as a whole; the same is true of quasars, radio galaxies, and unidentified sources considered individually. There is no apparent correlation between 21-cm polarization and brightness temperature, radio luminosity, distance to the source, linear dimensions, magnetic-field strength, or spectral characteristics of the visible light of the source.

The frequency distribution of the degree of polarization of the 21-cm-wavelength radiation from radio galaxies, quasars, and unidentified sources is illustrated in the figure.

Magnetic Fields and Particles in Our Galaxy. The radio radiation from extragalactic sources is modified in propagation through the magnetoionic medium which fills the space between the stars in our galaxy and possibly extends outside the plane of the spiral arms to form a galactic corona. In particular, the Faraday rotation of the plane of polarization of the radiation caused by the magnetic fields and free electrons along the path of propagation through the galaxy results in (1) rotations of the plane of polarization as observed from Earth and (2) depolarization of the radiation where the Faraday rotation differs across the diameter of the source. These effects provide an



Idealized cross section of our galaxy, showing the disk, the roughly spherical star halo, and the rough outline (dashed curve) of the electron-magnetic-field halo indicated by this work.

important new means for investigating the little-known galactic medium; this is the case particularly when the radiation sources are outside the galaxy, as are radio galaxies and quasars, because then the effects facilitate study of the magnetic fields and electron distributions along the total paths of the radiation through the galaxy.

We have found from an analysis of the polarization properties of 239 extragalactic sources (observed at 21-centimeter wavelength) relative to the path length of their radiation through the galaxy that the radiation of even very small-angular-diameter extragalactic sources is depolarized in traveling through our galaxy.

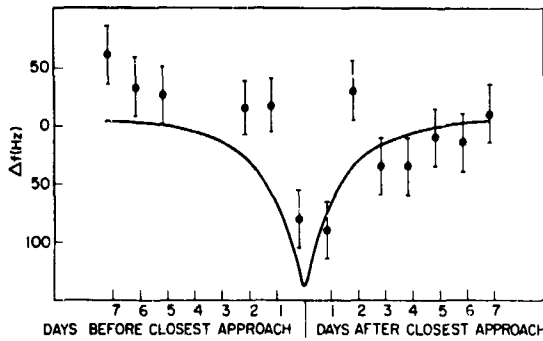
This depolarization is explained by differential Faraday rotation across the angular extent of the source. The differential Faraday rotation is caused by a variation in the product of the line-of-sight component of galactic magnetic-field and interstellar electron density with a scale of less than 1/2 parsec if the amplitude of this product is greater than 10^{-7} gauss cm^{-3} . If the average electron density in the galactic medium is of the order of 10^{-2} cm^{-3} , as was determined from recent pulsar observations, this product requires a magnetic field of 10^{-5} gauss. This figure is in good agreement with values for the galactic magnetic field of the order of 2×10^{-5} gauss, which were determined recently from measurements of the Zeeman splitting of the 21-cm line of galactic neutral hydrogen. Thus, the magnetic-field and electron-density requirements for the small-scale structure of the galactic magnetoionic medium derived from our observations of galactic depolarization are consistent with the most recently determined values for these quantities.

The 21-cm depolarization is appreciable for sources whose directions are within 120 degrees of the galactic plane in latitude. These results indicate that the magnetoionic medium responsible for the depolarization is not confined to the disk of the galaxy but extends into a galactic halo. The observations are consistent with a simple model in which the depolarization is proportional to the path length traveled by the radiation through an oblate-spheroidal region of the galactic halo having an axial ratio of between 2 and 3, as shown in the figure.

These investigations of the galaxy have given important new information on the fine structure of the magnetoionic medium and its probable extension into a galactic halo. Polarization measurements at different wavelengths are being combined to show the overall Faraday rotation through different parts of the galaxy and the large-scale distribution of the galactic magnetic field.

Effect of Mass on Frequency. Two known phenomena can change the frequency of electromagnetic radiation: the doppler effect and the gravitational red shift. Because in cosmology and astronomy so much importance is attached to deviations of the frequencies of lines from stars, galaxies, and quasars, NRL radio astronomers devised and performed experiments aimed at disclosing further influences on the frequency of radiation. The experiments described were designed to determine whether a large mass

GENERAL SCIENCES

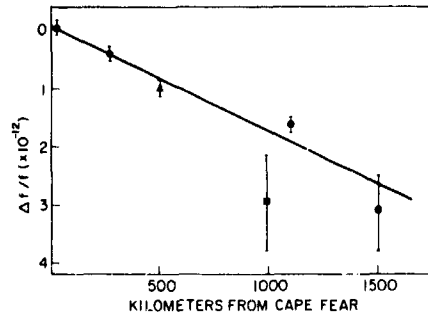


Plot of points representing the experimentally determined residual frequency (measured minus calculated) of the 21-centimeter line during the days before and after the closest approach of Taurus A to the sun, adding two years' measurements. The solid line is a $1/a$ dependence, where a is the distance from the center of the sun to the line of sight at closest approach. The probability that random fluctuations gave the red shift shown on the two days near closest approach is only 1 percent. After and before the days plotted here, the residuals were near the zero line. The error bars represent the actual spread of one day's measurement.

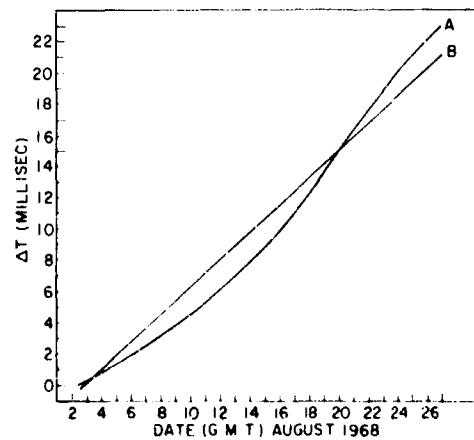
affects the frequency of electromagnetic radiation. In two of the experiments an apparent decrease in frequency was observed when the optical path was in the vicinity of a large mass, and in one of the experiments no apparent change was observed.

During the annual approach (every June) of the radio source Taurus A to the sun, the frequency of the 21-centimeter absorption line of the galactic neutral hydrogen in front of the supernova remnant can be measured to determine if its frequency changes. Such measurements, made by NRL in 1967 and 1968, indicated that the frequency of the 21-cm hydrogen absorption decreased by several orders of magnitude over the decrease that had been predicted on the basis of relativistic effects or effects of the solar corona when the optical path approached the sun. The first figure shows the observed apparent decrease (about 100 cycles per second) in the 1,420-million-cycles-per-second frequency of the hydrogen absorption line at the point of Taurus A's closest approach to the sun.

If mass affects radiation, it is logical to expect that the effect will be greater the longer the rays are under the influence of the mass. If a well-defined frequency is transmitted from a station on Earth, the effect of the mass of the Earth will depend on the length of the transmission path. In 1967 and 1968, measurements were made of the timing signals



Plot of points representing the experimentally determined difference in frequency between two cesium beam clocks as a function of distance between the two clocks. The four dots represent the results of an experiment started at Cape Fear, North Carolina, on May 2, 1968, and ended at Yarmouth, Nova Scotia, on June 10, 1968 (a northeastward path). The triangle represents the result on a northwestward path between Cape Fear and Washington, D.C. The square indicates the result on a southward path from Cape Fear to Jacksonville, Florida. The error bars were determined from the actual scatter in the time intervals between the two clocks.



Pulse arrival times from CP 0950. ΔT is the difference between the measured and predicted pulse arrival times based on a pulse period of 0.253 055 030 second UT. Curve A is the predicted differential arrival time, if one assumes the mass-on-frequency effect and a pulse period of 0.253 065 030 70 second UT. Line B is a least-squares straight-line fit to the observations.

emitted by the Loran C transmitter at Cape Fear, North Carolina. These measurements were taken at various distances from the transmitter and then accurately compared with timing signals derived from portable cesium-beam frequency standards. At the beginning of the experiment, the receiver and frequency standard were located 10 miles north of Cape Fear; and later they were moved to several other locations along the east coast. At the last location, in Nova Scotia, 1,500 kilometers from Cape Fear, the received timing signals were fractionally lower in frequency than the portable cesium-beam standard by $(1.7 \pm 0.5) \times 10^{-12}$. The results of these experiments indicate an apparent decrease in frequency with distance from the transmitter (see second figure). The apparent frequency shift cannot be explained by gravitational red shift, doppler effects, or relativistic effects.

As a further test, the pulsar CP 0950 was observed through the month of August 1968, during which the sun approached within 5 degrees of the line of sight. The measured pulse arrival times from the pulsar were consistent with an average pulse period of $0.253\ 065\ 032\ 0 \pm 4 \times 10^{-10}$ second UT, taking into account the error in the coordinates used for the position of the pulsar. No effect of the proximity of the mass of the sun on the pulse period, as predicted from the results of the two previous experiments, was observed (see third figure). The cause of this discrepancy has not yet been determined.

NUCLEAR PHYSICS

Analysis for Trace Amounts of Carbon and Oxygen. For some applications, it is desirable that the surfaces of metals be free of contaminants. Inasmuch as two of the most common surface contaminants are carbon and oxygen and that these elements are likely to occur on a surface if any contaminants are present, NRL scientists have developed techniques for detecting extremely small amounts of them. The procedure utilizes the NRL 5 million volt Van de Graaff accelerator as follows: The material whose surface is to be analyzed is placed in the target position within the vacuum system of the accelerator. It is then bombarded with high-speed ^3He particles. If carbon (common isotope, ^{12}C) is present, some of the ^3He particles undergo a nuclear reaction with the carbon, producing ^{11}C and ^4He . The isotope ^{11}C is radioactive (half life, about 20 minutes) and emits positrons. If

oxygen (common isotope, ^{16}O) is present, some of the ^3He particles interact to produce ^{18}F and ^4He . The isotope ^{18}F is also radioactive (half life, about 110 minutes) and emits positrons.

After a sample is bombarded, it is removed from the vacuum system and placed between two NaI(Tl) scintillation crystals, which detect the two positron-annihilation gamma rays (0.511 million electron volts each) in time coincidence. Automatic equipment then records the counting rate as a function of time. If carbon is on the sample during the bombardment, the counting rate exhibits the characteristic 20-minute half life; and if oxygen is present, the characteristic 110-minute half life. The amount of carbon or oxygen present may be ascertained from the magnitude of the counting rate.

This technique has been applied to the surface of gold samples whose cleanliness was critical to a series of chemical experiments.

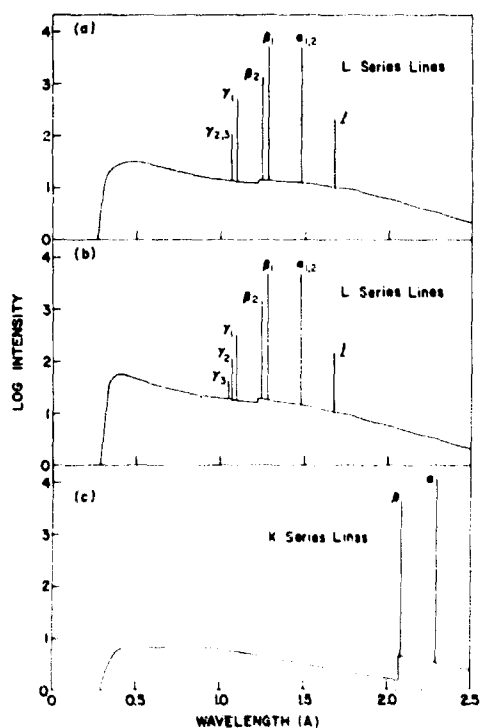
The sensitivity of the technique is such that as few as 10^{11} atoms of carbon per square centimeter (about 10^{-4} atomic layer) or 10^{12} atoms of oxygen per square centimeter (about 10^{-3} atomic layer) can be detected. This extreme sensitivity and selectivity are due to a number of factors: (1) the relatively high cross section for the nuclear reactions leading to the residual radioactive nuclides, (2) the energy discrimination (in the scintillation detector) against other radiations, (3) the discrimination afforded by the imposition of the time-coincidence requirement on the gamma-ray counts, and (4) the discrimination allowed by the decay half life characteristics.

X-Ray Spectrochemical Analysis. Since the early 1940's, NRL has pioneered in the area of quantitative chemical analysis by means of x-ray spectroscopy. In x-ray fluorescence analysis, a sample is irradiated by a high-energy, primary x-ray beam. The radiation excites the elements of the sample, causing them to emit x-rays whose characteristic lines indicate what elements are present. Measurements of the intensities of the spectral lines indicate how much of each element is present, providing that comparison standards or suitable mathematical relationships are available. In electron-probe microanalysis, a similar procedure is followed, except that a focused beam of electrons is used to produce the characteristic x-rays. The focused electron beam allows quantitative chemical analysis to be performed on individual precipitates or inclusions as small as

10^{-4} centimeters in size in alloys, minerals, or biological sections.

Extensive effort has been expended at NRL and other laboratories in government, industry, and universities to improve the mathematical-analysis approach to quantitative analysis because the comparison-standard method is always expensive, usually time consuming, and occasionally impossible to apply. In 1968, significant progress was made at NRL in three areas which will increase the Navy's capability in quantitative x-ray spectrochemical analysis:

(1) In x-ray fluorescence, the first accurate spectral distribution measurements of the radiation from x-ray tubes were obtained and compared with theoretical values on an absolute scale. These measurements enabled NRL investigators to accurately describe the detailed features of the primary exciting beam and thus to upgrade considerably the mathematical-analysis method.



Examples of measured x-ray spectral distributions: (a) tungsten target OEG-50 tube, 50-thousand-volt peak (full wave) excitation; (b) tungsten target OEG-50 tube, 45-thousand-volt constant potential excitation; (c) chromium target OEG-50 tube, 45-thousand-volt constant potential excitation.

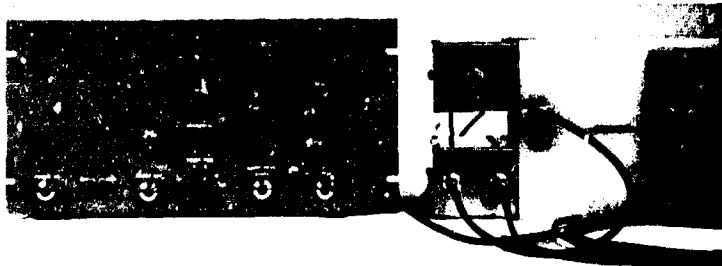
(2) Preliminary expressions were developed for x-ray fluorescence analysis of inhomogeneous specimens, such as heat-treated alloys and ore slurries. Heretofore, such analysis has presented an almost insurmountable problem because the characteristic x-ray intensities emitted from a sample are very sensitive to local variations in the x-ray mass absorption coefficient and hence to any variation in matrix composition. The preliminary expressions are limited to regular geometric shapes, such as spheres, rods, and cubes, and they are not in mathematical closed form except in special cases. Work continues on extending and generalizing the expressions.

(3) In electron-probe analysis, improvements were made in electron-transport equations for calculating both relative and absolute x-ray intensities due to each of several elements in a sample. The comparison of theory with experimental measurements indicates that the transport equations are now able to predict electron backscatter coefficients to within ± 3 percent accuracy and characteristic x-ray intensity to ± 10 percent. In the transport program, provision was made for fluorescent x-ray excitation by the electron-excited x-ray continuum (work originated in France in 1962) in addition to the usual secondary fluorescence by characteristic lines from other elements in the sample. The whole mathematical approach in electron-probe analysis is being prepared as a computer program. This program will be distributed to analysts as soon as it is available.

A Neutron Coincidence Detector for Safeguards Inspections. The possibility that a nation or even a private corporation might divert a certain portion of its fissile (i.e., thermal neutron fissionable) material intended for peaceful uses to the production of nuclear weapons has caused concern for a number of years. The seriousness of the problem is expected to increase enormously in the next decade as the expanded use of nuclear power leads to the production of large amounts of plutonium. Therefore, a number of national and international scientific organizations are examining the problem of safeguarding fissile material from possible diversion to weapon manufacture.

NRL has developed a neutron-coincidence detector which may prove to be very helpful in one type of plutonium inspection procedure. By means of four BF_3 tubes in a polyethylene moderator, the device measures neutrons produced in the spontaneous fission of ^{240}Pu . By taking advantage of the

The moderated array of BF_3 tubes which detect the neutrons is shown on the right. The coincidence unit displays simultaneously the total neutron count, the accidental coincidence count, and the real (true plus random) coincidence count.



fact that the fission of ^{240}Pu produces an average of 2.2 neutrons in coincidence, the instrument is also able to distinguish fission neutrons from those which might be produced by a radioactive source.

In October, NRL supplied a model of this instrument to the International Atomic Energy Agency (IAEA) in Vienna for use and evaluation. One of the functions of the IAEA is to conduct safeguards inspections at reactor sites throughout the world. The neutron-coincidence detector has already been used successfully in the examination of plutonium plates at the reactor in Winfrith, England, and is expected to be used in a forthcoming IAEA inspection of the Yankee reactor in Massachusetts.

Funds for the research leading to the development of this instrument were supplied by the U.S. Arms Control and Disarmament Agency. The model shown in the accompanying photograph was constructed for NRL by the Brookhaven National Laboratory.

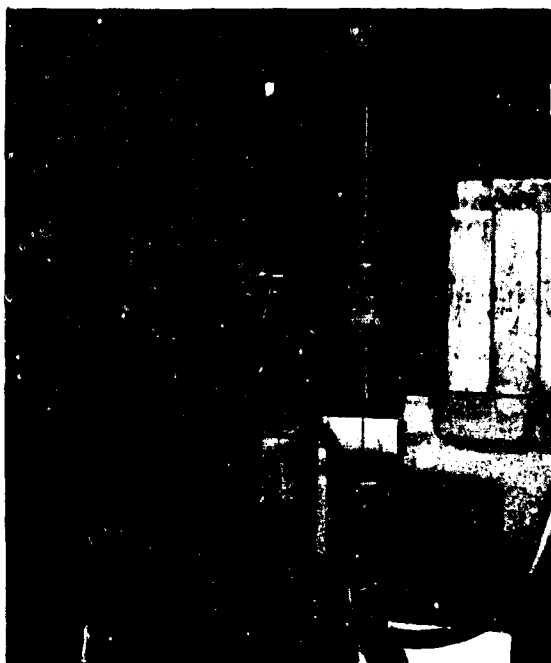
The Nature of Neutron Capture. According to the usually accepted theory of neutron capture, the highly excited capture states are of such a complex nature that they may only be described in statistical terms. This theory is well verified when one observes the gamma decay averaged over a set of resonances in the same nucleus. The theory would also imply that when one observes the gamma decays resulting from thermal capture in a set of nuclei which are similar in their low-lying levels, he would expect to see no regularity in the gamma transitions.

Recent studies of the high-energy electric dipole transitions following thermal neutron capture by even-even deformed nuclei with mass numbers ~ 180 have given results which seem to contradict this statistical theory. A set of seven neutron-capture reactions in ^{188}Er , ^{188}Yb , ^{178}Hf , ^{180}Hf , ^{184}W , ^{186}W , and ^{188}W samples showed an interesting regularity. Exceptionally strong transitions were observed to

go to rotational levels which have a quantum number known as "lambda" or "the third Nilsson number," which is either zero or one. Other transitions were either absent or greatly attenuated. Not only does such a regularity seemingly violate the statistical theory, but it violates it in a manner which is suggestive of a direct capture mechanism.

Advocates of a statistical model quite correctly argue that in any statistical phenomenon, seeming regularities can occur by accident. Three more cases— ^{170}Yb , ^{172}Yb , and ^{174}Yb —were, therefore, investigated employing the external beam of thermal neutrons at the NRL reactor. These cases were particularly interesting, both because they involved nuclei between those of erbium and tungsten, previously studied, and because their low-lying levels were well investigated by (d,p) and (d,t) studies. The NRL results showed that the regularity persists in all three reactions. In addition to the strong relative population of rotational Nilsson bands with lambda zero or one, the NRL results showed that there was a preference for particle states over whole states, further suggesting direct capture.

The existence of this regularity in an impressive number of thermal-neutron capture reactions indicates the desirability of extending capture measurements of the same nuclei to the resonance neutron energy range. Such measurements are now being made employing the NRL 60-million-electron-volt linear accelerator time-of-flight facility, which recently became operational. A pulse of neutrons less than a microsecond in duration is generated in a water-cooled tantalum target by means of (γ, n) reactions produced by the bremsstrahlung from the primary electron beam pulse. Appropriately moderated neutrons travel down a beam tube and are allowed to strike the sample under study. The 9-meter distance between source and sample is precisely known, and the energy of each neutron is then calculated from its arrival time after the source pulse—thus the term



Neutron-production target assembly for NRL's linear accelerator time-of-flight facility. The electron beam emerges from the accelerator's beam tube through thin, water-cooled metal foils and strikes the stainless steel target housing in the center of the picture. Inside the housing, the electrons generate fast neutrons via cascade electron-gamma-neutron reactions in a series of water-cooled tantalum plates. The fast neutrons are partly moderated in the slab of polyethylene located behind the target, and a fraction of them proceed down a four-inch-diameter flight tube through the wall behind the target. Discoloration in the polyethylene slab is due to radiation damage. Dimensions may be ascertained by comparison with the eight-inch-long lead bricks.

"time-of-flight." The linear accelerator is ideally suited to this work because of its pulsed nature and high intensity (more than 10^{13} neutrons per second (time average) are produced at the source).

For measurements of capture gamma rays due to neutrons in the 1-200 electron-volt resonance energy range, the element under study is placed in the neutron beam, and the gamma rays generated are measured by a high-resolution Ge(Li) detector. Presently, data are recorded in a 4,096-channel two-dimensional array, usually with 1,024 gamma-ray energy channels being associated with each of four time-of-flight channels. A projected data-acquisition computer with magnetic-tape storage will have a 4-

million-channel two-dimensional array capability; its use will permit 4,096 gamma-ray channels to be associated with each of 1,024 time-of-flight channels.

Preliminary analysis of data from ^{168}Yb indicates that the gamma spectrum for its first resonance is just like that for thermal capture and exhibits the same regularities seen in the thermal capture of ^{168}Yb and other nuclei.

Ion Implantation. Research on the effects of the implantation of ions in solids has been carried out by the Nuclear Physics Division and the Solid State Applications Branch of the Solid State Division. A number of samples have been irradiated by the 5-million-volt Van de Graaff accelerator using magnetically analyzed beams of ^3He , ^{40}Ar , ^{84}Kr , ^{86}Kr , and ^{136}Xe ions. The experiments performed thus far fall into two categories: (1) the implantation of an accurately known number of atoms into a solid in order to produce calibration standards and (2) the implantation of various heavy ions into solids for the study of radiation effects. A third type of experiment, in which the implanted ion affects the electrical properties of the target solid, will be started in 1969. In preparation for these studies, an improved ion-optic system and an analyzing magnet were added to a 30-thousand-volt apparatus, and the resolution of beams of ^{11}B ions was tested and found to be good.

A particularly interesting set of experiments involved the study of the coloration of LiF single crystals when irradiated with beams of 3.0-million electron-volt (MeV) ^3He , ^{40}Ar , and ^{84}Kr ions and 2.0 MeV ^{136}Xe ions. A number of new optical absorption bands were found as a result of irradiations with these massive ions. (Previously, the deuteron was the heaviest ion used to produce color centers in LiF.) For comparison, coloration in LiF was also produced by gamma ray irradiation, but the new bands were not observed. Precautions were taken during the irradiations to insure that effects due to heating or electrostatic charging were negligible and that the integrated beam flux over the area of the crystal sample was uniform.

The absorption spectra were measured with a Carey 14-spectrophotometer, and the resulting curves were analyzed with a digital computer and a Gaussian curve fitting program. In addition to the well-known F and M bands in LiF, three new absorption bands were found with the ^{40}Ar , ^{84}Kr , and ^{136}Xe irradiations at 3,860 angstroms (Å), 4,170Å, and 5,590Å. A

broad, small-amplitude absorption band was found at 4,280Å for the ^3He irradiations, but it is possible that this band is the same as one or a combination of the 3,860Å and 4,170Å bands produced by the more massive ions. Further experiments have been planned to determine the nature of the defects responsible for these absorption bands.

Successive etchings were performed to measure the F-center dependency of the density on the depth of ion penetration into the crystal. The etching measurements agree quite well with range calculations and show that for each type of bombarding ion the F-center density is fairly uniform along the particle's penetration range.

Charged-Particle Energy Losses and Fluctuations. Precise determinations of the energies and widths of nuclear levels are made at NRL by means of beams of charged particles from the 5 million volt Van de Graaff accelerator after the beams have passed through a magnetic beam analyzer and a very precise 2-meter-radius electrostatic beam analyzer. These well-defined beams of constant, known energy and small energy inhomogeneity may be used to produce (p, γ) reactions. A plot of the number of gamma rays per incident particle *versus* the particle energy in the neighborhood of a sharp resonance is called a yield curve. This curve has a shape which depends upon the following factors: (1) the beam energy distribution, (2) the width and energy of the nuclear resonance, (3) the rate at which the beam particles lose energy as they interact with atomic electrons and excite and ionize the atoms along their paths, and (4) the statistical fluctuations of these energy losses.

Studies based on a theory of energy-loss fluctuations advanced by P. V. Vavilov have been made. Vavilov solved a transport equation governing these loss distributions on the assumption that the formula which gives the probability for the energy loss in a single collision of the incident particle with an electron has a simple form which ignores the occurrence of "distant collisions." The analysis of precisely measured (p, γ) resonance yield curves provides an excellent means of testing this theory.

Preliminary results indicate that for targets of aluminum, which has an atomic number of 13, the theory affords a good description of experimental results. However, for a target material such as tantalum oxide, which has 186 electrons per molecule, it has been found that the description is not good

The single-collision loss probability assumed by Vavilov is proportional to the number of electrons per molecule (Z/A). Except for the light atoms, the inner electrons are bound so tightly that the probability of excitation or ionization of the atom by the incoming charged particle is very small. One might expect that if a change in the formula is made such that the real Z/A is reduced to a smaller "effective" Z/A a more realistic description would result. This has been shown to be the case, and it is anticipated that the "effective" Z/A will prove to be a useful parameter in the theory of energy loss and energy-loss distribution and in the application of the theory to problems in nuclear and atomic physics.

Triton-Induced Nuclear Reactions. In the 1967 *Annual Report*, success was reported in achieving a systematic analysis of the triton elastic scattering data taken with the NRL 2-million-volt Van de Graaff accelerator. The principal product of such studies is a set of parameters which generate wave functions. These wave functions give an accurate description of the interaction of the scattered particle with the target nucleus. The importance of these functions is that they can be utilized directly in nuclear reaction calculations.

The optical model parameters obtained from the scattering analysis were applied to a study of triton-induced reactions employing the distorted-wave Born approximation (DWBA). The two types of reactions studied can be represented as $T(t,p)R$ and $T(t,\alpha)R$, where T is the target nucleus and R is the residual nucleus. It is believed that the triton, a loosely bound particle consisting of two neutrons and a proton, interacts with a given nucleus predominantly by a one-step or direct process. The (t,p) reaction occurs when the triton, passing close by, transfers its two neutrons to the target nucleus; the (t, α) reaction occurs when the passing triton plucks a proton from the target nucleus. The DWBA method treats both processes as one-step transitions between scattering states. The initial scattering state is completely described by the elastic scattering parameters alluded to above. The final state is completely described by optical model analysis of the elastic scattering of protons (or alpha particles) of the proper energy by the appropriate nucleus. Since, in general, such experiments have not been performed, published values for optical model parameters describing processes that are about the same as (if not identical to) the desired ones are used.

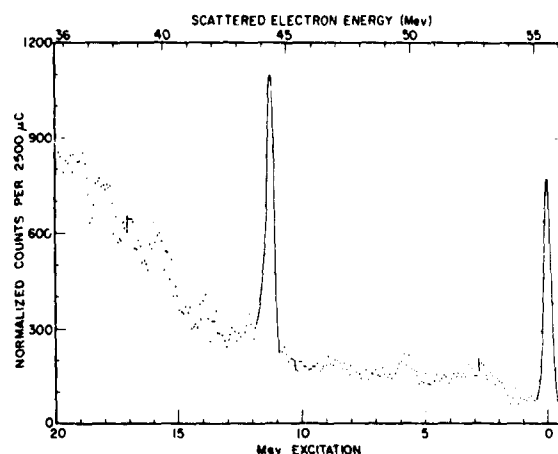
Studies have been made of (t,p) reactions with target nuclei ^{10}B , ^{12}C , ^{16}O , and ^{20}Ne at energies ranging from about 1.50 million electron volts (Mev) to 2.19 Mev. Most of the angular distribution data has been subjected to DWBA fitting procedures with excellent results. More than half of these distributions have been successfully fitted; some are still under investigation.

Analyses of (t, α) reactions have been carried out with the data of two experiments— $^{11}\text{B}(t,\alpha)^{10}\text{Be}$ and $^9\text{Be}(t,\alpha)^8\text{Li}$. The first reaction was studied at a range of energies between 1.0 and 2.1 Mev, and the second was studied only at 2.1 Mev. The analyses of both utilized the results of a recent detailed study of the ($^3\text{He},\alpha$) reaction that indicated the need to apply deep potential wells (about 150 Mev) instead of the customarily used shallow wells (about 50 Mev) to describe the interaction of alpha particles with nuclei. Use of the deep wells significantly improved the fits to our data. In addition to supplying information concerning the nature of the mechanism of the reaction, the DWBA analyses permitted the extraction of "spectroscopic factors" which yield structural information about the product nuclei.

Nuclear Structure Investigations by Inelastic Electron Scattering. New versatility has been added to the electron-scattering program of NRL's 60-million-electron-volt (Mev) electron linear accelerator (Linac). A chamber designed to contain gaseous target material, originally developed in 1966, has now been put into routine use. This chamber includes 0.00025-inch alloy windows for beam entry and exit. It is normally used at a 65-pounds-per-square-inch gas pressure and at a liquid-nitrogen temperature of 77°K. The recovery of expensive separated isotopes is provided for by a novel method of freezing them out at liquid-helium temperature.

The structure of nuclei having the same even number of protons and neutrons is particularly interesting since theoretical selection rules are unusually stringent in these cases. The 180-degree electron scattering should be dominated by a small group of transitions. These are magnetic dipole transitions to states which are analogs of states in neighboring nuclei. Further, Dieter Kurath, a prominent theoretician at Argonne National Laboratory, predicts the concentration of scattering in the lowest few transitions of this kind.

The results reported last year for ^{24}Mg (12 protons, 12 neutrons) are in agreement with these predictions,



Spectrum of electrons scattered at 180 degrees by ^{20}Ne when bombarded by 56-Mev electrons from NRL's linear accelerator. The peak at zero excitation energy is due to elastically scattered electrons which did not excite the nucleus. The lower energy electrons show a pronounced peak due to nuclear excitation and a continuum due to other forms of energy loss. A newly installed gas target chamber was employed to obtain these data.

with the dominant peaks corresponding to the two lowest-energy eligible states in ^{24}Na . Later results based on studies of ^{28}Si (14 protons, 14 neutrons) are similar, showing analogs of states in ^{28}Al . The recent results of studies of ^{20}Ne (10 protons, 10 neutrons) are even more striking. As can be seen in the accompanying figure, the spectrum of electrons scattered from ^{20}Ne shows only one pronounced peak in the region extending from the elastic scattering peak to 20-Mev excitation. This peak is due to the transition to the analog of the lowest eligible state in ^{20}F .

Research Program with the Sector Focusing Cyclotron. The first high-energy beam was extracted from the NRL cyclotron on February 12, 1968. On the following March 11, a particle beam was transported through the 9-foot radius-of-curvature analyzing magnet and, on April 27, was transported into experimental room No. 2. In May, isotope production was initiated in the cyclotron vault, and preliminary measurements on the doppler-shift attenuation experiment were started. Preliminary scattering studies were begun with the 30-inch-diameter scattering chamber in experimental room No. 3 during June.

By the end of the year, all of the planning for the initial start-up of the cyclotron facility had been accomplished. This included operation of the cyclotron for a variety of particles covering the energy range from about 10 to 50 million electron volts, the installation and operation of three beam paths (one to each of the three experimental rooms), and the full operation of several experimental programs. This work was sufficiently well advanced by the middle of September to permit four abstracts describing research results to be included in the program of the November (Miami) meeting of the Nuclear Physics Division of the American Physical Society. Subjects on which reports have been written and on which work continues include doppler-shift attenuation, J^π dependence in alpha induced reactions, multi-particle breakup mode of ${}^6\text{Li}-{}^4\text{He}$ and ${}^7\text{Li}-{}^4\text{He}$ reactions, and activation analysis. In addition, the cyclotron has provided service irradiations to NASA, Thompson Ramo Wooldridge, and The Space Sciences Division of NRL. Other studies actively under way involve neutron particle correlation, polarization, isospins, and the distribution of energy lost by fast charged particles in thin silicon solid-state detectors.

NRL and Georgetown University scientists have collaborated in nuclear research for several years; a new collaborative study, this one of (alpha, xn) reactions, was begun by NRL and Indiana University physicists in 1968.

New Approach to Bound States of Two Spin Waves in Heisenberg-Type Ferromagnets. In theoretical investigations of insulating ferromagnets, the Heisenberg model of ferromagnetism has proved to be a productive source of experimentally interesting and significant predictions. In this model, the spins of the magnetic ions are assumed to be coupled by exchange interactions, which may extend to any arbitrary number of neighbors. The low-energy collective excitations of such a system of coupled spins are called "spin waves." Such excitations are susceptible to detailed experimental investigation in a number of ways, the most accurate and general one being by means of the spin-wave scattering of polarized neutrons. This method was first proposed and used by NRL scientists in the early 1960's.

It has been known theoretically for some time that spin waves can cluster together to form bound states. Very recently, other theorists have predicted that

such states should be experimentally detectable by inelastic neutron scattering, just as free spin waves have been detected. In spite of the considerable experimental interest in this bound-state question, no theoretical investigations of a general scope have been carried out on this subject.

The present NRL investigation initiates a general theoretical attack on the problem of two bound spin waves in Heisenberg-like ferromagnets. In the formulation of this problem, a new and powerful calculational method has been introduced into solid-state physics. This method, the trace-inequality method, consists of a generalization of procedures from nonrelativistic scattering theory, heretofore neglected in solid-state applications.

By means of the trace-inequality approach, rigorous and practical sufficient conditions for the existence and nonexistence of bound spin-wave states have been discovered. These conditions are applicable to a wide class of crystal structures and to essentially arbitrary modes of coupling of the magnetic ions of the class of ferromagnets of interest. By using this approach on a high-speed electronic computer, it is possible in principle to map out the regions of existence and nonexistence of bound states of two spin waves under extremely general conditions.

The method has been successfully applied to the case of a body-centered ferromagnetic crystal with nearest-neighbor couplings. Comparisons of these results with those obtained previously indicate that crystal structure plays an important role in the bound-state spin-wave problem, a conclusion that had not been established by previous theoretical work.

Iteration Procedures for Analysis of Scattering Processes. The method perhaps most widely applied for analyzing scattering processes in quantum mechanics is the Born perturbation expansion, which expresses the solution as a power series in a coupling constant λ . This power series is a good approximation only for values of λ that are sufficiently small; the method is frequently successful in atomic physics where $\lambda \approx 1/137$, but usually fails for nuclear and particle processes where $\lambda \approx 15$. A completely different approach which shows promise of being applicable to these strong interactions has been conceived at NRL and the first stage of its development completed.

The NRL approach deals with the class of interaction procedures that can be written as a functional

$F(\psi)$ used, via the rule $\psi_{n+1} = F(\psi_n)$, to generate a sequence $\psi_0, \psi_1, \psi_2, \dots$ desired to converge quickly to the wave function of the quantum system. Given such a functional $F_1(\psi)$, one seeks methods of manipulating it to obtain an improved $F_2(\psi)$; the starting point is the functional which generates the Born expansion. Four such methods have been developed which, if applied serially, are capable of generating many useful and accurate iteration procedures. In these methods, a central role is played by matrix elements which measure the behavior of a functional for small and large distances from the scattering center.

In addition to their flexibility, an important advantage of such iteration procedures is that, in contrast to the standard perturbation expansion, the choice of ψ_0 need not be the (unperturbed) free wave solution. It is possible to select an input which better represents the average wavelength in the scattering region.

The NRL approach has been worked out and successfully applied to the case of simple potential scattering. For this case, it is much more powerful than the Born expansion and does indeed appear adequate for strong interactions. During their development, the iteration improvement methods were carefully restricted to those which seemed to promise straightforward extension to the more complex cases of actual physical interest.

A significant byproduct of this effort is a new approach for investigating the domain of validity of the Born expansion and of bounding the error involved in truncating it at any given stage.

Plasma Physics

Thermal Blooming of Laser Beams. Considerable effort is presently being directed toward developing laser beams for use in communications and ranging and for other applications where a continuous, intense beam or a pulsed beam with a high repetition rate is directed long distances through the atmosphere. It is now well known that in many practical cases there is sufficient absorption of energy from the beam to cause heating of the medium and a consequent change in its index of refraction. In many media, this change is negative and thus produces a diverging-lens effect leading to a lowering of the beam's power density and a degradation of its optical quality. Due to the increase in beam divergence, the phenomenon has become known as "thermal blooming" or

"self-defocusing." As a result of thermal blooming, the distance over which a given laser beam power density may be propagated is greatly reduced. It is of considerable importance, therefore, to understand the mechanisms controlling thermal blooming in order to find ways of minimizing the effect.

In response to the need for a detailed experimental analysis of thermal blooming, NRL initiated direct interferometric observations of the index changes arising in this phenomenon. A 65-milliwatt helium-neon laser (6,328 angstroms) was used to furnish the heating beam for propagation through a cell containing carbon tetrachloride doped with iodine to increase the absorption coefficient. The liquid cell was placed in one arm of a large Mach-Zehnder interferometer, with the optical path of the interferometer arm at right angles to the heating beam. A moving-picture camera simultaneously recorded the index changes in the medium as revealed by the interferometer fringe pattern and the intensity pattern of the laser beam as it exited from the liquid cell (see figure). In this way, spatially and temporally resolved data on the index variation could be correlated with the observation of thermal blooming.

In the initial phase of the experiment, a study was made of certain features of the phenomenon which could be described by theoretical expressions in closed form. The agreement between experiment and theory was satisfactory. The evolution of the

Interference fringe deflections due to the heating of iodine-doped carbon tetrachloride by the absorption of laser light are shown at three different times: (top) 0.9 second, before convection begins; (center) 2.5 seconds, near the onset of convection; and (bottom) 6.75 seconds, the beginning of the steady-state convective stage. The heating beam passes through the cell horizontally from left to right. The two small patterns at the right show the bloomed laser beam as viewed 55 centimeters from the exit window of the liquid cell. (Two patterns are produced because of reflections from the two surfaces of the beam splitter.)



0 1 2 3 (CM)

process from a conduction regime to a convection regime could be clearly seen in the interferometer fringe patterns.

In future experiments, an attempt will be made to eliminate the contribution of convection to heat dissipation by selecting a liquid medium in which convection does not occur; then the process will depend only on the equations governing heat conduction and light propagation. These equations are being solved on a digital computer so that the most general aspects of the phenomenon may be studied. Planned also is an investigation of thermal defocusing in air; techniques developed in the study of defocusing in liquids will be applied, although a carbon dioxide laser will be used as the beam source.

Collisionless Shock Wave Research. Research has been under way for several years at NRL and at various laboratories throughout the world to clarify the nature of collisionless shock waves. Such shocks can occur only in plasmas since they are caused by collective phenomena rather than the binary collisions that are responsible for ordinary gas dynamic shock waves. Collisionless shock waves are of interest for several reasons: They offer a new approach to controlled thermonuclear fusion, they occur in nature (for example, the solar wind impinging on the Earth's magnetic field is known to produce a collisionless "bow shock" between the Earth and the sun), and they display the collective dissipation and nonlinear phenomena that are so important in many laboratory and natural plasmas.

At NRL, collisionless shock waves have been produced in a small theta-pinch tube. The procedure begins with the injection of a plasma into the apparatus. An initial axial magnetic field is then established, following which a novel energy-storage system is rapidly discharged through the theta-pinch coil. This produces cylindrically symmetric shock waves which rapidly (up to 2×10^8 centimeters per second) implode toward the tube axis. The energy-storage system utilizes very high voltage transmission lines to deliver up to 10^{10} watts of electrical power to the coil during a period of 60 nanosecond.

The shock waves are detected by observing the compression of the initial magnetic field on miniature probes inserted into the tube. The magnetic structure of the shock, and particularly the thickness of the front, is of considerable theoretical interest. NRL physicists have observed shock thicknesses in an argon plasma that are two orders of magnitude

narrower than had been predicted. Recent reports of observations of the Earth's bow shock by the OGO-V satellite indicate that it is similarly thin.

Measurements have also been made of the electron heating in these waves by observing the x-ray bremsstrahlung that is produced. With the aid of an NRL-developed computer code, the relative x-ray fluxes through sets of metal foils of different composition have been interpreted to determine the thermal energy of the radiating electrons. The measurements indicate that the electrons, and probably the ions as well, are heated to enormous energies. In argon, electron temperatures of over 100 thousand electron volts have been measured. The heating rates are too fast to be accounted for by ordinary Joule heating. Considerable effort is therefore being devoted to identifying possible collective dissipation mechanisms that might be responsible for this phenomenon.

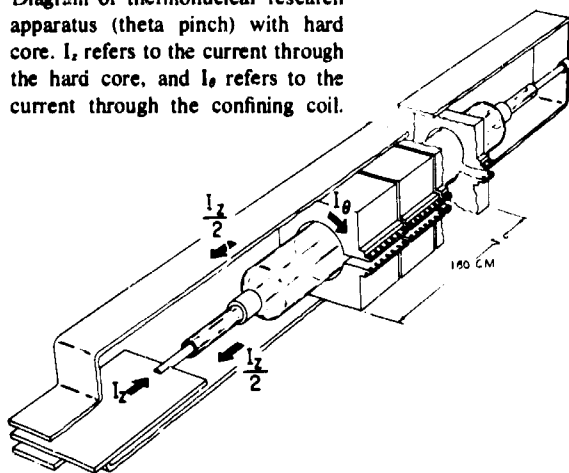
Equipment for a larger, complementary experiment has been built at the University of Maryland under the NRL-University of Maryland Joint Program in Plasma Physics. It is hoped that over the next year much progress can be made through the two experiments in understanding this fascinating plasma phenomenon.

Hard Core Theta-Pinch. For some years, scientists at NRL have been investigating methods of heating and confining ionized gases (plasmas) at extremely high temperatures. The principal device developed for this purpose has been a theta-pinch, in which a solenoid is used to produce an axial magnetic field that compresses radially, heats, and confines (free of cool walls) plasmas at temperatures as high as 10 million degrees. One of the problems that has arisen is that numerous instabilities occur in the coupling of hydrodynamic and electromagnetic processes. These instabilities are as yet not well understood theoretically. In addition to, but not entirely separate from, that problem is the difficulty of closing the "magnetic bottle" at the ends of the solenoid to increase the time that the hot, high-pressure plasma can be contained.

In an effort to improve the stabilization of the plasma while maintaining closed magnetic-field lines at the ends of the solenoid, radial shear was introduced in the field between the inner and outer radii of the annular plasma that forms between the 17-centimeter-diameter container and an insulated axial conductor ("hard core") through which a high current (up to 1 megampere) was passed (see diagram). The

GENERAL SCIENCES

Diagram of thermonuclear research apparatus (theta pinch) with hard core. I_z refers to the current through the hard core, and I_θ refers to the current through the confining coil.

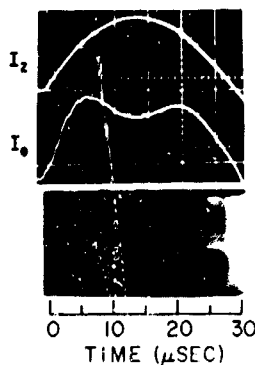


helical field lines resulting from the axial and azimuthal field components change direction across the plasma layer, thereby producing the desired shear. The radial evolution of the resulting plasma is illustrated here along with the two currents. The figure indicates gross stability and equilibrium for the peak-current portion of the discharge.

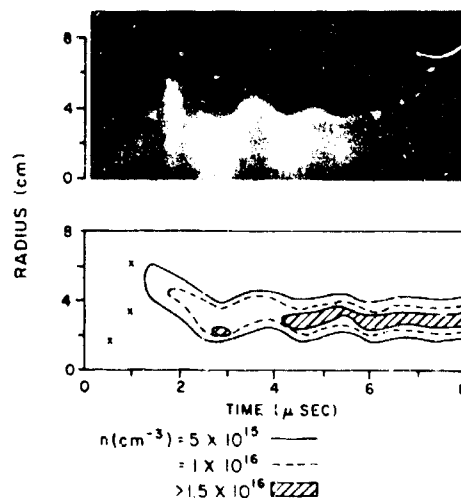
In order to better understand the detailed structure of the plasma, magnetohydrodynamic computer programs have been written and used successfully to predict both the observed macroscopic plasma behavior (see figure) and such basic plasma parameters as density, temperature, internal fields, and stability criteria within the plasma proper.

Under the present operating conditions, the lifetime of the plasma is limited by diffusion of the confining fields into the plasma and by rotational perturbations caused both by axial currents in the plasma near its ends and by slight asymmetries in the position of the central rod. These effects are being studied in more detail by means of improved diagnostic techniques.

High-Brightness Glass Lasers. Advances in laser technology in the past two years have made laser systems competitive with, and in some respects superior to, other methods of generating short-duration bursts of energy. Peak powers of 20 gigawatts (2×10^{10} watts) in a 30-nanosecond pulse have been obtained with a system consisting of a well-controlled master oscillator and a number of amplification stages. Because of the high degree of collimation, the beam can be focused to obtain



Hard core (I_z) and coil (I_θ) current waveforms and a streak-camera photograph of the hard-core theta-pinch experiment.



Radial-density distribution versus time determined on the basis of experimental streak photographs and computed constant-density zones. The x's represent computed peak-density regions at early times.

peak power densities of greater than 10^{16} watts/square centimeter.

The laser is attractive for plasma-confinement experiments because the light beam does not interact with magnetic fields. This makes it possible to create a plasma inside a magnetic "bottle" and avoid the difficulties that are encountered in injecting plasma into a confinement geometry.

In addition, the combination of high power and low divergence makes lasers of this type suitable for

experiments in frequency conversions and other non-linear optics phenomena.

Neodymium-doped laser glass has been the most desirable laser material for this type of system because of the ease with which large rods can be fabricated compared with such fabrication from crystalline laser media. However, domestically supplied laser glasses have such a low damage threshold that large systems would be exceedingly inefficient.

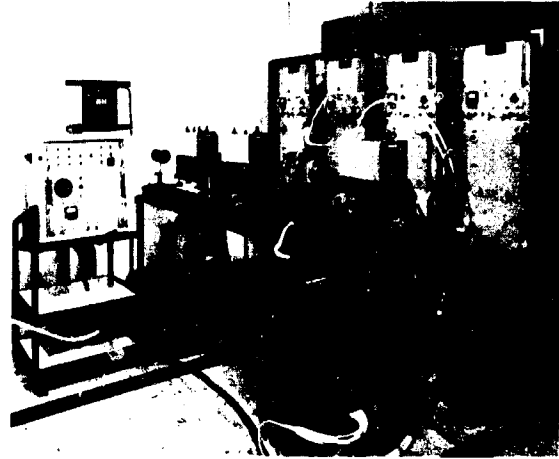
The French have succeeded in producing a laser glass with a very high damage threshold and in incorporating this into high-power laser systems. NRL has purchased and is now operating a three-stage system which produces 60 joules in a 30-nanosecond pulse. The system consists of a rotating prism switched oscillator and two amplifiers. The oscillator produces a well-collimated 3-joule pulse, and the amplifiers raise the beam energy to 60 joules. It is planned to add several more amplifier stages to this laser system to produce 500 joules in 30 nanoseconds. Additional oscillators are being designed to produce sub-nanosecond pulses, which will be amplified to high energy.

MATHEMATICS AND INFORMATION SCIENCES

Information Systems. Naval and other national authorities require an information system capable of designating the position and identity of all mobile platforms above, under, and on the world's oceans. NRL is conducting a multiphase research effort to develop this capability. The initial phases are aimed at providing a timely and accurate data base for such a system. Future efforts will examine methods of facilitating interaction between the data base and the decision makers or users of the information system.

The basic information flowing into the system consists of reports generated by various sensors and intelligence sources. These reports can be conflicting and incomplete, lacking the unique identifiers of the object of the report. Methodological investigations are being conducted to derive algorithms to permit association of such reports arising from a common object. Several candidate algorithms have been developed, and work is continuing in this area.

To support the analytic investigations, a computer test bed is being developed. The test bed will provide a means of evaluating candidate methodologies in



NRL's glass laser system (CGE VD320). The oscillator is on the right end of the optical bench, and the two amplifiers are on the left. The first amplifier raises the output level to 24 joules and the second to 60 joules. The control console is on the left, and the flashlamp power supplies are on the right.

a realistic report environment. In addition, it will provide a means of performing sensitivity analyses that can isolate areas requiring improvements in sensor technologies to supply information needs not presently satisfied.

Future studies will also consider associated problems of a total intelligence information system, including the man-machine interface. Development of query languages and computer-based artificial-intelligence techniques which imitate human activity in association and correlation are among the activities to be pursued.

Phased-Array Radar. A phased-array antenna is an inherently flexible sensor. As yet, no adequate methodology exists which systematically exploits this flexibility for its incorporation into an adaptive controlled radar. Such a radar is one which continually monitors its own performance relative to a given optimal condition and modifies its parameters by means of closed-loop action to approach the optimum. The NRL objective in this area is to develop a methodology.

A simulation model of the search mode of such a phased-array radar has been developed. The basic components are a search strategy, an evasion policy,

and a radar environment. The program is packaged so that each of the major radar functions is represented by a distinct module. Thus, modifications can be readily implemented.

The evasion policy permits the direction of a target to be shifted a random amount at random intervals of time. The radar environment is assumed to be one with random noise but no clutter or jamming. Various classical search procedures have been used.

A tracking package has been developed which uses a second order Kalman filter to predict future target positions.

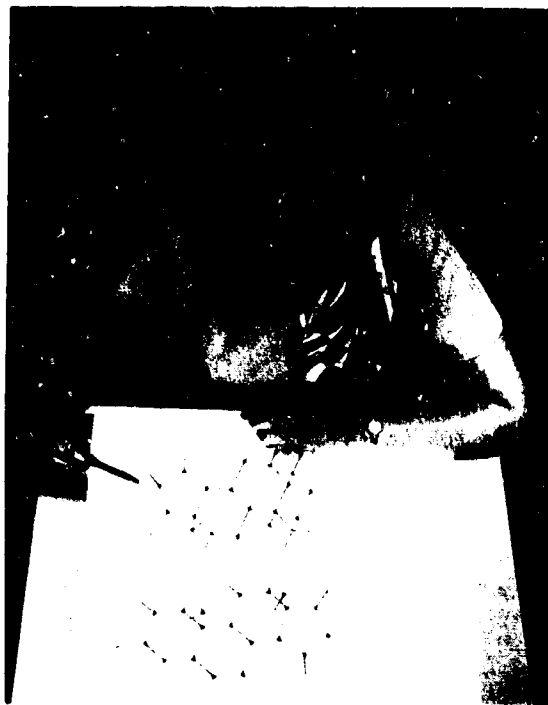
Analytic Functions and Their Applications. Analytic functions play a central role in many fields of pure and applied mathematics, and they have important applications to problems in science and engineering. Approximations to and with the use of analytic functions have become of increasing importance with the widespread use of automatic digital computers in scientific research. This project is concerned with the study of certain basic properties of analytic functions which are of particular importance for their applications and for the development of simple and accurate approximations.

These properties include the average size and rate of growth of the functions and their derivatives, their representations by power series, and their distribution of values and zeros. An especially useful and interesting class of entire functions of bounded index has been defined and studied with reference to these properties. These functions have also been found useful in the study of certain types of differential equations of infinite order, and a paper on this subject has appeared in volume 11 of the *Proceedings of Symposia in Pure Mathematics*, published by the American Mathematical Society.

A partial characterization of the class of functions of bounded index in terms of the important properties of order and type is given by NRL's determination that an entire function of bounded index is necessarily of exponential type and therefore does not have a rate of growth exceeding that of an exponential function. This important fact led to a more detailed investigation into the class of functions of exponential type and to the partial characterization of those functions in terms of their comparative rates of growth and their derivatives. This work was presented to the 1968 summer meeting of the American Mathematical Society and will be published in the *Journal of Mathematical Analysis and Applications*.

The importance of this work for applications and numerical approximations to problems in science and engineering is greatly enhanced by the following facts: (1) functions of bounded index possess particularly simple and accurate approximations by partial sums of their power series expansions, and (2) the class of functions of bounded index includes many of the standard functions of analysis, such as the exponential and trigonometric functions, and certain types of Bessel and confluent hypergeometric functions. In fact, any function which satisfies a linear differential equation with polynomial coefficients for which the degree of the leading polynomial is not less than the degree of any other of the polynomial coefficients is necessarily of bounded index.

Analysis of Noncentrosymmetric Crystal Structures. The occurrence of overlapping vectors usually complicates the problem of determining crystal structures. A mathematical formalism, developed at NRL, which facilitates recognizing and coping with this frequently occurring problem, has permitted the elucidation of



With reference to a structural model, an NRL mathematician points out a characteristic feature of two variants of androstane crystals (a single pentagonal ring of atoms among three hexagonal rings).

several complex noncentrosymmetric crystal structures. The method is strongly dependent on a recently derived probability distribution involving the phases of the crystal structure factors as well as on a novel least-squares technique, both obtained by the mathematics group at NRL. The crystal structures of estriol and two variants of androstane, sex hormones having important application in cancer research and crystallizing in noncentrosymmetric space groups, have been determined by these techniques using experimental data supplied by scientists at the Medical Foundation of Buffalo.

Polynomial Approximations on the Whole Real Line.

Frequently it is advantageous to approximate a mathematical function by another function more amenable to some particular use. (Such approximations are frequently used in machine computations.) Improved methods of determining the accuracy of approximate functions are obviously of prime importance.

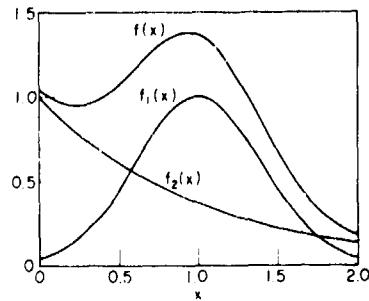
Given a continuous real-valued function $F(x)$ on $(-\infty, \infty)$ and a positive integer, N , it is desired to approximate $F(x)$ by a polynomial $P_N(x)$ of degree N (or less). As a measure of accuracy in performing this approximation, consider the quantity $|F(x) - P_N(x)|w(x)$ and let E_N be the maximum of this quantity over all x in the interval $(-\infty, \infty)$. Here, $w(x)$ is a "weight" function, a standard example of which is $w(x) = e^{-|x|^\alpha}$ for $\alpha \geq 1$.

It is desirable to choose $P_N(x)$ so as to minimize E_N and thus make the approximation as accurate as possible.

For the case $w(x) = e^{-|x|^\alpha}$, $\alpha \geq 2$, a lower bound has been found for E_N which matches the upper bound demonstrated by the Russian mathematician Dzrbasyan in 1955. In fact, for a general class of continuous functions there are two constants, A and B , with $0 < A < B$, such that $AN^{1/(\alpha-1)} < E_N < BN^{1/(\alpha-1)}$.

For the case $1 \leq \alpha < 2$, the question remains unresolved, and work is now proceeding on this aspect of the problem.

Statistical Decomposition of Mixtures. In various fields of scientific research are occurrences of populations consisting of mixtures of a number of subpopulations. For example, Karl Pearson considered mixtures consisting of two Gaussian subpopulations in his work on "the mathematical theory of evolution." More recently, mixtures of Gaussian subpopulations



A simple case of statistical decomposition of mixtures. Suppose the probability density function $f(x)$ is observed in a phenomenon of interest. The decomposition of this probability density function into its component parts, in this case a gaussian distribution $f_1(x)$, is useful in elucidating the characteristics of the phenomenon. Improved methods of solving the general statistical decomposition problem have been developed by NRL mathematicians.

have been considered in connection with a study of the composition of primary cosmic radiation. In general, the problem is this: *Given a sample from a population that is known to consist of a finite number of subpopulations, each of whose probability density functions depends upon a number of parameters, estimate the parameters on the basis of the sample.*

The ways of solving this problem are the "method of moments" and the "method of maximum likelihood." Both ways involve solving complicated systems of nonlinear equations. The maximum-likelihood estimate is better than the method-of-moments estimate, but its system of equation is by far the more difficult to solve. NRL mathematicians have shown that for certain types of mixtures, the maximum-likelihood estimate satisfies several comparatively simple equations, the use of which makes the maximum-likelihood equations easier to solve. The use of these equations also yields the following results:

1. The maximum-likelihood estimate of the various parameters for a mixture consisting of a finite number of subpopulations each having a Gaussian distribution and a finite number of subpopulations each having a gamma distribution satisfies the first method-of-moments equation.

2. The maximum-likelihood estimate of the various parameters for a mixture consisting of a finite number

GENERAL SCIENCES

of subpopulations each having a Gaussian distribution satisfies both the first and second method-of-moments equations.

Primitive Roots. The natural numbers together with the somewhat dependent operations of multiplication and addition modulo a prime, p , form a system that mathematicians call "a field." All of the integers in this field may be obtained by finding a suitable integer, g (called "a primitive root of p "), and then taking consecutive powers g, g^2, g^3, \dots modulo p .

The digits of the modulo p integers g, g^2, g^3, \dots give a long sequence of nonrepeating digits that have the appearance of being random. These generated random digits (together with some general modifications) can therefore be suitably employed in communications sciences (in the generation of random signals), in cryptography (for coding), in physics (when Monte Carlo methods are employed), etc.

Of particular interest is the distribution of the primitive roots themselves. The primitive roots appear to have a random distribution. It has been shown that among certain classes of integers (too complex to describe in detail here) there are arbitrarily long sequences of primitive roots in arithmetic progression (for all sufficiently large primes). Also, for large primes of a special form, there are arbitrarily long sequences of consecutive primitive roots. These results are generalizations of ones previously obtained.

The findings are somewhat surprising in view of the fact that primitive roots are defined in terms of the multiplication operation, and arithmetic progression is defined by the addition operation.

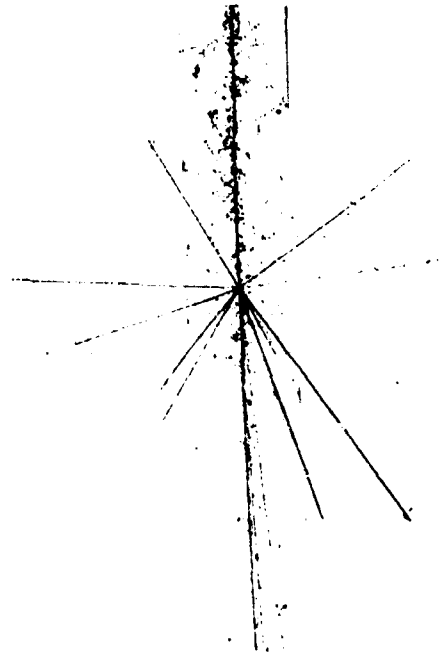
Research Computation Center Activities. During the calendar year 1968, NRL's Research Computation Center (RCC) continued to serve as the Laboratory's central computing facility, providing consulting, data retrieval, and programming services to all research areas. Computer usage continued to build steadily, and by the end of the year the Laboratory's CDC 3800 computer was operating almost around the clock, five days per week, and further augmentation of the equipment complex was being planned.

The RCC professional staff provided direct programming and analysis services on 30 different problems for 13 NRL divisions during the year. In addition, the RCC staff was able to complete a number of additional activities advantageous to all users of the facility. These included various types of improvements to the CDC 3800 operating system,

a number of general programs to facilitate the plotting of scientific results, and several scientific programs of general utility.

COSMIC RAY PHYSICS

Mean Path Length of Cosmic Rays. How much material do cosmic rays penetrate in the course of their space travels? The answer is of deep interest to astrophysicists, for it determines the transformations suffered by the primordial high-energy nuclei in their long galactic journey. The magnitude of this path length is closely connected with the regions and mechanisms of cosmic ray diffusion and trapping; it can be used, together with interstellar densities, to estimate the mean confinement time of the nuclei. Moreover, a knowledge of the path length is essential for deducing the distribution of cosmic ray elements at the source(s).



Breakup of a heavy cosmic-ray nucleus into lighter fragments by collision, as seen in a nuclear research emulsion exposed near the top of the atmosphere (magnified 2,000 times). Collisions such as this one also occur with interstellar hydrogen. Analysis of the arriving breakup products reveals the mean path length traversed by the primary cosmic rays in galactic space.

It has been realized for some time that the best source of information on path lengths is the abundance ratio of the so-called "light" nuclei to the heavier ones arriving at the top of the atmosphere. Since the light nuclei are the breakup products of heavier ones that have collided with interstellar atoms, the relative flux of light nuclei reflects the amount of material traversed. Striking confirmation of an early NRL determination of the relative flux of Li, Be, and B nuclei was obtained recently at the University of Minnesota by methods of detection completely different from those employed by NRL. The result: "light"/"medium" = 0.25 ± 0.02 . New laboratory data on the probability of various fragmentations of cosmic ray nuclei have been incorporated by NRL physicists in revised calculations of the mean path length. The best value is now 4 grams per square centimeter. This value has also been confirmed by NRL and other institutions through studies of the isotopic composition of cosmic ray helium.

Confinement of Cosmic Rays. Our ignorance of the regions in space where cosmic rays are magnetically trapped and of the duration of this confinement has been partly dispelled by NRL's analysis of information on the "light" cosmic ray elements and calculations of the effects of their nuclear fragmentation. The results indicate, but do not yet firmly establish, the confinement of these particles within the Milky Way disk.

Cosmic ray nuclei take a long time diffusing within the galaxy before they escape—at least as long as 100 thousand years. However, their "age" could be much greater. Present estimates range from 1 to 100 million years. If we knew which of these numbers is more nearly correct, we might be able to judge whether the cosmic rays are mainly confined to the galactic disk or spend most of their time in the vast space of the galactic "halo."

NRL scientists have estimated the amount, x , of material—about 4 grams per square centimeter—traversed by cosmic rays after they attain their high speeds, which are close to that of light. If the mean density of matter in the regions through which cosmic rays travel were also known, a direct determination of their mean *linear* path length ($x/\text{density}$, say, in light years) could be made. This path, L , is directly proportional to the "age," or confinement time, T ; i.e., $L = cT$, where c is the cosmic ray velocity.

Depending on where cosmic ray nuclei spend most of their time, different values of the density would be relevant. Within the galactic disk, the density of interstellar gas (mostly hydrogen) is known to be approximately 1 atom per cubic centimeter. By contrast, the density of gas in the tenuous galactic halo may be 100 times lower. Combining these numbers with the mean path length of material traversed (4 g/cm^2), we obtain the widely divergent estimates of "age" given above.

An independent means of estimating the age could resolve this dilemma, and a suitable "clock" for this purpose is radioactive ^{10}Be . This nuclide, produced along with other light isotopes by the collisional breakup of heavier cosmic ray nuclei in space, has a mean life of nearly 4 million years. The observed abundance of ^{10}Be (or of elemental beryllium) must be compared with the calculated rate of beryllium production in space relative to the rates of production of other cosmic ray species. If very little of this isotope is found in the arriving cosmic rays, then the cosmic rays must have been traveling for a time long enough for the ^{10}Be to die out. If, on the other hand, most of the beryllium has survived, this would signify that the cosmic rays had lived for a short time compared with the "mean life" of the beryllium nuclei. Not only would the ^{10}Be nuclei yield an estimate of age, they could also reveal the main storage region of cosmic ray nuclei and indicate the extent of galactic magnetic fields.

The main difficulty is in isolating fast ^{10}Be nuclei. However, this isotopic separation is not essential. Using laboratory data and theoretical estimates of the rates of production of ^7Be , ^9Be , ^{10}Be , ^{10}B , and ^{11}B from heavier elements, NRL physicists have calculated the elemental Be/B abundance ratio for the two cases: ^{10}Be surviving and ^{10}Be decaying into ^{10}B .

A critical review of published data on the relative fluxes of Li, Be, and B was carried out for comparison with the foregoing calculations. The analysis supports a "short" age, $T < 10$ million years, with confinement in the galactic disk. However, the data do not yet permit us to exclude entirely the possibility of a longer confinement time. The probability of the latter is still about 10 percent. In order to pin down the age more firmly, the NRL group is striving for a significant improvement in our knowledge of the individual abundances of cosmic ray lithium, beryllium, and boron.

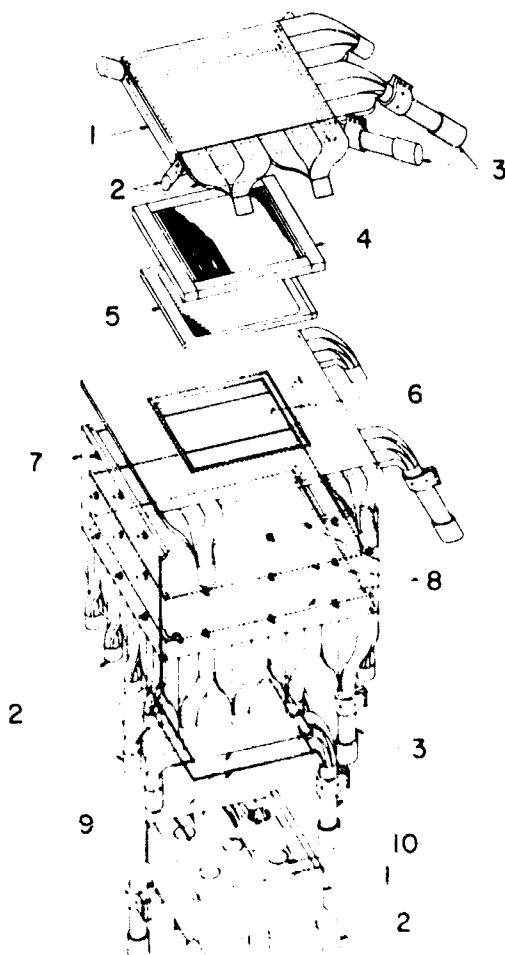
New Telescope for Detecting Cosmic Gamma Rays. One of the principal efforts of the Laboratory's cosmic ray physics program is in the pioneering field of gamma-ray astronomy. In furtherance of this effort, work was completed in 1968 on the design, development, and testing of prototype components of a large balloon-borne telescope for detecting cosmic gamma radiation in the energy interval of 20-120 million electron volts (Mev). Flight model components are being assembled in preparation for a test flight in 1969.

The telescope will seek to detect and measure both the diffuse, general background gamma radiation from outer space and the gamma radiation from suspected point sources (e.g., Crab Nebula). It will be oriented with a pointing accuracy of 1-3 degrees. Thus far, the only definitive observations of gamma rays at

high energies are those reported by Clark, Kraushaar, and Garmire on the basis of a satellite experiment conducted by MIT. These observations revealed a diffuse flux of gamma rays above 100 Mev originating within the galactic disk and peaking in the direction of the galactic center. The search for point sources has thus far been unsuccessful. Probably owing to limited sensitivity and inadequate discrimination, only the upper bounds of the fluxes have been delineated. The observation of discrete cosmic gamma-ray sources would, in effect, open a new window for astronomical studies. It promises to be of paramount importance in cosmic ray physics, astrophysics, and cosmology.

An exploded view of the NRL telescope is shown in the accompanying drawing. The instrument consists of a unique array of detectors (plastic scintillators, nuclear emulsions, a novel type of wide-gap spark chamber, and a Čerenkov detector), and it is designed to provide good angular and energy resolution for gamma rays of 20-120 Mev.

The domain of cosmic gamma-ray energies considered here has not yet been explored. Apart from the advantage such exploration presents of possibly detecting a higher flux, the spectral information obtained at these energies may allow discrimination between various mechanisms of gamma-ray production. The major obstacle hitherto has been that the low-energy electrons, which typically occur in pairs and reveal the incidence of the gamma rays, are easily scattered. The telescope was designed to minimize this multiple coulomb scattering and its degrading effect upon spatial resolution. The spatial resolution should be an order of magnitude higher than in the MIT experiment. Flux sensitivity for observations of point sources is expected to be $\approx 10^{-4}/\text{cm}^2 \text{ sec}$.



Exploded view of NRL's wide-gap spark chamber, emulsion, and counter array.

1. Anticoincidence scintillation cup.
2. Light pipe or pipes.
3. Photomultiplier assembly clamped to light pipe.
4. Emulsion stack.
5. Proportional counter.
6. Mylar window.
7. Wide-gap spark chamber with side walls and top plate made of scintillator.
8. Wire mesh electrodes.
9. Coincidence scintillation counters.
10. Čerenkov counter and absorber.

An Overview: by Ralph R. Goodman, Associate Director of Research for Oceanology

Programs carried out at the Naval Research Laboratory in the fields of oceanology, ocean engineering, and acoustics were brought together in 1967 to comprise, under the title "Oceanology," one of the Laboratory's current four major areas of research. This unification was effected to improve the efficiency of NRL studies of the environment in which most of the Navy's operations are conducted.

During 1968, the Acoustics Division assumed the leading responsibility among Navy laboratories for the Antisubmarine Warfare Underwater Surveillance Program. The research related to this program is, in part, a continuation of that begun at Columbia University's Hudson Laboratories, whose activities are scheduled to be discontinued on June 30, 1969. This added responsibility has led to a considerable expansion of the division in both personnel and facilities and to an enlargement of NRL's role in the study of long-range acoustic propagation in the oceans. During 1968, the Division participated in experiments in both the Atlantic and Pacific Oceans.

The Ocean Technology Division continued to work in the areas of ocean engineering and technology as well as in other fields which make use of the same techniques and approaches. The search for better materials and for methods for measuring their performance has been undertaken; the materials range from those used in the fabrication of body armor to those required for the construction of deep-ocean vehicles. Research was also begun on

the hydrodynamic response of large cabled structures in the deep sea; the need for this research is imperative because of the great potential of such structures for many naval applications.

Research on the sea-surface effects of transiting submarines is a major project in oceanology at NRL. Jointly, through the efforts of the Laboratory's Nonacoustic ASW (R&D) Task Group and Ocean Sciences Division, a program directed toward the understanding of ocean phenomena related to surface effects is in progress. Other principal areas of research are biological and chemical oceanography and atmospheric physics. The Ocean Sciences Division has an important role in the Maury Center for Ocean Science, which is located at NRL; the Center coordinates research in the Navy's ocean-science programs.

During 1968, the Laboratory acquired the services of the oceanographic ship USNS Gibbs to supplement its capability for marine research, which previously had been limited to the USNS Mizar. To accommodate the wide variety of needs for use of these ships, the Ship Facilities Group was established to schedule and coordinate scientific programs in oceanology.

For decades, NRL's programs in oceanology have played an important role in the Navy's effectiveness at sea. In the decades ahead, the research discussed briefly in this overview and in the reports that follow will be reflected in significantly improved operations of the Fleet.

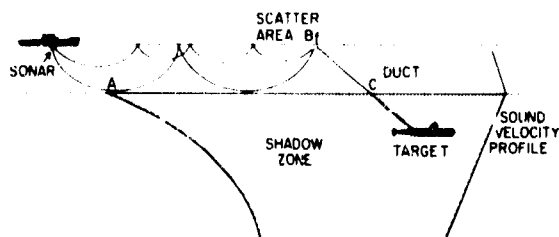
ACOUSTICS

Assured Range Studies. One problem of great importance to the Navy is the acoustic illumination of the region below the surface-bounded duct, called the shadow zone. A hostile submarine wishing to avoid detection can seek the relative security of this zone. Neither the bottom-bounce nor the towed, variable-depth sonar mode of operation has been satisfactory in dealing with this situation. Methods and techniques to extend the detection range into the shadow zone must be developed to give assured ranges of at least twice those now achieved.

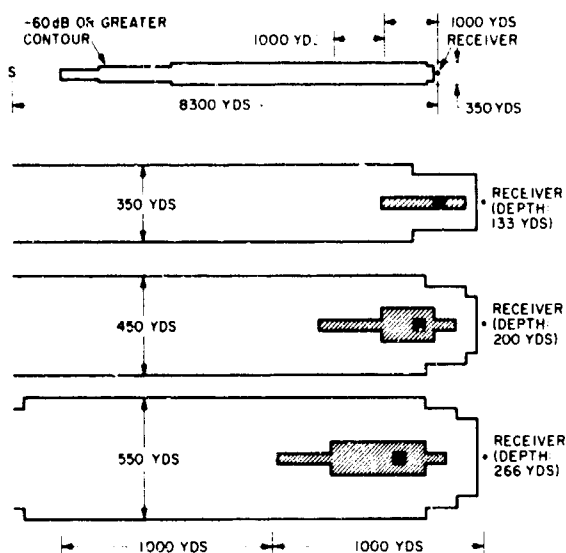
Since neither normal mode theory nor classical ray theory properly describes acoustics in the shadow zone, a three-part mathematical model has been developed at NRL. The first part, A, is the propagation loss in the duct. This value can be calculated from any of several theories. The second part, B, is

the forward scatter loss from an appropriate surface scattering area. This loss is calculated from a Bechmann-Spizzichino scattering model. The last part of the loss, C, from the scattering area to the target below the duct is computed from ray theory. This composite model has been programmed on the NRL CDC-3800 computer.

Two recent cruises yielded considerable field data, some of which have been analyzed and compared with calculated values. The average propagation loss was measured with a 5-thousand-cycle-per-second source and an echo repeater as a function of echo-repeater depth and the data compared to calculated losses using the prediction model. The scatter theory is found to fit the data much more closely in the shadow zone than does the normal mode theory. The high variability of levels within the duct found in



Three-part model of propagation losses. A, duct loss; B, forward scatter loss; and C, ray path loss.



Plan view of significant scattering areas at the ocean surface as seen from various receiver depths. The solid area is that which contributes the largest amount of energy to the receiver, and the shaded area is that over which the contribution is reduced by 3 decibels. The signal frequency is 5 thousand cycles per second.

the field data are thought to be caused by the interference between the several modes being propagated within the duct, whereas the relative stability below the duct is attributed to the averaging of a large number of acoustic paths from the surface scattering area to the receiver.

One benefit of the mathematical model is to help define the principal scattering area. The sizes and shapes of the total areas are similar with the sound source at one position, S, and the receiver at another. This area is defined as the space in which the scattering strength is -60 decibels or more. From the figures, several things are apparent. The principal

area in which the propagation and scattering losses are the least is confined to a relatively narrow region in the vicinity of the receiver. As the target goes deeper, the area lengthens, broadens, and moves away from the target.

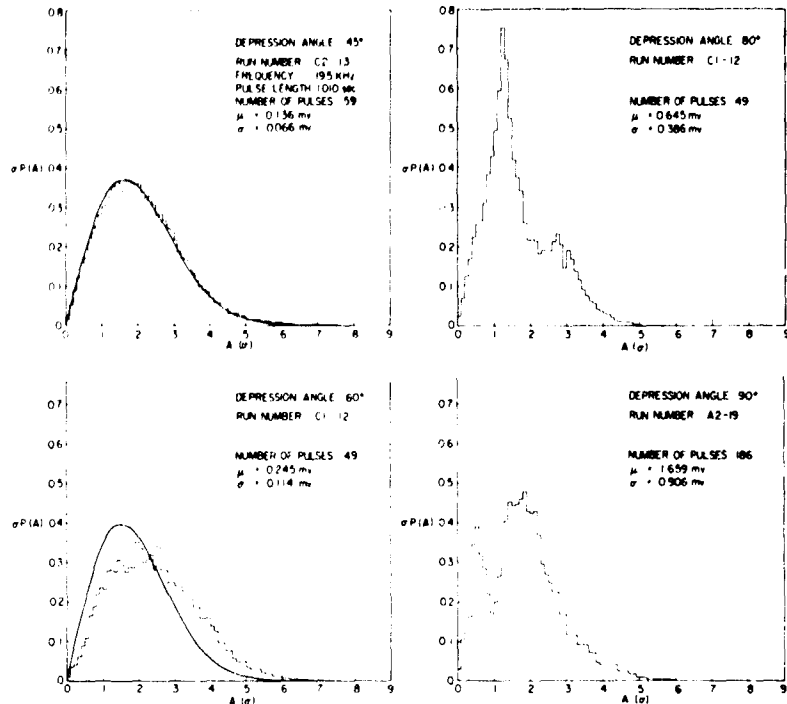
This information can be of great practical importance in the design of a sonar system for shadow-zone detection. Since the principal area of contribution to the sound level at the receiver is a rather narrow region far removed from the source, the transmitter-receiver beam pattern can be narrowed to maximize the energy on the target and reduce reverberation.

Statistics of Scattered Acoustic Pulses. In the search for a quantitative description of the scattering of underwater sound waves from a rough ocean bottom, an experiment was conducted to determine the amplitude statistics of the scattered signal. Echoes scattered in the monostatic direction were analyzed to obtain their distribution of amplitudes. The directional source within an 8-degree beamwidth transmitted 19.5-thousand-cycles-per-second constant-amplitude pulses of approximately 1-second duration at various inclinations of the beam axis with the ocean bottom. The scattered echoes were then received at the source, where the envelope was sampled digitally and recorded on magnetic tape. The data tapes were then inserted into a high-speed digital computer and the amplitude distributions obtained for each inclination of the source.

Photographs show that in areas where the ocean bottom is geographically flat, randomly oriented sand ripples occur which are estimated to have an elevation roughness of the order of one acoustic wavelength. For random surfaces, roughnesses of this order should result in scattered echoes with their amplitudes apportioned as the Rayleigh distribution.

The resultant amplitude structure, however, resembles Rayleigh distributions only in cases of incident angles of 45 degrees and below, i.e., small grazing angles. As the angle of incidence increases, the distributions show a transition from near Rayleigh to a multippeak structure at the high angles. Peaks in a distribution generally imply the presence of one or more coherent components. It was expected that there would be a coherent component present in the scattered pulse for the specular direction or that there would be more than one component in the case of acoustic highlights. If one assumes the presence

Four examples of the types of amplitude distributions observed when acoustic pulses are scattered monostatically from the ocean bottom. The ordinate is the product of the sample standard deviation and the probability density, and the abscissa is the amplitude measured in units of the standard deviation. The smooth curve is the Rayleigh density calculated on the basis of the sample standard deviation. For low depression angles (angles of incidence), the distribution resembles Rayleigh, but as the angle is increased, the distribution deviates markedly from Rayleigh.



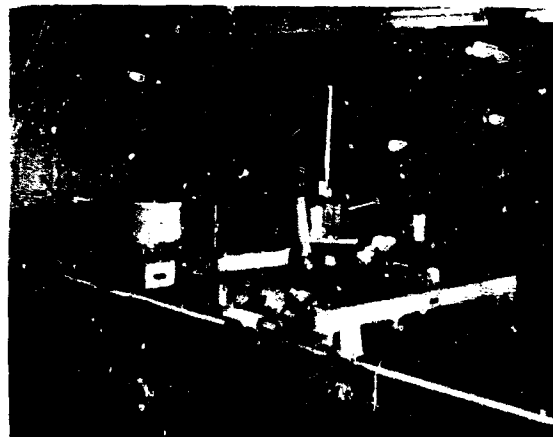
of coherent components, there is no acceptable physical theory for combining coherent and incoherent components to account for the observed distributions.

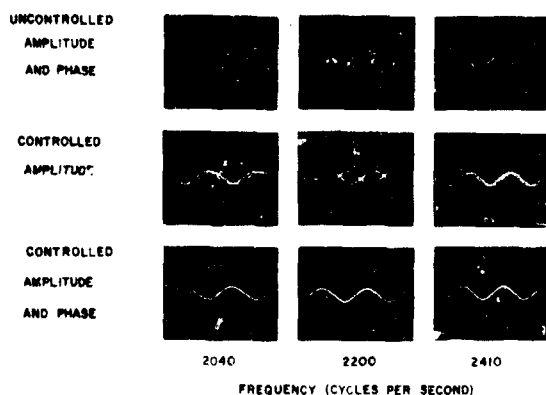
Scale Model Acoustic Studies. The Laboratory's need for a fairly large and well-instrumented acoustic research tool has been fulfilled with the construction of a 116,000-gallon water tank that is 30 feet in diameter and 22 feet in depth. The tank, which is made of cypress wood, has been installed in a 19-foot-deep pit and enclosed in a cinder-block house which contributes to the maintenance of the controlled environment necessary for accurate measurements. Associated electronic equipment provides an accurate, highly flexible, and manually convenient measuring system. Temperature and humidity are controlled, and a water filtering system is provided. Two carriages are supported by rails erected across the tank. One carriage supports and rotates transducer

arrays, and the other supports the programmable, triaxial hydrophone positioning and scanning system. The tank is the first of its kind to have the capability of positioning a test device variably in the x, y, and z planes. This feature was designed to NRL specifications.

Other equipment designed for the tank facility includes a multiaxial rotator for obtaining complex underwater acoustic beam patterns, which are then processed by a directivity index computer, and an

View of the top of the acoustic research tank, showing the two carriages on rails. The carriage at left supports and rotates transducer arrays, and the one at right positions hydrophones variably in x, y, and z planes.





adaptation of a radar radiation distribution printer for underwater measurements. This printer processes signals transmitted by an automatically scanning underwater hydrophone. It automatically types an acoustic pressure pattern in numerical decibel values that represent pressure variations in a selected area in the near or far field of a model transducer array.

In support of the research program scheduled for the tank facility, two model arrays, each consisting of 100 transducers, have been designed and fabricated. One array has been used to prove that directional acoustic beams can be obtained from biplanar arrangements of free-flooded ring transducers. The other array, in which the transducers vibrate in a piston-like longitudinal manner, is being used to study the suppression of undesirable acoustical interaction among transducers in low-frequency arrays.

This system is unique in that it provides control of the phase and amplitude of the displacement between two dissimilar transducers subjected to different acoustic loads; this is needed for a number of problems now being studied. It is unique also in having a rapid-response electronic feedback control system, which is now being used to study and control phase and amplitude.

UNDERWATER SOUND REFERENCE

Sonar Calibration at Simulated Great Depths and Low Temperatures. NRL has placed into operation a new facility in which, for the first time anywhere, underwater sound transducers up to 3 feet long and 5 inches in diameter can be calibrated in the frequency range

Control of the amplitude and phase of the displacements of two dissimilar transducers monitored by accelerometers and an electronic feedback system.

of 10 cycles per second to 4 thousand cycles per second (kHz) at static pressures as high as 10,000 pounds per square inch (equivalent to an ocean depth of 22,500 feet) and at temperatures in the range of -2°C to $+40^{\circ}\text{C}$.

Hydrophones now can be calibrated over the full range of temperatures usually cited in specifications of operating conditions. Previously, the lowest practical limit was $+2^{\circ}\text{C}$. The -2°C temperature, the freezing point of sea water, may be encountered in the arctic or at shallow depths in midwinter. The temperatures at great depths range from $+2^{\circ}\text{C}$ to $+4^{\circ}\text{C}$. The lower temperature limit is attained in an ethylene glycol solution. Its use has the advantage of permitting greater temperature differentials in the cooling equipment, which significantly decreases the operating time and costs for a series of calibrations over wide ranges of pressure and temperature.

To attain the frequency range, the theory and techniques associated with active impedance termination, developed at NRL, were applied to create a free-field acoustic environment in the presence of highly reflective boundaries within a steel tube 9 feet in length and 8 inches in inside diameter. Both absolute and comparison calibrations can be made. This facility extends the upper frequency limit of the technique from 1.5 kHz to the present 4 kHz.

During the first year of operation (1968), 47 hydrophones were calibrated at various combinations of pressure and temperature for a total of 289 calibrations, of which 115 were at pressures exceeding 1,000 pounds per square inch, the former limit of pressure.

Cavitation Threshold. Acoustical cavitation occurring within a sonar dome or other transducer housing produces reverberations and cancellations that limit the usable output of the entire device. In laboratory studies, such cavitation is induced to determine the effectiveness of new methods. The only apparent way to overcome cavitation induced by the high vibrational rate of the sound transducer is to increase the threshold at which it occurs. Although various methods are available, progress in applying them to operational sonar has been nearly negligible over the past two decades. The most common method of

retarding the onset of cavitation is to increase the pressure on the liquid surrounding the transducer.

In examining various means of water treatment to increase the cohesiveness or tensile strength of water, NRL has experimented with "Polyox" (ethylene oxide), the "giant" molecule that gained notoriety when a mixture of it and water siphoned itself from a beaker in an unconfined stream.

The cavitation threshold level as a function of Polyox concentration in water was measured in an end-lighted glass tank 14 centimeters square and 90 cm long. A 1-inch-diameter PZT-4 projector, resonant at 1 million cycles per second and having the ground electrode exposed to the water, was mounted at one end of the tank. The results showed that, at a concentration of about 80 parts per million by weight, the driving current of the transducer could be increased by 3 decibels before cavitation set in. Higher concentrations are impractical because the liquid becomes syrupy at 100 ppm by weight.

Additional measurements are planned at lower frequencies to determine whether shipboard experiments are justified.

High-Power Underwater Sound Source. Many underwater transducer calibrations made during the past few years have called for acoustic sources capable of producing sound pressure levels of 70 to 80 decibels referenced to 1 microbar and frequencies as low as 20 cycles per second (Hz). At times, the source is required to operate over the frequency range from 20 Hz to 10 thousand cycles per second (kHz). Special designs in which crystals drive flexure plates or bars generally have been used for this purpose, but they are very inconvenient and not completely satisfactory because each operates over a narrow frequency range and weighs several hundred or even thousand pounds. Frequently, therefore, several awkward transducers had to be used to satisfy the calibration requirements.

A new moving coil transducer, designed by NRL's Underwater Sound Reference Division (USRD type J13), weighs less than 120 pounds and provides high source levels over the frequency range of 20 Hz to 10 kHz. The diaphragm can be driven to a 0.5-inch peak-to-peak displacement. The output is displacement-limited below 80 Hz and current limited above that frequency. The response is linear, with a driving current to 25 amperes (rms), and produces an average sound pressure level of 75 decibels throughout the frequency range of 70 Hz to 5 kHz. To limit the

temperature rise, the transducer is operated at a 12-percent duty cycle.

The driving element can be used singly, or two or more elements can be operated together to produce a higher output. A single element weighs 60 pounds without the pressure-compensating housing. Some economy in weight for higher power requirements can be achieved by using one compensating mechanism for several elements.

Reliable Deep-Submergence Hydrophone. A new hydrophone for acoustic measurements and ocean surveillance at depths as great as 33,750 feet has been developed at NRL. Reliability at this depth has been achieved by employing the newest high-strength corrosion-resistant alloys and low-permeability elastomers. The new low-noise transistorized preamplifier used is substantially quieter than earlier designs.

An important feature of this hydrophone, designated USRD type H54, is a choice of sensitive element configurations and material types to allow the selection of frequency range, directivity characteristics, and sensitivity to satisfy a wide range of requirements. Elements of lead zirconate titanate, lead metaniobate, and lithium sulfate have been calibrated in the same basic hydrophone housing and acoustic boot; they offer sensitivities from -80 to -100 decibels referenced to 1 volt per microbar and frequencies as low as 1 cycle per second and as high as 150 thousand cycles per second. Each active material used for the sensitive element has been pressure cycled and calibrated to 15,000-pounds-per-square-inch static pressure, and the cable gland has withstood 15,000 psi without failure or degradation.

OCEAN SCIENCES

Marking the Ocean Surface with Artificial Sea Slicks. The success of air rescue operations at sea often depends upon the use of sea markers. Obviously, substances providing the greatest obtainable areal ranges and durations of visibility are sought. As the side benefit of an investigation of natural and artificial ocean-surface films, NRL discovered that certain organic substances produce intense light reflections and thus may prove highly valuable as components of sea markers.

The high visibility of these substances is due to their monomolecular structure, which has capillary wave-damping and wave-resistant characteristics. Compounds with optimum properties were found to

spread spontaneously and rapidly into very thin layers, one molecule thick, that resist the dispersive forces imposed by a dynamic, wind-driven sea. These water-insoluble, nonvolatile organic materials thus provide durable, visible artificial sea slicks.

A comparative field evaluation of these slick markers with the standard Navy dye marker showed that the visibility of the artificial surface films was best at certain viewing angles. The slick was visible at greater distances, since it affected a much greater area than the same weight of dye. Other viewing angles were better for the dye marker. Consequently, a combination of the two techniques proved to be the solution. The combination of dye and surface film-forming materials yields two substantially different marks, one or the other of which is visible from all viewing angles.

Dispensing methods have been developed to release an artificial slick slowly from a container tethered to a floating object, and tests have been carried out that show that small quantities of the monomolecular film-forming materials affect large areas of the sea surface; for example, 100 grams of pure compound will cover 60,000 square meters, or 14.6 acres, when completely spread.

Carbon Monoxide and Methane at the Air-Sea Interface. NRL scientists have been investigating the distribution of carbon monoxide (CO) and methane (CH₄) between the atmosphere and the ocean surface. The information obtained should prove useful in elucidating gaseous exchange mechanisms across the air-sea interface and in defining the role of the ocean as a sink for man-made pollutants in the atmosphere.

Results obtained during a cruise in June 1968 near Puerto Rico indicate that in that area atmospheric methane is in equilibrium with the surface waters in the open sea. More intriguing are results which show that the carbon monoxide concentration in ocean-surface waters is much greater than the equilibrium value calculated from the gas's atmospheric partial pressure and solubility coefficient. The ratio of measured to calculated carbon monoxide concentrations reached values as high as 90. This large disequilibrium indicates that the net transport of carbon monoxide is from the ocean into the atmosphere. These high carbon monoxide values in surface water at sea are thought to be related to biological processes, and laboratory studies are being conducted to determine the validity of this theory.

Studies conducted at the Chesapeake Light Station off Norfolk, Virginia, show that carbon monoxide at the sea surface undergoes diurnal variations, with maxima occurring during the daylight hours. Concentrations were found to increase by a factor of two between 4 a.m. and 2 p.m., providing evidence that biological processes are involved.

Atmospheric Space Charge Over Water. One of the electrical properties of the atmosphere over the oceans which is very different from its counterpart over the land is atmospheric space charge density. Exploratory research is being conducted by NRL to gain understanding of this electrical phenomenon of the air-sea interface.

Over water, there are at least two mechanisms which create atmospheric space charge. One is the separation of negative and positive ions near the surface by the geoelectric field, and the other is the injection into the atmosphere of charges carried on jet drops produced by the bursting of minute air bubbles. The bubbles are formed from air entrained in the water during periods of whitecap activity or breaking surf. The first mechanism is believed to be the most important during periods of low wind and quiet seas, and the second is most important during periods of rough seas accompanied by a well-mixed atmosphere. The failure to differentiate between these two mechanisms has led to confusion regarding the source of the space charge measured over water.

Measurements of space charge along coasts have shown that the surf zone is a prolific source of positive



Faraday cage apparatus aboard USNS *Eltanin*, 1968. The apparatus makes space electrical-charge measurements.

space charge. Recent observations by an NRL scientist aboard USNS *Eltanin* indicate that a positive space charge exists over the open ocean during periods of whitecap activity. Since a positive charge is also produced in the separation mechanism of the geoelectric field, it is difficult to determine whether the bubbling or the separation process predominates over salt water. In the laboratory, fresh water has been shown to produce a negative charge during bubbling and splashing. To differentiate between the two mechanisms, an experiment over Lake Superior was carried out by NRL scientists in the summer of 1968. Lake Superior was chosen not only because it is a body of fresh water but also because its low temperature adds stability to the adjacent atmosphere, thus enhancing the ionic separation process during quiet times. The spectrum of meteorological conditions encountered during this experiment was broad enough to show that during periods of stability and no splashing, a positive charge was produced, whereas when waves were breaking a negative charge was produced. These results agree well with the theoretical treatment proposed by NRL scientists for the two extreme cases.

The carriers of electrical charge produced by the splashing of fresh water were also investigated and found to have mobilities almost as great as the small atmospheric ions. Continued research of the atmospheric electric variables by the Navy will aid in understanding the marine atmosphere and its interaction with the sea.

Cloud Nuclei. During the formation of a cloud, each cloud droplet must have a small particle which can serve as a center (called "cloud nuclei") on which water vapor can condense. Only a small fraction of the total particles in the atmosphere have the necessary characteristics that make it possible for them to serve as cloud nuclei. A knowledge of the source and composition of these favored particles is important in understanding the formation and precipitation processes in natural clouds as well as in inducing man-made modifications to cloud processes.

Scientists at NRL have made long-distance (approximately 100,000 mile) flights in a Navy Super Constellation to sample cloud-nuclei distributions in different parts of the world. Special instrumentation, manually operated during flight, was used to measure the concentration of cloud nuclei in an air sample as a function of the supersaturation to which the

air sample is subjected. The range of supersaturations over which measurements were made covers the values which exist during cloud formation.

The results confirm the conclusion that air masses which have passed over continents are systematically richer (by a factor of 10 to 100) in cloud nuclei than are air masses which have been over the open ocean for several days. A comparison of the more industrialized North American continent with the less industrialized continents of Africa and Australia shows all three continents to be similar in their effects on the number of cloud nuclei, an indication that industrial and other man-made pollutants are not primary sources of cloud nuclei. The results indicate that the lifetime of a given cloud nucleus, at least over the ocean, is about three days. A widespread and relatively uniform source of cloud nuclei both over the ocean and over the land is indicated. Over the land, a large part of the cloud nuclei are known to be of surface origin because of an observed decrease in concentration with height, whereas over the ocean, the distribution is such that it leaves the question open as to whether marine nuclei originate at the sea surface or within the atmosphere.

Stratospheric Water-Vapor Distribution. Water vapor, a principal absorber and reradiator of infrared radiation in the atmosphere, plays an important role at very high altitudes, both in the energetics of the atmosphere and in the formulation of mathematical models for the numerical prediction of weather. It is also a factor in the chemistry of the upper atmosphere and may constitute a control for the concentration of ozone, thus exerting a further influence on atmospheric energetics.

While water-vapor measurements are easily obtainable in the lowest levels of the atmosphere, they can be made only with great difficulty at higher levels. Consequently, routine meteorological measurements have been limited to the lower half of the troposphere. Only in recent years, through special scientific programs, have efforts been made to determine the water-vapor distribution and its variability in the upper atmosphere.

Early observation of the vertical distribution of water vapor in the stratosphere produced only controversy because the findings from various programs did not agree with each other. One possible source of the disparity, as determined by NRL experiments in 1963, was that water vapor from the balloon-borne instrumentation contaminated the air being sampled.

This obstacle has been eliminated by using a sounding system, devised by NRL scientists, which measures the atmospheric water vapor during the descent of a balloon from 100,000 feet. The air is sampled from the lowest position in the balloon train and is thus essentially free from contamination from outside sources. The instrumentation used consists of an automatic hygrometer that directly measures the temperature at which frost forms in the atmosphere; this temperature, or frostpoint, uniquely defines the water-vapor concentration in the atmosphere.

In general, the air temperature places an upper limit on the amount of water vapor that can exist in the air. The lowest air temperatures in the stratosphere are in the tropics at 50,000 to 60,000 feet altitude. It has been proposed that the exchange of air with this low-temperature region limits the moisture content for the entire lower stratosphere. The observed concentrations are consistent with this limiting condition. The seasonal variability of water-vapor mixing at the level of the minimum air temperature is in the range of 1 to 4 parts per million; this is also consistent with the annual variability of the limiting air temperature. Stratospheric measurements over the latitudes 10°N to 75°N do not show a north-south gradient; if a gradient exists, it is presumed to be very small. An efficient lateral mixing process in the lower stratosphere is indicated.

Recent soundings made with the new instrumentation at low, middle, and high latitudes provided data for a broad survey of water-vapor distribution over the northern hemisphere. The most significant finding was that the water-vapor concentration does not increase with altitude above 90,000 feet as suggested by earlier data. Rather, it is nearly constant, with an average mixing ratio of about 2.5 parts per million.

Foam Separation of Trace Organic Substances in Sea Water. Knowledge of the organic compounds present in the ocean and the conditions affecting their production is of great importance both to the Navy and to marine science generally. There is ample evidence, for example, that small quantities of dissolved organic substances can significantly alter many of the physical properties of sea water, adsorb on surfaces and nourish fouling organisms, and control the aggregation or dispersal of many other organisms.

Although most of the usual chemical separation techniques have been applied to the isolation of or-

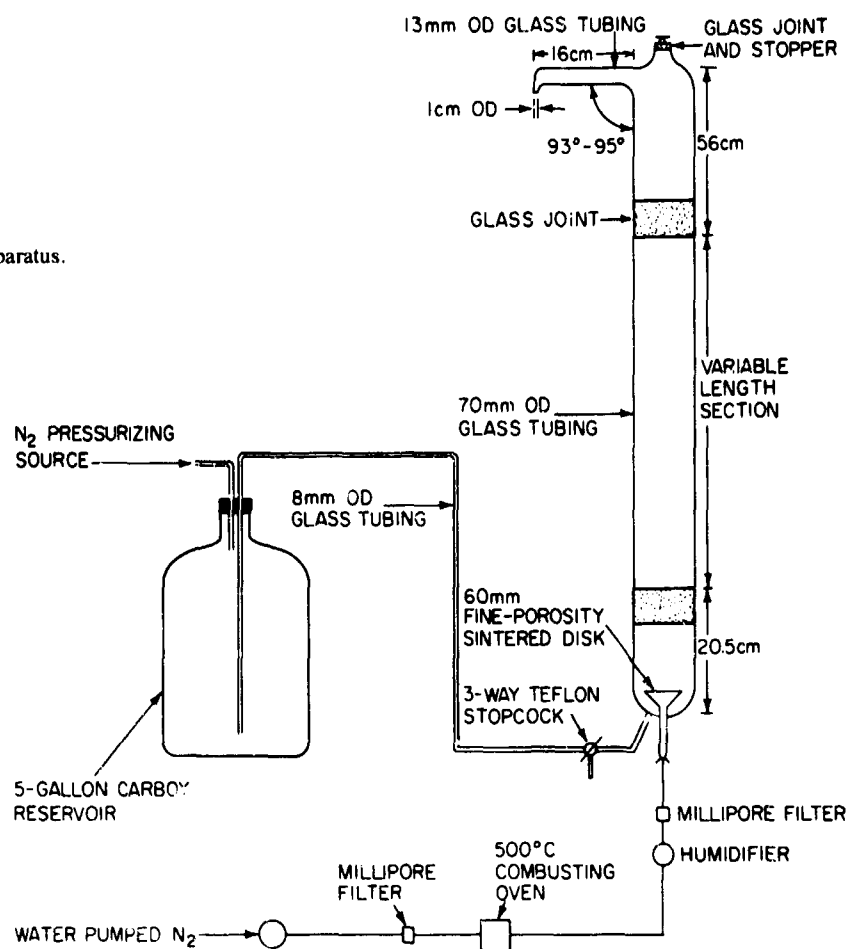
ganic compounds of sea water, all have important drawbacks. The principal difficulties stem from the fact that individual compounds occur in the parts-per-billion range or less, with the total of such compounds rarely exceeding a few parts per million. The salt content, on the other hand, lies in the range of 31-37 parts per thousand. Significant also is the fact that many organic compounds found in the sea have at least a moderate affinity for water, making extraction by immiscible solvents difficult or impossible.

One technique that does not seem to have been seriously investigated is that of foam separation (i.e., the isolation of substances in laboratory-generated foams). This has recently become an important method in chemical engineering, where it is used to purify solvents and recover by-products from effluent streams. The principal drawback of foam separation as a general method is that it is applicable only to compounds that can be scavenged by surfactants or to those substances that are surfactive (i.e., those compounds containing both hydrophobic and hydrophilic groupings that will cause them to accumulate preferentially at a gas-solution interface). Within this limitation, however, the process has the great advantage of becoming more efficient as the solution becomes more dilute. Thus it works best under those very conditions that cause most other separation processes to break down.

Since many important compounds which occur in the sea are surface active (e.g., proteins and enzymes, some polysaccharides, and lipids), the foam-separation process is being investigated systematically by NRL scientists as an additional tool of the chemical oceanographer. The essence of the technique is to create large quantities of gas-solution interfaces (bubbles) and allow them to rise through a column of sea water in a "foam tower." The surface-active compounds are adsorbed onto the bubble surfaces and carried to the top of the column as foam. The foam is removed, and when it collapses, the result is a solution preferentially enriched in the surface-active compounds. The foam tower has a capacity of 7.5 liters; middle sections of various lengths provide other capacities.

Experiments at NRL have thus far shown that 8-10 percent of the organic carbon in coastal sea water can be highly concentrated by this method and recovered in a small volume. Part of this material has been found to be protein. Protein is generally believed to occur in the sea, but the fact has not

Diagram of foam separation apparatus.



heretofore been actually demonstrated. Quantitative studies made with the apparatus and with known amounts of protein added to artificial sea water have shown that nearly 100 percent recoveries can be achieved with initial concentrations of 25 micrograms or less of protein per liter.

Trace-Element Measurements in Marine Animals. Among the most significant gaps in our basic understanding of the sea is a detailed knowledge of its chemical and physical evolution during geologic time. An effort is currently in progress to discover some of the properties of the ancient oceans, which have exerted such a profound influence on the biological and geochemical evolution of the Earth as we know it.

The problem is being studied through measurements of trace-element concentrations in the shells of

modern and fossil marine animals. The approach is to first collect marine invertebrates from different environments and to establish the influence of various ecological factors, such as temperature, salinity, and water chemistry, on the deposition of particular trace elements in their shells; then, by studying the same trace elements in the shells of their fossil ancestors, an attempt is made to reconstruct the chemical and physical parameters of the prehistoric seas they inhabited at various times in the geological past.

The initial experiments in this program have concentrated on determining the influence of salinity on the chemical composition of the shells of modern marine animals and establishing the trace-element content of 20-million-year-old marine fossils from the Miocene period.

The trace elements are measured by the nuclear technique of radio-activation analysis, in which

radioactive isotopes of the elements of interest are produced by bombarding the sample shells with neutrons in the NRL nuclear reactor. Specific chemical constituents are quantitatively identified by detecting gamma rays from the resultant radioactivated isotopes. Most of the work thus far has concerned the concentrations of Ca, Mg, Sr, Na, and Mn in certain molluscs and crustacea in relation to the salinity of their aquatic habitat. The measurements to date indicate that specific biochemical responses of marine animals to environmental factors are reflected in the trace-element concentrations in their shells. This positive result maintains the hope that trace-element measurements in marine fossils may provide a useful tool for establishing some of the physical and chemical parameters of the ancient oceans.

Marine Geochemistry of Fluorine. Although the element fluorine appears to be fairly uniformly distributed in the ocean, local excesses in deep water have been reported to occur, due either to submarine volcanic activity or to the dissolution of fluoride minerals. The mapping of these local excesses can provide information on the circulation of deep water. Equally interesting is the report that the ratio of fluorine to chlorine is much higher in the marine atmosphere than in the ocean itself. NRL scientists are utilizing radiochemical and electrochemical methods to investigate more thoroughly the sources and behavior of fluorine in the ocean and its role in air-sea interactions.

Radio chemical experiments were conducted to investigate the behavior of fluorides when sea water is evaporated and to study possible changes in the ratio of fluorine to chlorine during the formation of sea spray. Sea water samples spiked with fluorine were slowly evaporated by blowing warm air over them. Results showed that part of the fluorine is precipitated, with the $\text{CaCO}_3/\text{CaSO}_4$ fraction crystallizing first from the sea water. Some fluorine is found in the crystallized NaCl, but most of the element remains in solution, being precipitated after the precipitation of the minerals potassium and magnesium.

The air-sea interaction experiments were conducted by bubbling air through sea water spiked with fluorine and chlorine. The ratio of these two radioisotopes was measured in the original sea water as well as in the sea-spray droplets formed by the bursting air bubbles. No change was recorded in the ratio of

fluorine to chlorine during the formation of sea spray. These results are not in agreement with those of some other workers who do report fluorine and chlorine ion fractionation at the air-sea interface.

A new method for determining fluorine by photonuclear activation analysis was developed in 1967. It is based on counting the N^{16} radioactivity obtained from the reaction of "fast" photoneutrons with fluorine, $^{19}\text{F}(n,\alpha)^{16}\text{N}$. Analysis by this method is very fast, requiring only two minutes per sample. In addition, it permits nondestructive analysis of fluorine in rocks, fossils, marine animals, and sediments. The detection limit, however, is 0.05 percent fluorine, but the sample types indicated above usually contain sufficient fluorine for accurate analysis.

Using an ion-specific electrode, NRL scientists developed during 1968 a simple, rapid, accurate method for the analysis of fluoride in sea water. Its accuracy was verified by independently measuring the fluoride in sea water samples which had been analyzed by the well-established photonuclear activation method developed at NRL. The technique was used at sea (aboard ship) to measure fluoride distributions at several locations in the Atlantic Ocean.

The fluoride ion-specific electrode was utilized to evaluate the formation constant of the equilibrium $\text{Mg}^{++} + \text{F}^- \rightleftharpoons \text{MgF}^+$ in H_2O and in sea water as a function of temperature and total ionic strength. These results were of value in increasing our knowledge about ionic equilibria operative in the sea as well as contributing information necessary for the electrochemical analysis of total fluoride.

It must be emphasized that the method developed for the fluoride electrode should be generally applicable to several types of ion-specific electrodes which are now available. These devices offer an attractive approach to the analysis of minor constituents in sea water by virtue of their ability to measure individual chemical species and their adaptability for continuous *in situ* measurements. Their adaptation for operation at high hydrostatic pressures will also be useful for laboratory studies of the effects of pressure on chemical equilibria.

The Density Gradient Column as a Tool for Measuring Sea-water Density. Density is one of the most important physical properties of sea water; from an accurate knowledge of the *in situ* density structure over a given region, it is possible to predict the movement of water masses, the formation of currents, and the sea-surface slope. Density is not, however,

an isolated property. It is intimately associated with and dependent upon salinity, temperature, and pressure. In the open ocean, it ranges from about 1.02400 to about 1.03000 grams per cubic centimeter. The usual method of determining density is by calculations based on a knowledge of these variables. For most oceanographic purposes it is necessary to know this value correctly to at least one part in the fifth decimal.

There are several direct and indirect methods for measuring the density of sea water. Pycnometry, the timing of a falling drop, and hydrostatic weighing are not suitable for shipboard use. Other methods, such as stem hydrometry, usually are not sensitive enough for oceanographic purposes. The Laboratory has made a preliminary study to determine the feasibility of adapting another method, the density-gradient column, for use in determining the density of sea water. In this approach, a column of liquid, immiscible with water and having a vertical density gradient, is prepared. The water-drop sample is inserted in the column, where it falls until it reaches the level of its own density. The resting position of the sample drop is compared to the positions of samples with known density. The density is computed on the basis of a linear density gradient.

The liquids finally adopted for this study were bromobenzene (density 1.48531) and kerosene

(density 0.80437). Two mixtures of high and low density, respectively, were prepared at the extremes of the selected density range (from approximately 1.02000 to 1.02800) by combining the two liquids in the proper ratios. The lighter mixture was carefully layered over the heavier one in the density gradient tube. After the liquids were gently mixed across the interface, the tubes were allowed to stand until the gradients stabilized.

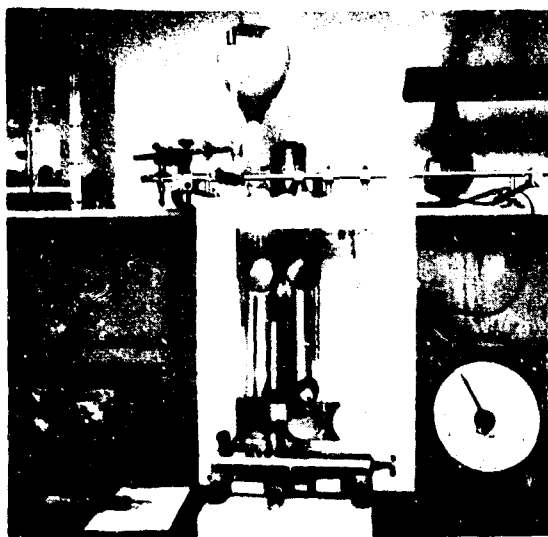
All experiments to date have been conducted with salt solutions of known densities as determined by a pycnometer. The effects of several variables on the procedure have been examined. It is believed that, under laboratory conditions at least, it is possible to determine routinely the density of sea water to 1 part in 10^5 . The problems of shipboard operation have not yet been investigated.

Study of Phytoplankton by Spectroreflectometry. Little is known about the fine-scale distribution of phytoplankton and the nutrient and environmental factors that induce "blooms," or localized concentrations of organisms.

More frequent sampling, to achieve better detail in plankton data, has required that the various mechanical and chemical sampling methods be improved. It has also required that ways be found to decrease the amount of labor involved in collecting and measuring organisms and in reducing the data to suitable indices. These needs have resulted in the current use of a trichromatic method which filters but does not involve an extraction procedure. The results are given in terms of pigment content per unit of water filtered.

It seemed possible to NRL scientists that small concentrations of minute phytoplankton organisms deposited on a white filter might be detectable in a useful way with the Beckman DK2A spectrophotometer and its integrating sphere accessory, which have high sensitivity and scanning capability. One hastens to add that some types of cells are difficult to break up sufficiently to allow the escape of all pigments, thus introducing an uncertainty in the data obtained.

To establish the feasibility of applying spectroreflectivity methods to the estimation of phytoplankton, unialgal cultures of known organisms in known concentrations were used. The organisms were *Chlorella* sp., *Chaetoceros galvestonensis* Collier and Murphy, *Gymnodinium breve* Davis, and *Cyclotella nana* Hustedt. Other cultures are now being prepared. All of these organisms were made up in



The vertical density gradient column used to determine the densities of sea water samples in a constant-temperature bath. The cathetometer for measuring drop position is in the foreground.

200 milliliters of suspension in their final concentrations. The suspension was filtered through a millipore disc with a pore size of 0.45 microns. Immediately following filtration, the discs were transferred to plastic petri dishes and stored in the dark under refrigeration until submitted to the spectrophotometer. Each sample was scanned against a blank millipore filter as a reference.

Work to date indicates that the spectrophotometric method has considerable promise for the qualitative differentiation and quantitative estimation of dominant planktonic types. Absorption at a single wavelength (670 millimicrons, an absorption maximum for chlorophyll c) can be a useful index of concentrations of phytoplanktonic material. Samples analyzed recently in the Caribbean Sea gave data on plankton distribution in that area.

OCEAN TECHNOLOGY

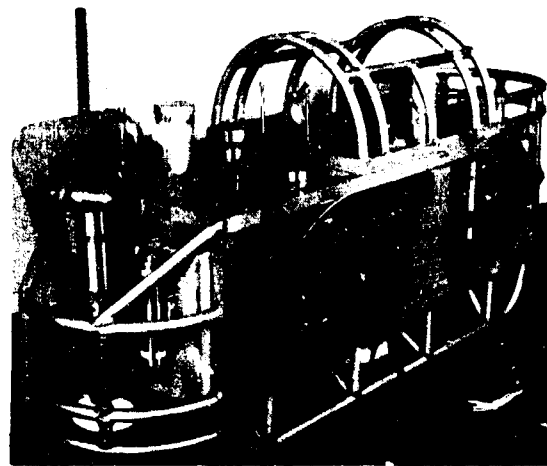
Scorpion Search. The successful search for the lost submarine *USS Scorpion* was probably the longest continuous operation aboard a ship ever undertaken by a group from NRL. The search operations were conducted aboard *USNS Mizar* (T-AGOR 11), which steamed from Norfolk, Virginia, on June 2, 1968, and returned to New York on November 22. During this 172-day interval, *Mizar* steamed approximately 10,000 miles, of which 2,600 miles were traveled at a search speed of about one knot.

Once a month *Mizar* visited Praia in Terceira, Azores, to take on supplies and exchange scientific parties. Each scientific party normally consisted of 12 personnel from NRL, 4 satellite navigation operators from the Naval Oceanographic Office, and one operations analyst from Wagner Associates. During the first two months there also were four ocean-bottom scanning-sonar operators from Westinghouse. The commodore of Task Group 42.2.1 and one officer from Submarine Development Group One were aboard during the last three months. Only 19 berthing spaces were available for scientific personnel, but there were times when the scientific party was as large as 25.

The towed search vehicle was an aluminum structure, called a "fish," which was built at NRL. Mounted in this structure was the integrated search system. The principal sensors used were the proton precession magnetometer, a wide-angle-lens survey camera, and a side-looking sonar. A transponder for determining the position of the fish relative to the ship, a frequency-multiplexing telemetry and com-



USNS *Mizar*.



Aluminum carriage ("fish") containing search instrumentation.

mand-control unit, two 200 watt-second stroboscopic lights, and a 28-volt battery power supply made up the remaining components mounted in the fish. An off-the-bottom depth indicator (essentially a pinger system) was used to maintain the fish at the desired height above the ocean floor.

A 20,000-foot-long armored, single coaxial cable provided the only electrical link for all information from the sensors to the ship and for commands from the ship to the fish. (Maintaining a full battery charge was also done through this same coaxial cable.) The fish was retrieved only when the camera ran out of film, which was after 35 hours of continuous photography. When searching at a speed of one knot, with the fish 30 feet above the bottom, a 100-foot-diameter view of the bottom was photographed each 30 seconds. Sufficient overlap of the photographed

area was provided so that a continuous mosaic of the ocean bottom could be reconstructed. A total of 119,000 photographs was taken of the area. At times, two cameras were mounted in the fish. The second camera carried film for an additional 24,000 photographs. The total ocean bottom photographed equaled an area of 12 square miles.

Major shipboard navigational equipment included the acoustic tracking system, which computed the position of the fish relative to the ship, and a satellite navigation system, which indicated the ship's geographic position. When a systematic search of an area was desired, transponders were mounted on the ocean bottom and "fixed" geographically. The acoustic-tracking system also used these transponders to compute their position relative to the ship.

The first photographic evidence found of the whereabouts of *Scorpion* was a bent piece of sheet metal, which was detected after 18 days of operation. In that same area, there was a sharp geomagnetic outcropping that gave a signal from the magnetometer having characteristics similar to those of a man-made object. However, no further magnetic anomalies were recorded. The bent piece of metal could not be positively identified as being from the *Scorpion*, so the search was continued in other areas.

After five months of futile searching, it was decided to return to the general vicinity in which the metal had been found. Within a few days, on October 28, the magnetometer recorded a signal of the proper characteristics, and the side-looking sonar showed an object standing clear of the bottom. When the film was developed, the object was identified as being a large section of the hull.

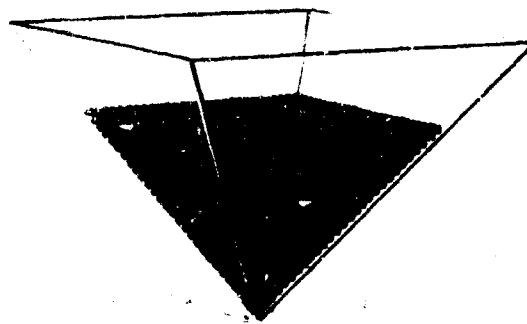
On the following run, after the fish had been near the bottom but a few hours, the main drive-shaft coupling on the deep-sea winch failed. The fish plummeted to the ocean floor, but it was retrieved by the operation of a small auxiliary motor. After 4-1/2 hours of inhauling, the fish finally broke surface. Suddenly, the tow cable parted, and the fish (valued at \$75,000) plunged 10,000 feet to the ocean bottom. This was a serious loss of equipment, but more so of search capability. Two days were spent preparing the spare fish and repairing the hoist. During the remaining three days, 10,000 photographs were obtained of parts of the hull and debris from it.

NRI was charged with the responsibility for coordinating the analysis of all data. A large mosaic photograph of the ocean floor was completed, and pertinent data were made available to the Navy's Board of Inquiry.

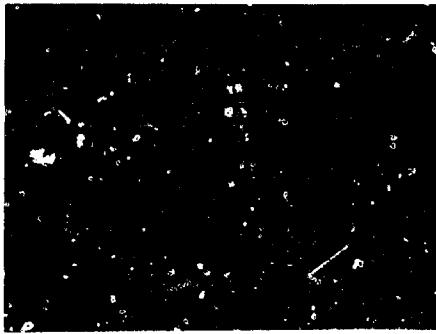
Optimum Packing of Hollow Spheres in Buoyancy Materials. Improved syntactic foams and arrays of hollow spheres are in great demand to provide buoyancy for deep-diving vehicles and instrument packages. Currently, the buoyancy is limited by the packing of the spheres, which is far from ideal. The collapse of individual spheres under the applied pressures is also a problem.

The volume fraction of spheres in syntactic foam can be increased to a major degree through close packing if certain rules and precautions are observed. A first requirement is provision for a main set of spheres that are sufficiently uniform in size to permit them to be closely packed. A second requirement is that the geometry of the container is such that the spheres can be poured into it so as to allow later infusion by the matrix. If the shape of the container is not correct, the entire volume will be disturbed by dislocations and vacancies analogous to defects in plastically deformed metal crystals. For nonuniform spheres, the packing may be even poorer.

Perfect packing can be obtained without dislocations if the container is a regular tetrahedron or octahedron or a truncated version of either. Perfect natural packing can be achieved in an octahedral container. A substantial further improvement in buoyancy can be obtained by infiltrating the main set of spheres with a population of smaller size which can shake down through the interstices. For this purpose, the diameter should be one seventh (or less) of the diameter of the main spheres. Although major improvements are theoretically possible, their future realization depends on the development of industrial manufacturing techniques capable of



Perfect packing of hollow spheres in a truncated version of a regular octahedron.



Hollow buoyancy spheres in an inappropriately shaped container. Dislocations and vacancies are apparent.

producing hollow glass spheres sufficiently uniform in size and sufficiently high in individual buoyancy and strength.

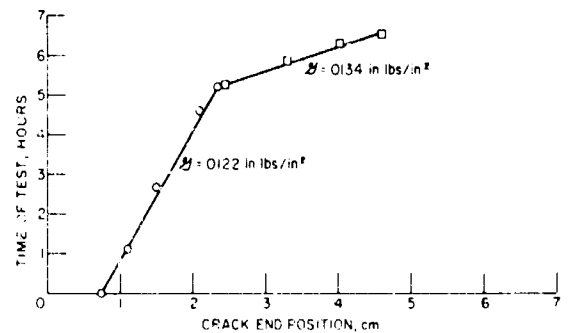
The goals of this investigation also include the calculation and measurement of the stresses on the glass spheres which contribute to individual collapse by elastic buckling. Two of the contributing factors are (1) stresses caused by shrinkage in the resin as it cools from the curing temperature and (2) point loads on a sphere applied by the nearest neighbors in contact or in near contact.

The Strength of Annealed Bulk Glass for Possible Deep-Submergence Structures. Although chemical strengthening and surface quenching are well-established processes which can greatly increase the strength and reliability of glass, they are not as yet generally applicable to thick sections and complicated shapes of large structures. Also, only certain glass compositions can respond to these processes. For the next two or three years, annealed bulk glasses

will be considered for deep-submergence structures in spite of the well-known fact that their strength is limited by surface flaws. Etching can remove most of these flaws, but there is no guarantee that all flaws will be removed or that new ones will not be created accidentally. Surface cracks can grow to critical depths under low tensile stresses and moist conditions. The critical depth for surface cracks is of the order of 30 microinches if the glass is to accept a tensile stress of 100,000 pounds per square inch.

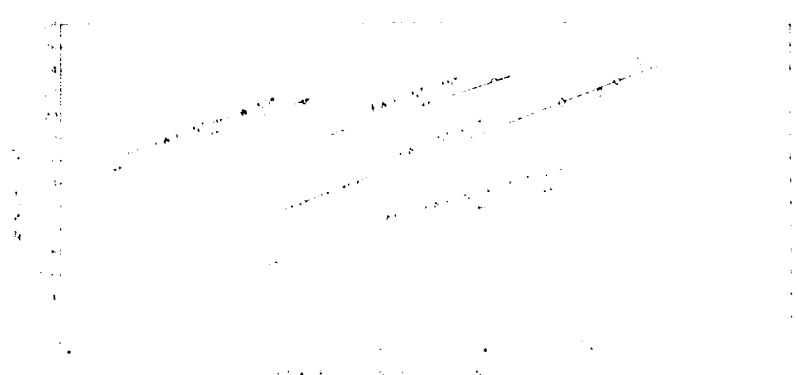
The time necessary for subcritical crack growth to result in critical crack depth was investigated by measuring the rates of growth under arbitrary constantly applied fracture driving forces. Having established the rates as a function of the driving force and the humidity, it was found possible by integration to predict the times for small surface cracks to grow to critical size.

Chemical rate theory was modified to incorporate fracture mechanics, and the resulting equations are useful as a theoretical framework for explaining the



Crack length as a function of a constantly applied driving force, G . The slope of the line gives the rate of crack propagation. (Test for $3 \times 12 \times 0.127$ -inch plate glass conducted at 74°F and at almost 100 percent relative humidity.)

Crack velocity versus G for different dewpoints. The test was conducted at temperatures ranging from 22°C to 25°C .



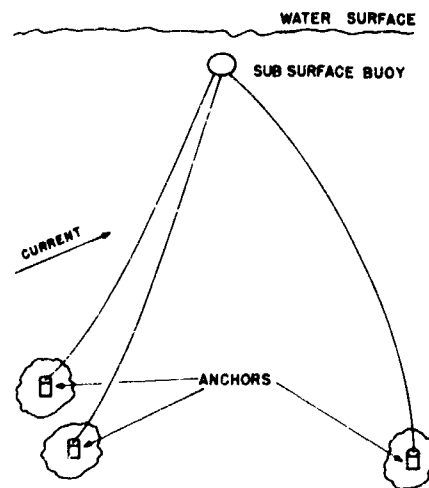
experimental results. The rate at which the short-time strength degrades is proportional to the rate at which the square root of the crack depth increases. A strong dependence of crack growth rate on composition was found, but the selection of an optimum composition will require the acquisition of much more information.

Structural Analysis of Cable Systems. Cables are employed as the basic structural elements in a large number of scientific, engineering, and military developments, such as suspension bridges, power lines, towlines, and tethers, because of their convenient handling and storage properties as well as their extremely favorable ratios of strength to weight. For such use, it is desirable to calculate the tensions in, and shapes of, the loaded cable structure so that the reliability and performance of a system can be predicted.

For a wide range of cable stress *versus* strain relationships and applied loadings, no adequate analysis techniques have been available. This was particularly true for cables with nonlinear stress *versus* strain relationships and for structures subjected to current-induced drag forces that are dependent upon both the position and orientation of the system in space. The primary reason for limited analytical techniques is the large inherent nonlinearities in the equations of equilibrium and of the forcing functions.

NRL scientists became actively engaged in the development of techniques for the analysis of such systems during the past year. This effort has culminated in the formulation of a new structural-analysis technique called "the method of imaginary reactions." This method is capable of providing rapid and accurate engineering answers relating to stress and deflection patterns when applied to cables. A lumped-parameter description of the cable system is applied. However, since the number of unknown variables equals only the number of redundant reactions for any representation of the structure, a closely spaced division of the structure into lumped-parameter elements can be made without grossly affecting the number of calculations needed.

This method is being used to study several cable systems which have previously defied accurate analysis. One such system, of particular interest to oceanographers and the Navy, is Sea Spider. This system consists of a subsurface buoy anchored to the bottom by three cables. It is designed to provide



Schematic representation of the Sea Spider cable installation which supports undersea instrumentation. The pyramidal arrangement and large flotation buoy improve stability, but water currents and gravity cause displacements from desired straight-line orientation.

a platform for a wide variety of oceanographic experiments that require an ultrastable base and a long life. The float is stationed deeply enough to avoid surface-wind and -wave effects, and its large buoyancy imparts high tensions to the anchoring cables. Because of the high tensions and the pyramidal arrangement of the cables, the system is structurally resistant to current-induced deflections from its gravity equilibrium position.

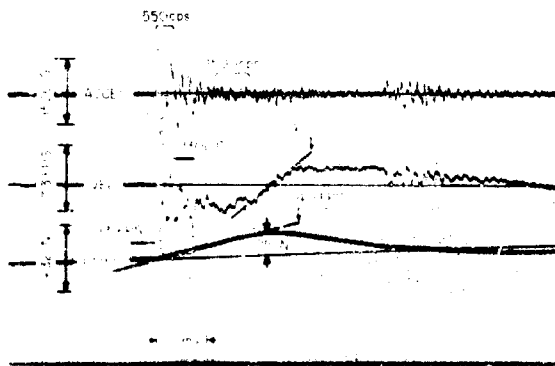
The general method of analysis has been developed, and example computations for representative arrays have been performed with the aid of digital-computer coding. A large variety of problems can be solved by making relatively minor variations in the basic analytical approach.

Experimental Approaches in Shock Design Research.

As is true of most technologies, the progress in devising methods to design "shock-hardened" ship-board structures depends on the creative interplay between physical experimentation and theoretical ingenuity. In structural shock design research, physical experimentation has long been dominated—one might almost say "inhibited"—by measurement and analysis problems which stem from the inherent complexity of real structures and from their equally complex response to shock environments. Some years

ago attempts to interpret structural shock records in the time domain were largely abandoned in favor of approaches involving the same records transformed into a frequency domain; the complex data included in the available single-parameter records (usually relative velocity) seriously impeded physically significant interpretation. Recent improvements in instrumentation have produced new possibilities for analytical insight.

More or less central to the improved instrumentation system is an integrated-accelerometer concept, in which small, lightweight accelerometer transducers are coupled with electronic circuitry capable of producing the velocity and displacement integrals of a measured absolute acceleration transient. While the concept is fairly obvious, the practical problems have been formidable. In a typical shipboard shock-measurement problem, accurate integration requires that the system be linear and stable over a dynamic range of 10,000 to 1, that it respond to frequencies from near zero to approximately 2,000 cycles per second, and that it be insensitive to higher structural frequencies which would otherwise require a further extension of dynamic range. In addition, the com-



An accelerometer record reproduced with successive integrations. This record was obtained from an acceleration transducer attached to a standard Navy lightweight shock machine. The displacement record tends to emphasize rigid body motions common to the entire structure, while the velocity and acceleration records emphasize motions common to progressively smaller portions which correspond to higher modes of the structure. From the three waveshapes, their peak values, and averaged rate-of-change values taken at selected times, it is possible to infer many characteristics of the instrumented structure from which this record was taken.

ponents of the system must be operationally compatible with the primitive experimental conditions frequently encountered during field measurement programs. These difficulties have been surmounted with the NRL shock instrumentation system, which has been proved during usage in a series of laboratory and field measurement programs.

For the experimental researcher, simultaneous recording of shock response in a convenient three-parameter format (acceleration, velocity, and displacement) provides new options for the interpretation of structural response under shock. The ready recognition of coupled structural modes, impacts within the structure, dynamically induced deformations, and instrumentation malfunctions is frequently possible. Further, the interpretive flexibility that would accrue from having a set of filtered records can now result from a simple manual averaging of the slopes of the velocity or the displacement records over selected time intervals. In general, the successive integrals emphasize motions common to different proportions of the total structure while maintaining a physically meaningful interrelationship between these motions. An interpretive study of time-history records in the three-parameter format, in conjunction with frequency-decomposition techniques already developed, can stimulate another step in the evolution of shock design methods.

The Reliability of Nuclear-Power Instrumentation for Oceanographic Research. Because of the long life and low maintenance of the nuclear power plant, nuclear systems will play a large role in ocean technology. The difficulties involved in adapting the nuclear reactor to these new applications for energy and propulsion will include the problem of providing for reliability in the measurement and control circuits of the primary units. This particularly troublesome area in reactor technology has been receiving close scrutiny in a related field of research at NRL.

Scientists at this Laboratory have long sought a capability for the accurate measurement of the physical properties of materials irradiated in a nuclear environment. The unreliability of components in the in-pile portions of the circuits (i.e., those exposed to high nuclear flux) blocked this effort. The inability of these components to perform properly was, of course, due to the continuous attack of the high-intensity neutron and gamma radiation upon the materials used in their construction.

In an effort to surmount these difficulties, a series of in-pile experiments with an electromechanical instrumentation system were conducted. During these studies, the functional response of each of the circuit components was examined separately with respect to the influence of the different radiation phenomena. It was then possible to provide a number of necessary adjustments in circuit design and to develop the correct design criteria for the complete instrumentation system. In a final test, the in-pile measurement system was subjected to 643 hours of full-power exposure in the core of the NRL reactor. Circuit reliability was directly comparable to that normally expected in conventional systems.

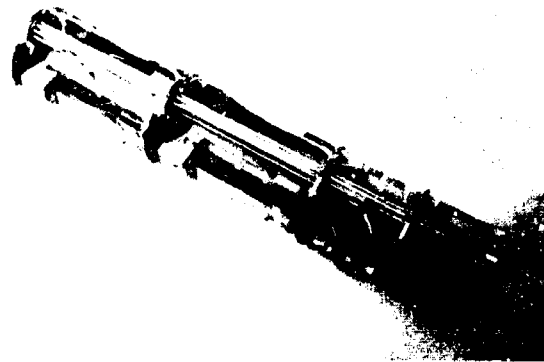
A 3-inch-diameter research probe was used in conjunction with specially designed electronic circuits. The probe, with 12 of these circuits attached, was used to test 4 different mechanical strain sensors under conditions of load, no load, and intermittently applied loading.

Success was achieved through the following measures:

1. Materials which were least subject to degradation through transmutation of their elements were selected for the construction of new components.

2. Instabilities introduced into the electrical signal output through ionization of the insulation mediums and of the experimental atmosphere were eliminated through the spatial readjustment of components, the addition of ceramic insulators, and the provision for a dried helium atmosphere.

3. A symmetrical open-loop design in the mechanical load train removed undesirable thermal stresses caused by gamma heating of the materials.



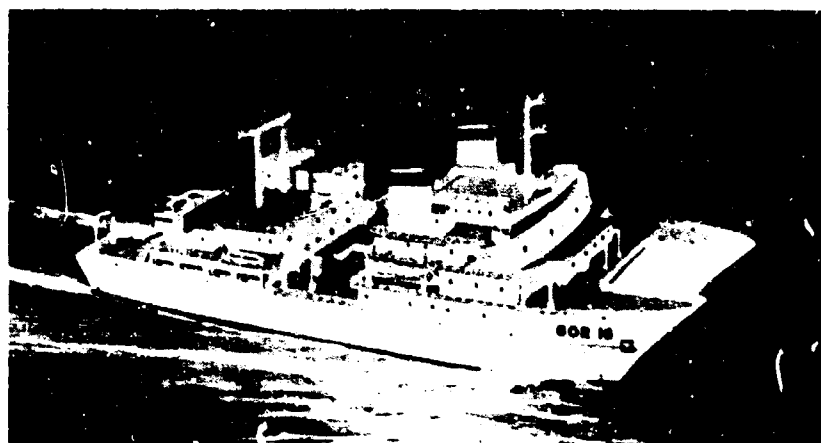
A nuclear reactor probe. The measurement systems in this probe withstood a total exposure of 2.78×10^{18} neutrons per square centimeter, with energies greater than 1 million electron volts, without disruption of functional properties.

4. A rearrangement of the mechanical components was made to provide an equal-temperature platform upon which the dissimilar metallic junctions of the electrical circuit could be mounted. The generation of undesirable thermoelectric electromotive forces within the circuit was thus prevented.

5. The remaining small, spurious influences of the environment upon the test configuration were removed from the electric output by opposing or compensating for their effects in paired elements of the instrumentation system.

In addition to providing for an increased reliability in reactor measurement and control circuits, the results obtained also supply much-needed data on the in-pile behavior of materials.

During 1968, the design of an oceanographic ship which will have many entirely new features - a 230-foot-long catamaran type vessel - was completed. The ship, a drawing of which is shown here, will be put into operation for NRL in the early 1970's.



CONTRIBUTIONS TO SCIENCE AND TECHNOLOGY

During 1968, the Research Department staff produced over 1,100 scientific and technical papers. Its productivity total includes 171 formal NRL reports, 95 memorandum reports, 490 oral presentations at scientific and technical meetings in the United States and in foreign countries, and 362 papers published in professional society journals. Of the published works, 20 papers appearing in the open literature and 6 formal NRL reports were selected for NRL publication awards; these award-

winning papers and reports are identified by an asterisk preceding their titles in the following list.

In addition, 71 patents were issued in 1968 on inventions made by present and former employees of the Naval Research Laboratory. This figure brings the grand total, through the calendar year 1968, to 2,110.

A bibliography of papers published in scientific journals, a list of U.S. patents awarded, and a bibliography of NRL formal reports are presented below.

PAPERS PUBLISHED IN SCIENTIFIC JOURNALS

ACOUSTICS

Acoustic Measurements in the Deep Ocean Convergence Zone, by C. L. Buchanan and R. B. Patterson, *Proc. 24th Navy Symposium on Underwater Acoustics*, New London, Conn., November 12-14, 1968, p. 71

Amplitude Distributions of Monostatically Bottom Scattered Signals, by B. G. Hurdle, K. D. Flowers, and K. P. Thompson, *Acous. Soc. Am. J.* **44**:356, July 1968

Axially Symmetric Vibration of a Thin Cylindrical Elastic Shell Filled with Nonviscous Compressible Fluid, by V. A. Del Grosso, *Acustica* **20**:313, July 1968

Energy Spectral Density of the Sonic Boom, by J. S. Lee, H. L. Peterson, and C. McCoy, *Acous. Soc. Am. J.* **44**:299, July 1968

Experimental Measurement of 'Creeping' Waves on Solid Aluminum Cylinders in Water Using Pulses, by W. G. Neubauer, *Acous. Soc. Am. J.* **44**:298, July 1968

Experimental Observation of Three Types of Pulsed Circumferential Waves on Solid Aluminum Cylinders, by W. G. Neubauer, *Acous. Soc. Am. J.* **44**:1150, October 1968

The Influence of Reverberation and Surface Scattering on the Detection of Targets in the Shadow Zone, by B. J. Schweitzer and H. N. Van Ness, *Proc. 24th Navy Symposium on Underwater Acoustics*, New London, Conn., November 12-14, 1968, pp. 130-144

International Standardization in Underwater Sound Measurements, by W. J. Trott, *Acustica* **20**:182 (1968)

Long Baseline Correlation Experiments, by D. C. Coulter and C. McCoy, Jr., *Proc. 24th Navy Symposium on Underwater Acoustics*, New London, Conn., November 12-14, 1968, pp. 413-423

Near Field Calibration Array, by G. Pida, D. J. G. Gregan, and S. Hanish, *Proc. 24th Navy Symposium on Underwater Acoustics*, New London, Conn., November 12-14, 1968, pp. 234-257

Passive Range Determination, by A. T. McClinton and J. C. Cybulski, *Proc. 24th Navy Symposium on Underwater Acoustics*, New London, Conn., November 12-14, 1968, pp. 705-719

Results of an Experiment on Acoustic Reflection from the Sea Surface, by R. H. Ferris and W. A. Kuperman, *Proc. 24th Navy Symposium on Underwater Acoustics*, New London, Conn., November 12-14, 1968, pp. 438-453

Sound Scattering Into the Shadow Zone Below an Isothermal Layer, by B. J. Schweitzer, *Acous. Soc. Am. J.* **44**:525, August 1968

CHEMISTRY AND CHEMICAL PHYSICS

Adhesion: Mechanisms That Assist or Impede It, by R. V. Baier, Elaine G. Shafrin, and W. A. Zisman, *Science* **162**:1360, December 20, 1968

The Adsorption of C¹⁴-Labeled Stearic Acid on Iron, by C. O. Timmons, R. L. Patterson and L. B. Lockhart, Jr., *J. Coll. and Interface Science* **26**:120, January 1968

Anion-Radicals of Polyphenylsiloxanes, by D. H. Eargle, Jr., and W. B. Moniz, *J. Polymer Sci.* **6**:1153, May 1968

Anisotropy in Energy Calculations for Graphite, by E. F. Meyer, *J. Chem. Phys.* **48**:5284, June 1, 1968

Anodic Oxidation of Hydrogen on Iron and Platinum in Sodium Hydroxide Solution, by S. Schuldiner and C. M. Shepherd, *Electrochem. Soc. J.* **115**:916, September 1968

***Barrier Films Increase Service Lives of Prelubricated Miniature Ball Bearings**, by V. G. Fitzsimmons, C. M. Murphy, J. B. Romans, and C. R. Singleterry, *Lubrication Eng.* **24**:35, January 1968

Characteristics of an Improved Inert-Cathode/Magnesium Anode Sea Water Battery, by B. J. Wilson, *Intersociety Et. al., Conversion Engineering Conference Record*, pp. 852-860, 1968

Changes in the Microstructure of a Sintered Silver Electrode After Repeated Cycling at a Low Current, by C. P. Wales and A. C. Simon, *Electrochem. Soc. J.* **115**:1228, December 1968

- Charging of the Silver Oxide Electrode With Periodically Varying Current. III. 60 CPS Asymmetric A.C.**, by C. P. Wales, *Electrochem. Soc. J.* **115**:680, July 1968
- Charging the Silver Oxide Electrode with Periodically Varying Current. IV. Intermittent Constant Current Reversals During Charge**, by C. P. Wales, *Electrochem. Soc. J.* **115**:985, October 1968
- Coriolis Coupling in a Very Nearly Symmetric-Top Molecule**, by A. B. Harvey, *Spectroscopy Ltrs.* **1**:197, May 1968
- Corrosion of Metals in Tropical Environments—Copper and Wrought Copper Alloys**, by C. R. Southwell and A. L. Alexander (NRL), and C. W. Hummer, Jr. (Naval Station, Rodman, Canal Zone, Panama), *Mat. Prot.* **7**:41, January 1968
- Determination of Trace Contaminants in Air by Concentrating on Porous Polymer Beads**, by F. W. Williams and M. E. Umstead, *Anal. Chem.* **40**:2232, December 1968
- Effect of Adsorbed Water on the Critical Surface Tension of Wetting on Metal Surfaces**, by Marianne K. Bernett and W. A. Zisman, *J. Colloid & Interface Science* **28**:243, October 1968
- Electrical Discharges from a Fuel Surface**, by J. T. Leonard and H. W. Carhart, *Static Electrification Conference, Proc.*, London, England, May 8-10, 1967, pp. 100-111, British Institute of Physics and the Physical Society, 1968
- The Electrochemical Characteristics of Several Proprietary Aluminum Galvanic-Anode Alloys in Sea Water**, by T. J. Lennox, Jr., M. H. Peterson, and R. E. Groover, *Mat. Prot.* **7**:33, February 1968
- Electron Spin Resonance Study of the Photolysis of Polystyrene and Poly(α -Methylstyrene)**, by R. F. Cozzens, W. B. Moniz, and R. B. Fox, *J. Chem. Phys.* **48**:581, January 15, 1968
- Estimation of Absolute Entropies from Gas Chromatographic Retention Data**, by F. W. Williams and H. W. Carhart, *J. Gas Chromatography* **6**:280, May 1968
- Fluorine-Containing Epoxy Components and Plastics**, by J. R. Griffith and J. E. Quick, American Chemical Society, 155th Meeting, *Proc., Division of Organic Coatings and Plastics Chemistry*, Vol. XXVIII, No. 1, p. 342, 1968
- Fundamental Aspects of Polymer Photodegradation**, by R. B. Fox, *The Chem. Bull.* **55**:18, November 1968
- Generation and Dissipation of Electrostatic Discharges in Aircraft Fuel Systems**, by J. T. Leonard, *Proc. Conference on Fire Safety Measures for Aircraft Fuel Systems* (Federal Aviation Agency, December 1967), pp. 35-64 (1968)
- Growth Characteristics of Iron Oxide Films Generated in Dilute Lithium Hydroxide Solution at 300°C**, by J. B. Moore and R. L. Jones, *Electrochem. Soc. J.* **115**:576, June 1968
- High Resolution Vacuum Ultraviolet Absorption Spectra of $B^1\Sigma^+ - X^1\Sigma^+$, $C^1\Sigma^+ - X^1\Sigma^+$, and $j^3\Sigma^+ - X^1\Sigma^+$ Transitions in Carbon Monoxide**, by S. G. Tilford and J. T. Vanderslice, *J. Molec. Spectros.* **26**:419, August 1968
- Hydrolysis of Oil-Soluble Organic Amine Salts in the Two-Phase Water-Benzene System**, by M. A. Scheiman and H. R. Baker, *J. Chem. & Eng. Data* **13**:394, July 1968
- Ionization from the Heterogeneous Catalytic Oxidation of Hydrocarbons in the Vapor Phase**, by J. E. Johnson, F. J. Woods, and M. E. Umstead, *Advances in Chemistry Series* **76**:313 (1968)
- The Mass Spectra of Trifluorophosphinecarbonylcobalt Hydrides**, by F. E. Saalfeld and M. V. McDowell (NRL), and S. K. Gondal and A. G. MacDiarmid (U. of Pa.) *Am. Chem. Soc. J.* **90**:3684 (1968)
- The Mass Spectrum of Methyl difluorosilyltetracarbonylcobalt**, by F. E. Saalfeld and M. V. McDowell (NRL), S. K. Gondal and A. G. MacDiarmid (University of Pennsylvania), *Inorganic Chem.* **7**:1465 (1968)
- The Mass Spectrum of Trifluorosilyltetracarbonylcobalt**, by F. E. Saalfeld and M. V. McDowell (NRL), A. P. Hagen and A. G. MacDiarmid (University of Pennsylvania), *Inorganic Chem.* **7**:1665 (1968)
- Membrane Potentials and Ion Selectivity of Fused Silica in Molten Salts**, by K. H. Stern, *J. Phys. Chem.* **72**:1963, June 1968
- Microvoids in Glass-Resin Composites. Their Origin and Effect on Composite Strength**, by W. D. Bascom and J. B. Romans, *I&EC Product Research and Development* **7**:172, September 1968
- On the Activity of Platinum Catalysts in Solution. II. Kinetics of the Pt-O Reaction with Hydrogen and of Pt-H Deposition Using a Double Pulse Technique**, by T. B. Warner and S. Schuldiner, *Electrochem. Soc. J.* **115**:28 (1968)
- On the Activity of Platinum Catalysts in Solution. III. Facets on Flame-Formed Platinum Spheres**, by T. B. Warner, *Electrochem. Soc. J.* **115**:615, June 1968
- Oxidation of Hydrogen on a Passive Platinum Electrode**, by S. Schuldiner, *Electrochem. Soc. J.* **115**:362, April 1968
- Passivation of Anodic Reactions**, by S. Schuldiner, *Electrochem. Soc. J.* **115**:897, September 1968
- Potentiostatic Current-Potential Measurements on Iron and Platinum Electrodes in High-Purity Closed Alkaline Systems**, by C. M. Shepherd and S. Schuldiner, *Electrochem. Soc. J.* **115**:1124, November 1968
- Preparation and Wettability of Terminally Chlorophenyl-Substituted Carboxylic Acid Films**, by Elaine G. Shafrin and W. A. Zisman, in *Advances in Chemistry Series*, **87**:20, American Chemical Society, 1968

CONTRIBUTIONS

Pressure Effects on the Friction Coefficient of Thin-Film Solid Lubricants, by R. C. Bowers and W. A. Zisman, *J. Appl. Phys.* **39**:5385, November 1968

Products of Strength Times Self-Broadened Half-Widths of Absorption Lines in the ν_2 Band of Water Vapor, by D. K. Prinz, *Appl. Opt.* **7**:689 (1968)

Quantitative Measurement of Void Content in Glass-Filament-Wound Composites and Correlation of Interlaminar Shear Strength with Void Content, by E. J. Kohn, A. G. Sands, and R. C. Clark, *I&EC Product Research and Development* **7**:179, September 1968

Quelques observations sur l'état actuel de la nomenclature des polymères, by R. B. Fox, *Rev. Gén. Caoutchouc et. Plast.*, Ed. Plastiques **5**:152 (1968)

The Relation of Initial Spreading Pressure of Polar Compounds on Water to Interfacial Tension, Work of Adhesion, and Solubility, by C. O. Timmons and W. A. Zisman, *J. Colloid & Interface Science* **28**:106, September 1968

Removal of Water from Jet Fuel, by R. N. Hazlett, *U.S. Naval Aviation Weapons System Digest* (Aeronautics Ed.), pp. 17-22, October 1968

Ring-Puckering Vibration of 2,5-Dihydrothiophene, by W. H. Green and A. B. Harvey, *J. Chem. Phys.* **49**:177, July 1, 1968

The Solid-Liquid Interface—An Essential and Active Frontier of Science, by W. A. Zisman, in *Advances in Chemistry Series* **87**:1, American Chemical Society, 1968

Spectroscopic Analysis of Polypeptide Conformation in Polymethyl Glutamate Monolayers, by G. I. Loeb and R. E. Baier, *J. Colloid & Interface Sci.* **27**:38, May 1968

A Structure-Based Nomenclature for Linear Polymers, by R. B. Fox, *et al.*, *Macromolecules* **1**:193 (1968)

A Study of the Conformation of Surface Films of Polybenzyl-L-Glutamate by Multiple Internal Reflection Spectroscopy, by G. I. Loeb, *J. Coll. Interface Sci.* **26**:236 (1968)

Surface Potentials of Aqueous Electrolyte Solutions, by N. L. Jarvis and M. A. Scheiman, *J. Phys. Chem.* **72**:74 (1968)

Vibrational Spectra and Structure of Dimethyl Diselenide and Dimethyl Diselenide-d₆, by W. H. Green and A. B. Harvey, *J. Chem. Phys.* **49**:3586, October 15, 1968

Wettability and Constitution of Photooxidized Polystyrene and Other Amorphous Polymers, by R. B. Fox, T. R. Price and D. S. Cain, *Advances in Chemistry Series* **87**:72 (1968)

The Wettability of Fluoro- and Chlorocarbon Trialkoxysilane Films Adsorbed on Glass and Metal Surfaces, by W. D. Bascom, *J. Colloid & Interface Science* **27**:789, August 1968

The Wettability of n-Octadecylamine, n-Octadecyl Alcohol and n-Octadecanoic Acid Films Adsorbed on Thermally

Treated Metal Oxide Surfaces, by W. D. Bascom, *J. Colloid & Interface Science* **26**:89, January 1968

CRYSTAL AND MOLECULAR STRUCTURE

The Crystal Structure of the Alkaloid Reserpine, C₃₃H₄₀N₂O₆, by I. L. Karle and J. Karle, *Acta Crystall.* **B24**:81, January 23, 1968

The Crystal Structures of Two Novel Polycyclic Products, C₂₆H₂₂O₆ and C₂₄H₁₈, from the Photolysis of anti-[2.2]Paracyclonaphthene, by A. V. Fratini, *Am. Chem. Soc. J.* **90**:1688, March 27, 1968

Derivatives of Morphine VII. The Structure of Pentachloro-oxo-and-ethoxycodides; an Unusual Addition Reaction to an Aromatic Ring, by U. Eisner, T. J. Batterham, U. Weiss and I. L. Karle, *Chemical Communications*, p. 774, 1968

Noncentral Force Model for Hexagonal Close-Packed Crystal Lattices (II), by E. A. Metzbowler, *Phys. Stat. Solidi* **25**:403, January 1, 1968

Partial Structural Information Combined with the Tangent Formula for Noncentrosymmetric Crystals, by J. Karle, *Acta Crystall.* **B24**:182, February 1968

Self-Diffusion in the Molecular Crystal Adamantane: Comparison of NMR and Plastic-Flow Methods, by H. Resing (NRL); N. T. Corke and J. N. Sherwood (U. of Strathclyde), *Phys. Rev. Ltrs.* **20**:1227, May 27, 1968

The Structure of Batrachotoxinin A, a Novel Steroidal Alkaloid from the Colombian Arrow Poison Frog, Phylllobates aurotaenia, by T. Tokuyama, J. Daly, B. Witkop, I. L. Karle and J. Karle, *Am. Chem. Soc. J.* **90**:1917 (1968)

INSTRUMENTATION AND SYSTEMS

Absorption Edge Effects in Electron Probe Analysis, by D. Nagel, in *Quantitative Electron Probe Microanalysis* (Proc., NBS Seminar, Gaithersburg, Md. June 12-13, 1967), Ed., K. F. J. Heinrich, NBS, Spec. Pub. 298, October 1968, pp 189-196

Calculation Methods for Fluorescent X-Ray Spectrometry—Empirical Coefficients vs. Fundamental Parameters, by J. W. Criss and L. S. Birks, *Analytical Chem.* **40**:1080, June 1968

The Design for an Optical Rate Display, by Patricia Anne Griffin, *Human Factors* **10**, August 1968

Ein neuer Magnetograph zur simultanen Messung des longitudinalen und des transversalen Zeemaneffektes im Sonnenspektrum, by G. Bruckner, *Z. Astrophys.* **68**:48 (1968)

Guard Ring Shielding to Eliminate Instability of Collecting Volume in Ionization Chambers, by F. H. Attix and S. G. Gorbies, *Rev. Sci. Instr.* **39**:1766, November 1968

- Joystick Dynamics, by Barbour Lee Perry and H. P. Birmingham, *Human Factors* 10:413, August 1968
- LIF and $\text{CaF}_2\text{:Mn}$ Thermoluminescent Dosimeters in Tandem, by S. G. Gorbics and F. H. Attix, *Intern. J. Rad. Isotopes* 19:81, February 1968
- *Method for Computing Magnet Coil Current Settings for the NRL Isochronous Cyclotron, by R. G. Allas, C. M. Davisson, A. G. Pieper, and R. B. Theus, *Nuclear Instr. & Meth.* 64:333, October 1, 1968
- A MgF_2 Soleil Compensator for the Near Infrared, by E. D. Palik, *Appl. Optics* 7:978, May 1968
- A Neutron Spectrometer Using Pulse Shape Discrimination, by D. W. Jones, *Nuclear Instr. & Meth.* 62:19 (1968)
- On the Structure of Formulas for Quantitative Analysis, by John Criss, in *Quantitative Electron Probe Microanalysis*, (Proc., NBS Seminar, Gaithersburg, Md. June 12-13, 1967), Ed., K. F. J. Heinrich, NBS, Spec. Pub. 298, Oct. 1968, pp. 53-62
- Sample Orienting Device Providing Two Rotational Degrees of Freedom in a Solenoid, by J. E. Ivory, *Rev. Sci. Instr.* 39:1225, August 1968
- Spectral Distribution of X-Ray Tubes for Quantitative X-Ray Fluorescence Analysis, by J. V. Gilfrich and L. S. Birks, *Analytical Chem.* 40:1077, June 1968
- Techniques for Minimizing Edge Effects in Nuclear Emulsions, by R. L. Kinzer, N. Seeman, and G. H. Share, *Nuclear Instr. & Meth.* 60:340, April 1, 1968
- LASER PHYSICS AND TECHNOLOGY**
- Compensating for Pump-Induced Distortion in Glass Laser Rods, by J. N. Bradford and R. C. Eckardt, *Appl. Opt.* 7:2418, December 1968
- Definition of Laser Radar Cross Section, by P. W. Wyman, *Appl. Opt.* 7:207, January 1968
- Hydrogen Molecular Vacuum Ultraviolet Laser Theory, by A. W. Ali (Catholic Univ.) and A. C. Kolb (NRL), *Appl. Phys. Ltrs.* 13:259, October 1968
- Linear and Circularly Polarized Laser Radiation in Optical Third Harmonic Generation, by P. P. Bey, J. F. Giuliani, and H. Rabin, *Phys. Ltrs.* 26A:128 (1968)
- Measurements on the Stimulated Raman Effect in H_2 in Terms of Laser Oscillator and Amplifier Theories, by A. J. Glass (NRL), P. V. Avizonis, K. C. Jungling, A. H. Guenther, and R. M. Heimlich (Air Force Weapons Lab., Kirtland AFB), *J. Appl. Phys.* 39:1752, February 15, 1968
- Interferometric Observation of Absorption Induced Line Change Associated with Thermal Blooming, by E. A. McClain, L. Sica, and A. J. Glass, *Appl. Phys. Ltrs.* 13:359, December 1, 1968
- *Phase-Matched Optical Harmonic Generation in Liquid Media Employing Anomalous Dispersion, by P. P. Bey, J. F. Giuliani, and H. Rabin, *IEEE J. Quantum Electronics* QE-4:932, November 1968
- Third-Harmonic Nonlinear Reflection from a Liquid with Adjustable Momentum Matching, by P. P. Bey, J. F. Giuliani, and H. Rabin, *Phys. Ltrs.* 28A:89, November 4, 1968
- Time Development of Strokes Pulsed in Raman Lasers, by A. J. Glass and J. M. McMahon, *Am. Phys. Soc. Bull.* 13:55 (1968)
- MATHEMATICS**
- *Differential Equations of Infinite Order Hyperdirichlet Series and Entire Functions of Bounded Index, by B. Lepson, *Proc. of Symposia in Pure Mathematics* 11:298 (1968)
- *On the Distribution of Values of Meromorphic Functions, by F. Gross, *Am. Math. Soc. Trans.* 131:199, April 1968
- *On the Equation $f^n + g^n = 1$, II, by F. Gross, *Am. Math. Soc. Bull.* 74:647, July 1968
- Orthogonal Expansion of a Real Rational Function Having Hurwitz Denominator, by G. V. Trunk (NRL) and W. H. Huggins (Johns Hopkins U.), *IEEE Trans.* CT-15:144, June 1968
- *Pairs of Consecutive Primitive Roots Modulo, by E. Vegh, *Am. Math. Soc. Proc.* 19:1169 (1968)
- Statistical Estimation of the Intrinsic Dimensionality of Data Collections, by G. V. Trunk, *Info. & Contr.* 12:508, May-June 1968
- Sufficient Conditions for Stability of the Faddeev Equations, by W. W. Zachary, *Am. Phys. Soc. Bull.* 13:1419 (1968)
- MECHANICS**
- Agenda Discussion on High Speed Dislocation, by J. Weertman and J. M. Krafft, *Proc. Battelle Colloquium on Dislocation Dynamics*, Seattle-Harrison, Brit. Columbia (McGraw Hill, New York, 1968) pp. 609-620
- Dynamic Mechanical Behavior of Metal at the Tip of a Plane Strain Crack, by J. M. Krafft, in *Mechanical Behavior of Materials Under Dynamic Load*, Ed., U.S. Lindholm (Springer-Verlag, 1968) pp. 134-151
- Empirical Relationship Between Shear Strength, Pressure, and Temperature - II, by L. C. Towle (NRL) and R. E. Riecher (AF CRL), *Appl. Phys. Ltrs.* 13:159, September 1, 1968
- Linear Fracture Mechanics, Fracture Transition, and Fracture Control, by G. R. Irwin (now at Lehigh Univ.), *Eng. Fracture Mechanics* 1:241, August 1968

CONTRIBUTIONS

Normal Modes and Theory for Combined Structures, by W. L. Fourney and G. J. O'Hara, *Acous. Soc. Am. J.* **44**:1220, November 1968

The Pressure and Temperature Dependence of the Shear Strength of Minerals, by L. C. Towle and R. F. Riecker, *J. Appl. Phys.* **39**:4807, September 1968

Theoretical and Experimental Study of Longitudinal Impact of Tapered Rods, by L. R. Hettche, *NBS J. Res.* **72C**:231, October-December 1968

METALLURGY AND METAL PHYSICS

The Adsorption Model for Environmental Effects in Fatigue Crack Propagation, by M. R. Achter, *Scripta Metallurgica* **2**:525, September 1968

Advances in Fracture Toughness Characterization Procedures and in Quantitative Interpretations to Fracture-Safe Design for Structural Steels, by W. S. Pellini, *Weld. Res. Council Bull. No. 130*, May 1968

Anomalies in the Thermopower of Pd Ni Alloys, by A. I. Schindler (NRL) and C. L. Foiles (Michigan State U.), *Phys. Ltrs.* **26A**:154, January 15, 1968

Bound States of Two Spin Waves in the Heisenberg Ferromagnet, by A. W. Saenz and W. W. Zachary, *Am. Phys. Soc. Bull.* **13**:92 (1968)

***Chromium Solubility in Wustite at 1000°C: Changes in Oxygen Activity and Lattice Parameter**, by C. T. Fujii and R. A. Meussner, *AIME Met. Soc. Trans.* **242**:1259, July 1968

Comments on Theoretical Analyses of Isenthalpic Solidification, by M. E. Glicksman and R. J. Schaefer, *J. Crystal Growth* **2**:239 (1968)

A Comparison of Fracture Toughness Parameters for Titanium Alloys, by C. N. Freed, *Eng. Fracture Mechanics* **1**:175, June 1968

Comparison of Paraboloidal Models of Dendrite Tips, by R. J. Schaefer and M. E. Glicksman, *J. Metals* **20**:67A (1968)

Determination of Absolute Solid/Liquid Interfacial Energies in Metals, by M. E. Glicksman and C. L. Vold, *J. Metals* **20**:28A (1968)

Deviation from Matthiessen's Rule in the Low Temperature Thermal and Electrical Resistivities of Very Pure Copper, by J. L. Schriempf, *NBS Spec. Pub. No. 302*, September 1968, pp. 249-252

Dislocation Structures in Niobium (Columbium) Single Crystals Observed by Optical Microscopy, by R. G. Vardiman and M. R. Achter, *AIME Met. Soc. Trans.* **242**:196, February 1968

Effects of Heat Treating Environmental Conditions on the Stress-Corrosion Cracking Resistance of Several Titanium Alloys, by D. G. Howe and R. J. Goode, in *Applications Related Phenomena in Titanium Alloys*, ASTM STP 432, pp. 189-201 (1968)

The Effects of Some Alloying Elements on the Decomposition of Cementite and Graphitization Kinetics in Cast Irons, by G. Sandoz, in *Recent Research on Cast Iron* (Gordon and Breach, 1968) pp. 509-550

***Effects of a 3.5 Per Cent Sodium Chloride Aqueous Saline Environment on the Fatigue Crack Propagation Characteristics of Titanium Alloys**, by T. W. Crooker and E. A. Lange, *Applications Related Phenomena in Titanium Alloys*, ASTM STP 432 (1968), pp. 251-267

Electron Microscope Image Intensifier Studies of Metallic Solid/Liquid Interfaces, by C. L. Vold and M. E. Glicksman, *J. Metals* **20**:69A (1968)

Electron-Paramagnon Scattering in Pt-Ni Alloys, by D. J. Gillespie and A. I. Schindler, *Am. Phys. Soc. Bull.* **13**:364 (1968)

Evaluation of Materials for Hydrospace Applications, by R. J. Goode, in *Weld Imperfections (Proc. Symposium at Lockheed Palo Alto Research Laboratory, Palo Alto, California)*, Eds., A. R. Pfluger and R. E. Lewis (Addison-Wesley, 1968) pp. 393-426

Fatigue Crack Propagation and Plane Strain Fracture Toughness Characteristics of a 9Ni-4Co-0.25C Steel, by T. W. Crooker, L. A. Cooley, E. A. Lange, and C. N. Freed, *ASM Trans. Quart.* **61**:568, September 1968

Flaws and Performance of Metals in Structures, by E. A. Lange, *Proc. 1964 Symposium on Physics and Non-destructive Testing*, pp. 29-53 (1968)

Fracture Characteristics of Welded Quenched and Tempered Steels in Various Specimens, by L. J. McGeady, *Weld. J.* **47**:563-s, December 1968

Fracture by Microscopic Plastic Deformation Processes, by C. D. Beachem and D. A. Meyn, in *Electron Fractography*, ASTM Spec. Tech. Pub. No. 436, pp. 59-88 (1968)

Hall Effect in Pd Containing Small Amounts of Fe, Ni, Ru, or Pt, by D. J. Gillespie and A. I. Schindler, *Am. Phys. Soc. Bull.* **13**:642 (1968)

Low-Temperature Electrical Resistivity of Pd and Pd-Ni Alloys, by A. I. Schindler (NRL) and B. R. Coles (Imperial College, London), *J. Appl. Phys.* **39**:956 (1968)

Low Temperature Magnetoresistance in Nearly Ferromagnetic Pd-Ni Alloys, by A. I. Schindler and B. C. La Roy, *Am. Phys. Soc. Bull.* **13**:364 (1968)

Low Temperature Specific Heat of Ni and Some FCC Based Alloys, by R. Ehrat, A. C. Ehrlich, and D. Rivier, *J. Phys. Chem. Solids* **29**:799 (1968)

- Low Temperature Thermal and Electrical Resistivities of Osmium**, by J. T. Schriempf, *Am. Phys. Soc. Bull.* **13**: 510 (1968)
- Low Temperature Thermal and Electrical Resistivities of Ultrapure Silver**, by A. C. Ehrlich and J. T. Schriempf, *Am. Phys. Soc. Bull.* **13**:510 (1968)
- Measurement of Atomic Kinetics of Solidification Using Peltier Heating and Cooling**, by R. J. Schaefer and M. E. Glicksman, *Acta Met.* **16**:1009, August 1968
- Metal Mixing During Electron Beam Welding**, by P. Shahinian, J. T. Atwell, and E. J. Brooks, *Electrochem. Tech.* **6**:282, July-August 1968
- Metals and Corrosion**, by B. F. Brown, *Mach. Design.* **40**:165, January 18, 1968
- The Nature of Fatigue-Crack Propagation in Air and Vacuum for 2024 Aluminum**, by D. A. Meyn, *ASM Trans. Quart.* **61**:52, March 1968
- Observations on Micromechanisms of Fatigue-Crack Propagation in 2024 Aluminum**, by D. A. Meyn, *ASM Trans. Quart.* **61**:42, March 1968
- Procedures for Fracture Toughness Characterization and Interpretations to Failure-Safe Design for Structural Titanium Alloys**, by R. J. Goode, *Welding Research Council Bulletin No. 134*, 17 pp., October 1968
- Progress in Quantitative Electron Probe Microanalysis**, by J. W. Criss, in *Fifty Years of Progress in Metallographic Techniques*, ASTM STP 430, pp. 291-314 (1968)
- Relative Interfacial Free Energies in Pure Nickel, Dispersion Hardened Nickel, and a Precipitation Hardened Nickel-Base Alloy**, by C. M. Gilmore (NRI), L. E. Murr (U. of Southern California), and P. J. Smith (Stevens Inst. Tech.), *Phil. Mag.* **17**:89, January 1968
- Report of the Washington Electron Probe Users' Group**, by L. S. Birks, J. V. Gilfrich, and H. Yakowitz, in *Fifty Years of Progress in Metallographic Techniques*, ASTM STP 430, pp. 343-353 (1968)
- Some Quantitative Aspects of Solid/Liquid Interface Morphology**, by M. E. Glicksman and C. L. Vold, *J. Metals* **20**:94A (1968)
- Specific-Heat Enhancement in Strongly Paramagnetic Pd-Ni Alloys**, by A. I. Schindler and C. A. MacKliet, *Phys. Rev. Lett.* **20**:15, January 1, 1968, also in *Am. Phys. Soc. Bull.* **13**:124 (1968)
- Spin Fluctuation Effects in Nearly Ferromagnetic Pd-Ni and Pt-Ni Alloys**, by A. I. Schindler, *Am. Phys. Soc. Bull.* **13**:642 (1968)
- Thermal and Electrical Resistivities of Dilute Pd-Ni Alloys from 2 to 20 K**, by J. T. Schriempf and A. I. Schindler, *Am. Phys. Soc. Bull.* **13**:1644 (1968)
- Three-Term Analysis of the Ideal Thermal and Electrical Resistivities of Transition Metals**, by J. T. Schriempf, *Phys. Rev. Lett.* **20**:1034, May 6, 1968

NUCLEAR AND ATOMIC PHYSICS

- Anomalous Isotope Shift in C^{12} and C^{13}** , by R. Raphael and M. Rosen, *Am. Phys. Soc. Bull.* **13**:719 (1968)
- Computational Methods for X-Ray Emission From Targets Excited by Electrons**, by D. B. Brown, in *Quantitative Electron Probe Microanalysis* (Proc., NBS Seminar, Gaithersburg, Md., June 12-13, 1967), Ed., K. F. J. Heinrich, NBS, Spec. Pub. 298, October 1968, pp. 63-69
- Computed Values of the Specific γ -Ray Constant Γ for ^{137}Cs and ^{60}Co** , by F. H. Attix, *Phys. in Med. and Biol.* **13**:119 (1968)
- Decay of ^{44}K and ^{40}K** , by R. E. Larson, C. M. Gordon, and J. A. Eisele, *Am. Phys. Soc. Bull.* **13**:1383 (1968)
- The D(p,p,n)p Reaction at 46 MeV**, by E. L. Petersen, P. Thomas, R. O. Bondelid, J. W. Verba, and J. R. Richardson, *Am. Phys. Soc. Bull.* **13**:569 (1968)
- DWBA Analysis of Low Energy (t,p) Angular Distributions**, by L. Cohen and G. H. Herling, *Am. Phys. Soc. Bull.* **13**:1388 (1968)
- Energy Spectra of Photoneutrons from O^{16} at 70°, 90°, 110°, 130°, and 150°**, by D. W. Jones and M. Elaine Toms, *Am. Phys. Soc. Bull.* **13**:718 (1968)
- Gamma Rays from the Decay of ^{44}Sc , and ^{46}Sc ; and Energy Levels in ^{44}Ca and ^{46}Ti** , by J. A. Eisele and R. E. Larson, *Am. Phys. Soc. Bull.* **13**:1384 (1968)
- Gamma Spectra Arising from Thermal Neutron Capture by Even-Even Yb Isotopes**, by A. I. Namenson and J. C. Ritter, *Am. Phys. Soc. Bull.* **13**:722 (1968)
- Gamma Spectra of Yb^{170} (n, γ) Yb^{171} and Yb^{172} (n, γ) Yb^{173}** , by A. I. Namenson and J. C. Ritter, *Am. Phys. Soc. Bull.* **13**:1391 (1968)
- (γ ,2n), (γ ,n) and (γ , α n) Reactions on ^{63}Cu and the Decay of ^{63}Co** , by J. C. Ritter, R. E. Larson, and J. I. Hoover, *Nuclear Phys.* **A110**:463, March 22, 1968
- Generalized Helm Model for Electron Scattering from Deformed Nuclei**, by R. Raphael and M. Rosen, *Am. Phys. Soc. Bull.* **13**:175 (1968)
- Inelastic Electron Scattering from ^{24}Mg at 180°**, by W. I. Fagg, W. I. Bendel, R. A. Tobin, and H. F. Kaiser, *Phys. Rev.* **171**:1250, July 20, 1968
- Inelastic Electron Scattering from ^{24}Mg at 180°**, by W. I. Bendel, W. I. Fagg, R. A. Tobin, and H. F. Kaiser, *Phys. Rev.* **173**:1103, September 20, 1968

CONTRIBUTIONS

- J-Dependence in the Reaction $^{60}\text{Ni}(\alpha, p)^{61}\text{Cu}$ at 30 MeV**, by L. R. Cooper, L. S. August, and P. Shapiro, *Am. Phys. Soc. Bull.* 13:1446 (1968)
- Lifetimes of the First Four Excited States in Si^{28}** , by S. I. Baker and R. E. Segel, *Phys. Rev.* 170:1046, June 20, 1968
- Lifetime Limits for the Excited State Transitions from the O^{16} Giant Resonance**, by K. Murray and J. Ritter, *Am. Phys. Soc. Bull.* 13:1423 (1968)
- Lifetimes of States in ^{24}Mg** , by S. I. Baker, C. R. Gossett, P. A. Treado, J. M. Lambert, and L. A. Beach, *Am. Phys. Soc. Bull.* 13:1371 (1968)
- The $\text{Li}^7(\text{He}^3, t_0)\text{Be}^7$ and $\text{Li}^7(\text{He}^3, t_1)\text{Be}^7$ Reactions from 8.0 to 10.0 MeV**, by R. V. Mancuso, A. R. Knudson, and E. A. Wolicki, *Am. Phys. Soc. Bull.* 13:606 (1968)
- ^6Li States from the $^7\text{Li}(^3\text{He}, \alpha)^6\text{Li}$ Reaction**, by P. A. Treado, J. M. Lambert, V. E. Alessi, R. J. Kane, and D. Haddad, *Am. Phys. Soc. Bull.* 13:1386 (1968)
- Low-Energy Argon Implantation in (111) Silicon**, by J. Comas and E. A. Wolicki, *Am. Phys. Soc. Bull.* 13:967 (1968)
- Nuclear Particle and Photon Decay Following Electroexcitation**, by D. Drechsel and H. Überall, *Am. Phys. Soc. Bull.* 13:718 (1968)
- Numerical Analysis of (p, γ) Resonance Yields**, by K. L. Dunning, *Am. Phys. Soc. Bull.* 13:1444 (1968)
- On the Sensitivity of Multiple-Scattering Calculations to the Single-Scattering Phase Functions**, by H. B. Howell, *J. Atmos. Sci.* 25:1090, November 1968
- On the Trouton-Noble Experiment**, by J. W. Butler, *Am. J. Phys.* 36:939, November 1968
- 180° Electron Scattering on ^{28}Si and ^{20}Ne** , by W. L. Bendel, L. W. Fagg, E. C. Jones, Jr., H. F. Kaiser, and S. Numrich, *Am. Phys. Soc. Bull.* 13:1373 (1968)
- Optical Model Analysis of Low Energy Triton Scattering**, by G. H. Herling and L. Cohen, *Am. Phys. Soc. Bull.* 13:93 (1968)
- Polarization of Neutrons from the $^2\text{H}(d, n)^3\text{He}$ Reaction Below 400 keV**, by A. F. Behot, T. H. May and W. I. McGarry, *Nuclear Phys.* A108:250, February 5, 1968
- Positive Parity Excited State Transitions from the O^{16} Giant Resonance**, by K. Murray and J. C. Ritter, *Am. Phys. Soc. Bull.* 13:717 (1968)
- Sequential Decay in the $^7\text{Li}(\alpha, d)^6\text{Be}$ and $^7\text{Li}(\alpha, t)^6\text{Be}$ Reactions at 50 MeV**, by J. N. Lambert, P. A. Treado, L. A. Beach, R. B. Theus, and E. L. Petersen, *Am. Phys. Soc. Bull.* 13:1450 (1968)
- Study of $\text{C}^{12}(n, \alpha)n$ at 14.1**, by F. H. Berkowitz, A. W. Barrows, R. V. Mancuso, and S. L. Bard, *Am. Phys. Soc. Bull.* 13:607 (1968)
- The Study of the Quasi-Free Process in the p-d Breakup Reaction**, by R. O. Bondelid, E. L. Petersen, G. Paic, J. R. Richardson, P. Thomas, and J. W. Verba, *Am. Phys. Soc. Bull.* 13:1368 (1968)
- Triple Correlation in the $^{60}\text{Ni}(p, \gamma)^{60}\text{Cu}$ and $^{62}\text{Ni}(p, \gamma)^{62}\text{Cu}$ Reactions**, by P. A. Treado, C. R. Gossett and L. S. August, *Nuclear Phys.* A112:32 (1968)

OCEAN SCIENCES AND ENGINEERING

- Clear-Air Echoes and Corresponding Atmospheric Structure Determined by Aircraft**, by I. Katz (APL) and D. L. Randall (NRL), *Proc., 13th Radar Meteorology Conference*, pp. 274-278, Montreal, August 20-23, 1968
- Comments on "Anomalous Cloud Lines,"** by S. Twomey, H. B. Howell, and T. A. Wojciechowski, *J. Atmos. Sci.* 25:333, March 1968
- The Determination of Fluorine in Sea Water by Photon Activation Analysis**, by P. E. Wilkiss and V. J. Linnenbom, *Limnol. and Oceano.* 13:530, July 1968
- Glaciation of a Cumulus at Approximately -4C** , by R. E. Ruskin, S. C. Mossop, and K. J. Heffernan, *J. Atmos. Sci.* 25:889, September 1968
- Guarded Double Field Meter**, by S. Gathman, *Rev. Sci. Instr.* 39:43, January 1968
- The Influence of Monomolecular Surface Films on the Production of Condensation Nuclei from Bubbled Sea Water**, by W. D. Garrett, *J. Geophys. Res.* 73:5145, August 15, 1968
- Invasion of Some Tropical Timbers by Fungi in Brackish Waters**, by D. D. Ritchie, *Elisha Mitchell Sci. Soc. J.* 84:221, April 1968
- Künstliche Veränderungen der Grenzfläche Ozean/Atmosphäre?** by W. D. Garrett, *Umschau in Wissenschaft und Technik No. 18*, pp. 568-569 (1968)
- Photographic Techniques for Ocean Floor Search and Research**, by R. B. Patterson, *Marine Sciences Instrumentation* 4:354 (1968)
- Search and Serendipity**, by W. L. Brundage, Jr., C. L. Buchanan, and R. B. Patterson, Chapter 6, in *Deep-Sea Photography*, Ed. J. B. Hersey (Baltimore Johns Hopkins Press, 1967), pp. 75-87.
- A Sensitive Gas Chromatographic Method for Determining Carbon Monoxide in Seawater**, by J. W. Swinnerton, V. J. Linnenbom, and C. H. Check, *Limnol. Ocean.* 13:193, January 1968
- Space Charge Over the Open Ocean**, by S. Gathman and Eva Mae Trent, *J. Atmos. Sci.* 25:1075, November 1968
- Wake Collapse in Stratified Fluid: Experimental Exploration of Scaling Characteristics**, by A. H. Schooley, *Science* 160:763, May 17, 1968

*Water Vapor Distribution in the Stratosphere and High Troposphere, by H. J. Mastenbrook, *J. Atmos. Sci.* 25:299, March 1968

PLASMA PHYSICS

Experimental Investigations of Normal Ionizing Shock Waves, by L. Levine, *Phys. of Fluids* 11:1479 (1968)

*Observation of Two-Photon Continuum Emission from Neon IX, by R. C. Elton, L. J. Palumbo, and H. R. Griem, *Phys. Rev. Lett.* 20:783, April 8, 1968

Plasma. Introductory Remarks, by A. C. Kolb, *J. Quant. Spectros. Radiat. Transfer* 8:387, January 1968

Similarities in Soak and Exploding Wire Discharges, by I. M. Vitkovitsky, *Exploding Wires* 4:35 (1968)

Stability of the NRL Hard Core Theta-Pinch, by D. Duchs, R. H. Dixon, R. C. Elton, and A. C. Kolb, *Am. Phys. Soc. Bull.* 13:1551 (1968)

Two-Dimensional Theta-Pinch Dynamics with Transverse Magnetic Fields, by D. Duchs, *Phys Fluid* 11:2010 (1968)

Two-Photon Continuum Emission from Helium-Like Ne IX, by L. J. Palumbo, R. C. Elton, and R. H. Dixon, *Am. Phys. Soc. Bull.* 13:634 (1968)

Vacuum Ultraviolet Radiation from Plasmas, by R. C. Elton, *J. Quant. Spectros. Radiat. Transfer* 8:393, January 1968

RADIATION EFFECTS

An Annealing Study of Electron-Irradiated Silicon Solar Cells, by R. L. Statler and B. J. Faraday, in *Proc. Symposium on Radiation Effects on Semiconductor Components*, Toulouse, France, March 7-10, 1967, Vol. II, Paper B25, 1968

Basic Concepts of Dosimetry, by W. C. Roesch and F. H. Attix, in *Radiation Dosimetry*, 2nd ed., Eds. F. H. Attix and W. C. Roesch, Academic Press, 1968

Basic γ -Ray Dosimetry, by F. H. Attix, *Health Phys.* 15:49 (1968)

Critique of In-Place Annealing of SM-1A Nuclear Reactor Vessel, by U. Potapovs (NRL), G. W. Knighton, and A. S. Denton (Fort Belvoir, Va.), *Nuclear Eng. & Design* 8:39 (1968)

Defect Clusters in Electron-Irradiated Silicon, by N. D. Wilsey, R. L. Statler, and B. J. Faraday, *IEEE Trans.* NS-15:55, December 1968

The Effects of Coupling Nuclear Radiation with Static Service Stresses on Pressure Vessel Material Behavior, by J. R. Hawthorne and F. J. Loss, *Nuclear Eng. & Design* 8:108 (1968)

Effects of ^3He Irradiation on the Anisotropy-Field Inhomogeneity and Coercive Force in Thin Permalloy Films, by C. M. Williams, *J. Appl. Phys.* 39:4741, September 1968

Excitation Transfer in Radiation-Damaged Organic Solids, by H. B. Rosenstock and J. H. Schulman, in *Localized Excitations in Solids* (Plenum Press, 1968), pp. 330-334

Neutron Radiation Embrittlement of Lacrosse Reactor Pressure Vessel Steel and Weldment: Properties and Directionality Considerations, by C. Z. Serpan, Jr., *Nuclear Eng. & Design* 8:95 (1968)

Notch Ductility Properties of SM-1A Reactor Pressure Vessel Following the In-Place Annealing Operation, by U. Potapovs, J. R. Hawthorne, and C. Z. Serpan, Jr., *Nuclear Appl.* 5:389, December 1968

One-MeV Electron Damage in Silicon Solar Cells, by R. L. Statler, *Intersociety Energy Conversion Engineering Conference Record*, pp. 122-127, 1968

Radiation Embrittlement of 14Ni-5Cr-3Mo Maraging Steel and Companion Weld Metal at <250°F and at Elevated Temperatures, by R. A. Gray, Jr., and J. R. Hawthorne, *Am. Nuclear Soc. Trans.* 11:147, June 1968

Radiation Embrittlement of Pressure Vessels and Procedures for Limiting This Effect in Power Reactors, by L. E. Steele and U. Potapovs (NRL) and C. W. Knighton (Fort Belvoir), *Nuclear Appl.* 4:230, April 1968

Radiation Embrittlement of Reactor Vessel Steels and Suggestions for Its Control, by L. E. Steele and U. Potapovs, *Nuclear Eng. & Design* 8:58 (1968)

Reverse Annealing of Conductivity in Electron Irradiated N-Type Silicon, by Regina V. Tauke and B. J. Faraday, in *Lattice Defects in Semiconductors* (Univ. of Tokyo Press, Tokyo, Japan, 1968), pp. 168-182

Ruby Fluorescence as a Dosimeter for Pulsed, High Energy, Ionizing Radiation, by J. J. Halpin and R. F. Weagel, *Rev. Sci. Instr.* 39:1117, August 1968

Shielding of Solar Cells Against Van Allen Belt Protons, by C. A. Carosella, *J. Spacecraft & Rockets*, 5:878, July 1968

Surface Effects of Radiation, by H. L. Hughes, in *Proc. Symposium on Radiation Effects on Semiconductor Components*, Toulouse, France, March 7-10, 1967, Vol. II, Paper B3, 1968

Test of PM-2A Reactor Vessel, by C. Z. Serpan, Jr., *Nuclear Safety* 9:271, May-June 1968

Test of PM-2A Reactor Vessel, by C. Z. Serpan, Jr., *Nuclear Safety* 9:410, September-October 1968

Thermal Annealing of Proton-Irradiated Silicon Solar Cells, by B. J. Faraday, Regina V. Tauke, and R. L. Statler, in *Proc. Symposium on Radiation Effects on Semiconductor Components*, Toulouse, France, March 7-10, 1967, Vol. II, Paper B24, 1968

CONTRIBUTIONS

- * **Thermal Quenching of Luminescence in Six Thermoluminescent Dosimetry Phosphors**, by S. G. Gorbics, A. E. Nash, and F. H. Attix, *Proc. 2d International Conference on Luminescent Dosimetry*, AEC Document CONF-68090, 1968.
- Thermoluminescent Dosimeters for Personnel Monitoring**, by F. H. Attix and T. L. Johnson, *Proc., Congress on Nuclear Electronics and Radio-protection*, Toulouse, France, March 4-8, Vol. 3, 1968.
- RADIO AND RADAR**
- Acceleration and Velocity Signal Processing for Over-the-Horizon Radar Detection**, by G. K. Jensen, *Anti-Missiles Research Advisory Council Proc.*, Vol. 18, Pt. 1, Meeting of April 24-26, 1968, pp. 1199-1211.
- Comments on a Paper 'A Note on the Millimeter and Submillimeter Wave Dielectric Constant and Loss Tangent Value of Some Common Materials'** by K. H. Brecken and A. P. Sheppard, by L. V. Blake, *Radio Sci.* 3:975, September 1968.
- Contour Pattern Analysis of a Monopulse Radar Cassegrain Antenna**, by D. D. Howard, *Microwave J.* 11:61, December 1968.
- A Crystal Oscillator Satellite Experiment**, by R. L. Easton, *Proc., 22nd Annual Symposium on Frequency Control*, Atlantic City, N.J., April 22-24, 1968, pp. 342-353.
- Design of a Successful System**, by R. Easton, *Telemetry J.* 3:56, April-May 1968.
- * **An Improved Electronic Decoy**, by C. R. Kohler, J. K. Brown, P. F. Lloyd, and T. J. Jesswein, *Proc., Joint ECM Planning Conference*, October 1968, Section 1, p. 7.
- Matrix Fed Circular Array for Continuous Scanning**, *IEEE Proc.*, Special Issue on Electronic Scanning, November 1968, pp. 2016-2027.
- * **A New Model for Sea Clutter**, by J. V. Wright, *IEEE Trans.* AP-16:217, March 1968.
- A New Circuit for Pulse Shape Discrimination**, by D. W. Jones, in *Proc., 11th IEEE Science Scintillation Counter Symposium*, February 28-March 1, 1968, Wash., D.C., *IEEE Trans.* NS-15:491, June 1968.
- The Omega Navigation System**, by J. W. Brogden, *J. Inst. Navigation* 15:115 (1968).
- * **Radar Target Amplitude, Angle, and Doppler Scintillation from Analysis of the Echo Signal Propagating in Space**, by J. H. Dunn and D. D. Howard, *IEEE Trans. Microwave Theory & Tech.* MTT-16:715, September 1968.
- Radio Ray (Radar) Range-Height-Angle Charts**, by L. V. Blake, *Microwave J.* 11:49, October 1968.
- * **Rapid Look-Through Technique**, by G. C. Page, Jr., *Proc., Joint ECM Planning Conference*, October 1968, Section 3, p. 23.
- * **Ray Height Computation for a Continuous Near Atmospheric Refractive-Index Profile**, by L. V. Blake, *Radio Sci.* 3:85, January 1968.
- RC Null Network Requiring Only Two Components of Prescribed Value**, by C. F. White, *IEEE Proc.* 56:1129, June, 1968, Special Issue on Studies of Neural Elements and Systems.
- Scattering of Electromagnetic Waves from a Slightly Rough Surface Moving with Uniform Velocity**, by G. R. Valenzuela, *Radio Sci.* 3:1154, December 1968.
- Scattering of Electromagnetic Waves from a Tilted Slightly Rough Surface**, by G. R. Valenzuela, *Radio Sci.* 3:1057, November 1968.
- Sea Clutter Measurements on Four Frequencies**, by J. C. Daley, *URSI Digest, 1968 Fall Meeting, Boston, Mass., September 10-12, 1968*, p. 23.
- Wideband Ambiguity Function of Pseudo-Random Sequences: An Open Problem**, by D. A. Swick, *IEEE Trans. Info. Theory* IT-14:602, July 1968.
- World's Most Powerful VHF Transmitting Station**, by L. D. Breetz, *Electronics and Aerospace Systems Convention Record*, pp. 247-251, 1968.
- SOLID STATE PHYSICS**
- Anomalous Fundamental Absorption in Germanium Films**, by J. E. Davey and T. Pankey, *Am. Phys. Soc. Bull.* 13:727 (1968).
- Carbon Tetrachloride: Plastic Properties**, by L. C. Towle, *Science* 159:629, February 9, 1968.
- Conversion of F₂⁻ Centers and Destruction of R Centers in LiF with R Light**, by K. L. Vander Lugt (NRL) and Y. W. Kim (Wayne State Univ.), *Phys. Rev.* 171:1096 (1968).
- The Effect of Iron on the Ultraviolet Absorption of High Purity Soda-Silicate Glass**, by G. H. Sigel and R. J. Ginther, *J. Glass Tech.* 9:66, June 3, 1968.
- Effects of Electron-Optical-Phonon Interaction in the Combined Resonance Spectra of InSb**, by B. D. McCombe and R. Kaplan, *Phys. Rev. Ltrs.* 21:756, September 9, 1968.
- Effects of Surface Force-Constant Changes on the Atomic Mean Square Displacements in Face-Centered Cubic Crystals with a Free Surface**, by R. F. Wallis, B. C. Clark, and R. Herman, *Phys. Rev.* 167:652, March 15, 1968.
- Ejection Patterns in Low Energy Sputtering of GaAs and GaP Crystals**, by J. Comas (NRL) and C. B. Cooper (Univ. of Del.), *J. Appl. Phys.* 39:5736, November 1968.
- Electrical Conductivity of Potassium Chloride**, by R. G. Fuller, M. H. Reilly, C. L. Marquardt, and J. C. Wells, *Phys. Rev. Ltrs.* 20:662, March 25, 1968.

- Energy Transfer in Organic Solids, by H. B. Rosenstock, *J. Chem. Phys.* 48:532, January 1, 1968
- Epitaxial GaAs Films Deposited by Vacuum Evaporation, by J. E. Davey and T. Pankey, *J. Appl. Phys.* 39:1941, March 1968
- ESR Studies of Lithium Borate Glasses and Compounds Irradiated at 77K: Evidence for a New Interpretation of the Trapped-Hole Center Associated with Boron, by D. L. Griscom (NRL) and P. C. Taylor, D. A. Ware, and P. J. Bray (Brown Univ.), *J. Chem. Phys.* 58:5158 (1968)
- Evidence for Zero-Point Spin Deviation in K_2MnF_6 , by M. Rubinstein and V. J. Folen, *Phys. Lett.* 28A:108, November 4, 1968
- Examination of the Thermal Variation of the Mean Square Atomic Displacements in Zinc and Evaluation of the Associated Debye Temperatures, by E. F. Skelton (NRL) and J. L. Katz (Rensselaer), *Phys. Rev.* 171:801, July 15, 1968
- F_2 -Center in Additively Colored KCl, by I. Schneider, *Phys. Lett.* 20:790, April 8, 1968
- F-Center in Ammonium Halides, by F. W. Patten, *Solid State Comm.* 6:65 (1968)
- Ferromagnetic Resonance in the Highly Anisotropic Ferromagnet Gallium Iron Oxide, by J. Dweck, *Phys. Rev.* 168:602, April 10, 1968
- Hall Effect, Magnetoresistance, Resistivity and Size Effect in Ni, by A. C. Ehrlich and D. Rivier, *J. Phys. Chem. Solids* 29:1293 (1968)
- Hyperfine Field Spectra of Binary Fe-Co Alloys: Nuclear Magnetic Resonance of ^{57}Fe and ^{59}Co , by M. Rubinstein, *Phys. Rev.* 172:277, August 10, 1968
- Implantation and Detection of Low Energy Argon Ions in Silicon Single Crystals, by J. Comas and C. A. Carosella, *Electrochem. Soc. J.* 115:974, September 1968
- Impurity Effects on F to M Conversion in NaF, by R. A. Andrews and Y. W. Kim, *J. Phys. & Chem. Solids* 29:1909, October 1968
- Impurity-State-Optical-Phonon Coupling in a Magnetic Field in InSb, by R. Kaplan and R. F. Wallis, *Phys. Rev. Lett.* 20:1499, June 24, 1968
- *Magnetic Properties of K_2CoF_6 , a Highly Anisotropic Two-Dimensional Magnetic Structure, by V. J. Folen, J. J. Krebs, and M. Rubinstein, *Solid-State Comm.* 6:865, December 1968
- Magnetoacoustic Excitation of Radio-Frequency Resonances and Echoes in Magnetic Materials, by M. Rubinstein and G. H. Stauss, *J. Appl. Phys.* 39:81, January 1968
- Magneto-Oscillatory Excitation Spectra of Shallow Acceptor Impurities in InSb and Ge, by R. Kaplan, *Phys. Rev. Lett.* 20:329, February 12, 1968
- Measurement of the Conduction Band g-Value Anisotropy in InSb, by B. D. AcCombe, *Solid State Comm.* 6:533, August 1968
- Nuclear Magnetic Resonance and Magnetization Studies of $CdCr_2Se_4$, by C. H. Stauss and M. Rubinstein (NRL); J. Feinleib, K. Dwight, and N. Menyuk (Lincoln Lab. MIT); and A. Wold (Brown University), *J. Appl. Phys.* 39:667, February 1, 1968
- Nuclear Magnetic Resonance Relaxation of Molecules Adsorbed on Surfaces, by H. A. Resing, *Advances in Molec. Relaxation Processes* 1:109 (1968)
- NMR Subspectral Analysis Applied to Polyfluorobenzenes $C_6H_2F_4$ - III-Pentafluorobenzene, by W. B. Mcnz (NRL), E. Lustig (FDA), and P. Diehl and M. Bodmer (Univ. of Basel), *J. Chem. Phys.* 49:4550, November 15, 1968
- Optical Properties—Dynamical Processes in Solid State Optics, by H. B. Rosenstock, *Science* 160:981, May 31, 1968
- Paramagnetic NH_2Cl and NH_2Br Color Centers in Irradiated Ammonium Halide Single Crystals, by F. W. Patten, *Phys. Rev.* 175:1216, November 15, 1968
- Paramagnetic Resonance of I_2 -Centers in PHJ Single Crystals, by C. L. Marquardt, *J. Chem. Phys.* 48:994, February 1, 1968
- Phase Fields and Thermal Expansion of Oxides of Copper, by A. L. Pranatis, *Am. Ceramic Soc. J.* 51:182, March 1968
- Polymorphism in Vacuum-Deposited GaP Films, by J. E. Davey and T. Pankey, *Appl. Phys. Lett.* 12:38, January 15, 1968
- Reflectivity Measurements of Coupled Collective Cyclotron Excitation-Longitudinal Optical Phonon Modes in Polar Semiconductors, by F. D. Fulk, Bertha W. Hennis, and J. R. Stevenson (NRL) and S. Iwasa (MIT), *Solid State Comm.* 6:721 (1968)
- Relativistic and Spin Effects for Crystal Electrons in Uniform Electric and Magnetic Fields, by S. Teitler, *Solid State Comm.* 6:485, July 1968
- A Study of Surface Diffusion by NMR: Sulfur Hexafluoride Adsorbed on Synthetic Faujasite, by J. K. Thompson and H. A. Resing, *J. Colloid and Interface Science* 26:279, March 1968
- The Valence Bond Approximation in Crystals—Application to an Analysis of the Ultraviolet Spectrum in Quartz, by A. R. Ruffa, *Phys. Stat. Solidi* 29:605, October 1, 1968
- Vibrations of Disordered Solids, by H. B. Rosenstock and R. E. McGill, *Phys. Rev.* 176:1004 (1968)

CONTRIBUTIONS

SPACE SCIENCES

- Analysis of the Solar Spectrum in the Spectral Range 33-110A**, by K. G. Widing and G. D. Sandlin, *Astron. J.* 73:S83, June 1968
- Analysis of the Solar Spectrum in the Spectrum Range 33-110A**, by K. G. Widing and G. D. Sandlin, *Astrophys. J.* 152:545, May 1968
- The Army's Role in Space**, by T. C. Winter, Jr., *Military Review* 48:52, July 1968
- The BN Andromeda Complex: An Example of Star Formation in a Low Mass Cloud**, by Hunter, Jr., H. James and A. F. Aveni, *The Astron. J.* 73:86 (1968)
- The Character and Origin of Coronal Streamers as Observed from Rockets**, by G. D. Sandlin, M. J. Koomen and R. Tousey, *Astron. J.* 73:S75, June 1968
- Comparison of Elemental and Isotopic Methods of Deducing Cosmic-Ray Confinement Time**, by M. M. Shapiro and R. Silberberg, *Amer. Phys. Soc. Bull.* 13:694 (1968)
- Considerations Affecting the Estimation of Cosmic-Ray Age**, by M. M. Shapiro and R. Silberberg, *Can. J. Phys.* 46:S561, May 15, 1968
- Cosmic Ray Abundances Measured at Near-Equatorial Latitudes above the Atmosphere**, by F. W. O'Dell, M. M. Shapiro, R. Silberberg, B. Stiller, C. H. Tsao (NRL), N. Durgaprasad, C. E. Fichtel, D. E. Guss, and D. V. Reames (NASA-Goddard), *Am. Phys. Soc. Bull.* 13: 694 (1968)
- Cosmic-Ray Nuclei**, by M. M. Shapiro, *Astronaut. & Aeronaut.* 6:6, July 1968
- Cosmic X-Rays**, by H. Friedman, *Nature* 220:862, November 30, 1968
- Detection of Lyman- β and Helium Resonance Radiation in the Night Sky**, by J. M. Young, C. R. Carruthers, J. C. Holmes, C. Y. Johnson, and N. P. Patterson, *Science* 160:990, May 31, 1968
- Determination of the Astronomical Unit from Hydrogen-Line Radial-Velocity Measurements**, by S. H. Knowles, *Astron. J.* 73:S102, June 1968
- Discrete X-Ray Sources**, by H. Friedman, in *Stars and Stellar Systems, Vol. VII: Nebulae and Interstellar Matter*, edited by Barbara M. Middlehurst and L. H. Aller (The University of Chicago, 1968), pp. 685-706
- The Distribution of Lyman- α Radiation as Observed in the Sky from Satellite OGO-III, OGO-IV, and OSO-IV**, by P. Mange, *AGU Trans.* 49:254 (1968)
- The Effect of Mass on Frequency**, by D. Sadeh, S. Knowles, and B. Au, *Science* 161:567, August 9, 1968
- Extreme Ultraviolet Hellograms and the Sun's Corona**, by J. D. Purcell, R. Tousey, and M. J. Koomen, in *Space Research VIII* (Amsterdam:North-Holland Publishing Co., 1968), pp. 450-457
- The Far Ultraviolet Spectral Intensity of a B3V Star**, by R. C. Henry (NRL) and C. B. Opal, H. W. Moos, W. G. Fastie, and M. Bottema (Johns Hopkins Univ.), *Astrophys. J.* 153:L179, September 1968
- *Far-Ultraviolet Spectroscopy and Photometry of Some Early-Type Stars**, by G. R. Carruthers, *Astrophys. J.* 151:269, January 1968
- Flux Densities of Radio Sources at 9.55-mm Wavelength**, by R. W. Hobbs, H. H. Corbett, and N. J. Santini, *Astrophys. J.* 152:43, April 1968
- High-Energy Galactic Cosmic-Ray Composition Measured in Gemini XI**, by F. W. O'Dell, M. M. Shapiro, R. Silberberg, B. Stiller, C. H. Tsao (NRL), and N. Durgaprasad, C. E. Fichtel, D. E. Guss, and D. V. Reames (NASA, Greenbelt, Md.), *Can. J. Phys.* 46:S569, May 15, 1968
- Hydrogen-to-Helium Ratio in the Solar Photosphere**, by C. A. Rcuse, Final Report on NSF Grant GP-7788, University of California (Berkeley), *Space Science Lab. Series 9, Issue 36* (1968)
- IGY, IQSY and the Future of International Cooperation in Solar-Terrestrial Research**, by H. Friedman, *Astronaut. & Aeronaut.* 16:23, January 1968
- Intensity Measurements of Chromospheric Fine Structures in Lyman- α** , by W. A. Sloan, *Solar Physics* 5:329 (1968)
- Intensity Profiles of the 6300- \AA and 5577- \AA OI Lines in the Night Airglow**, by I. S. Gullidge, D. M. Packer, S. G. Tilford, and J. T. Vanderslice, *J. Geophys. Res.* 73: 5535, September 1, 1968
- Interpretation of Satellite Lyman- α Airglow Measurements**, by R. R. Meier, *AGU Trans.* 49:254 (1968)
- Ion Composition Measurements in the Polar Region from the Explorer Satellite**, by J. H. Hoffman, *AGU Trans.* 49:253 (1968)
- Ionic Species in the Sun as Identified from XUV and X-Ray Lines**, by R. Tousey and K. G. Widing, *Astron. J.* 73: S80, June 1968
- Linear Polarization Observations at 3.6-cm Wavelength**, by J. P. Hollinger and R. W. Hobbs, *Astrophys. J.* 151:771, February 1968
- Linear Polarization of Radio Sources at 2.07-Centimeter Wavelength**, by R. W. Hobbs and J. P. Hollinger, *Astrophys. J.* 154:423, November 1968
- The Lunar Crescent and Earthshine Observed at 2° Solar Elongation**, by M. J. Koomen, R. Tousey, and R. T. Seal, Jr., in *Moon and Planets II* (Amsterdam:North-Holland Publishing Co., 1968), pp. 187-195

- Lunar Radius from Radar Measurements**, by A. Shapiro, E. A. Uliana, B. S. Yaplee, and S. H. Knowles, in *Space Research XIX, Moon and Planets II* (Amsterdam: North-Holland Publishing Co., 1968), pp. 34-46
- Measurements of Mars at 1.55-cm and 0.95-cm Wavelengths**, by R. W. Hobbs, T. P. McCullough, and J. A. Waak, *Icarus* 9:360, September 1968
- Metal Abundance in A Stars**, by R. C. Henry, *Astrophys. J.* 152:L87, May 1968
- New X-Ray Spectra of Sco XR-1, Cyg XR-1, and Cyg XR-2**, by J. F. Meekins, G. Fritz, R. C. Henry, E. T. Byram, and H. Friedman, *Astron. J.* 73:S106, June 1968
- A Note on the Seasonal Variation of the Ionospheric Electron Content and Slab Thickness over Washington, D.C.**, by J. M. Goodman, *Planetary & Space Sci.* 16:1073 (1968)
- Observations of Aurora in the Far UV from OGO-IV**, by T. A. Chubb and G. T. Hicks, *AGU Trans.* 49:248 (1968)
- Observations of Solar Chromospheric Fine Structures in the Light of Lyman- α** , by W. A. Sloan, *Solar Phys.* 4:196 (1968)
- On Some Aspects of XUV Spectroheliograms**, by R. Tousey, G. D. Sandlin, and J. D. Purcell, in *Structure and Development of Solar Active Regions*, edited by Kiepenheuer (International Astronomical Union, 1968), pp. 411-419
- 1-8A X-ray Spectra of the Active Sun from OSO-IV**, by J. F. Meekins, T. A. Chubb, R. W. Kreplin, and H. Friedman, *Astron. J.* 73:S106 (1968)
- Photographs of Coronal Streamers from a Rocket on May 9, 1967**, by R. Tousey, G. D. Sandlin, and M. J. Koomen, in *Structure and Development of Solar Active Regions*, edited by Kiepenheuer (International Astronomical Union, 1968), pp. 385-388
- Photography of the Night Airglow Layer from the Gemini Series of Manned Spacecraft**, by M. J. Koomen, R. T. Seal, Jr., and R. Tousey (NRL), and J. Lintott (NASA), *Astron. J.* 73:S103, June 1968
- Photography of the Night Airglow from the Gemini Series of Manned Spacecraft**, by M. J. Koomen and R. T. Seal, Jr. (NRL) and J. Lintott (NASA), in *Space Research VIII* (Amsterdam: North-Holland Publishing Co., 1968), pp. 683-691
- Physics of the Earth in Space, A Program of Research: 1968-1975**, Report of a Study by the NAS-NRC Space Science Board, August 1968, Chaired by H. Friedman, Assisted by F. S. Johnson, National Academy of Sciences, October 1968
- Polarization of Strong Radio Sources at 9.55-mm Wavelength**, by R. W. Hobbs, *Astrophys. J.* 153:1001, September 1968
- Polarized Brightness Distribution Over Cassiopeia A, the Crab Nebula, and Cygnus A at 1.55-cm Wavelength**, by C. H. Mayer and J. P. Hollinger, *Astrophys. J.* 151:53, January 1968
- Possible Detection of a Dense Hot Intergalactic Medium**, by G. Fritz, J. F. Meekins, R. C. Henry, E. T. Byram, and H. Friedman, *Astron. J.* 73:Suppl. No. 1360, June 1968
- Possible Detection of a Dense Intergalactic Plasma**, by R. C. Henry, G. Fritz, J. F. Meekins, H. Friedman, and E. T. Byram, *Astrophys. J.* 153:L11, July 1968
- Preliminary Observations of the Far-Infrared Night-Sky Background Radiation**, by K. Shivanandan (NRL), J. R. Houck, and M. O. Harwit (Cornell-Sydney Univ. Astronomy Center), *Phys. Rev. Lett.* 21:1460, November 1, 1968
- A Radio Determination of the Sun's Distance**, by S. H. Knowles, *Sky and Telescope* 36:81, August 1968
- Reply to 'X-rays from Source 3C 273' by Edw. Argyle**, by H. Friedman, E. T. Byram, and T. A. Chubb, *Science* 159:747, February 16, 1968
- Rocket Observations of Bright Celestial Infrared Sources in Ursa Major**, by P. D. Feldman, D. P. McNutt, and K. Shivanandan, *Astrophys. J.* 154:131, December 1968
- Search for an Effect of Mass on Frequency During a Close Approach of Pulsar CP 0950 to the Sun**, by D. Sadeh, J. P. Hollinger, S. H. Knowles, and A. B. Youmans, *Science* 162:897, November 22, 1968
- Search for a Frequency Shift of the 21-Centimeter Line from Taurus A Near Occultation by the Sun**, by A. Sadeh, S. H. Knowles, and B. S. Yaplee, *Science* 159:307, January 19, 1968
- A Search for X-Rays from Helium and Air Discharges at Atmospheric Pressure**, by R. C. Noggle, E. P. Krider, and J. R. Wayland, *J. Appl. Phys.* 39:4746, September 1968
- Soft X-Rays from Scorpius XR-1**, by G. Fritz, J. F. Meekins, R. C. Henry, E. T. Byram, and H. Friedman, *Astrophys. J.* 153:L199, September 1968
- The Solar XUV Spectrum**, by H. Friedman, *Astron. J.* 73:S61 (1968)
- Some Measurements of Electron Content Enhancements Associated with Magnetic Storms**, by J. M. Goodman, *Planetary & Space Sci.* 16:951 (1968)
- Surveys of X-Ray Sources**, by H. Friedman, in *Highlights of Astronomy* (I.A.U., 1968), pp. 180-183
- Theoretical and Practical Limitations of Solar Magnetic Field Measurements**, by G. Brueckner, *Astron. J.* 73:S56, June 1968
- Variability of the Linear Polarization of 3C 120 and 3C 279**, by R. W. Hobbs, J. P. Hollinger, and G. E. Marandino, *Astrophys. J.* 154:L49, November 1968

CONTRIBUTIONS

X-Ray Astronomy: New Window to Space, by H. Friedman. *Britannica Yearbook of Science and the Future*. pp. 196-209 (1968)

X-Ray Line and Continuum Spectra of Solar Flares from 0.5 to 8.5 Angstroms, by J. F. Meekins, R. W. Kreplin, T. A. Chubb, and H. Friedman. *Science* 162:891, November 22, 1968

X-Rays from Source 3C 273, by H. Friedman, E. T. Byram and T. A. Chubb. *Science* 159:747 (1968)

THEORETICAL PHYSICS

Approximate Solutions for S-Wave Scattering by an Exponential Potential, by I. Manning. *Am. Phys. Soc. Bull.* 13:106 (1968)

Collapse of Thick Hollow Cylinders by External Pressure, by T. Y. Thomas. *J. Math. & Mech.* 17:987, April 1968

A Formal Numerical Solution of the Equation of Radiative Transfer, by C. A. Rouse. *J. Quant. Spectros. Radiat. Transfer* 8:1167 (1968)

A New Relativistic Rigid Body Concept Involving Simply Transitive Subgroups $G_4(q)$ of the Poincaré Group, by E. J. Schremp. *Am. Phys. Soc. Bull.* 13:591 (1968)

The Pauli Principle in the Center-of-Mass System, by J. B. Aviles, Jr.. *Ann. Phys.* 42:403, May 1967

Quasi-Inertia and Gravitation, by S. Teitler. *Nuovo Cim.* 53B:329, February 11, 1968

The Screened Coulomb Electronic Partition Function, by C. A. Rouse, in *International Conference on Phenomena in Ionized Gases*, 8th, Vienna, 1967, p. 267 (1968)

Screening Effects in the Quantum Theory of Radiation, by C. A. Rouse. *Am. Phys. Soc. Bull.* 13:574 (1968)

Separation of the Center-of-Mass in Independent Particle Systems, by J. B. Aviles. *Ann. Phys.* 50:393, December 1968

Singular Variations Near the Contact Discontinuity in the Theory of Interplanetary Blast Waves, by T. S. Lee and W. W. Balwanz. *Solar Phys.* 4:240, June 1968

Use of Iteration Procedures to Generate Scattering Approximations, by I. Manning. *Phys. Rev.* 168:1875, April 25, 1968

OTHER

The Navy's Response to the Forrestal Disaster and Future Carrier Survivability from Fire, by H. B. Peterson and R. L. Tuve. *Fire J.* 62:46, November 1968

Who Should Support Scholarly Research, by H. B. Rosenstock. *Bull. Atomic Sci.* 24:60, January 1968

FORMAL NRL REPORTS

ACOUSTICS

6673 "Power Spectrum Estimates of Sampled Pseudo-Random Sequences," by C. McCoy, Jr.

6682 "Some Investigations of Sound-Scattering Layers Near Key West, Florida," by D. F. Wilson, L. C. Ricalzone, and R. C. Beckett

6685 "Tables of Radial Spheroidal Wave Functions. Vol. 1-Prolate Radial Functions of the First and Second Type," by S. Hanish, R. V. Baier, W. H. Buckler, and Berthel K. Carmichael

6686 "Tables of Radial Spheroidal Wave Functions. Vol. 2-Oblate Radial Functions of the First and Second Type and Their First Derivatives," by S. Hanish, R. V. Baier, W. H. Buckler, and Berthel K. Carmichael

6728 "A PDP-8 FORTRAN Program for Near-Field Array Testing," by G. A. Sabin

6734 "Application of the Near-Field Technique to Sonar Evaluation," by W. J. Trott and I. B. Groves

6758 "Tables of Radial Spheroidal Wave Functions. Vol. 4-Prolate Radial Functions of the 1st and 2nd Type and Their 1st Derivatives for $m=0$; $\xi=1.01, 1.1(0.1)1.9, 2(1)10$," by S. Hanish, R. V. Baier, W. H. Buckler, and Berthel K. Carmichael

6759 "Tables of Radial Spheroidal Wave Functions. Vol. 5-Prolate Radial Functions of the 1st and 2nd Type and Their 1st Derivatives for $m=1$; $\xi=1.01, 1.1(0.1)1.9, 2(1)10$," by S. Hanish, R. V. Baier, W. H. Buckler, and Berthel K. Carmichael

6760 "Tables of Radial Spheroidal Wave Functions. Vol. 6-Prolate Radial Functions of the 1st and 2nd Type and Their 1st Derivatives for $m=2$; $\xi=1.01, 1.1(0.1)1.9, 2(1)10$," by S. Hanish, R. V. Baier, W. H. Buckler, and Berthel K. Carmichael

6770 "Theoretical Computations for a Wavelength Square Array of 144 Radiators Including Effects of Various Arrangements of 'Tuning' the Electrical Terminals," by R. V. Baier

*6791 "The Experimental Examination, by Means of Pulses, of Circumferential Waves on Aluminum Cylinders in Water," by W. G. Neubauer

6817 "Performance Characteristics of a Parabolic and a Conical Underwater Acoustic Reflector," by J. B. Gregory

6822 "A New NRL Acoustic Research Tank Facility," by J. Chervenak

6852 "Systematic Errors in Ultrasonic Propagation Parameter Measurements. Part 4-- Effect of Finite Thickness Elastic Solid Tubes Enclosing the Liquid Cylinder of Interest," by V. A. Del Grosso

6856 "Tables of Eigenvalues of the Wave Equation in Prolate Spheroidal Coordinates," by S. Hanish and B. King

APPLICATIONS RESEARCH

- 6643 "Kelvin Wake Optical Filter Synthesis," by G. L. Hall
- 6646 "A Comparison of Three Types of Manual Controls on a Third-Order Tracking Task," by P. N. Ziegler and R. Chernikoff
- 6660 "A Subsatellite Area-of-View Circuit," by R. J. Orsino and H. G. Talmadge, Jr.
- 6694 "Satellite Prediction and Display. A Review of SPAD," by H. G. Talmadge, Jr.
- 6746 "A Study of the Acquisition and Tracking Problems of Optical Systems for Space Object Identification," by R. J. Orsino
- 6752 "High Density Satellite Surveillance," by Space Application Branch, Applications Research Division
- *6773 "Low-Frequency EMP Calculations," by J. E. Rogerson and A. D. Anderson
- 6781 "The TIMATION I Satellite," by Space Applications Branch, Space Applications Research Division
- 6785 "A Digital Computer System for Signal Analysis," by G. V. Olds
- 6801 "Theory on Afterburning in a Low-Altitude Rocket Exhaust Plume," by R. Shao-Lin Lee and W. W. Balwanz.
- 6813 "Calculation of the Retarded Electric Field for an Arbitrary Charge and Current Distribution," by R. J. Radin

ATMOSPHERE AND ASTROPHYSICS

- 6615 "Measurement of Spectral Radiance of the Horizon Sky," by G. L. Knestrick and J. A. Curcio
- 6652 "Atmospheric Electric Characteristics of Regions," by J. H. Kraakevik and W. A. Hoppel
- 6692 "Measurements of the Solar Brightness Distribution at 14.50 GHz," by J. P. Hollinger
- 6725 "Measurement of Atmospheric Dewpoint From Aircraft," by R. E. Ruskin
- 6766 "Attenuation of Microwave Radiation for Paths Through the Atmosphere," by R. A. LeFandre
- 6827 "On the Scaling of Dipole Radiation in the Ionosphere," by M. J. Smith

BIOLOGICAL SYSTEMS

- 6691 "Mechanisms Assisting or Impeding Adhesion in Biological Systems," by R. E. Baier and F. G. Shafrin
- 6699 "Biophysical Studies of Microbial Cell Walls. Part 1—The Preparation of Isolated Cell Walls," by R. A. Neihof and W. H. Echols
- 6795 "Biophysical Studies of Microbial Cell Walls. Part 2—Electrophoresis: Apparatus and Exploratory Experiments," by R. A. Neihof and W. H. Echols

CHEMISTRY (Also see Mathematics and Information Sciences; Biological Systems; and Metallurgy)

- 6613 "The Plate Materials of the Lead-Acid Cell. Part 3—Anodic Oxidation of Tetragonal PbO," by Jeanne Burbank
- 6622 "On the Activity of Platinum Catalysts in Solution. Part 1—Effects of Thermal Treatment and Chemical Etching on the Pt-O/Hydrogen Specific Reaction Rate," by T. B. Warner, S. Schuldiner, and B. J. Piersma
- 6626 "Identification and Characterization of Electrochemical Reaction Products by X-Ray Diffraction," by Jeanne Burbank
- 6627 "On the Activity of Platinum Catalysts in Solution. Part 2—Kinetics of the Pt-O Reaction with Hydrogen and of Pt-H Deposition Using a Double-Pulse Technique," by T. B. Warner and S. Schuldiner
- 6636 "The Sealab II Trace-Contaminant Profile," by R. A. Saunders and R. H. Gammon
- 6639 "Electron Impact Studies of Volatile Inorganic Compounds," by F. E. Saalfeld and M. V. McDowell
- 6642 "The Interaction of Otto Fuel with the Atmosphere Control Systems Used in Nuclear Submarines," by J. K. Musick and J. E. Johnson
- 6644 "The Wettability of Ethyl- and Vinyltriethoxysilane Films Formed at Organic-Liquid/Silica Interfaces," by W. D. Bascom
- 6647 "Feasibility of Microscopy for Investigating the Silver Oxide Electrode," by C. F. Wales and A. C. Simon
- 6653 "Identification of Free Radicals in the Photodegradation of Polystyrene and Its Homologs," by R. F. Cozzens and R. B. Fox
- 6656 "Studies of the Naval Facilities Engineering Command Protective Shelter. II. Summer Trials," prepared cooperatively by Naval Research Laboratory (NRL authors, H. F. Bogardus and E. A. Ramskill), Naval Facilities Engineering Command, Naval Medical Research Institute, and Army Medical Research and Nutrition Laboratory
- 6658 "Chlorophenylalkyl-Substituted Carboxylic Acids and Silanes Designed as Adhesion Promoters," by J. G. O'Rear, P. J. Sniegoski, and F. L. James
- 6659 "Oxidation of Hydrogen on a Passive Platinum Electrode," by S. Schuldiner
- 6665 "The Solubility of Air in Otto Fuel II," by E. T. Johnson, D. D. Williams, and R. R. Miller
- 6667 "Neopentyl Polyol Esters for Jet Engine Lubricants—Effect of Tricresyl Phosphate on Thermal Stability and Corrosivity," by R. L. Cottingham and H. Ravner
- 6669 "Factors in the Coalescence of Water in Fuel," by R. N. Hazlett
- 6674 "Thermal Stability of Ethylenedinitrotetraacetic Acid and Its Salts. Part 1—A Literature Survey," by D. I. Venezky

CONTRIBUTIONS

- 6690 "Filament-Winding Plastics Part 5—Epoxy-Amine Reactions and the Practical Use of High-Strength Plastics," by J. R. Griffith and Mary E. McGraw
- 6691 "Mechanisms Assisting or Impeding Adhesion in Biological Systems," by R. E. Baier, Elaine G. Shafrin, and W. A. Zisman
- 6695 "Effects of Constant-Current Reversals During Charge of the Silver Oxide Electrode," by C. P. Wales
- 6701 "Crystallographic Changes During Oxidation (Charging) of the Silver Electrode. Part 1—Initial Oxidation of an Industrial Sintered Plaque," by C. P. Wales and A. C. Simon
- 6703 "Passivation of Anodic Reactions," by S. Schuldiner
- 6705 "Effect of Adsorbed Water on Wetting Properties of Borosilicate Glass, Quartz, and Sapphire," by Marianne K. Bennett and W. A. Zisman
- 6707 "Crystallographic Changes During Oxidation (Charging) of the Silver Electrode. Part 2—Oxidation Following Five Charge-Discharge Cycles at a Low Rate," by C. P. Wales and A. C. Simon
- 6708 "Halogenated Hydrocarbons in the Atmospheres of Submarines in Squadron FIFTEEN," by F. W. Williams and J. E. Johnson
- 6716 "The Relation of Initial Spreading Pressure of Polar Compounds on Water to Interfacial Tension, Work of Adhesion, and Solubility," by C. O. Timmons and W. A. Zisman
- 6718 "Anodic Oxidation of Hydrogen on Iron and Platinum in Sodium Hydroxide Solution," by S. Schuldiner and C. M. Shepherd
- 6722 "Sixth Annual Progress Report. The Present Status of Chemical Research in Atmosphere Purification and Control on Nuclear-Powered Submarines," edited by R. R. Miller and V. R. Piatt
- 6723 "Microporosity in Lead-Antimony Grid Alloys," by A. C. Simon
- 6724 "The Growth of Oxide Films in High-Temperature Aqueous Environment. Part 1—Growth Characteristics of Iron Oxide Films Generated in Dilute Lithium Hydroxide Solutions at 300°C," by J. B. Moore, Jr., and R. L. Jones
- 6727 "Effect of Adsorbed Water on the Critical Surface Tension of Wetting on Metal Surfaces," by Marianne K. Bennett and W. A. Zisman
- 6730 "A Preservative-Lubricant for Small Arms," by H. R. Baker, R. N. Bolster, and V. G. FitzSimmons
- 6735 "Pressure Effects on the Friction Coefficients of Thin-Film Solid Lubricants," by R. C. Bowers and W. A. Zisman
- 6737 "Effects of Oxidizable Anion Adsorption on the Anodic Behavior of Platinum," by S. Schuldiner
- 6741 "Wear and Friction Studies of Neopentyl Polyol Ester Lubricants," by R. C. Bowers and J. M. Hall
- 6747 "Thermal Stability of Ethylenedinitrilotetraacetic Acid and Its Salts. Part 2—Rate of Decomposition in Aqueous Solution Determined by NMR Techniques," by D. L. Venezky and W. B. Moniz
- 6748 "Potentiostatic Current-Potential Measurements on Iron and Platinum Electrodes in High-Purity Closed Alkaline Systems," by C. M. Shepherd and S. Schuldiner
- 6750 "Determination of the Ester Composition of Neopentyl Polyol Ester Lubricants," by P. J. Sniegoski
- 6754 "Initial Fungus Attack on Tropical Woods in Panamanian Estuarine Waters," by D. D. Ritchie
- 6755 "Wettability and MAIR Infrared Spectroscopy of Solvent-Cast Thin Films of Polyamides and Polypeptides," by R. E. Baier and W. A. Zisman
- 6763 "Effect of Solubilized Methanol on Micelle Size in a Nonpolar Solvent," by A. J. Fryar and S. Kaufman
- 6768 "The Plate Materials of the Lead-Acid Cell. Part 4—Anodic Oxidation of Three Representative Oxides," by Jeanne Burbank
- 6775 "Nondestructive Testing for Void Content in Glass-Filament-Wound Composites," by B. E. Walker, Jr., C. T. Ewing, and R. R. Miller
- 6786 "On the Porosity of Protective Films on Mild Steel," by T. A. Kovacina
- 6788 "Diffusion Limited, Liquid Phase Oxidation of n-Dodecane at 200°C," by B. D. Boss and R. N. Hazlett
- 6818 "The Wettability of Fluoro- and Chloro-Carbon Trialkoxysilane Films Adsorbed on Glass and Metal Surfaces," by W. D. Bascom

COMMUNICATIONS SCIENCES (Also see Radar and Applications Research)

- 6663 "Theoretical VLF Multimode Propagation Predictions," by C. B. Brookes, Jr., J. H. McCabe, and F. J. Rhoads
- 6677 "Phase-Shift Enhancement by Mode-Suppression Techniques," by M. L. Reuss, Jr.
- 6696 "A Matrix-Fed Circular Array for Continuous Scanning," by B. Sheleg
- *6712 "Impedance of LOFTI IIA Very-Low-Frequency Antennas in the Ionosphere," by C. E. Young
- 6749 "NRL Terrain Clutter Study—Phase II," by J. C. Daley, W. T. Davis, J. R. Duncan, and M. B. Laing
- 6751 "A Semiautomatic Jam-Accept (SAJAC) Decoder for Mode 4 of the IFF Mark XII," by W. B. Bishop
- 6764 "The Waveguide Tunnel-Diode Amplifier. Design Considerations," by J. J. Ayoub, Jr.
- 6860 "A 2 MHz to 30 MHz Broadband Solid State Power Amplifier for Use in a Shipboard Radio Transmitter," by D. A. Venn and M. R. Webb

COMPUTER SCIENCE AND TECHNOLOGY (See Mathematics and Information Sciences)

CRYOGENICS (Also see Energy Conversion)

- 6711 "The Production of Temperatures Below 1°K by the Adiabatic Demagnetization of 50% Ce(PO₃)₂-Ba(PO₃)₂ Glass," by F. L. Althouse

ENERGY CONVERSION

- 6618 "Torque on a Superconducting Toroid in a Uniform Field," by B. J. Wilson, E. E. King, and J. R. Miller
- 6714 "A DC-to-DC Converter with Constant Output Voltage," by J. M. Marzolf
- 6715 "Characteristics of an Improved Inert-Cathode/Magnesium-Anode Sea-Water Battery," by B. J. Wilson
- 6726 "Superconducting Lead Pressure Contacts," by E. E. King and P. I. Peterson
- 6769 "Seawater Battery with Converter-Regulator as a Power Source for the AN/SSQ-38 Sonobuoy," by J. M. Marzolf and B. J. Wilson

FRACTURE MECHANICS (Also see Metallurgy)

- 6635 "Environmentally Assisted Crack Growth in Glass," by G. M. Sinclair and S. P. Withrow
- 6654 "Effect of Side Grooves and Fatigue Crack Length on Plane-Strain Fracture Toughness," by C. N. Freed
- 6675 "Theoretical Thermodynamic Properties of Gases at High Temperatures and Densities with Numerical Results for Hydrogen," by J. R. Baker, W. H. Geatches, and H. F. Swift

LASER PHYSICS AND TECHNOLOGY (Also see Radar)

- 6771 "Nitrogen Laser Power Density and Some Design Considerations," by A. W. Ali and Nancy V. Alberico

MATHEMATICS AND INFORMATION SCIENCES (Also see Radar)

- 6632 "A Computer Method for the Automatic Reduction of Spectroscopic Data," by E. F. Ditzel and L. E. Giddings, Jr.
- 6655 "A Computer Program for the Quantitative Interpretation of Mass Spectrographic Photoplates," by P. P. Bey and J. G. Allard
- 6664 "NELIAC-N—The NAREC Version of the NELIAC Programming Language," by J. W. Kallander
- 6689 "A Continuous Inventory Problem," by H. Hauptman and A. Ziffer
- 6697 "The Tangent Formula Program for the X-Ray Analysis of Noncentrosymmetric Crystals," by S. A. Brenner and P. H. Gum
- 6706 "A Particular Class of Penti-Hexagonal Polyhedra," by G. Chayt and H. Hauptman
- 6710 "FORTRAN Programs for First Order Calculation of Properties of Beam Transport Systems," by P. Shapiro
- 6733 "A Table of Central-Force Geometrical Coefficients Associated with Talmi Integrals. For Use in Calculating Nuclear Two-Body Matrix Elements Using Harmonic Oscillator Wave Functions," by J. B. Langworthy and S. Podgor

METALLURGY (Also see Chemistry; Fracture Mechanics; and Radiation Effects)

- 6588 "The Effects of an Aqueous Environment on the Fatigue Crack Propagation Characteristics of Titanium Alloys," by T. W. Crooker and E. A. Lange
- 6637 "Measurement of Atomic Kinetics of Solidification Using Peltier Heating and Cooling," by R. J. Schaefer and M. E. Glicksman
- 6698 "Subcritical Flaw Growth in 9Ni-4Co-0.25C Steel—A Fatigue and Fractographic Investigation and Its Relationship to Plane Strain Fracture Toughness," by T. W. Crooker, L. A. Cooley, E. A. Lange, and C. N. Freed
- 6713 "Advances in Fracture Toughness Characterization Procedures and In Quantitative Interpretations to Fracture-Safe Design for Structural Steels," by W. S. Pellini
- *6761 "Fatigue Crack Growth in Three 180-KSI Yield Strength Steels in Air and In Salt-Water Environments," by T. W. Crooker and E. A. Lange
- 6869 "Dislocation Pipe Diffusion in Silver Single Crystals," by R. G. Vardiman and M. R. Achter

NONLINEAR OPTICS (Also see Mathematics and Information Sciences)

- 6662 "Second Harmonic Generation by Reflection from GaAs," by J. B. Langworthy

NUCLEAR AND ATOMIC PHYSICS (Also see Radiation Effects)

- 6670 "The Demineralized Water System for the NRL Cyclotron," by R. O. Bondelid
- 6704 "Thermal Neutron Flux in the Thermal Column of the NRL Reactor," by R. H. Vogt and Christine M. Gosgrove
- 6709 "Reactor Utilization in Support of Research and Technology," by C. V. Strain
- 6729 "Topics in Electron Scattering and Nuclear Models. Notes on Lectures Given at NRL in the Fall of 1966," by H. Uberall
- 6745 "Nuclear Physics Division Progress Report on NRL Problem H01-29," by D. C. Cook, R. J. Omohundro, C. W. Peters, A. I. Snyder, and D. J. Walker
- 6757 "Project Doorstop-Phase III Report," by C. W. Peters and L. Ruby
- 6783 "An Empirical Approach to Thermal Neutron Absorption Cross Sections," by S. Podgor
- 6868 "Nuclear Physics Division Progress Report on NRL Problem I201-29," by D. C. Cook, R. J. Omohundro, C. W. Peters, A. I. Snyder, D. J. Walker, and A. S. Gallia, Jr

CONTRIBUTIONS

OCEAN SCIENCES AND ENGINEERING (Also see Applications Research; Atmosphere and Astrophysics; Chemistry; and Radar)

- *6610 "Optical Detection of Kelvin Waves Generated by Submerged Submarines," by K. G. Williams and T. Myles Thomas
- 6672 "The Influence of Monomolecular Surface Films on the Production of Condensation Nuclei From Bubbled Sea Water," by W. D. Garrett
- 6736 "Infrared Characteristics of Ocean Water (1-1/2 to 15 Microns)," by D. Friedman
- 6762 "Modification of the Air/Sea Interface by Artificial Sea Slicks," by W. R. Barger and W. D. Garrett
- 6767 "The Density-Gradient Column as a Tool for Measuring Sea Water Density," by J. D. Bultman and J. M. Leonard
- 6854 "Some Operating Characteristics of a Xenon-Mercury Short Arc Lamp Immersed in Water," by G. L. Stamm, R. L. Denningham, and A. G. Rockman
- 6855 "Controlled Destructive Testing of Pressure Vessels," by J. J. Gennari and E. Czul

PLASMA PHYSICS

- 6738 "Determination of Electron Temperatures Between 50 keV and 100 keV from X-Ray Continuum Radiation in Plasma," by R. C. Elton
- 6784 "Apparent Local Jump in the Momentum-Transfer Rate at the Front of Flare-Fresh Solar Plasma in the Interplanetary Space," by W. W. Balwanz and T. S. Lee
- 6801 "Theory on Afterburning in a Low-Altitude Rocket Exhaust Plume," by R. S. Lee and W. W. Balwanz

RADAR

- 6608 "A Mathematical Model of a Rotational Frequency Translation Device," by D. Sachs
- 6623 "Some Basic Aspects of Radar Target Imaging," by H. A. Brown
- 6628 "Large Antenna Systems," by M. J. Skoleik
- 6641 "Scintillation Range Noise and Related Phenomena in Water Wave Profiling with Microwave Radar," by A. M. King, C. M. Morrow, C. G. Myers, and C. L. Moody
- 6650 "Radio Ray (Radar) Range-Height-Angle Charts," by L. V. Blake
- 6651 "Eliminating Radar Ambiguities by Processing Staggered Pulse Trains or Spectra," by H. H. Woerrlein
- 6657 "Analysis of Laser-Radar Eye Hazard," by P. W. Wyman
- 6661 "Sea-Clutter Measurement by Radar-Return Sampling," by A. M. Findlay
- 6666 "Radar Scattering from Array Antennas," by R. D. Tompkins
- 6680 "Dynamic Measurement of Aircraft Reflectivity Characteristics," by I. D. Olin
- 6681 "The Scattering of a Plane Electromagnetic Wave by a Linear Array of Center-Loaded Cylinders," by O. D. Sledge
- 6684 "A Multiple Sensor Digital Map-Matching Technique," by J. D. Wilson
- 6702 "Target Noise Characteristics of a CH-21 Helicopter," by M. C. Licitra
- 6717 "On the Transient Response and Backscatter Properties of Linear Antennas," by S. Sandler
- 6719 "NRL Radar Division Technical Highlights (1967)," by W. N. Shaddix
- 6720 "Noise Filtering Improvements," by C. F. White
- 6731 "Applications of Computer-Aided Ionospheric Ray Tracing Techniques to the Analysis of Over-the-Horizon Radar Signatures from Launch-Phase Rockets," by J. R. Davis, M. E. Harding, F. H. Utley, and J. W. Willis
- 6744 "X-Band Doppler Signature of the A-6A," by R. E. Gardner and R. Hynes
- 6790 "A Statistical Estimation of Aerospace Radar Ground Coverage," by J. D. Wilson
- 6796 "The Detection of Nonfluctuating Targets in Log-Normal Clutter," by S. F. George
- 6804 "Ocean Surveillance-Statistical Considerations," by G. V. Trunk
- 6807 "The Determination of Target Course and Speed from Radar Data," by J. P. Barry

RADIATION EFFECTS

- 6620 "The Effects of Coupling Nuclear Radiation with Static and Cyclic Service Stresses and of Periodic Proof Testing on Pressure Vessel Material Behavior," by J. R. Hawthorne and F. J. Loss
- 6625 "Availability of Data on Irradiated Materials as Related to Design Requirements for Water Cooled Reactor Pressure Vessels," by J. R. Hawthorne and F. J. Loss
- 6649 "The Tensile Properties of Selected Steels for Use in Nuclear Reactor Pressure Vessels," by E. P. Klier, J. R. Hawthorne, and L. F. Steele
- 6721 "Notch Ductility Properties of SM-1A Reactor Pressure Vessel Following the In-Place Annealing Operation," by U. Potapovs, J. R. Hawthorne, and C. Z. Serpan, Jr.
- 6739 "Notch Ductility and Tensile Property Evaluation of the PM-2A Reactor Pressure Vessel," by C. Z. Serpan, Jr.
- 6765 "Hot Cell Equipment Developed for Remote Tension Test Specimen Evaluations at NRI," by J. R. Hawthorne and H. F. Watson
- 6772 "Initial Assessments of Notch Ductility Behavior of A533 Pressure Vessel Steel with Neutron Irradiation," by J. R. Hawthorne and U. Potapovs

- 6797 "Effects of High-Energy Protons on Photographic Film," by T. C. Winter, Jr., and G. E. Brueckner
 6803 "The Effect of Residual Elements on 550°F Irradiation Response of Selected Pressure Vessel Steels and Weldments," by U. Potapovs and J. R. Lockhart, Jr.

SHOCK AND VIBRATION

- *6630 "Evaluation of Modifications to Shock-Mitigating Shipboard Stowage System for Terrier Surface-to-Air Missile," by R. L. Bort and M. W. Oleson
 6676 "The Effect of a Second Mode and Nearby Structures on Shock Design Values," by G. J. O'Hara and L. P. Petak
 6776 "Normal Mode Theory for Combined Structures," by W. L. Fournay and G. J. O'Hara
 6819 "The Static Equilibrium Configuration of Cable Arrays Using the Method of Imaginary Reactions," by R. A. Skop and G. J. O'Hara

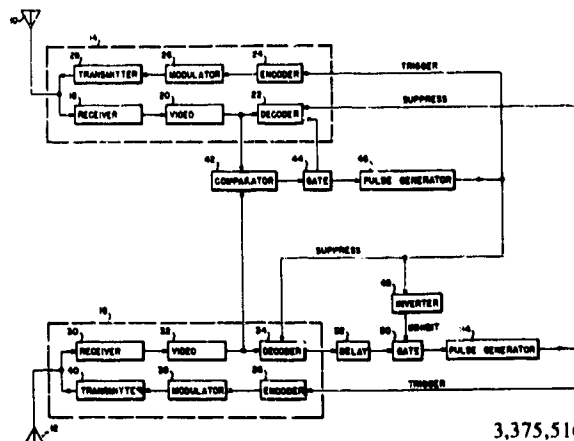
SPACE SCIENCE (See Applications Research: Plasma Physics; and Atmosphere and Astrophysics)

SPECTROSCOPY (Also see Atmosphere and Astrophysics; Chemistry; and Mathematics and Information Sciences)

- 6638 "Measurement and Identification of Laboratory-Produced Vacuum Ultraviolet Spectral Lines," by Nancy V. Roth and R. C. Elton
 6648 "Atomic Emission Lines Below 2000 Angstroms—Hydrogen Through Argon," by R. L. Kelley
 6679 "The Relative Speed of Several X-Ray Films," by Jacqueline S. Vierling
 6732 "Intensification and Reduction of Kodak No-Screen Medical X-Ray Film," by Jacqueline Vierling

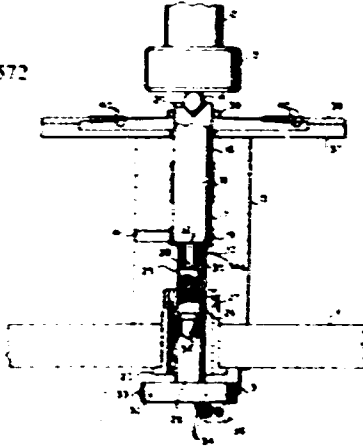
PATENTS RECEIVED

- 3,363,118 — Radially Driven Flexure Plate Transducer, issued January 9, 1968, to Claude C. Sims.
 3,364,365 — Pulse Amplitude-to-Time Conversion Circuit, issued January 16, 1968, to Robert E. Eisenhauer.
 3,364,457 — Electrical Adapter, issued January 16, 1968, to Robert J. Veith, Raymond C. Wilkinson, and Claude C. Martin.
 3,364,461 — Transducer Array with Constant-Pressure Plane-Wave Near Field, issued January 16, 1968, to Winfield J. Trott.
 3,364,466 — Data Collection System Having Plural Channel Storage of Sequential Signals, issued January 16, 1968, to Paul T. Stine.



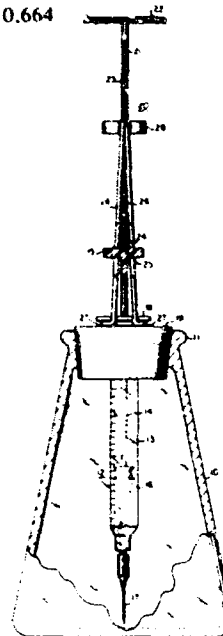
- 3,366,962 — Grounded Sleeve Antenna, issued January 30, 1968, to John J. Kulik and Richard F. Schmidt.
 3,367,172 — Air Gage Heads for Internal Measuring of Waveguide Bends, issued February 6, 1968, to David W. McCormick.
 3,368,189 — Obstacle Locator System, issued February 6, 1968, to Robert M. Page.
 3,369,934 — Method for Removing Vanadium Deposits from the Fire Side of Heat Transfer Surfaces, issued February 20, 1968, to Albert J. Pollard.
 3,371,309 — Thermomechanical Transducer, issued February 27, 1968, to Alar H. Rich.
 3,372,981 — Stabilization of Monoethanolamine Solutions in Carbon Dioxide Scrubbers, issued March 12, 1968, to Harold Ravner and Charles H. Blachly.
 3,373,263 — Gunfire Control System for Supplying Aiming Information for Guns Having Different Ballistic Characteristics, issued March 12, 1968, to Densil M. Cooper, Charles F. Wysong, and Thomas W. Chappelle.
 3,373,353 — Electron Beam Scanning System for Quality Control of Materials, issued March 12, 1968, to Franklin H. Harris.
 3,374,050 — Paint Dispensing Pen, issued March 19, 1968, to Harold S. Goulart and Herbert Rabin.
 3,374,307 — Electrical Connector, issued March 19, 1968, to Theodore J. Rauen, Edwin C. Myers, Jr., and Arthur B. Cooke.
 3,374,313 — Cathode Ray Tube Overlay Including a Rotatable Disc with a Plurality of Range Scales, issued March 19, 1968, to Robert H. Mathes and Lauro C. Ricalzone.
 3,374,383 — Accumulation Means for Reduction of Sputter in Gas-Filled, Lyman-Alpha Source Tube, issued March 19, 1968, to George J. Bergen and Arnold H. Singer.

CONTRIBUTIONS

- 3,374,662 - Flexural Fatigue Machine, issued March 26, 1968, to Meyer R. Achter, Hugh H. Smith, Robert J. Rieve, and Richard L. Stegman.
- 3,374,762 - Pressure Indicator, issued March 26, 1968, to Alan W. Baldwin.
- 3,375,516 - Dual Antenna System for Transponder Beacon Devices, issued March 26, 1968, to Gerald E. Hart and Charles E. Quigley.
- 3,379,901 - Fetal Heart Transducer and Method of Manufacture, issued April 27, 1968, to James R. Richards.
- 3,379,997 - Magneto-hydrodynamic Light Source Excited Laser, issued April 23, 1968, to Leonard J. Melhart.
- 3,380,019 - Pressure-Gradient Hydrophone, issued April 23, 1968, to Claude C. Sans.
- 3,381,147 - Measuring Device Employing Negative Resistance, issued April 30, 1968, to George Abraham.
- 3,382,722 - Indicating Instrument Having Vibration for Removing Effects of Static Friction, issued May 14, 1968, to Richard B. Bridge and Thomas E. Maersch, III.
- 3,382,785 - Pulsed Eddy Current Motivated Shutter, issued May 14, 1968, to Leonard J. Melhart.
- 3,383,238 - Method and Apparatus of Controlling Thin Film Deposition in a Vacuum, issued May 14, 1968, to Arlyn E. Unzicker and Blair J. Zajac.
- 3,383,328 - Water Displacing and Rust Preventive Composition, issued May 14, 1968, to Hayward R. Baker and Paul E. Leach.
- 3,383,405 - Method of Preparing Mixed Diesters, issued May 14, 1968, to Paul J. Smigowski.
- 3,383,458 - Modular Power Distribution System, issued May 14, 1968, to Nicholas M. Raskhodoff and Douglas A. Venn.
- 3,397,572 - 
- 3,383,538 - Proportional Counter Tube Including a Plurality of Anode-Cathode Units, issued May 14, 1968, to Charles S. Bowyer.
- 3,383,602 - Signal Amplitude Selector, issued May 14, 1968, to Elvin E. Herman.
- 3,383,603 - Precision Electronic Current Amplifier and Integrator, issued May 14, 1968, to Mervin W. O'Connor.
- 3,383,606 - Diverse Frequency Echo Detection System, issued May 14, 1968, to John R. Davis, James M. Hendrick, and Irving H. Page.
- 3,386,364 - Synchronous Intervalometer, issued June 4, 1968, to Leonard O. Hayden.
- 3,386,659 - Method and Means for Producing Electrical Energy Utilizing a Bacterial Organism, issued June 4, 1968, to Hector J. Wilson and Martin B. Cavatagh (deceased).
- 3,386,266 - Pulse Processor, issued June 11, 1968, to Raymond A. Njar.
- 3,388,332 - Computer Device for Aircraft Carrier Approach System, issued June 11, 1968, to Albert Brodzinsky, Joseph E. Reynolds, Jr., and Irving M. Saffitz.
- 3,388,397 - Radio Navigation Receiver System Utilizing AGC for Switching from Phase-Measuring Mode of Operation to a Dead Reckoning Mode, issued June 11, 1968, to Alexander F. Thornhill and Melvin F. Williams.
- 3,388,399 - Antenna Feed for Two-Coordinate Tracking Radars, issued June 11, 1968, to James E. Lewis.
- 3,392,951 - Variable Pitch Bracket, issued July 16, 1968, to Robert K. Chaimson.
- 3,393,400 - Calibration Method Using Transducer Array with Constant-Pressure Phase-Wave Near-Field, issued July 16, 1968, to Winfield J. Trott.
- 3,394,323 - Zero Phase-Shift Filter, issued July 23, 1968, to Maxine G. Kaufman and Hugh B. Gardner.
- 3,394,341 - High-Pressure Contact for Electrical Connectors, issued July 23, 1968, to Douglas A. Venn.
- 3,395,516 - Airborne Aerosol Collector, issued August 6, 1968, to Roger M. Schecter and Robert G. Russ.
- 3,396,120 - Thermoluminescent Glass and Method of Preparing the Same, issued August 6, 1968, to Robert J. Gintner.
- 3,396,300 - Proportional Counter Tube Having a Plurality of Interconnected Ionization Chambers, issued August 6, 1968, to Charles S. Bowyer.
- 3,397,572 - Device for Measuring Stress-Strain Curve, issued August 20, 1968, to Walter A. Stolz (deceased), Joseph M. Krafft, and Frank W. Bird.
- 3,397,851 - Nutation Damper Assembly, issued August 20, 1968, to Douglas P. McNutt.

- 3,398,277 - Electro-Optical Altimeter, issued August 20, 1968, to Dwight L. Randall.
- 3,398,330 - Bistable Command Module, issued August 20, 1968, to John S. Poole.
- 3,398,374 - Time Gated Filter, issued August 26, 1968, to Maxine G. Kaufman.
- 3,400,399 - System and Method for Obtaining Accurate Tactical Navigation, issued September 3, 1968, to Evans L. Kline.
- 3,403,253 - Humidimeter Having Feedback Means to Control the Energization of the Tube, issued September 24, 1968, to Oliver K. Larison.
- 3,403,344 - Commutated Linear Multiple Gate, issued September 24, 1968, to Spencer M. Cork, Garoid K. Jensen, and James E. McGeogh.
- 3,403,543 - Apparatus for Forming Flattened Tubes with Constant Radii Edge Sections, issued October 1, 1968, to John B. Gregory, Arthur T. McClinton, and Patrick A. Whittington.
- 3,404,229 - System for Reducing Phase Distortion in the Phase Reference Signals of a Multichannel Phase Shift Data System, issued October 1, 1968, to Francis X. Downey and Charles H. Weaver.
- 3,406,397 - Satellite Angle and Altitude Measuring System, issued October 15, 1968, to Roger L. Easton and Thomas B. McCaskill.
- 3,407,354 - Motor and Self-Synchronous Generator Frequency Synchronization Units for Swept Frequency Secret Communications System, issued October 22, 1968, to Joseph P. Wheeler.
- 3,409,895 - Time Recording System, issued November 5, 1968, to Leonard O. Hayden.
- 3,410,664 - Titration Apparatus, issued November 12, 1968, to George H. Fielding.
- 3,412,347 - Transistorized Phase Modulator Suitable for Analog Data Conversion, issued November 19, 1968, to Francis X. Downey and Alick Frank.
- 3,412,377 - Integrated Fresnel Rainbow Optical Landing System, issued November 19, 1968, to Barbour Lee Perry.

3,410,664



- 3,413,555 - Analog Data Converter for a Phase Comparison Telemetry System, issued November 26, 1968, to Francis X. Downey.
- 3,417,251 - Towed Instrument for Continuous Measurement of Ocean Turbidity, issued December 17 to John M. Leonard and John D. Bultman.
- 3,417,523 - Folding Antenna Mount, issued December 24, 1968, to William U. Matson.
- 3,417,602 - A Tube-Bending Mandrel, issued December 24, 1968, to John G. Schmidt.
- 3,418,510 - Triggered Spark Gap Electric Arcing Device, issued December 24, 1968, to Leonard J. Melhart.
- 3,418,584 - Control Circuit for an Indicating Device, issued December 24, 1968, to Henry P. Birmingham.
- 3,418,602 - Direct-Coupled Regenerative Feedback Starting Circuit for Common-Emitter Power Oscillators, issued December 24, 1968, to Charles A. Lauter, Jr.
- 3,418,634 - Delay Line Switch Prefire and Failure-Indicating System, issued December 24, 1968, to Marvin P. Young.

RECOGNITION OF PERSONNEL

HONORS AND INCENTIVE AWARDS

Employees of the Naval Research Laboratory are recognized for their distinguished achievements through the Navy Incentive Awards Program, through appropriate honors offered and conferred by professional societies and academic institutions, and also through letters of commendation from various research sponsors and consumers. Approximately 900 NRL employees were so recognized in 1968. Members of the Laboratory staff who received some of the more significant of these honors and awards during the past year are listed below.

George Abraham: *Elected Chairman of the Washington, D.C., Section of the Institute of Electrical and Electronic Engineers*

Frank H. Attix: *Elected to Board of Directors (3-year term), Health Physics Society; Associate Editor, Radiation Dosimetry, Vol. 1, 2d ed., Academic Press, 1968; Program Chairman, 2d International Conference on Luminescence Dosimetry, Galinburg, Tenn., September 23-26, 1968, and Chairman of the Session on Relative Response of TL Phosphors to X-rays, V-rays, and Charged Particles; and Chairman of the Radiation Physics*



Dr. B. Floyd Brown receives the 13th Annual E. O. Hulburt Award from Capt James C. Matheson, USN, Director of NRL, for his work in fundamentals of stress corrosion cracking. The Hulburt Award is the highest science award conferred by NRL.



Dr. Martin E. Glicksman, left, and **Dr. Henry Shenker**, right, received the 1968 awards for pure science and for applied science, respectively, granted annually by the NRL chapter of the Scientific Research Society of America. **Dr. Clifford C. Klick**, center, NRI, RESA president for 1968, made the presentations.

Session, 15th Annual Meeting of the Health Physics Society, Denver, Colo., June 16-20, 1968

Henry P. Birmingham: *Program Chairman, 9th Annual IEEE Symposium on Human Factors, Washington, D.C., May 6-7, 1968*

LaVerne S. Birks: *Elected first President of the Electron Probe Analysis Society; chairman of a session at the Eastern Analytical Symposium, New York, N.Y., November 13-15, 1968*

Emanuel L. Brancato: *Appointed to a 2-year term as Chairman of the NAS/NRC Board of the Conference on Electrical Insulation and Dielectric Phenomena*

B. Floyd Brown: *NRL E. O. Hulburt Science Award*

Chester L. Buchanan and colleagues: *Letters of Commendation for contributions to the successful Scorpion search from the Chief of Naval Operations, from the Commander, Submarine Force Atlantic, and from Congressman Alton Lennon (D., N.C.)*

Rube Chernikoff: *General Chairman, 9th Annual IEEE Symposium on Human Factors, Washington, D.C., May 6-7, 1968*

Robert B. Fox: *President of the Chemical Society of Washington, 1968; appointed member of the Editorial Advisory Board for the ACS monthly publication, Macromolecules*

Herbert Friedman: *Appointed by President Johnson to membership on the General Advisory Com-*



Mr. Emerick Toth receives the Superior Civilian Service Award from RAdm Thomas B. Owen, USN, Chief of Naval Research. Mr. Toth has long been an expert in the field of radio communications. He received the award upon his retirement early in 1968.

mittee on Atomic Energy; appointed Chairman of the Space Science Board of the National Research Council; elected President of the Planetary Sciences Section of the American Geophysical Union

Martin E. Glicksman: *Pure Science Award, NRL Chapter, Scientific Research Society of America*
Wayne C. Hall: *Certificate of Appreciation, Joint Board on Science Education of the Greater Washington Area*

Joseph J. Halpin: *Selected by editorial staff of Applied Optics to write a review of the IEEE Annual Conference on Nuclear and Space Radiation Effects, held at Missoula, Mont., July 15-18, 1968*

J. Heaston Heald: *Navy Superior Civilian Service Award*

John Hill: *Publicity Chairman, 9th Annual IEEE Symposium on Human Factors, Washington, D.C., May 5-7, 1968*

Alexander J. Hiller: *Chairman, Coastal Oceanography Session, 5th U.S. Navy Symposium on Military Oceanography, Panama City, Fla., May 1-3, 1968*

Isabella L. Karle: *1968 Achievement Award, Society of Women Engineers*

Jerome Karle: *Navy Distinguished Civilian Service Award; appointed to NRL Chair of Science for the Structure of Matter*

John M. Leonard: *Certificate of Appreciation, Joint Board on Science Education of the Greater Washington Area*

Herbert S. Poole: *Certificate of Appreciation, Joint Board on Science Education of the Greater Washington Area*

Dror S. Sadeh: *Third Prize, Gravity Research Foundation, for paper entitled "The Effect of Mass on Frequency"*

Albert I. Schindler: *Elected to Board of Governors (3-year term), Scientific Research Society of America*

Elaine G. Shafrin: *Certificate of Appreciation, Joint Board on Science Education of the Greater Washington Area*

Henry Shenker: *Applied Science Award, NRL Chapter, Scientific Research Society of America*

Curtis R. Singleterry: *Awarded Doctor of Humane Letters by Aurora College, Aurora, Ill.*

Merrill I. Skolnik: *Elected Fellow of the Institute of Electrical and Electronics Engineers*

Emerick Toth: *Navy Superior Civilian Service Award*

Richard L. Tuve: *Letter of Commendation from the Chief of Naval Operations for accomplishments with the twin-agent firefighting chemicals, Light Water and purple-K powder*

Richard F. Wallis: *Editor, Localized Excitation in Solids, Plenum Press, 1968*



Dr. Jerome Karle, Chief Scientist of the Laboratory for Structure of Matter, receives the Navy's Distinguished Civilian Service Award from the Honorable Robert A. Frosch, Assistant Secretary of the Navy (R&D), for his pioneering research in the analysis of the structure of matter by electron x-ray, and neutron diffraction

RECOGNITION

Dean I. Walter: *Certificate of Appreciation, Joint Board on Science Education of the Greater Washington Area*

William A. Zisman: *Navy Captain Robert Dexter Conrad Award*



Dr. William A. Zisman, Chief Scientist of the Laboratory for Chemical Physics and formerly Superintendent of the Chemistry Division, and Mrs. Zisman admire the Navy's Captain Robert Dexter Conrad Award, presented by the Honorable Paul R. Ignatius, Secretary of the Navy. Dr. Zisman received the award for his "... notable research in chemistry during the past twenty-nine years."

DISTRIBUTION OF INCENTIVE AWARDS DURING 1968

Navy Robert Dexter Conrad Award	1
Navy Distinguished Civilian Service Award	1
Navy Superior Civilian Service Award	3
NRL E. O. Hulburt Science Award	1
Award of Merit for Group Achievement	1
Invention and Patent Disclosures	132
Research Publication Awards	48
Sustained Superior Performance	47
Outstanding Performance Rating	131
Quality Salary Increase	85
Beneficial Suggestion	84
Fifty-Year Federal Length of Service	1
Forty-Year Federal Length of Service	2
Thirty-Year Federal Length of Service	43
Twenty-Five-Year NRL Length of Service	64
Twenty-Year Federal Length of Service	128
Ten-Year NRL Length of Service	90

136

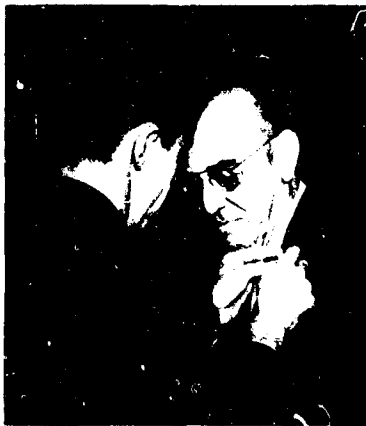
RESEARCH PUBLICATION AWARDS

Awards for research publications were established at NRL in 1968 for presentation annually to single or multiple authors of technical articles and formal NRL reports that are judged by select committees to be the best produced in each division of the Research Department during a given calendar year. The authors selected to receive the first NRL annual publication awards are listed here. (The 20 award-winning papers are included in the bibliographies of published works which appear in the section "Contributions to Science and Technology.")

Richard G. Allas	Benjamin Lepson
Arlo D. Anderson	Patrick P. Lloyd
Frank H. Attix	Henry J. Mastenbrook
Paul P. Bey	Russell A. Meussner
Lamont V. Blake	Charles M. Murphy, Jr.
Robert L. Bort	Werner G. Neubauer
Joseph K. Brown	Albert E. Nash
George R. Carruthers	Merval W. Oleson
Thomas W. Crooker	George C. Page, Jr.
Charlotte M. Davisson	Louis J. Palumbo
John H. Dunn	Arthur G. Pieper
Raymond C. Elton	Herbert Rabin
Vincent G. FitzSimmons	John E. Rogerson
Vincent J. Folen	James B. Romans
Charles T. Fujii	Mark Rubinstein
John F. Giuliani	Sigmund Schuldiner
Steven G. Gorbics	Clarence M. Shepherd
Hans R. Griem	Curtis R. Singleterry
Fred Gross	Richard B. Theus
Dean D. Howard	T. Myles Thomas
Thomas J. Jesswein	Kingsley G. Williams
Charles R. Kohler	John W. Wright
James J. Krebs	Emanuel Vegh
Eugene A. Lange	Charles E. Young



Mr. Ralph G. Taylor, of the Space Science Division, receives an award from Capt James C. Matheson, USN, Director of NRL, for disclosing a patentable invention, a 40-60A photometer having an aluminum-coated Mylar window.



Dr. Louis A. Gebhard receives a 50-year length-of-service pin from Capt James C. Matheson, USN, Director of NRL. Dr. Gebhard recently retired as Superintendent of the Radio (now Communications Sciences) Division and at present is a consultant to the Associate Director of Research for Electronics. He is a pioneer in the development of radio and radar.

SCHOLARSHIP AWARDS

Twenty-eight employees received educational "scholarships" in 1968 under the Naval Research Laboratory's Edison Memorial and Sabbatical Study Programs, both of which are designed to help NRL maintain a highly competent corps of professional personnel. Under the Edison Program, which was established at NRL in 1961, selected employees devote three days per week to graduate study and three days per week to their work at NRL. The Laboratory's Sabbatical Program, now in its fifth year, permits selected employees to pursue an academic year of full-time research or graduate study at either foreign or domestic institutions. NRL staff members in either program continue to receive their regular salaries, annual and sick leave privileges, and the numerous fringe benefits of Federal employment. Up through the academic year 1968-1969, ninety-nine employees (61 Edison and 38 Sabbatical) have been selected to participate in these educational programs at NRL. The roster of current participants is as follows:

Dr. George R. Carruthers, of the E. O. Hulburt Center for Space Research, receives a Research Publication Award from Dr. Alan Berman, Director of Research at NRL. The title of Dr. Carruthers' paper, which appeared in *Astrophys. J.* 151:269 (1968), was "Far-Ultraviolet Spectroscopy and Photometry of Some Early-Type Stars."

Robert V. Anderson, Ocean Sciences: *Sabbatical*
 Frank H. Attix, Nuclear Physics: *Sabbatical*
 Willard D. Bascom, Chemistry: *Edison*
 James N. Bradford, Solid State: *Sabbatical*
 Roderick A. Carr, Ocean Sciences: *Edison*
 Joe O. Elliot, NonAcoustic ASW (R&D)
 Task Group: *Sabbatical*
 Lawrence W. Fagg, Nuclear Physics: *Sabbatical*

RECOGNITION

Andrew M. Findlay, Radar: *Edison*
John M. Goodman, Radar: *Edison*
Sam Hanish, Acoustics: *Edison*
Gary H. Herling, Nuclear Physics: *Sabbatical*
James M. Hudnall, Radar: *Edison*
Edward C. Jones, Nuclear Physics: *Edison*
Michael J. Marrone, Solid State: *Edison*
Robert M. Mason, Mathematics and Information Sciences: *Sabbatical*
Caldwell McCoy, Jr., Acoustics: *Edison*
Daniel R. Mulville, Ocean Technology: *Edison*
David J. Nagel, Nuclear Physics: *Edison*
Manuel R. Pablo, Electronics: *Edison*
Edward D. Palik, Solid State: *Sabbatical*
Richard I. Perlut, Engineering Services: *Edison*
Chester F. Poranski, Chemistry: *Edison*
Robert J. Sanford, Ocean Technology: *Edison*
Glenn D. Sandlin, Space Science: *Edison*
Thomas J. Schriempf, Metallurgy: *Sabbatical*
David A. Swick, Acoustics: *Edison*
Joseph F. Weller, Solid State: *Edison*
Conrad M. Williams, Metallurgy: *Edison*

RESEARCH ASSOCIATESHIP AWARDS

Hulburt Center Research Associates

A program of educational and research stimulation carried out by the Space Science Division is known as the Hulburt Center Program (after E. O. Hulburt, NRL's first Director of Research and a pioneer in space science). It is sponsored jointly by the National Science Foundation, the Office of Naval Research, and the National Aeronautics and Space Administration. Under the Hulburt Center plan, National Science Foundation appointments are established at NRL so that university people—advanced graduate students, postgraduates, and faculty members—may participate in an augmented program of space research.

Normally, the tenure of a Hulburt Center appointment is one year, but assignments for periods of two or three years are not uncommon. Applications are reviewed by the staff of the Hulburt Center and the Astronomy Section of the National Science Foundation. During 1968, there were eight Hulburt Center appointees at the Laboratory:

George Doschek
Paul D. Feldman
Richard Henry
Robert R. Meier

N. Paul Patterson
Dianne K. Prinz
Carl A. Rouse
Dror S. Sadeh

Postdoctoral Research Associates

The Naval Research Laboratory, in cooperation with the National Research Council of the National Academy of Sciences and the National Academy of Engineering, supports a postdoctoral research associateship program whereby recent recipients of the doctorate degree are offered the opportunity to work at the Laboratory for one year (occasionally for two years). During that time an appointee engages in advanced training and basic research under the guidance of one of NRL's senior scientists.

Awards are made annually in any field included in the Laboratory's research program. They are based on the recommendations of a panel of nationally known scientists appointed by the National Academy of Sciences.

During 1968 there were 31 postdoctoral associates active at NRL. Their names are listed below, together with the area of research in which they were engaged.

Robert E. Baier, Biochemistry
C. Edward Bailey, Solid State Physics
Samuel I. Baker, Nuclear Physics
Stephen G. Bishop, Solid State Physics
James S. Byrnes, Mathematics
James Comas, Solid State Physics
Larry R. Cooper, Nuclear Physics
Alexander C. Ehrlich, Physics
David R. Flinn, Chemistry
Richard D. Gilardi, Physical Chemistry
Manuel Gomez-Rodriguez, Solid State Physics
William H. Green, Chemistry
David L. Griscom, Solid State Physics
Robert J. Hansen, Solid State Physics
Uwe J. Hansen, Solid State Physics
Richard K. Jeck, Jr., Physics
John C. Kershenstein, Physics
Robert L. Kinzer, Physics
John H. Konnert, Physical Chemistry
Leslie S. Levine, Physics
Richard V. Mancuso, Nuclear Physics
Michael H. Reilly, Solid State Physics
Murray Rosen, Chemistry
Gerald H. Share, Physics
Charles W. Sink, Chemistry
Earl F. Skelton, Solid State Physics
Edward H. Takken, Physics
Karel Vander Lugt, Physics
Joseph L. Verble, Solid State Physics
Robert J. Wagner, Solid State Physics
Alan W. Webb, Chemistry